Palacký University Olomouc
Faculty of Medicine and Dentistry

EPIGENETIC STUDY OF 5-AZACYTIDINE NUCLEOSIDES AND THEIR DERIVATIVES

DISSERTATION

Presented in Partial Fulfillment of the Requirements for the Degree of Doctor of Philosophy in Pediatrics

By

Khushboo Agrawal, M.Sc.

June 2017

*****

Supervisor

Marián Hajdúch, M.D., Ph.D.

I, the undersigned, hereby declare that this Ph.D. dissertation has been composed solely by myself, and embodies the original research work of my own investigation. I played the major role in the preparation and execution of the experiments, and the data analysis and interpretation are entirely by own work. Any collaborative contributions from colleagues have been explicitly acknowledged, and references to all supporting literatures and resources have been duly cited.

I further declare that this dissertation has not been submitted, in whole or in part, for any other degree or professional qualification.

In Olomouc
June 2017

Khushboo Agrawal, M.Sc.

I, the undersigned, have examined the dissertation entitled

EPIGENETIC STUDY OF 5-AZACYTIDINE NUCLEOSIDES
AND THEIR DERIVATIVES

presented by Khushboo Agrawal,

a candidate for the degree of Doctor of Philosophy in Pediatrics,

and hereby certify that, in my opinion, it is fully adequate in scope and quality as a dissertation for the degree of Doctor of Philosophy, and is worthy of acceptance.

Assoc. Prof. MUDr. Marián Hajdúch, Ph.D.
(Principal Advisor)

Prof. MUDr. Vladimír Mihál, C.Sc.
(Opponent)

Prof. RNDr. Vladimír Král, Ph.D., D.Sc.
(Opponent)

Dedicated to

Cancer Patients and Survivors

Abstract

DNA methylation plays a pivotal role in the etiology of cancer by mediating epigenetic silencing of cancer-related genes. Since the relationship between aberrant DNA methylation and cancer has been understood, there has been a significant amount of research at developing anti-cancer therapies that work by inhibiting DNA methylation. The first epigenetic drugs azacytidine and its congener decitabine are currently most advanced hypomethylating agents in clinic for the treatment of hematological malignancies, and have shown promising results in solid tumors in early clinical trials. Yet, the clinical success of these prototypal drugs is limited due to accqusition of primary and secondary resistance, and their hydrolytic instability which decreases their plasma circulation time. In this study, a cell-based DNA demethylation detection system was developed for high throughput screening of potent hypomethylating epi-drugs. The described detection system provides an efficient tool for large-scale epigenetic drug screenings, and would therefore benefit academic and industrial drug discovery. Using this system, the newly synthesized biodegradable, polyanhydride formulations of azanucleoside drugs were characterized for their therapeutic effectiveness, and it was found that microbead formulations of the hydrolytically labile azanucleoside drugs could prevent their chemical decomposition in aqueous solution, and effectively increase their plasma circulation time. The detection system was further used to study the effect of stromal cells of the tumor-microenvironment on the response of cancer cells to hypomethylating agents. The study showed the increased activity of hypomethylating agents in high stromal environment which suggests the potential of tumor-stroma ratio for predicting the outcome of epigenetic therapy in cancer. Finally, the molecular mechanism of secondary resistance to azanucleoside drugs was investigated in colorectal cancer. The study revealed the response predicting biomarker genes which may differentiate between resistance and sensitivity to azanucleoside drugs, and further proposes alternative therapeutics for overcoming resistance to azanucleosides.

Abstrakt

Methylace DNA hraje klíčovou roli v etiologii nádorů tím, že zprostředkovává epigenetické utlumení exprese genů souvisejících s rozvojem nádorových onemocnění. Poté co byl popsán vztah mezi aberantní methylací DNA a rakovinným bujením bylo vyvinuto velké množství protirakovinných léčiv, které fungují na základě inhibice DNA methylace. Prvním léčivem ovlivňujícím DNA na epigenetické úrovni byl azacytidin a vedlejší produkt jeho syntézy gemcitabin. Tyto dvě látky jsou v současnosti nejvíce používanými léčivy pro snížení methylace DNA v klinické praxi při léčbě hematologických nádorů a vykazují slibné výsledky také v raných fázích klinických studií pro léčbu solidních nádorů. Širší využití těchto léků je bohužel limitováno častým výskytem primární a sekundární rezistence a také jejich značnou nestabilitou ve vodném prostředí, resp. v krevní plazmě. V této studii byl vyvinut vysoce propustný testovací systém (tzv. high-throughput screening) umožňující detekci snížené methylace DNA v jednotlivých savčích buňkách. Tento detekční systém poskytuje velmi efektivní způsob testování velkého množství látek modifikujících epigenetické procesy uvnitř buněk a může tak být využíván jak v primárním tak i v aplikovaném výzkumu protinádorových léčiv. S pomocí tohoto systému byla popsána terapeutická účinnost nově syntetizovaných biodegradabilních polyanhydridových derivátů azanukleosidových léčiv. Bylo zjištěno, že stabilitu hydrolyticky labilních forem azanukleosidových léčiv lze vylepšit jejich vazbou na mikrokuličky. Tato modifikace zabraňuje rozkladu látek ve vodném roztoku a efektivně tak prodlužuje jejich setrvání v krevní plazmě. Detekční systém byl dále použit pro studium vlivu buněk nádorového stromatu na nádorové buňky. Studie ukázala zvýšenou aktivitu látek a tedy výrazný stupeň hypomethylované DNA v nádorech s vysokým zastoupením stromatu. Studie tak poukazuje na možnost predikce efektivity léčby těmito látkami na základě zhodnocení poměrného zastoupení buněk stromatu a nádorových buněk u daného rakovinného onemocnění. Molekulární mechanismy vzniku sekundární rezistence k azanukleosidovým léčivům byly studovány v buňkách nádoru tlustého střeva. Studie odhalila některé geny, které mohou sloužit jako biomarkery pro predikci sensitivity nebo rezistence k azanukleosidovým léčivům a navrhuje také alternativní způsoby léčby, které by umožnily překonání rezistence k azanukleosidovým léčivům.

Acknowledgements

First and foremost I want to express my sincere gratitude to my advisor and director of the Institute of Molecular and Translational Medicine, Marián Hajdúch. Without you I wouldn't be where I am today. You have contributed both consciously and un-consciously in making my Ph.D. experience productive and stimulating. I appreciate all your contributions of time, enduring support, encouragement, and words of wisdom which always helped me during tough times in the Ph.D. pursuit. I am extremely thankful to you for always trusting and believing in me, and for allowing me the freedom to learn from my own mistakes. Apart from being a wonderful Ph.D. mentor, the unconditional love that I received from you always made me feel like your daughter, than a Ph.D. student. You said to me once that why I miss my family when I have my scientific family here in Czech, and you really kept your words during my entire Ph.D. tenure. I cannot express myself, I am so grateful Sir.

I would especially like to thank Petr Džubák for his constant involvement during project discussions and throughout support with technical difficulties, and other senior lab members at the institute, Josef Srovnal, Martin Mistrík, Jiří Drábek, and Radek Trojanec for sharing their expertise.

I am indebted to Viswanath Das for his immense support throughout my Ph.D. He has played a significant role in process of my learning, and has set an excellent example at work. This thesis would not have been possible without your tangible guidance Viswanath Bhai.

I want to thank Ivo Frydrych and Juraj Kramara for always helping me with technical difficulties in lab and patience for answering all my questions. To my dearest colleague Eva Veselá for her enormous help during all the difficult times in lab and for providing great motivation and strength to overcome challenges.

I want to acknowledge other members that I have had the pleasure to work with, and without contribution of whose expertise, my Ph.D. project would not have been successfully completed. In regards to transcriptomics and methylomics sequencing, I thank Petr Vojta and Rastislav Slavkovský for carrying next-generation sequencing runs on my samples. I very much appreciate Petr for his willingness to help me with hierarchical clustering of genes everytime I needed. I thank Rastislav for teaching me how to design primers for methylation analysis, and highly appreciate his enthusiasm and interest to understand the theory of my project. It was really a great pleasure to work with you guys.

The 3D culture studies presented in this dissertation were done by Viswanath. We worked together on three research articles and I really appreciate his collaboration. His perceptive comments on drafts of my manuscripts significantly improved my writing skills.

For flow-cytometric analysis, I thank Ivo for measuring my samples. I also thank Ivo and Narendran Annadurai for their valuable help with my wet lab experiments during last academic year of my Ph.D. Thank you so much guys for making it possible at the last moment.

I am thankful to Dalibor Doležal for his kind cooperation with animal experiments, to Jiří Večerka for xenografts transplantations and *in vivo* drug administrations, and to Zbyněk Nový for *in vivo* fluorescence imaging of tumors. I acknowledge Jana Vrbková for performing statistical analysis on my *in vivo* data.

The biodegradable microbeads formulations of azanucleoside drugs discussed in this dissertation were developed, and physically and chemically characterized by Martin Hrubý and members of his group at Institute of Macromolecular Chemistry AS CR, v.v.i., Prague. I appreciate their collaboration and the impressive skills of Martin who designed the microbeads system. I also thank Marcela Krečmerová from the Institute of Organic Chemistry and Biochemistry, Czech Academy of Sciences, Prague for providing azanucleoside drugs in bulk to perform all my experiments.

I cannot thank enough to Toshikazu Ushijima at National Cancer Center Research Institute, Tokyo for his kind gift of FLJ32130 targeting vector without which it would have been very difficult to achieve the goal of establishing DNA methylation detection system. I will be forever grateful to him for his generous help.

I am exceptionally thankful to Jean-Pierre Issa from Fels Institute for Cancer Research and Molecular Biology and numerous scientists in field of cancer epigenetics who visited my poster sessions at American Association of Cancer Research Annual Meetings in USA for their expert comments on my research which steered my project in the right direction. I am highly obliged to my advisor, Marián for repeatedly providing me the precious opportunities to attend the biggest cancer convention, it truly benefited me.

I want to direct my sincere thanks to Martin Modrianský, vice-dean for development and postgraduate studies for his good comments on my work, and for nominating me to represent Palacký University at International Medical Postgraduate Conference in Hradec Králové. As a Ph.D. student it meant a lot for me.

I express special thanks to all our past and present lab managers who kept us organized, especially to my favorite, Renata Buriánová, and to Anna Janošťaková from whom I received so many wonderful gifts, and our perfect IT technicians, Tomáš Novotný and Jan Moucha. To all

our administrative assistants, especially our comical Vera Drozdova and Barbora Miklášová who were always ready to help and our sweet receptionist Petra Vránová and Jiří Krajča. I gratefully acknowledge Helga Hromádková in office of student's affair for being remarkably organized and for her incredible cooperation throughout my Ph.D.

I owe a great debt to all my colleagues at IMTM who supported me in one way or another, and put up with me being married to my Ph.D. for the past few years. Most especially to my buddy Jiří Řehulka whose help cannot be described in few words. Dude, I troubled you throughout my Ph.D., million thanks for helping me always.

My time at IMTM was made enjoyable in large part due to many friends and groups that became a part of my life. I am grateful for fun time spent with my officemates, Lakshman Varanasi, Ermin Schadich, and Pawel Znojek for all the laughter.

I share the most beautiful part of my memories in Olomouc with my friend cum loving sister Laura Ledwoń who is now a part of my family and without whose emotional support my life was not possible in a country 7,000 miles away from my home.

I pay deep respect to all my honorable teachers who taught me at School and University, whatever little I am today, all because of them.

I am extremely thankful to God for giving me the best parents of this world, Mummy Papa you are the pillar of my strength, love you sooooo much ^◡^ To my adorable, loving, and caring sister Bhavana Agrawal and my brother Priyesh Agrawal who have enriched my life beyond measure, and are the biggest reasons of happiness in my life. I cannot imagine myself without you two ^◡^

Khushboo Agrawal
Palacký University Olomouc
June, 2017

This Ph.D. was supported by Palacký University of Olomouc Doctoral Scholarship to Khushboo Agrawal. The research was supported by the generous grants awarded by the European Social Fund (CZ.1.07/2.3.00/20.0009), Czech Ministry of Education (MSM 6198959216), Czech Science Foundation (GAČR 303/09/H048), Medical Faculty Internal Grant Agency of Palacký University (IGA UP LF_2010_006, LF_2012_018, LF_2013_016, LF_2016_019), Ministry of Industry and Trade of the Czech Republic (MPO TIP FR-TI4/625), Ministry of Education, Youth and Sports (CZ09/7F14009, LO1304, LF2015091, LM2015064), Grant Agency of the Czech Republic (1402652S, 1403636S), Ministry of Health of the Czech Republic (15-31984A), and Technology Agency of the Czech Republic (TE010200028). Infrastructural part of the research (Institute of Molecular and Translational Medicine) was supported by the Operational Programme Research and Development for Innovations (project BIOMEDREG; CZ.1.05/2.1.00/01.0030).

Table of contents

List of figures

Chapter 5

List of tables

Chapter 1

Chapter 5

List of major abbreviations

α-DAC	Alpha anomer of 2’-deoxy-5-azacytidine
ALL	Acute lymphoblastic leukemia
AML	Acute myeloid leukemia
AUC	Area under the curve
AZA	5-azacytidine; azacytidine
BED	Biologically effective dose
BET	Bromodomain and extra-terminal motif
BSC	Best supportive care
CCR	Conventional care regimen
CDA	Cytidine deaminase
CM	Conditioned medium
Cmax	Maximum observed plasma concentration
CMML	Chronic myelomonocytic leukemia
CR	Complete remission
CRC	Colorectal cancer
DAC	2'-deoxy-5-azacytidine; decitabine
dCK	Deoxycytidine kinase
DFS	Disease free survival
DHDAC	2′-deoxy-5, 6-dihydro-5-azacytidine
DLT	Dose limiting toxicities
DNMT	DNA methyltransferase
DNMTI	DNA methyltransferase inhibitors
DOR	Duration of response
EFS	Event free survival
HCS	High content screening
MCS	Multicellular spheroids
MDS	Myelodysplastic syndrome
MTD	Maximum tolerated dose
ORR	Overall response rate

OS	Overall survival
PD	Pharmacodynamics
PFS	Progression free survival
PK	Pharmacokinetics
PSA-co-PCH	poly(sebaccic acid-co-1,4- cyclohexanedicarboxylic acid)
RFS	Relapse free survival
SAE	Serious adverse events
SID	Signal integrated density
T1/2	Terminal phase half-life
Tmax	Time to maximum plasma concentration
TSG	Tumor suppressor gene
TTP	Time to progression
uCK	Uridine cytidine kinase

Chapter 1

General introduction

1.1. DNA methylation – ‘A key epigenomic instructor’

‘Epigenetics’ is an emerging frontier in science, especially due to the fact that unlike genetic changes such as point mutations, gene deletions, and rearrangements which occur in DNA sequence, epigenetic changes impart temporal and spatial control on gene expression without changing the underlying DNA sequence (Melki & Clark, 2002). Thus, epigenetic marks are potentially reversible and offer increased opportunities to ameliorate the disease phenotype. The potential utility of epigenetics in cancer research has long been established, and it is being widely accepted that cancer is as much a disease of dysregulated epigenetic alterations as it is a genetic disease (Lambert & Herceg, 2008). Within cancer cells there are three fundamental epigenetic mechanisms that operate along the common pathway, associated with chromatin repression and gene silencing: DNA methylation, histone modifications, and mutations in chromatin remodeling complexes (Grant, 2009). Since five decades of discovery, DNA methylation is the most widely studied lesion of the malignant cell.

As a rule, DNA methylation occurs by covalent addition of a methyl group to the 5' carbon of the cytosine ring, resulting in 5-methylcytosine. Methylated DNA then interacts with various proteins including methyl-CpG binding domain proteins which drives the recruitment of chromatin-remodeling proteins responsible for transcriptional repression (Bogdanović & Veenstra, 2009). Modifications of core histone proteins (particularly the N-terminal ‘‘tails’’) such as acetylation and phosphorylation further play the role in recognition of chromatin by multiprotein complexes which either facilitates chromatin relaxation and genes “switched on” or chromatin compaction and genes “switched off” (Dario *et al.*, 2008).

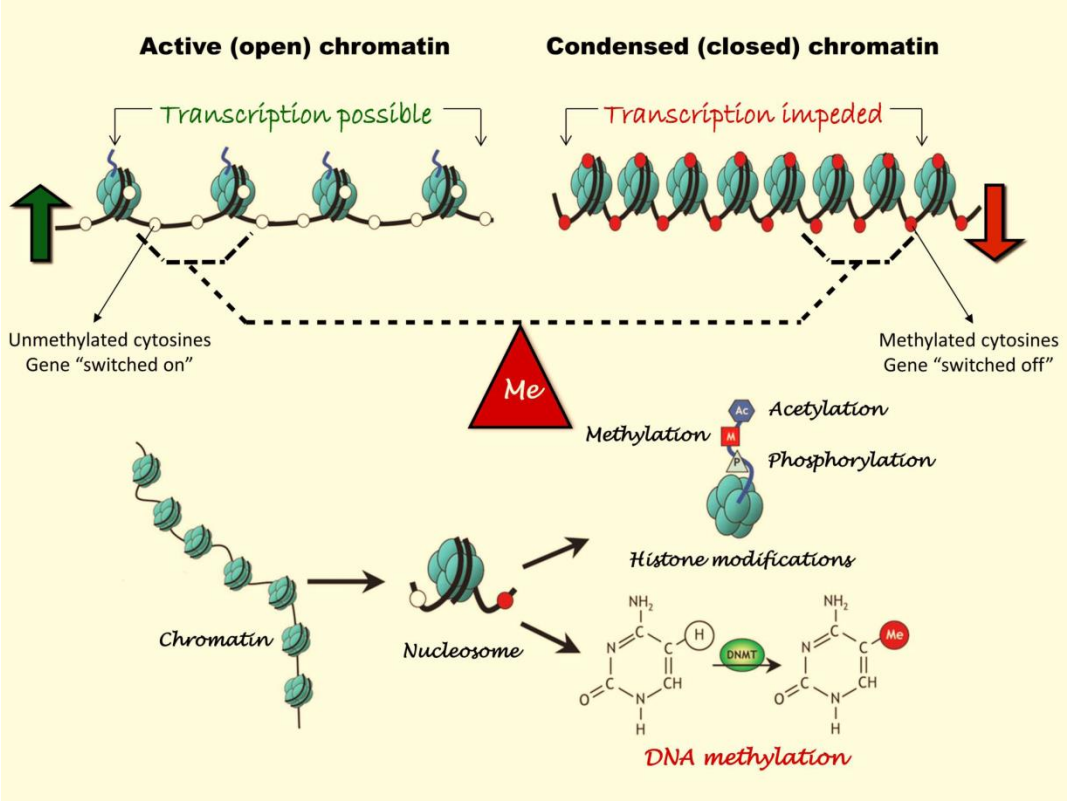

Figure 1.1 Interplay between DNA methylation, gene transcription and chromatin structure

DNA methylation is an "epigenetic switch" that regulates the balance between 'open' and 'closed' form of chromatin by changing the interactions between DNA and protein. The rate of DNA methylation is directly proportional to transcription. The increase in amount of methyl group (red circles) accompanied by modifications of core histone proteins (such as acetylation and phosphorylation) results in alteration of the chromatin structure from open to closed conformation, in which case DNA is less accessible for transcriptional machinery, and hence transcription is impeded, ultimately resulting in gene silencing. Figure is modified from Luong, P. Basic Principles of Genetics (http://cnx.org/contents/QcTHfqRM@1/Basic-Principles-of-Genetics).

1.1.1. DNA methyltransferases – regulators of DNA methylation machinery

The transfer of a methyl group from S-adenosyl-methionine that serves as a methyl donor to the cytosine residues is catalyzed by a highly conserved family of proteins, DNA methyltransferases (DNMTs). All known DNA cytosine-methyltransferases bears ten conserved sequence motifs involved in catalytic, cofactor binding, and DNA targeting functions (Bestor, 2000). In mammals, the global cytosine methylation patterns are established by the complex interplay of at least three independently

encoded DNMTs: DNMT1, DNMT3A, and DNMT3B (Robertson, 2001). The three enzymes consist of similar C-terminal catalytic region, but significantly diverge N-terminal regulatory region, consistent with their differing functions (Okano *et al*., 1998). Based on their key function, DNMTs are further classified as *de novo* methyltransferases, enzymes that are able to methylate previously unmethylated CpG sequences, and maintenance methyltransferases, which copy pre-existing methylation marks onto newly biosynthesized DNA during replication (Robertson, 2001). DNMT1, the first eukaryotic methyltransferase to be discovered is the most abundant DNMT in mammalian cells (Bestor *et al*., 1988). The enzyme has been shown to have 10-40 fold preference for hemi-methylated DNA and is referred as maintenance methyltransferase, considered to be primarily responsible for copying methylation patterns after DNA replication (Robertson *et al*., 1999), but it has also been shown to be involved in certain types of *de-novo* methylation (Vertino *et al*., 1996). In general, it has been revealed that DNMT1 is required for proper embryonic development, imprinting, and X-chromosome inactivation (Robertson, 2001). The recently discovered and characterized DNMT3 family consists of two related proteins, DNMT3A and DNMT3B. Both DNMT3 enzymes show equal affinity for hemi-methylated and unmethylated DNA substrates (Okano *et al*., 1998), and are classified as *de-novo* methyltransferases, required for genome-wide DNA methylation that occurs after embryo implantation (Okano *et al*., 1999), but DNMT3A/3B can also fill the role of a maintenance DNMT (Rhee *et al*., 2000). In general, both DNMT3A/3B are essential for early development, and the loss of either is lethal (Okano *et al*., 1999). In addition to DNMT1, DNMT3A, and DNMT3B, there are two non-canonical family members, DNMT3L and DNMT2. DNMT3L is homologus to DNMT3s but does not possess catalytic activity, however, when bound to DNMT3A/3B it significantly increases their catalytic activity, and plays an essential role in development (Gowher *et al*., 2005). DNMT2 which shares strong sequence homology with other DNMTs potentially methylate RNA instead of DNA (Jeltsch *et al*., 2006).

1.1.2. DNA methylation and cancer

During early mammalian development, normal tissue-specific DNA methylation patterns are established through the combination of demethylation and *de novo* methylation (Baylin *et al*., 2001), and these methylation patterns are maintained through subsequent cell divisions by the action of DNMTs (Holliday *et al*., 2002). Traditionally, in normal mammalian cell 70% of CpG-enriched sequences are methylated, and are established in a precise location and defined pattern. However, DNA from a malignant cell is characterized by the decrease in amounts of genomic 5-methylcytosine, accompanied by concomitant elevation of DNMTs causing localized increase in methylation of CpG

dinucleotides, near promoter and proximal coding regions of genes where transcription is initiated, and are otherwise unmethylated (Melki & Clark, 2002).

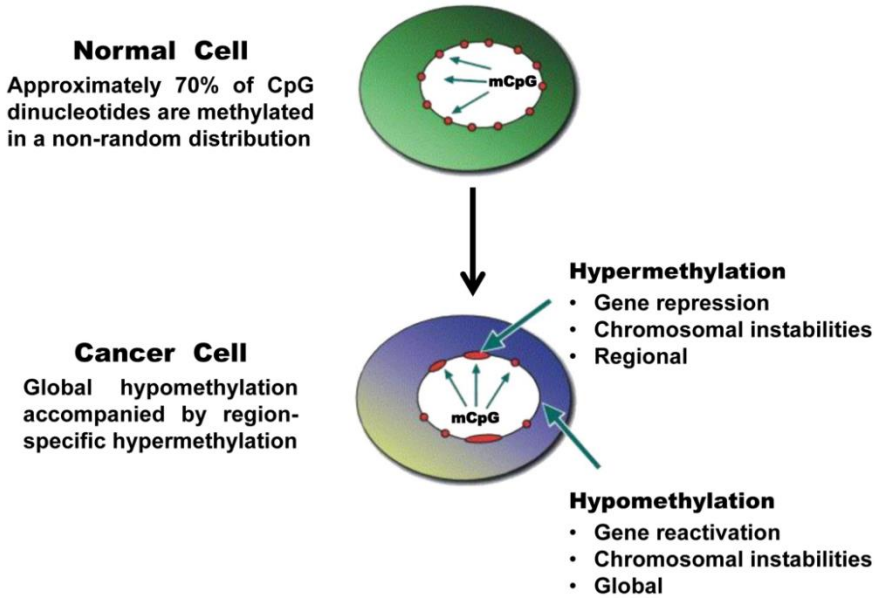

Figure 1.2 DNA methylation changes in cancer cell (Melki & Clark, 2002)

In general, modification of the epigenome due to DNA methylation, resulting in altered gene expression is categorized as hyper-methylation and hypo-methylation. DNA hyper-methylation events at CpG islands frequently demonstrate transcriptional silencing of many genes involved in cell cycle regulation, tumor cell invasion, DNA repair, and other critical growth regulators that suppress malignancy. Conversely, genome-wide hypo-methylation mediate stimulation of proto-oncogenes, eventually triggering the cancer phenotype (Melki & Clark, 2002; Agrawal *et al*., 2007).

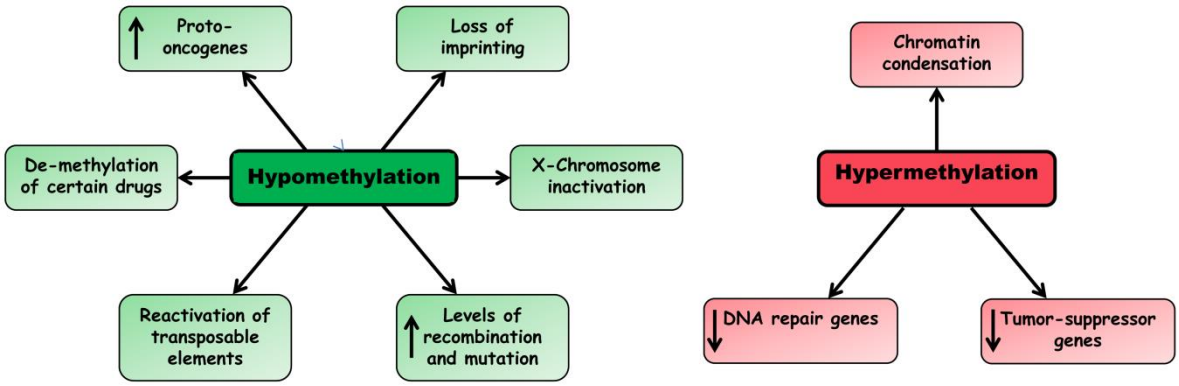

Figure 1.3 Functional outcomes of hypo-methylation and hyper-methylation (Agrawal *et al*., 2007)

1.1.3. DNA methyltransferase inhibitors – A promising anti-cancer drug class

DNA methylation-mediated epigenetic silencing of cancer-related genes has greatly emphasized on the development of anti-cancer therapies that work by inhibiting DNA methylation and restore normal epigenetic landscape by reprogramming of genes involved in disease mechanisms. The azanucleoside drugs, 5-azacytidine (azacytidine, 5-aza-CR, AZA) and 2′-deoxy-5-azacytidine (decitabine, 5-aza-CdR, DAC) are currently most advanced drugs for epigenetic cancer therapies. These prototypal drugs have long been approved by Food and Drug Administration (FDA) for the treatment of hematologic malignancies (Mack, 2010), and have also gained significant interest as priming agents for treatment of solid tumors (Cowan *et al*., 2010). Apart from these established therapies, the cohort of many DNA methylation targeting drugs are currently in clinical trial phases for a variety of cancer types, and several others in pre-clinical development. This includes nucleoside analogs which sequester DNMTs by incorporating into DNA during replication, and non-nucleoside analog classes which directly bind to the catalytic region of DNMTs and render the enzyme inactive, without covalent enzyme trapping. This Chapter extensively summarizes the far developed nucleosidic DNA methyltranferase inhibitors (DNMTIs) in various stages of pre-clinical investigation and advanced stages of clinical development, with particular emphasis on their role in epigenetic cancer therapy.

1.2. First generation FDA approved DNMTIs

The first epigenetic drugs, azacytidine and decitabine, synthesized in 1964 at Institute of Organic Chemistry and Biochemistry, Czech Academy of Sciences in Prague, and originally developed as conventional cancerostatics for use at higher doses (Sorm *et al*., 1964) were first linked with DNA methylation in 1980s when cellular differentiation induced by these azanucleosides (AZN) was associated with changes in DNA methylation (Jones & Taylor, 1980; Jones & Taylor, 1981). Consequently, the anti-tumor activity of azanucleoside analogs were determined to be due to dual mechanisms of action (i) at high doses, azacytidine induce pronounced cytotoxicity via incorporation into RNA and DNA, and decitabine inhibit cell proliferation via incorporation into DNA, and (ii) at low doses, these drugs induce DNA hypomethylation by inhibiting DNMTs, causing reactivation of silenced genes and affecting the processes of cell differentiation and tumor suppression (Gnyszka *et al*., 2013).

The molecular action of these azanucleoside drugs is completed in three main steps which include cellular uptake, intracellular metabolism, and incorporation into nucleic acids. The cellular uptake of AZN is mediated by human concentrative nucleoside transporter 1, hCNT1 (Rius *et al*.,

2009). After their cellular uptake, AZN are metabolically converted into their active forms through different metabolic pathways. This involves ATP-dependent phosphorylation of the nucleosides to the mono-phosphorylated nucleotides, catalyzed by uridine-cytidine kinase (uCK) and deoxycytidine kinase (dCK) for azacytidine and decitabine respectively (Momparler *et al*., 1979), and subsequent phosphorylation by two different kinases yielding the active metabolites 5-aza-2'-cytidine-triphosphate (5-aza-CTP) and 2'-deoxy-5-azacytidine-triphosphate (5-aza-dCTP) for azacytidine and decitabine respectively. During replication, decitabine-derived 5-aza-dCTP is incorporated into newly synthesized DNA, whereas, 80-90 % of azacytidine is incorporated into RNA as 5-aza-CTP, and only 10-20 % is incorporated into DNA after multistep conversion by the enzyme ribonucleotide reductase to 5-aza-dCTP (Li *et al*., 1970).

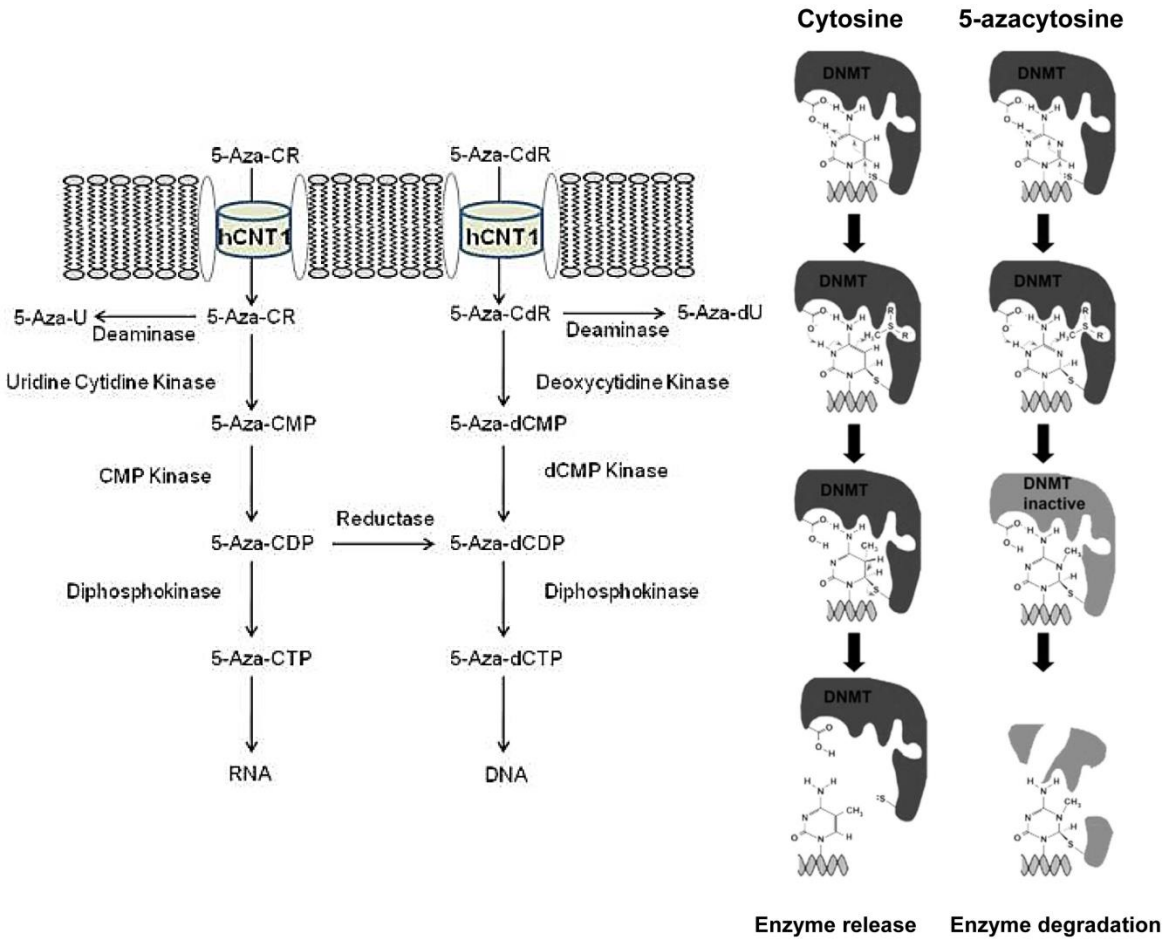

Figure 1.4 Mechanism of action of azanucleosides

After incorporation into DNA as 5-aza-dCTP, azacytosines substitute for cytosine forming azacytosine-guanine dinucleotides which are recognized by DNMTs as natural substrate (DNMT1 at low doses and DNMT3A/3B only at high doses). Consequently, the covalent bond formed between

azacytosine-containing DNA and DNMTs results in irreversible trapping of DNMTs and loss of its functionality, and eventual degradation resulting in the depletion of cellular DNMTs and loss of methylation marks during replication, ultimately leading to re-activation of silenced tumor suppressor genes (TSGs). (Stresemann & Lyko, 2008). In addition, covalent DNMT-azacytosine DNA adducts also triggers DNA damage ATM/ATR response pathways resulting in growth inhibition, G2 cell cycle arrest, and apoptosis (Palii *et al*., 2008). Besides, as azacytidine is mostly incorporated into RNA, its partial efficacy is due to RNA-dependent (cell-cycle-independent) effects. 5-aza-CTP on incorporation into RNA inhibits methylation of tRNA at DNMT2 target sites (Schaefer *et al*., 2009) and further disrupts rRNA processing ultimately leading to inhibition of protein synthesis and induction of apoptosis (Lee & Karon, 1976). Furthermore, a recent study has shown that 5-aza-CTP incorporation into RNA inhibits ribonucleotide reductase and interferes with the conversion of ribonucleotides to deoxyribonucleotides leading to inhibition of DNA synthesis and repair (Aimiuwu *et al*., 2012).

Apart from mechanism-based inhibition of DNA methylation and RNA metabolism, the azanucleoside-induced effects may also be via DNMT-independent mechanisms. AZN inhibit *NFkB* pathway through reduction of the phosphorylation of the *NFκB*-activating kinase IKKα/β (Fabre *et al*., 2008). Further, AZN have been reported to impair *de novo* synthesis of pyrimidine through inhibition of uridine monophosphate synthase (Cihák, 1974). Recently, AZN have been shown to induce specific immune responses in cancer cells (Wrangle *et al*., 2013; Li *et al*., 2014; Chiappinelli *et al*., 2015) which highlight their significance in cancer immunotherapy.

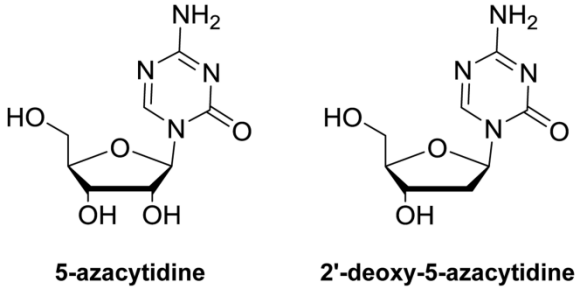

Figure 1.5 FDA approved hypomethylating agents

1.2.1. 5-azacytidine

5-Azacytidine (Azacytidine, Vidaza®, Celgene, Summit, NJ, USA) is the first hypomethylating agent to receive regulatory approval by FDA in 2004 for the treatment of myelodysplastic syndrome (MDS), following the first successful clinical trial (Silverman *et al*., 2002) which demonstrated superiority of azacytidine over best supportive care (BSC) in MDS patients, at recommended dose of 75 mg/m^2 administered over a prolonged period of 7 days in a 4-week cycle.

Presently, azacytidine has received regulatory approval for the treatment of MDS and acute myeloid leukemia (AML) with 20-30% bone marrow (BM) blasts in USA, Canada, and European Union (EU), and for the treatment of AML with > 30% BM blasts in EU and several other countries. The complete list of clinical trials (296 studies until May 2017) registered with ClinicalTrials.gov for azacytidine, as single agent therapy, and in combination with various chemotherapeutic, epigenetic or immunomodulatory agents can be found at https://clinicaltrials.gov/ct2/results?cond=&term=5azacytidine&cntry1=&state1=&SearchAll=Search+all+studies&recrs. The data presented in Table 1.1 and 1.5 summarizes 15 years of experience and outcomes in clinical trials with azacytidine as single agent (Table 1.1) or in combinatorial therapies (Table 1.5). The data collectively indicates the effectiveness of azacytidine at increasing overall survival (OS) to similar or greater extent in comparison to currently approved AML treatment but with less toxicity, and recommends the use of azacytidine in the treatment of AML, especially for elderly patients who are unfit and ineligible for intensive chemotherapy regimens. Furthermore, the ongoing and future investigations of azacytidine in combinatorial therapies may lead to better treatment outcomes in hematologic malignancies as well as in various solid tumors.

Table 1.1 Azacytidine in clinical trials

This table summarizes all registered clinical trials of azacytidine as single agent therapy for which study results have been posted or are available as publications.

Conditions	Phase	Study start, Status	Brief summary	NCT number (References)
MDS	Phase 3	2003, Completed	Randomized study of azacytidine in high-risk MDS, for determining the effectiveness of azacytidine + BSC as compared to CCR (physician choice of low-dose cytarabine + BSC, standard chemotherapy + BSC or BSC only) at (i) improving survival (ii) response (iii) effect on DOR, and (iv) TTP to AML; • **Azacytidine:** 75 mg/m^2/day, *s.c.*, daily, 1-7 d, every 4 w • **Result** [(Azacytidine vs. CCR): ORR: 51/179 (28%) vs. 21/179 (12%), DOR: 13.6 months vs. 5.2 months, TTP to AML: 20.7 months vs. 15.4 months, OS: 24.5 months vs. 15.0 months], [SAE: Azacytidine: 114/175 (65%), BSC only: 71/102 (70%), Low-dose Cytarabine: 27/44 (61%), Standard Chemotherapy: 14/19 (74%)]	NCT00071799 (Fenaux *et al*., 2009)
MDS	Phase 2	2005, Completed	Randomized study of azacytidine in MDS, for determining the safety and effectiveness of three alternative dosing regimens of azacytidine in combination with BSC; • **Regimen A:** 75 mg/m^2, *s.c.*, 1-5 d, every 4 w; **Result:** ORR: 4/50 (8%), SAE: 18/50 (36%) • **Regimen B:** 75 mg/m^2, *s.c.*, 1-5 d and 8-9 d, every 4 w; **Result:** ORR: 3/50 (6%), SAE: 27/50 (54%) • **Regimen C:** 50 mg/m^2, *s.c.*, 1-5 d and 8-12 d, every 4 w; **Result:** ORR: 4/51 (8%), SAE: 22/48 (46%)	NCT00102687
Myelofibrosis	Phase 2	2005, Completed	Non-randomized study of the safety and effectiveness of azacytidine in myelofibrosis; • **Azacytidine:** 75 mg/m^2, *s.c.*, daily, 1-7 d, every 4 w • **Result:** ORR: 8/34 (24%), SAE: 17/34 (50%)	NCT00569660
AML	Phase 2	2006, Completed	Study of azacytidine as maintenance therapy for determining the effectiveness of azacytidine, at increasing survival and decreasing the rate of leukemia relapse in older patients > 60 years with AML in CR after induction chemotherapy; • **Azacytidine:** 50 mg/m^2, *s.c.*, daily, 1-5 d, every 4 w • **Result:** DFS-1 year: 50%, OS: 20.4 months, SAE: 2/24 (8%)	NCT00387647
MDS	Phase 2	2006, Completed	Study of azacytidine for determining ORR in MDS; • **Azacytidine:** 75 mg/m^2, *i.v.*, daily, 1-5 d, every 4 w • **Result:** ORR: 6/22 (27%), DOR: 15.0 months, PFS: 11.3 months, OS: 14.8 months, SAE: 12/24 (50%)	NCT00384956
Myelofibrosis	Phase 2	2006, Terminated	Study of azacytidine in patients with myelofibrosis with myeloid metaplasia, for determining (i) safety and effectiveness of azacytidine (ii) pertinent biologic characteristics of myelofibrosis before and during azacytidine therapy (iii) effects of treatment on constitutional symptoms in these patients, and (iv) time to event distributions for OS and progression; • **Azacytidine:** 75 mg/m^2, *s.c.*, daily, 1-5 d, every 4 w • **Result:** ORR: 0/10 (0%), OS: 16.9 months, SAE: 4/10 (40%)	NCT00381693
Prolymphocytic leukemia	Phase 2	2006, Terminated	Study of the safety and effectiveness of azacytidine in fludarabine-resistant chronic lymphocytic leukemia, Richter's transformation, and T-cell-prolymphocytic leukemia; • **Azacytidine:** 75 mg/m^2, *s.c.*, daily, 1-7 d, every 3-8 w • **Result:** ORR: 0/9 (0%), SAE: 0/9 (0%)	NCT00413478 (Malik *et al*., 2013)

MDS	Phase 3	2007, Completed	Randomized study (an extension to study NCT00071799) allowing for continuation of azacytidine treatment in MDS for ethical and safety reasons until the commercial availability of the drug; • **Azacytidine:** 75 mg/m^2/day, *s.c.*, daily, 1-7 d, every 4 w • **Result:** ORR: 91/179 (51%), SAE: 20/40 (50%)	NCT01186939 (Silverman *et al*., 2011)
MDS, CMML, AML	Phase 1	2007, Completed	Non-randomized dose-escalation study of oral azacytidine in patients with MDS, CMML, and AML, for determining (i) long term safety and effectiveness (ii) PK and PD, and (iii) MTD and BED based on safety, PK, and PD data; • **Azacytidine:** 75 mg/m^2/day, *s.c.*, daily, 1-7 d, 4 w (cycle 1) followed by 120-600 mg/day, *p.o.*, daily, 1-7 d of each additional 4 w cycle • **Result:** ORR: 6/17 (35%) in previously treated and 11/15 (73%) in untreated MDS and CMML patients and no response in AML patients, PK [Tmax: 0.5 h (*s.c.*) vs. 1.0 h (*p.o.*), mean elimination half-life: 1.6 h (*s.c.*) vs. 0.62 h (*p.o.*), mean relative oral bioavailability: 6.3% to 20%], PD: Azacytidine (*s.c.*, *p.o.*) decreased DNA methylation in blood with maximum effect at day 15 of each cycle, MTD: 480 mg, SAE: ≥ 20% of patients	NCT00528983 (Garcia-Manero *et al*., 2011)
MDS	-	2008, Completed	Pilot study of pre-transplant azacytidine in patients with high-risk MDS who are candidates for allogeneic hematopoietic cell transplantation, for determining the effectiveness of azacytidine in preventing MDS relapse; • **Azacytidine:** 75 mg/m^2/day, *s.c.*, daily, 5-7 d, every 4 w • **Result:** ORR: 10/21 (48%), DFS-1 year: 52%, OS-1 year: 62%, SAE: 8/25 (32%)	NCT00660400 (Nishihori *et al*., 2014)
MDS	Phase 2	2008, Completed	Study of the feasibility and effectiveness of azacytidine as pre-transplant cytoreduction prior to allogeneic hematopoietic cell transplantation in patients with high-risk MDS; • **Azacytidine:** 75 mg/m^2, *s.c.* or *i.v.*, daily, 1-7 d • **Result:** EFS-1 year: 47%, EFS-2 year: 37%, OS-1 year: 47%, OS-2 year: 37%, SAE: 13/16 (81%)	NCT00721214
AML	Phase 2	2008, Completed	Study of the safety and effectiveness of azacytidine in elderly patients with newly diagnosed previously untreated or secondary AML who are unsuitable for intensive chemotherapy; • **Azacytidine:** 100 mg/m^2/day, *s.c.*, daily, 1-5 d, every 4 w • **Result:** CR: 8/45 (18%), DOR: 8.0 months, OS: 6.0 months, SAE: 8/45 (18%)	NCT00739388 (Passweg *et al*., 2014)
MDS, CMML, AML, Lymphoma, Multiple myeloma	Phase 1	2008, Completed	Randomized study of azacytidine in patients with MDS, CMML, AML, lymphoma, and multiple myeloma, for determining PK and safety of different *p.o.* formulations versus *s.c.* formulations; • **Study 1:** 75 mg/m^2, *s.c.*, d 1, d 15; 180 mg, *p.o.* (IRT-A, IRT-B, ECT, or 200 mg CAP), d 3; 360 mg, *p.o.* (IRT-A, IRT-B, ECT, or 400 mg CAP), d 5; individualized doses in formulation IRT-A, IRT-B, ECT or CAP, calculated to deliver 80% on d 17 and 120% on d 19 of the mean *s.c.* azacytidine exposure (AUC d 1-15), not to exceed 1200 mg • **Study 2 (Part 1):** 3 way crossover: 3 x 100 mg IRT-B tablets (under fasted conditions), d 1; 2 x 150 mg IRT-C tablets (under fasted conditions), d 2; 2 x 150 mg IRT-C tablets (under fed conditions), d 3 • **Study 2 (Part 2):** 2 x 150 mg IRT-C tablets (under fasted conditions), d 1; 40 mg omeprazole, d 2-4; 2 x 150 mg IRT-C tablets after 1 h of 40 mg omeprazole, d 5 • **Result:** Oral azacytidine is rapidly absorbed with little or no effect of food on PK parameters, and does not require dose adjustments when taking a proton-pump inhibitor such as omeprazole	NCT00761722 NCT01519011 (Laille *et al*., 2014)
MDS, AML, Solid tumors, Multiple myeloma, Non-hodgkin's lymphoma, Hodgkin's disease	Phase 1	2008, Completed	Randomized study of azacytidine in adult cancer patients with and without impaired renal function, for determining (i) if azacytidine is absorbed in the body at the same rate or proportion for different concentrations (ii) the effect of renal impairment on azacytidine PK, and (iii) safety and tolerability of azacytidine in patients with renal function impairment; • **Regimen A:** 25 mg/m^2, *s.c.*, d 1 - 75 mg/m^2, *s.c.*, daily, 1-7 d, every 4 w • **Regimen B:** 50 mg/m^2, *s.c.*, d 1 - 75 mg/m^2, *s.c.*, daily, 1-7 d, every 4 w • **Regimen C:** 75 mg/m^2, *s.c.*, d 1-5 - 75 mg/m^2, *s.c.*, daily, 1-7 d, every 4 w • **Regimen D:** 100 mg/m^2, *s.c.*, d 1 - 75 mg/m^2, *s.c.*, daily, 1-7 d, every 4 w	NCT00652626

			• **Regimen E:** 75 mg/m^2, *s.c.*, d 1-5 - 75 mg/m^2, *s.c.*, daily, 1-7 d, every 4 w; severe renal impairment • **Result** [Regimen A, B, C, D: Cmax (ng/mL): 34%, 61%, 58%, 39%, Tmax: 0.25 h, 0.25 h, 0.25 h, 0.27 h, T1/2: 1.38 h, 0.63 h, 1.19 h, 1.03 h], [Normal renal function vs. severe renal impairment: Cmax (ng/mL): 58% vs. 93% on d 1 and 46% vs. 92% on d 5, Tmax: 0.25 h vs. 0.50 h on d 1 and 0.38 h vs. 0.64 h on d 5, T1/2: 1.19 h vs. 0.97 h on d 1 and 1.03 h vs. 1.15 h on d 5], [SAE: Regimen A, B, C, D, E: 0/5 (0%), 0/5 (0%), 4/6 (67%), 1/5 (20%), 1/6 (17%)]	
AML	Phase 3	2010, Completed	Randomized study of the effectiveness of azacytidine versus CCR (physician choice of low-dose cytarabine + BSC, intensive chemotherapy + BSC or BSC only), for determining OS in older patients with newly diagnosed AML; • **Azacytidine:** 75 mg/m^2, *s.c.*, daily, 1-7 d, every 4 w • **Result** [(Azacytidine vs. CCR): ORR: 67/241 (28%) vs. 62/247 (25%), DOR: 10.4 months vs. 12.3 months, EFS: 6.7 months vs. 4.8 months, RFS: 9.3 months vs. 10.5 months, OS: 10.4 months vs. 6.5 months, OS-1year: 47% vs. 34%], [SAE: Azacytidine: 188/236 (80%), BSC only: 30/40 (75%), Low-dose Cytarabine: 118/153 (77%), Standard Chemotherapy: 27/42 (64%)]	NCT01074047 (Dombret *et al*., 2015)
MDS, AML	-	2010, Recruiting	Study of azacytidine in patients with high-risk MDS and AML with multilineage dysplasia, for characterizing (i) molecular mechanism of action and resistance to azacytidine: role of apoptosis versus autophagy, and (ii) reversion of azacytidine resistance using different drugs targeting apoptosis and/or autophagy; • **Result:** *BCL2L10* was discovered as a predictive factor for resistance to azacytidine in MDS and AML patients	NCT01210274 (Cluzeau *et al*., 2012)
MDS	Phase 4	2010, Completed	Study of the safety, effectiveness, and PK of azacytidine in adult Taiwanese patients with high-risk MDS; • **Azacytidine:** 75 mg/m^2/day, *s.c.*, daily, 1-7 d, every 4 w • **Result:** ORR: 0/44 (0%), Cmax (ng/mL): 44%, Tmax: 0.29 h, T1/2: 1.0 h, SAE: 28/44 (64%)	NCT01201811
Non-small cell lung cancer	Phase 2	2011, Active	Pilot study of azacytidine in patients with previously treated advanced non-small cell lung cancer, for determining (i) the ability of azacytidine to cause DNA hypomethylation and re-expression of silenced TSGs when stratified for high or low expression of mir29a, b, c (ii) ORR, PFS, and OS, and (iii) correlation of miRNA profiles with response to azacytidine; • **Azacytidine:** 75 mg/m^2, *s.c.*, daily, 1-7 d, every 4 w • **Result:** SAE: 1/1 (100%)	NCT01281124
CMML	Phase 2	2011, Completed	Study of the safety and effectiveness of azacytidine in CMML, for determining (i) ORR, PFS, and OS (ii) to develop biomarkers for response and gain insights into mechanisms determining response, and (iii) the gene expression and promoter methylation profiling pre- and post-azacytidine therapy; • **Azacytidine:** *s.c.* or *i.v.* 10-40 min, daily, 1-7 d • **Result:** CR: 3/11 (27%), SAE: 2/11 (18%)	NCT01350947
MDS	Phase 2	2012, Active	Study of the safety, effectiveness, and PK of azacytidine in adult Chinese patients with high-risk MDS; • **Azacytidine:** 75 mg/m^2/day, *s.c.*, daily, 1-7 d, every 4 w • **Result:** ORR: 9/72 (13%), OS: 22.0 months, Cmax (ng/mL): 31%, Tmax: 0.25 h, T1/2: 0.8 h, SAE: 38/72 (53%)	NCT01599325

1.2.2. 2'-deoxy-5-azacytidine

2'-deoxy-5-azacytidine (Decitabine, Dacogen®, MGI Pharma, Bloomington, MN, USA) is the second hypomethylating agent, to be approved by FDA in 2006 for the treatment of higher-risk MDS, after showing its clinical effectiveness over BSC in treating elderly patients with intermediate- or high-risk MDS, ineligible for intensive chemotherapy (Lübbert *et al*., 2011), at low-dose schedule of 15 mg/m^2 every 8 h for 3 days in a 6-week cycle. Later, the lower-dose regimen with higher-dose intensity of 20 mg/m^2 over 5 days in a 4-week cycle was suggested as a superior regimen (Kantarjian *et al*., 2007). Presently, decitabine has received regulatory approval for the treatment of MDS in USA and for the treatment of elderly AML in EU so far. The complete list of clinical trials (225 studies until May 2017) registered with ClinicalTrials.gov for decitabine, as single agent therapy, and in combination with various chemotherapeutic, epigenetic or immunomodulatory agents can be found at https://clinicaltrials.gov/ct2/results?cond=&term=2%27-deoxy-5-azacytidine&cntry1=&state1=&Search=Search.The data presented in Table 1.2 and 1.6 summarizes 17 years of experience and outcomes in clinical trials with decitabine as single agent (Table 1.2) or in combinatorial therapies (Table 1.6). The data collectively indicates the effectiveness of decitabine at prolonging median time to progression (TTP) to AML or death, but no improvement in OS in comparison with BSC. The inferior outcome in terms of OS might be due to higher cytotoxicity observed. Nevertheless, the ongoing and future investigations of decitabine in combinatorial therapies may lead to better treatment outcomes in hematologic malignancies as well as in various solid tumors.

Apart from beta-D-anomer of 2'-deoxy-5-azacytidine, the alpha-D-anomer of this agent was also characterized for putative anti-leukemic effects and toxicity in mouse and human leukemic cells. The results of the studies indicated lower anti-leukemic activity as well as toxicity of alpha-anomer (Veselý *et al*., 1984; Fojtova *et al*., 2007). But the efficient ability of alpha-anomer to hypomethylate genomic DNA (Fojtova *et al*., 2007; Matoušová *et al*., 2011) or induce demethylation of specific tested gene (Agrawal *et al*., 2017) at concentrations comparable to beta form, combined with low cytotoxicity (Veselý *et al*., 1984; Fojtova *et al*., 2007; Matoušová *et al*., 2011; Agrawal *et al*., 2017) indicates towards the potential use of alpha-anomer in epigenetic therapy.

Table 1.2 Decitabine in clinical trials

This table summarizes all registered clinical trials of decitabine as single agent therapy for which study results have been posted or are available as publications.

Conditions	Phase	Study start, Status	Brief summary	NCT number (References)
MDS	Phase 3	2001, Completed	Randomized study for comparing the safety and efficacy profiles of decitabine versus supportive care in adults with advanced-stage MDS; • **Decitabine:** 15 mg/m^2, *i.v.*, 3 h, every 8 h x 3 d, every 6 w • **Result:** ORR: 44/157 (28%), DOR: 9.9 months, OS: 16.6 months, SAE: > 4%	NCT00043381 (Jabbour *et al*., 2013)
MDS, CMML	Phase 2	2003, Completed	Randomized study of the safety and effectiveness of three different schedules of low-dose decitabine in MDS; • **Schedule A:** 10 mg/m^2, *i.v.*, 1 h daily, 1-10 d, every 4-8 w; **Result:** ORR: 10/17 (59%), SAE: 5/17 (29%) • **Schedule B:** 20 mg/m^2, *i.v.*, 1 h daily, 1-5 d, every 4-8 w; **Result:** ORR: 68/93 (73%), SAE: 32/93 (34%) • **Schedule C:** 20 mg/m^2, *s.c.*, twice daily, 1-5 d, every 4-8 w; **Result:** ORR: 8/14 (57%), SAE: 7/14 (50%)	NCT00067808 (Oki *et al*., 2008)
Thyroid cancer	Phase 2	2004, Completed	Study of decitabine in patients with metastatic papillary or follicular thyroid cancer unresponsive to iodine I 131 (131I), for determining (i) if decitabine can restore 131I uptake (ii) the efficacy of 131I therapy administered after restoration of 131I uptake (iii) the effect of decitabine on clinical and molecular markers of thyroid cancer cell differentiation, and (iv) the safety and tolerability of decitabine in patients undergoing thyroid hormone withdrawal-induced hypothyroidism and 131I therapy; • **Decitabine:** 6 mg/m^2, *i.v.*, 1 h, 1-5 d and 8-12 d with possible second course • **131I:** thyrotropin-alfa stimulated radioactive iodine scan on w 3 • **Result:** Restoration of 131I uptake in metastatic lesions: 0/12 (0%), SAE: 9/12 (75%)	NCT00085293
Myelofibrosis	Phase 2	2004, Active	Study of the safety and ORR of decitabine in primary and secondary myelofibrosis, and determination of (i) the epigenetic effects including methylation status and re-expression of specific target genes, and (ii) the potential utility of CD34+ as surrogate biomarker for biological activity of decitabine in myeloid metaplasia with myelofibrosis; • **Decitabine:** 0.3 mg/kg/day, *s.c.*, 1-5 d and 8-12 d, every 6 w • **Result:** ORR: 7/19 (37%), SAE: 15/21 (71%)	NCT00095784
MDS, CMML	Phase 2	2005, Terminated	Non-randomized study of the ORR of low-dose decitabine in MDS following the failure of the standard azacytidine therapy; • **Decitabine:** 20 mg/m^2, *i.v.*, 1 h daily, 1-5 d, every 4-8 w • **Result:** CR: 3/16 (19%), SAE: 6/16 (38%)	NCT00113321
AML	Phase 2	2005, Completed	Non-randomized study of decitabine for determining the rate of CR and OS in older patients with AML; • **Decitabine:** 20 mg/m^2, *i.v.*, daily, 1-5 d, every 4 w • **Result:** CR: 13/55 (24%), SAE: 40/55 (73%)	NCT00358644
AML, MDS	Phase 1	2005, Completed	Non-randomized PK study of decitabine in AML or MDS; • **Decitabine:** 15 mg/m^2, *i.v.*, 3 h, every 8 h x 3 d • **Result:** Cmax (ng/mL): 73.8 (d 1), 64.8 (d 2), 77.0 (d 3), Tmax: 2.49 h (d 1), 2.53 h (d 2), 2.29 (d 3), SAE: 9/16 (56%)	NCT01378416
MDS	Phase 2	2005,	Non-randomized study of the ORR of decitabine in adults with advanced-stage MDS;	NCT00260065

		Completed	• **Decitabine:** 20 mg/m^2, *i.v.*, daily, 1-5 d, every 4 w • **Result:** ORR: 33/99 (33%), SAE: 65/99 (66%)	(Jabbour *et al*., 2013)
AML, MDS	Phase 2	2005, Completed	Randomized study of decitabine in AML or MDS (i) to generate additional information about the overall safety profile (ii) safety information of hepatically or renally impaired patients, and patients taking concomitant medications and/or therapies without trial restrictions; • **Decitabine:** 20 mg/m², *i.v.*, 1 h daily, 1-5 d, every 4 w • **Result:** Patients with adverse events: 10/10 (100%), SAE: 6/10 (60%)	NCT00760084
AML	Phase 3	2005, Completed	Randomized study of decitabine versus supportive care or low-dose cytarabine for comparing the treatment results in older patients with newly diagnosed *de novo* or secondary AML; • **Decitabine:** 20 mg/m^2, *i.v.*, 1 h daily, 1-5 d, every 4 w • **Result** (decitabine vs. cytarabine or supportive care): OS: 7.7 months vs. 5 months, SAE: 190/238 (80%) vs. 162/237 (68%)	NCT00260832 (Mayer *et al*., 2014)
AML	Phase 2/3	2006, Completed	Randomized study of decitabine as maintenance therapy for adults with unfavorable risk AML in first CR or with relapsed AML in second CR; • **Decitabine:** 20 mg/m^2, *i.v.*, 1 h daily, 1-5 d, every 4-8 w • **Result:** DFS-1 year: 50%, SAE: 1/20 (5%)	NCT00398983
AML	Phase 2	2006, Active	Study of decitabine as maintenance therapy after standard therapy (chemotherapy: busulfan, cytarabine, daunorubicin hydrochloride, etoposide; bone marrow transplantation; allogeneic hematopoietic cell transplantation) in treating younger patients < 60 years with previously untreated AML, for determining (i) efficacy, feasibility, and toxicities (ii) 1-year DFS rate (iii) biologic response to decitabine (iv) DNA demethylation, down-regulation of DNMT1, and gene re-expression; • **Decitabine:** 20 mg/m^2, *i.v.*, 1 h daily, 1-5 d, every 6 w • **Result:** DFS-1 year: 80%, SAE: 0/132 (0%)	NCT00416598 (Blum *et al*., 2017)
AML	Phase 2	2007, Completed	Study determining (i) the rate of CR (ii) rate of OS at 1-year (iii) ORR, and (iv) pharmacological and biological correlative studies of decitabine with clinical endpoints and/or response in patients with previously untreated AML; • **Decitabine:** 20 mg/m^2/day, *i.v.*, 1 h daily, 1-10 d, every 4 w • **Result:** CR: 25/55 (45%), SAE: 0/53 (0%)	NCT00492401 (Blum *et al*., 2010)
AML	Phase 1	2007, Completed	Non-randomized study of the feasibility, safety, and biologic activity of epigenetic priming with decitabine prior to standard cytarabine, daunorubicin (7+3) induction chemotherapy in younger patients with less-than-favorable risk AML, for determining (i) the appropriate dose level (ii) safety and expected toxicities (iii) optimal dose schedule of decitabine, and (iv) molecular and cellular consequences of decitabine-induced hypomethylation; • **Decitabine:** 20 mg/m^2/day, *i.v.*, 1 h (Arm A) or 24 h (Arm B), 1-3/5/7 d • **Result:** ORR: 25/30 (83%), toxicity similar to standard induction chemotherapy	NCT00538876 (Scandura *et al*., 2011)
Myelofibrosis	Phase 2	2008, Terminated	Study of the safety and effectiveness of low-dose decitabine in patients with symptomatic primary myelofibrosis (PMF) or post essential thrombocythemic (ET) or polycythemic vera (PV) MF, and analysis of the ability of decitabine at decreasing pathologic angiogenesis and other stromal reactive features intrinsic to PMF or post ET/PV MF; • **Decitabine:** 20 mg/m^2/day, *i.v.*, 1 h daily, 1-5 d, every 4 w • **Result:** ORR: 1/4 (25%), SAE: 1/4 (25%)	NCT00630994
MDS	Phase 2	2008, Completed	Randomized study of the safety and effectiveness of two different schedules of low-dose decitabine in adults with low or intermediate-1 risk MDS; • **Schedule A:** 20 mg/m^2/day, *s.c.*, daily, 1-3 d, every 4 w; **Result:** ORR: 10/43 (23%), SAE: 18/43 (42%) • **Schedule B:** 20 mg/m^2/day, *s.c.*, d 1, d 8, d 15, every 4 w; **Result:** ORR: 5/22 (23%), SAE: 10/22 (45%)	NCT00619099 (Garcia-Manero *et al*., 2013)
MDS	Phase 1	2008, Completed	Non-randomized study of decitabine for determining the recommended dose level, safety and effectiveness in MDS; • **Dose A:** 15 mg/m^2, *i.v.*, 1 h daily, 1-5 d, every 4 w; **Result:** ORR: 2/3 (67%), Cmax (ng/mL): 151.7 (d 1), 142 (d 5), SAE: 1/3 (33%)	NCT00796003 (Oki *et al*., 2012)

			• **Dose B:** 20 mg/m^2, *i.v.*, 1 h daily, 1-5 d, every 4 w; **Result:** ORR: 3/6 (50%), Cmax (ng/mL): 166.4 (d 1), 190.6 (d 5), SAE: 1/6 (17%)	
MDS	Phase 2	2008, Completed	Study of the safety and ORR of decitabine in previously treated and untreated Taiwanese patients with MDS; • **Decitabine:** 20 mg/m^2, *i.v.*, 1 h daily, 1-5 d, every 4 w • **Result:** ORR: 8/34 (24%), OS: 22.8 months, SAE: 28/37 (76%)	NCT00744757
CMML	Phase 2	2008, Completed	Study of the therapeutic efficacy of decitabine in patients with previously treated or untreated CMML; • **Decitabine:** 20 mg/m^2/day, *i.v.*, 1 h daily, 1-5 d, every 4-7 w • **Result:** ORR: 15/39 (38%), OS-2 year: 48%	NCT01098084 (Braun *et al*., 2011)
MDS	Phase 4	2008, Completed	Study of the safety and effectiveness of decitabine in MDS; • **Decitabine:** 20 mg/m^2, *i.v.*, daily, 1-5 d, every 4 w • **Result:** ORR: 56/101 (55%), DOR: 13.2 months, OS: 17.7 months	NCT01041846 (Lee *et al*., 2011)
MDS	Phase 4	2009, Terminated	Randomized study for demonstrating the effectiveness and safety of decitabine over azacytidine in patients with intermediate or high-risk MDS; • **Decitabine:** 20 mg/m^2/day, *i.v.*, daily, 1-5 d, every 4 w • **Azacytidine:** 75 mg/m^2/day, *s.c.*, daily, 1-7 d, every 4 w • **Result** (Decitabine vs. Azacytidine): ORR: 1/11 (9%) vs. 1/12 (8%), SAE: 7/13 (54%) vs. 7/13 (54%)	NCT01011283
MDS	Phase 3	2009, Completed	Randomized study of the safety and effectiveness of two different schedules of low-dose decitabine in MDS; • **Schedule A:** 15 mg/m^2, *i.v.*, 3 h, every 8 h x 3 d, every 6 w • **Result:** ORR: 10/34 (29%), OS-6 and 12 months: 91% and 76%, SAE: 8/34 (24%) • **Schedule B:** 20 mg/m^2, *i.v.*, 1 h daily, 1-5 d, every 4 w • **Result:** ORR: 25/98 (26%), OS-6 and 12 months: 85% and 66%, SAE: 26/98 (27%)	NCT01751867 (Wu *et al*., 2015)
MDS	Phase 1/2	2010, Completed	Study of decitabine as differentiation therapy in MDS, for demonstrating (i) the effectiveness of DNMT1 depleting but non-DNA damaging doses of decitabine (ii) the safety of the regimen (iii) response by aberrant methylation signature (iv) correlation of DNMT1 depletion, cytogenetic and methylome profile, and CDA genotype and expression with clinical response criteria; • **Induction phase:** 0.2 mg/kg/day, *s.c.*, twice weekly for 4 w or thrice weekly until achieving bone marrow blasts < 5% • **Maintenance phase:** 0.2 mg/kg/day, *s.c.*, twice weekly for up to 52 w in the absence of disease progression or unacceptable toxicity • **Result:** CR: 4/25 (16%), SAE: 12/25 (48%)	NCT01165996 (Saunthararajah *et al*., 2015)
MDS, AML	Phase 1	2011, Active	Dose-escalation study of decitabine as maintenance therapy in patients with higher-risk MDS and MDS/AML receiving allogeneic stem cell transplantation; • **Decitabine:** 5-15 mg/kg/day, *i.v.*, 1 h daily, 1-5 d, every 4 w • **Result:** Median maintenance dose: 7 mg/m^2/day	NCT01277484 (Han *et al*., 2015)
MDS	-	2012, Completed	Study determining the prognostic impact of mutations in spliceosome machinery genes (*SRSF2*, *U2AF1*, and *ZRSR2*) on the outcomes of 1st line decitabine treatment in MDS; • **Result** (Spliceosome wild-type group vs. mutated group): ORR: 43% vs. 47%, OS: 22.0 months vs.15.9 months	NCT02060409 (Hong *et al*., 2015)
AML, MDS	Phase 2	2013, Recruiting	Study determining the potential genetic markers of decitabine response in patients with AML or MDS; • **Decitabine:** 20 mg/m^2, *i.v.*, 1 h daily, 1-10 d, every 4 w • **Result:** ORR (unfavorable-risk vs. favorable-risk cytogenetic profile): 29/43 (67%) vs. 24/71 (34%), ORR (TP53 mutations vs. wild-type TP53): 21/21 (100%) vs. 32/78 (41%)	NCT01687400 (Welch *et al*., 2016)

1.3. First generation nucleosidic DNMTIs in pre-clinical or clinical development

The first nucleosidic modulators of DNMTs, azacytidine and decitabine are undeniably the most effective hypomethylating drugs with exceptional epigenetic modulatory effects, and substantial anti-proliferative activity. On the other hand, apart from these prototypal drugs, various other nucleoside analogs that work by a similar mechanism, targeting DNMTs have shown promising DNA hypomethylation activity during pre-clinical studies or have entered into clinical trials. These include cytosine analogs with modification at 5 C position of the pyrimidine ring: pseudoisocytidine, 5-fluoro-2'-deoxycytidine, 5,6-dihydro-5-azacytidine, fazarabine, 2′-deoxy-5,6-dihydro-5-azacytidine, and 5-aza-4'-thio-2'-deoxycytidine, as well as other molecular variations which do not incorporate 5 C modification of the pyrimidine ring: zebularine, 6-thioguanine, and 4′-thio-2′-deoxycytidine (Fig.1.6, Table 1.3).

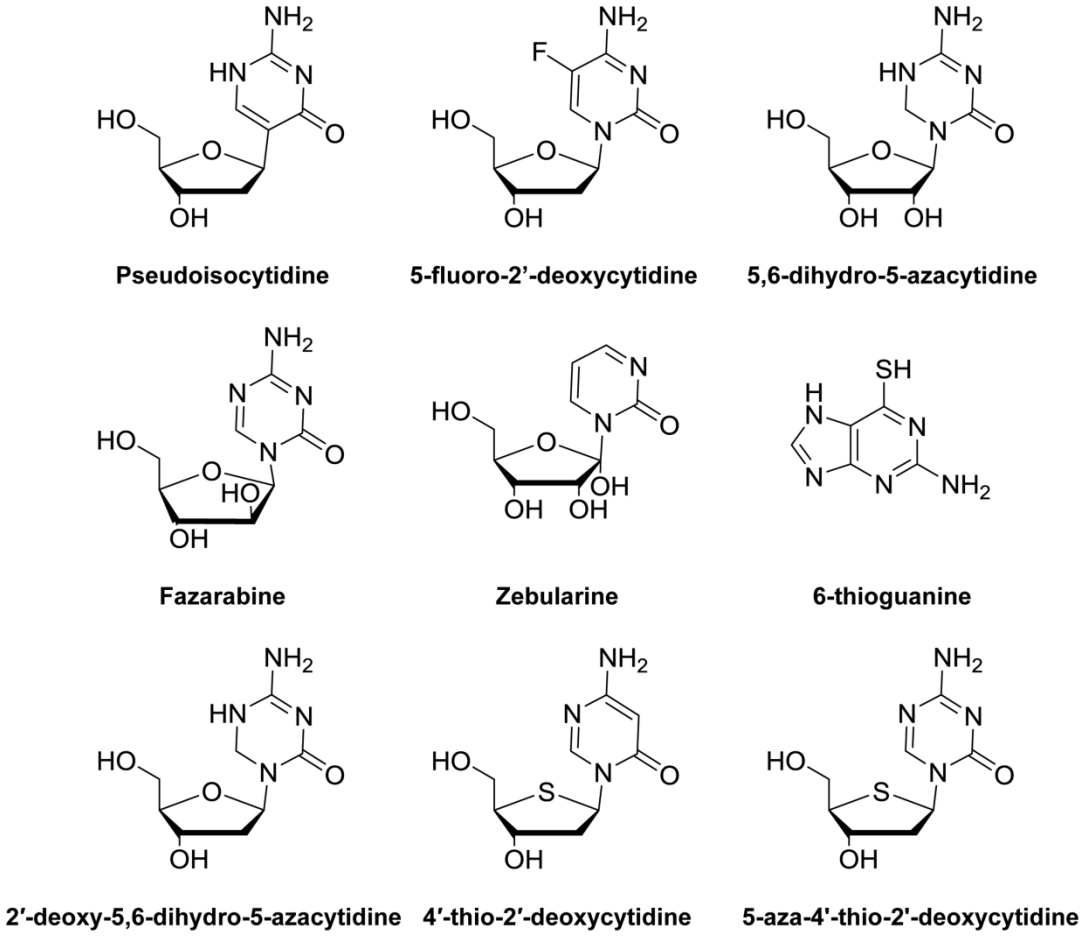

Figure 1.6 First generation nucleosidic DNMTIs in developmental stage

1.3.1. Pseudoisocytidine

Pseudoisocytidine or 2-amino-5-β-D-ribofuranosylpyrimidin-4(1H)-one (ψ ICyd), an isostere of cytidine and 5-aza-CR is a synthetic pyrimidine C-nucleoside with hydrolytically stable ring structure (Fig.1.6). The exceptional stability of ψ ICyd (stable at pH 7.4 for 6 days at 22°C and for at least 3 days at 37° C) may be due to substitution of C-N glycosyl linkage with C-C bond between C-1 of the β-D-ribofuranose moiety and C-5 of the aglycon (Chu *et al*., 1975). The mechanism of action is similar to 5-aza-CR, however, ψ ICyd has been reported to be comparatively less cytotoxic (Burchenal *et al*., 1976). Also, ψ ICyd is resistant to enzymatic deamination by cytidine deaminase (CDA), in comparison with 5-aza-CR and 1-beta-D-arabinofuranosylcytosine (Woodcock *et al*., 1980), and was recently discovered as inhibitor of CDA (Costanzi *et al*., 2011). The low cytotoxicity combined with stability against both enzymatic and chemical catabolism supported biological evaluation of ψ ICyd, *in vitro* and *in vivo*. The study conducted in human and mouse leukemic cell lines demonstrated equal or significantly higher anti-leukemic effects of ψ ICyd, compared to 5-aza-CR. Remarkably, ψ ICyd showed no cross-resistance to cytosine arabinoside or cytarabine (Ara-C), but exhibited strong inhibitory effects in Ara-C resistant mouse leukemias, in contrast to 5-aza-CR. Further, the *in vivo* anti-leukemic activity of *i.p.* or *p.o.* administered ψ ICyd was also proven to be equal or better than comparatively toxic doses of 5-aza-CR (Burchenal *et al*., 1976). Apart from interesting anti-leukemic activity, ψ ICyd displayed effective DNA demethylation activity and perturbed the cellular differentiated state (Jones & Taylor, 1980). The encouraging pre-clinical results indicated towards clinical evaluation of ψ ICyd, especially in AML patients resistant to Ara-C. Unfortunately, the phase 1 clinical evaluation of ψ ICyd was precluded due to dose limiting accumulative hepatotoxicity (Woodcock *et al*., 1980).

1.3.2. 5-fluoro-2'deoxycytidine

5-fluoro-2'-deoxycytidine (FdCyd) is a chemically stable fluoro-pyrimidine analog, currently undergoing phase 1/2 clinical trial in combination with the CDA inhibitor, tetrahydrouridine (THU). Structurally, FdCyd bears a chemical modification at position 5 of the pyrimidine ring, where fluorine replaces hydrogen, fig.1.6 (Wempen *et al*., 1961). The mechanism of action of FdCyd involves deamination by CDA to 5-fluoro-2'-deoxyuridine (FdUrd), phosphorylation by thymidine kinase to 5-fluoro-2'-deoxyuridine monophosphate, and subsequent inhibition of deoxythymidine monophosphate (dTMP) synthetase. The inhibition of dTMP synthetase results in the decreased production of dTMP which in turn leads to depletion of

thymidine triphosphate, and inhibition of DNA synthesis and cell division (Newman & Santi, 1982). The tumor inhibitory activity of FdCyd was first reported by an *in vitro* study which evidenced complete growth inhibition of human cervical cancer cells in culture (Eidinoff *et al*., 1959). In addition to its function as a prodrug for FdUrd, the specific mechanism of action of FdCyd involves inhibition of DNMT after incorporation into DNA as FdCyd triphosphate. The hypomethylation potential of FdCyd was confirmed by its ability to inhibit DNA methylation and induce muscle formation in cultured mouse embryo cells (Jones & Taylor, 1980). However, DNMT inhibitory properties of FdCyd are limited due to CDA mediated rapid conversion of FdCyd *in vivo* to pharmacologically active, yet unwanted metabolites, FdUrd, 5-fluorouracil (FU), and 5-fluorouridine (FUrd) which do not inhibit DNMT. In this context, a pre-clinical study characterizing the pharmacokinetics (PK) and metabolism of FdCyd in mice demonstrated that co-administration of FdCyd + THU significantly reduced the first pass effect of CDA on FdCyd, evidenced by increased exposure to FdCyd and decreased exposure to its metabolites (Beumer *et al*., 2006). Similar PK study conducted in cynomolgus monkeys and humans proved that co-administration of FdCyd + THU resulted in increased exposure to FdCyd and improved oral bioavailability (Holleran *et al*., 2015). Consequently, it was proposed that the degradation of FdCyd to inactive metabolites can be inhibited by combining with CDA inhibitor, THU, without inhibiting its activation by dCK. Sequentially conducted clinical studies in patients, simultaneously treated with FdCyd and THU further showed that following co-administration of FdCyd + THU, the plasma concentrations of FdCyd required for *in vitro* inhibition of DNA methylation was achieved, and accompanying plasma concentration of unwanted metabolites, FdUrd and FU was diminished. This resulted in less cytotoxic side effects and increased hypomethylation efficacy (Beumer *et al*., 2008). Apparently, studies were conducted in various cancer cell lines, to investigate the ability of FdCyd (i) to induce demethylation and cause re-expression of hypermethylation-silenced genes (ii) the association between hypomethylation activity and cellular biological activities, and (iii) the underlining molecular mechanism behind cytotoxicity. The study conducted in *MAGE-1* negative melanoma cell line demonstrated that FdCyd treatment resulted in decreased methylation of CpG sites in the *MAGE-1* promoter region, induced the expression of *MAGE-1* mRNA, and increased *MAGE-1* protein in a dose- and time-dependent manner (Hou & Newman, 2005). The demethylation effect of FdCyd was also proven by another study conducted in breast cancer cells, where, FdCyd treatment resulted in decreased methylation and increased mRNA expression of various originally silenced TSGs, specifically *TWIST1*, in a dose- and time-dependent manner (Li *et al*., 2006). However, no correlation was found between cytotoxic activity and hypomethylation activity of FdCyd, studied in several

human cancer cell lines, although incorporation of FdCyd into DNA was evidenced (Liu *et al*., 2009). Instead, a study conducted in FdCyd sensitive colon cancer cells showed that inhibition of cell proliferation by FdCyd which arrested cells in G2/M phase was mediated by activation of DNA damage response pathway (Zhao *et al*., 2012). Recently, an extensive study was conducted *in vitro* and *in vivo* to investigate the combination of FdCyd + THU as a demethylation regimen in tumor cells. The results of the study showed that continuous exposure to the combination of FdCyd + THU modified tumor cell growth by inhibiting DNMT1, and decreased long interspersed nuclear elements 1 (LINE1) promoter methylation in bladder cancer cells. DNMT1 and LINE1 methylation changes in tumor cells isolated from patients with FdCyd + THU treatment protocol, enrolled in a Phase 1 clinical trial further confirmed the mechanism of this combination regimen (Kinders *et al*., 2011). Besides, the study also showed the upregulation of *p16* expression in bladder cancer, following treatment with FdCyd + THU. Importantly, an immunofluorescence assay for *p16* expression in circulating tumor cells (CTCs) was developed and implemented in phase 1 trial. Determination of DNMT1 and LINE1 methylation in tumor biopsies, and *p16* expression in CTCs will also be included in phase 2 trial of this regimen (Kinders *et al*., 2011). The first-in-human phase 1 trial of FdCyd was conducted in patients with advanced solid tumors, to establish the best dose of FdCyd which can be combined with THU, and to determine the side effects of the combination. The maximum tolerated dose (MTD) of the combination was established at 134 mg/m^2 FdCyd + 350 mg/m^2 THU, 1-5 and 8-12 days, every 4 weeks, with the recommended phase 2 dose of 100 mg/m^2/day FdCyd + 350 mg/m^2/day THU (Newman *et al*., 2015). Recently, in an attempt to develop pre-clinical drug development pipeline to reduce the attrition of drugs in clinical trials, the combination of FdCyd + THU was tested in pediatric brain tumor models. The results of the study revealed that despite potent *in vitro* activity and *in vivo* PK properties, FdCyd showed no significant *in vivo* therapeutic response, and therefore was deprioritized for the treatment of pediatric brain tumors in clinic (Morfouace *et al*., 2016).

1.3.3. 5,6-dihydro-5-azacytidine

5,6-dihydro-5-azacytidine (DHAC) is a reduced analog of 5-aza-CR that surpasses the disadvantage of hydrolytic instability due to saturated 5,6-double bond, fig.1.6 (Beisler *et al*., 1977), and facilitates prolonged *i.v.* infusion, potentially avoiding acute toxicities associated with bolus administration of 5-aza-CR (Curt *et al*., 1985). The mechanism of action is similar to the parent drug that involves phosphorylation by uCK and incorporation into nucleic acids, resulting in inhibition of RNA synthesis and DNA methylation (Avramis *et al*., 1989). The therapeutic

potential of DHAC has been mainly characterized in lymphoid and leukemic cell lines. The studies demonstrated the defined effects of DHAC on cell survival and cell cycle kinetics (Traganos *et al*., 1981), and inhibition of DNA methylation (Avramis *et al*., 1989; Antonsson *et al*., 1987; Kees *et al*., 1995) resulting in induced dCK re-expression (Antonsson *et al*., 1987). The hypomethylation activity of DHAC was further confirmed *in vivo*, where *i.p.* administered DHAC significantly reduced DNA methylation levels in xenografted mouse model of leukemic cells. In addition, the hypomethylation level correlated with dCK expression in these cells (Powell *et al*., 1988). But, the comparative studies of the parent drug, 5-aza-CR and DHAC established lower hypomethylation activity (Jones & Taylor, 1980; Matoušová *et al*., 2011), as well as less potency of DHAC as cytotoxic agent, and requirement of 10-fold higher drug concentration to achieve similar growth inhibitory activity as the parent drug (Voytek *et al*., 1977). The lower potency of the reduced analog may be due to its greater affinity towards CDA causing rapid deamination at lower therapeutic concentrations, and consequently inefficient conversion to active metabolite, 5-aza-dCTP resulting in poor DNA incorporation (Futterman *et al*., 1978). However, the advantage of increased stability in aqueous solution over a wide range of pH necessitated clinical investigation of DHAC. During the phase 1 study, MTD was attained at 7 g/m^2 of DHAC, administered as a 24 h constant *i.v.* infusion, every 4 weeks, demonstrating pleuritic chest pain as the dose limiting toxicity. Other toxicities included nausea and vomiting with no evidence for myelosuppression, nephrotoxicity or hepatotoxicity. Transient disease responses were observed in two patients with aggressive lymphoma, and one patient with progressive Hodgkin's lymphoma showed disease stabilization for 7 treatment cycles (Curt *et al*., 1985). Subsequently, phase 2 trials were conducted in extensive, untreated non-small cell lung cancer, pleural malignant mesothelioma, and disseminated malignant melanoma. However, low response rate during initial clinical trials, accompanied by cardiac toxicity ceased further development of DHAC (Holoye *et al*., 1987; Dhingra *et al*., 1991; Creagan *et al*., 1993; Yogelzang *et al*., 1997). Nevertheless, definite antitumor activity in chemo-refractory malignant mesothelioma (Yogelzang *et al*., 1997), and meaningful regressions in disseminated malignant melanoma (Creagan *et al*., 1993), combined with modest hematologic toxicity profile favors the use of DHAC with other agents, and warrants further trials testing synergistic combination regimens. But caution regarding cardiac arrhythmias and pericardial effusion is essential. Recently, the studies conducted in estrogen- and androgen-refractory, breast and prostate cancers respectively evidenced the effectiveness of DHAC to restore estrogen and androgen sensitivity. This suggests the clinical application of DHAC in treatment of hormone-refractory breast and prostate cancer patients by

re-sensitizing them to conventional therapies with estrogen and androgen antagonists (Izbicka *et al*., 1999a; Izbicka *et al*., 1999b).

1.3.4. Fazarabine

Fazarabine also known as Kymarabine or 1-β-D-arabinofuranosyl-5-azacytosine (Ara-AC) is a pyrimidine analog, synthesized by combining the structural features of cytotoxic nucleosides, Ara-C and 5-aza-CR. Structurally, Ara-AC bears stereochemical inversion of hydroxyl group at the 2' position of cytidine, analogus to Ara-C, and bioisosteric replacement of carbon-5 with nitrogen in the pyrimidine base, analogus to 5-aza-CR, fig.1.6 (Beisler *et al*., 1979). Similar in mechanism of action to Ara-C, Ara-AC is phosphorylated by dCK to triphosphate form which incorporates into DNA in place of thymidine, and exerts its anti-neoplastic effect by causing DNA hypomethylation, and direct cytotoxicity by inhibiting DNA synthesis (Barchi *et al*., 1996). A study investigating the mechanisms of native and acquired resistance to Ara-AC further showed dCK as the important determinant for tumor sensitivity to this drug. It was shown that leukemic and solid tumor cell lines exhibiting resistance towards Ara-C due to marked decrease in dCK level, also showed cross-resistance towards Ara-AC. But, Ara-AC is protected from deamination by CDA, unlike Ara-C (Ahluwalia *et al*., 1986). During pre-clinical evaluations, Ara-AC showed cytocidal activity against human colon cancer cells *in vitro* by inhibition of DNA synthesis (Glazer & Knode, 1984), and *in vivo* Ara-AC demonstrated marked anti-tumor activity in wide spectrum of murine leukemias and solid tumors, and human tumor xenografts of National Cancer Institute (NCI) tumor panel. The studies also demonstrated the equal effectivity of Ara-AC by the *p.o.* route, compared with *i.p.* administration (Veselý & Pískala, 1986; Dalai *et al*., 1986; Wallace *et al*., 1989). Further, an *in vitro* study conducted in Ara-C sensitive and resistant human leukemia cell lines confirmed the DNA hypomethylation potency of Ara-AC (Kees & Avramis, 1995). Consequently, several phase 1 studies were conducted in past decades, in cases of both, children and adult with refractory or solid tumor malignancies. The studies aimed to determine the toxicity, MTD, and therapeutic efficacy for low-dose 72 h continuous *i.v.* infusions, as well as for high dose short infusions, using a daily bolus administration for 5 days. In both schedules, predominant dose limiting toxicities (DLT) observed was myelosuppression including reversible granulocytopenia and thrombocytopenia. Other toxicities observed were moderate nausea and vomiting which did not appear to be dose dependent. A rare case of one patient with stable disease for 65 days was noted (Heideman *et al*., 1989; Surbone *et al*., 1990; Bailey *et al*., 1991; Amato *et al*., 1992; Bernstein *et al*., 1993; Goldberg *et al*., 1997; Wilhelm *et al*., 1999). After promising pre-clinical activity and reasonable

toxicity in phase 1 clinical trials, several phase 2 studies of Ara-AC were also published in solid tumors. Using the continuous *i.v.* infusions for 3 days, no major clinical responses were observed in advanced colorectal and pancreatic adenocarcinoma, metastatic breast and colon cancer, and advanced non-small cell lung carcinoma (Hubbard *et al*., 1992; Casper *et al*., 1992; Walters *et al*., 1992; Ben-Baruch *et al*., 1993; Williamson *et al*., 1995). The studies employing the bolus regimens for five days in advanced head and neck cancer, high grade gliomas, advanced squamous cell carcinoma of the cervix, and ovarian cancer also reported unsatisfactory results (Kuebler *et al*., 1991; Selby *et al*., 1994; Manetta *et al*., 1995a; Manetta *et al*., 1995b). No significant activity of this drug in various phase 2 clinical trials blocked further investigation.

1.3.5. Zebularine

Zebularine or 1-(β-D-ribofuranosyl)-1,2 dihydropyrimidin-2-one (Zeb) is a mechanism based inhibitor of DNA methylation, without apparent modification at position 5 of the pyrimidine ring. Structurally, Zeb is a cytidine analog containing 2-(1H)-pyrimidinone ring which lacks exocyclic amino group at position 4 of the ring, originally designed as the potent inhibitor of CDA, fig.1.6 (Kim *et al*., 1986). In addition to concomitant CDA inhibitory activity, Zeb has also been reported to induce selective inhibition of DNMTs. Its mechanism of action is similar to AZN analogs, and involves incorporation into DNA, and subsequent formation of covalent adduct with DNMTs at position 6 of the pyrimidinone ring, resulting in proteasomal-mediated enzyme degradation (Zhou *et al*., 2002). Further, Zeb features a remarkable property of being preferentially selective towards the tumor cells, in terms of incorporation into DNA, cell growth inhibition, demethylation, and depletion of DNMTs, suggesting minimal toxicity (Cheng *et al*., 2004b; Tan *et al*., 2013). Furthermore, unlike AZN drugs Zeb is chemically stable in aqueous solution which enables its oral administration (Holleran *et al*., 2005). Also, due to low toxicity Zeb can be used for long term treatment with minimal side effects (Yoo *et al*., 2008). Thus, favorable pharmacological properties of Zeb, stability combined with minimal toxicity allows for continuous treatment. This sustains demethylation effects for prolonged periods and prevents gene re-silencing, demonstrated by induction and maintenance of *p16* expression, global demethylation, and complete depletion of DNMT1 following Zeb treatment in bladder cancer cells (Cheng *et al*., 2004a). During pre-clinical studies, the hypomethylation and anti-tumor activity of Zeb was evaluated in wide range of cancer cell lines, including myeloid malignancies and selected solid tumors. The studies demonstrated the potential role of Zeb as demethylating agent in epigenetic therapy, as well as via cell cycle arrest and induction of apoptosis by various other pathways independent of DNA methylation. The first study characterizing Zeb as a

demethylating agent reported slight cytotoxicity and demethylation-mediated reactivation of silenced *p16* gene in bladder cancer cells, *in vitro*. Also, Zeb administered *i.p.* or *p.o.* induced *p16* re-expression and significantly reduced tumor volume in *in vivo* established human bladder cancer xenografts (Cheng *et al*., 2003). The study designed in radiation-induced T-cell lymphoma mouse model showed the positive effects of *i.p.* administered Zeb with minimal toxicity against the development of thymic lymphoma, evidenced by longer OS, and accompanied therapeutic changes including global genomic hypomethylation, DNMT1 depletion, and demethylation-induced re-expression of *p16INK4a*, *MGMT*, *MLT-1*, and *E-cadherin* genes (Herranz *et al*., 2006). The study in AML cell lines and primary patient samples demonstrated demethylation and dose-dependent increase in *p15INK4B* expression, along with inhibition of cell proliferation, blockade in G2/M phase, and induction of apoptosis (Scott *et al*., 2007). Another study using human promyelocytic leukemia cell lines again reported decreased DNMT1 expression, time-dependent expression of *pan-cadherin* and partial demethylation of *E-cadherin*, together with dose- and time-dependent cell growth inhibition, dose-dependent apoptosis manifested by procaspase-3 and PAR-1 cleavage, and onset of early apoptosis (Savickiene *et al*., 2012b). Yet, another study in p53 mutant leukemic T cells reported caspase-mediated apoptosis induction and activation of intrinsic apoptotic pathway by inducing mitochondrial alterations such as *BAK* activation, loss of transmembrane potential, and generation of reactive oxygen species, paralleled by induction of DNA damage, following Zeb treatment (Ruiz-Magaña *et al*., 2012). In gastric cancer cell lines, Zeb treatment caused DNMT inhibition and re-expression of hypermethylation silenced *p16* in a dose- and time-dependent manner. This most likely activated mitochondrial apoptosis pathway by upregulating pro-apoptotic *BAX* and inhibiting anti-apoptotic *Bcl-2* expression associated with increase of caspases-3 activity. The study also reported the anti-tumor effect of *p.o.* administered Zeb in human gastric cancer xenografted mouse model (Tan *et al*., 2013). In cervical cancer cells, Zeb inhibited cell growth in a dose-dependent manner by causing S-phase arrest of the cell cycle, accompanied by increased levels of S-phase marker, *Cyclin A*/*CDK2* proteins, and induction of apoptosis, accompanied by loss of mitochondrial membrane potential (MMP), PARP-1 cleavage, and activation of caspase-3, -8 and -9 (You & Park, 2012). In lung cancer cell lines, Zeb induced cell death in a dose-dependent manner, accompanied by loss of MMP, *Bcl-2* decrease, *BAX* and *p53* increase (You & Park, 2014), and/or caspase-3 and -8 activations, and S-phase arrest of the cell cycle (You & Park, 2014; You & Park, 2013). Besides, Zeb treatment resulted in depletion of glutathione (GSH) levels in both cervical and lung cancer cell lines, and GSH content was inversely correlated with apoptotic effect induced by Zeb (You & Park, 2012; You & Park, 2014; You & Park, 2013). The study in pancreatic cancer models

reported dose- and time-dependent decrease in cell proliferation and increase in apoptosis, associated with up-regulation of *BAX* and increased expression of *CK7, in vitro*. Also, *i.p.* administered Zeb caused delayed growth of *in vivo* established human pancreatic xenografts, accompanied with up-regulation of *CK7* and down-regulation of de-differentiation markers (Neureiter *et al*., 2007). In human mammary tumors, Zeb-induced inhibition of cell growth was associated with increased *p21* expression, decreased expression of *cyclin D*, and induction of S-phase arrest in a dose- and time-dependent manner. At high doses, Zeb mediated alterations in apoptotic proteins, *caspase-3*, *BAX*, *Bcl-2,* and PARP cleavage. However, at low doses, Zeb inhibited DNMTs and induced re-expression of epigenetically silenced estrogen and progesterone receptor mRNA (Billam *et al*., 2010). The anti-tumor study conducted in genetically engineered mouse model of breast cancer further evidenced high apoptotic index and significantly delayed growth of mammary tumors following *p.o.* administration of Zeb. The study also reported the depletion of DNMTs and up-regulation of various methylation regulated as well as cancer related cell cycle regulatory genes (Chen *et al*., 2012). In hepatocellular carcinoma cells, Zeb induced cell cycle arrest independent of DNA methylation via MAPK pathway, and induced apoptosis by decreasing the activity of *PKR* resulting in *Bcl-2* down-regulation and apoptotic cell death (Nakamura *et al*., 2013), and via DNA methylation pathway by reactivating *Ras* and *Jak/Stat* inhibitors resulting in cell growth suppression and extensive cell death (Calvisi *et al*., 2006). The study conducted in colorectal cancer further described the anti-cancer activity of Zeb via induction of *p53* dependent apoptosis, by down-regulation of the increased expression of pro-survival marker of endoplasmic reticulum stress, *GRP78* and autophagy, *p62,* and by up-regulating the pro-apoptotic CHOP in colorectal cancer patients and tumor-derived stem cells. Also, *p.o.* administered Zeb significantly inhibited both tumor weight and tumor volume in human colorectal cancer xenografts (Yang *et al*., 2013). The anti-cancer activity of Zeb was also explored in cholangiocarcinoma. The study demonstrated that Zeb treatment resulted in DNMT depletion, and to an extent, the alteration in DNA methylation status was associated with suppression of the Wnt signaling pathway leading to apoptotic cell death. In addition, decrease in β-catenin protein levels was also reported in Zeb treated cells (Nakamura *et al*., 2015). The anti-cancer effects of Zeb were further characterized in brain cancers. In glioblastoma cells, Zeb induced cytotoxic effects in a dose-dependent manner and caused rapid global and gene-specific demethylation. The major determinant for cellular response to Zeb was found to be combination of DNA repair and cell cycle checkpoint defects (Meador *et al*., 2010). In pediatric medulloblastoma cell lines, Zeb treatment inhibited cell proliferation and clonogenicity by increasing expression of TSGs, *p53* and *p21*, induced S-phase cell cycle arrest and decreased

expression of *cyclin A*, and induced apoptosis by increasing *BAX* and decreasing *Bcl-2* and *survivin* proteins. In addition, Zeb treatment also modulated the activation of SHH pathway, and altered global gene expression profile, significantly upregulating *BATF2* expression in medulloblastoma cells (Andrade *et al*., 2017). In human osteosarcoma cells, Zeb treatment inhibited viability and promoted apoptosis in a dose- and time-dependent manner by disturbing the interaction between DNMT1 and histone methyltransferase, G9a, thereby causing demethylation-induced expression of hypermethylation silenced TSG, *ARHI* (Ye *et al*., 2016). In oral squamous cell carcinoma, treatment with Zeb inhibited *VEGF* expression via proteasome-based ubiquitination of the *HIF-1α* pathway, which suggests the potential of Zeb in modulation of angiogenic properties in these cells (Suzuki *et al*., 2008). Altogether, the spectrum of Zeb effects in myeloid malignancies and wide range of solid tumors demonstrate the anti-cancer mechanisms of Zeb, as demethylating agent and as a promising adjuvant chemotherapy agent via DNMT independent pathways, and provide strong rationale to continue the research with Zeb. However, the poor bioavailability of Zeb, resulting from its complex metabolism into endogenous inactive compounds and its limited DNA incorporation (Ben-Kasus *et al*., 2005), and secondly, requirement of higher dose to induce similar levels of demethylation as 5-aza-CR and 5-aza-CdR, due to lack of permanent covalent complex with DNMTs (Champion *et al*., 2010) has prevented Zeb from entering into clinical trials, yet. Nevertheless, the combinatorial therapy of Zeb with other demethylating agents may lower its required dose for clinical approaches, and provide effective anti-cancer treatment. Moreover, the depletion of cancer-related antigen genes suggests anti-tumor potential of Zeb in combination with immunotherapy (Cheng *et al*., 2004b).

1.3.6. 6-thioguanine

6-thioguanine also known as Thioguanine; Tioguanine; Thioguanine Tabloid ® or 2-amino-1,7-dihydro-6H-purine-6-thione (6-tG), is a synthetic guanosine analogue antimetabolite with remarkable anti-neoplastic and immuno-suppressive activity, used in maintenance therapy of childhood acute lymphoblastic leukemia (ALL) and lymphoblastic non-hodgkin's lymphoma (Munshi *et al*., 2014). Chemically, 6-tG is synthesized by substitution of oxygen with sulphur at carbon 6 of guanine, fig.1.6 (Hitchings & Elion, 1954). The mechanism of action of 6-tG involves incorporation into DNA and RNA as 6-tG nucleotide. At nucleotide level, 6-tG competes with hypoxanthine and guanine for the enzyme hypoxanthine-guanine phosphoribosyltransferase, and is converted to 6-thioguanilyic acid (TGMP). At therapeutic doses, TGMP reaches high intracellular concentrations and interferes with the synthesis of guanine nucleotide by inhibiting several enzymes involved in purine biosynthesis, and consequently resulting in blockade of DNA

and RNA synthesis and cell death (Nelson *et al*., 1975). Moreover, a study using human embryonic kidney cell line suggested that cytotoxic effects induced by thiopurine drugs may also be contributed in part by inhibition of DNA methylation, as evidenced by dose-dependent decrease in global DNA methylation and DNMT activity following exposure of cells to 6-tG, which was comparable to decitabine (Hogarth *et al*., 2008). Eventually, another study conducted in human embryonic kidney cell line and leukemia derived cell lines demonstrated appreciable decrease in the level of global cytosine methylation following treatment with 6-tG (Wang & Wang, 2009; Yuan *et al*., 2011). The study also reported promoter demethylation and 4-fold increases in mRNA levels of epigenetically silenced genes *DCC*, *KCNK2*, *LRP1B*, *NKX6-1*, *NOPE*, *PCDHGA12*, and *RPIB9* in ALL cells following treatment with 6-tG (Yuan *et al*., 2011). The underlying mechanism behind the global cytosine demethylation was substantiated using ALL derived Jurkat-T cells. The study showed that epigenetic effect of 6-tG was mediated by down-regulation of histone lysine-specific demethylase 1 expression which stimulated lysine methylation of DNMT1, and triggered its degradation via the ubiquitin-proteasomal pathway (Yuan *et al*., 2011). Yet, another study conducted in canine malignant lymphoid cells further confirmed the demethylation activity of 6-tG, evidenced by decrease in level of DNMT1 protein and global DNA methylation (Flesner *et al*., 2014). Altogether, inhibition of DNA methylation by thiopurine drugs may contribute in part to their cytotoxic activity.

1.3.7. 2′-deoxy-5,6-dihydro-5-azacytidine

2′-deoxy-5,6-dihydro-5-azacytidine (DHDAC, KP-1212) is another recently developed, hydrolytically stable congener of DAC with advantages of high aqueous stability and minimal cytotoxicity (Fig.1.6). DHDAC has already been known for its anti-HIV activity mediated by lethal mutagenesis of the viral genome (Harris *et al*., 2005) and has also been tested in phase 2 clinical trial against HIV (Mullins *et al*., 2011). However, the demethylation potential of DHDAC in cellular models was discovered very recently. The study reported the efficient ability of DHDAC to decrease the methylation level of two epigenetically silenced genes, *CDKN2B* and *THBS-1*, and increase mRNA expression of *THBS-1* in human leukemic cell lines, similar to DAC. The study also demonstrated that hypomethylation activity of DHDAC was comparable to DAC (Matoušová *et al*., 2011). Furthermore, the studies proved DHDAC as less toxic alternative of DAC, evidenced by time-dependent increase in DAC toxicity against negligible or no effect of DHDAC on cell cycle progression at 100-fold higher concentration or at dose that induced DNA hypomethylation and gene reactivation comparable to DAC (Matoušová *et al*., 2011; Agrawal *et al.*, 2017). Overall, efficient hypomethylation activity combined with low toxicity and aqueous

stability might represent DHDAC as a superior hypomethylating agent over DAC. But, further pre-clinical studies and clinical trials validating DHDAC as feasible alternative of DAC is clearly required.

α-anomer of DHDAC (α-DHDAC) was reported with no significant hypomethylation potency. This may be due to absence of the 5,6-double bond, required for spontaneous conversion of α-DHDAC to corresponding β-anomer. Also, incorporation of α-anomer into DNA is unlikely (Matoušová *et al*., 2011).

1.3.8. 4′-thio-2′-deoxycytidine and 5-aza-4′-thio-2′-deoxycytidine

4′-thio-2′-deoxycytidine (TdCyd) was synthesized as a 5’-protected phosphoramidite (Fig.1.6), and was initially discovered as inhibitor of methylation by bacterial HhaI methyltransferase (Kumar *et al*., 1997). Recently, TdCyd and its 5-aza analogue (Fig.1.6), 5-aza-4'-thio-2'-deoxycytidine (5-aza-TdCyd) were reported for their potential activity in depleting human DNMT1 and concomitant inhibition of tumor growth, in both *in vitro* and *in vivo* cancer models (Thottassery *et al*., 2014). The study demonstrated that both TdCyd and 5-aza-TdCyd decreased cell viability and caused marked depletion of DNMT1 in leukemic and solid tumor cells, and effectively induced CpG demethylation and re-expression of TSG, *p15* in leukemia cells. Both TdCyd and 5-aza-TdCyd administered *i.p.* also showed DNMT1 depleting activity in human leukemic and lung cancer xenograft models, and caused efficient reduction of tumor growth in lung cancer xenografts (Thottassery *et al*., 2014). Furthermore, the study also indicated better tolerance of 5-aza-TdCyd as compared to decitabine, evident by at least 10-fold greater selectivity index (ratio of MTD to that of minimal DNMT1 depleting dose) than decitabine. The data suggest minimal off target toxicity of 5-aza-TdCyd, however, the reason of less toxicity remains ununderstood (Thottassery *et al*., 2014). It was also distinguished that 5-aza-TdCyd was indefinitely stable in aqueous solution with three times longer half-life over decitabine, thereby supporting adequate bioavailability of oral formulations (Thottassery *et al*., 2014). Collectively, the data emphasize towards further development of 4′-thio modified deoxycytidine analogs as novel clinically effective DNA methylation inhibitors with less toxicity and increased stability, and approval of their use in treatment of solid tumors. Now, TdCyd has entered into phase 1 clinical trial, to establish safety, tolerability, and MTD of oral TdCyd in patients with refractory solid tumors (NCT02423057).

Table 1.3 Nucleoside analogs as DNA methylation inhibitors in pre-clinical or clinical development stage

This table presents the beneficial characteristics of first generation nucleosidic DNA methylation inhibitors, their in vitro cellular potency in various cancer types, in vivo anti-tumor activity, and current phase of clinical development.

Drug	Specific characteristics	Types of cancer (*In vitro*)	*In vitro* cellular potency	Pre-clinical activity	Clinical phase	References
ψICyd	• Exceptional hydrolytic stability • Resistant to enzymatic deamination by CDA • Reduced cytotoxicity • Orally bioavailable	Leukemia	0.04-3.8 µg/mL	• Anti-leukemic activity at 60-150 mg/kg, *i.p.* or 100-150 mg/kg, *p.o.* doses in leukemia mouse models	-	Burchenal *et al*., 1976; Chu *et al*., 1975; Costanzi *et al*., 2011; Jones *et al*., 1980; Woodcock *et al*., 1980
FdCyd	• Stable in aqueous solution • Orally bioavailable when co-administered with CDA inhibitor, THU	Cervix, Melanoma, Breast, Colon, Bladder, Brain	25 nM-10 µM	• The combination of 6 mg/kg FdCyd + 100 mg/kg THU, *i.v.* dose showed no significant *in vivo* activity	Phase 1/2	Beumer *et al*., 2006; Beumer *et al*., 2008; Eidinoff *et al*., 1959; Holleran *et al*., 2015; Hou *et al*., 2005; Kinders *et al*., 2011; Li *et al*., 2006; Morfouace *et al*., 2016; Newman *et al*., 2015; Wempen *et al*., 1961; Zhao *et al*., 2012
DHAC	• Stable in aqueous solution • Modest hematologic toxicity profile	Lymphoma, Leukemia, Breast, Prostate	10-200 µM	• 25.1% and 46.3% decrease in DNA methylation at 1500 mg/kg, *i.p.* dose in dCK(0) and dCK(-) mouse leukemic cancer xenografts	Phase 1/2	Antonsson *et al*., 1981; Avramis *et al*., 1989; Beisler *et al*., 1977; Creagan *et al*., 1993; Curt *et al*., 1985; Dhingra *et al*., 1991; Holoye *et al*., 1987; Izbicka *et al*., 1999a; Izbicka *et al*., 1999b; Kees *et al*., 1995; Powell *et al*., 1988; Traganos *et al*., 1981; Yogelzang *et al*., 1997
Ara-AC	• Protected from deamination by CDA • Orally bioavailable	Colon, Leukemia	0.75-10 µM	• Ara-AC, administered *i.p* or *i.v.* demonstrated wide therapeutic activity against several murine leukemias, and human xenografts of the NCI tumor panel	Phase 1/2	Ahluwalia *et al*., 1986; Amato *et al*., 1992; Bailey *et al*., 1991; Ben-Baruch *et al*., 1993; Bernstein *et al*., 1993; Casper *et al*., 1992; Dalai *et al*., 1986; Glazer & Knode, 1984; Goldberg *et al*., 1997; Heideman *et al*., 1989; Hubbard *et al*., 1992; Kuebler *et al*., 1991; Manetta *et al*., 1995a; Manetta *et al*., 1995b; Selby *et al*., 1994; Surbone *et al*., 1990; Veselý &; Pískala, 1986; Wallace *et al*., 1989; Walters *et al*., 1992; Wilhelm *et al*., 1999; Williamson *et al*., 1995
Zeb	• Stable in aqueous solution • Potent inhibitor of CDA • Selective specificity for cancer cells ensures minimal general toxicity • Continuous long-term treatment possibility prevents gene re-methylation • Orally bioavailable	Bladder, Leukemia, Stomach, Cervix, Lung, Pancreas, Breast, Liver, Colon, Cholangiocarcin	10 µM-1 mM	• Significant reduction in tumor volume at high dose of 1000 mg/kg, *i.p.* or *p.o.* in human bladder cancer xenografts • Improved OS in radiation-induced T-cell lymphoma mouse model at 400 mg/kg, *i.p.* dose • Significant inhibition of tumor volume at 10, 50, and 100 mg/kg, *p.o.* doses in human gastric cancer xenografts	-	Andrade *et al*., 2017; Billam *et al*., 2010; Calvisi *et al*., 2006; Chen *et al*., 2012; Cheng *et al*., 2003; Cheng *et al*., 2004a; Cheng *et al*., 2004b; Herranz *et al*., 2006; Holleran *et al*., 2005; Kim *et al*., 1986; Meador *et al*., 2010; Nakamura *et al*., 2013; Nakamura *et al*., 2015; Neureiter *et al*., 2007; Ruiz-Magaña *et al*., 2012; Savickiene *et al*., 2012b; Scott *et al*.,

		oma, Brain, Osteosarcoma, Oral squamous cell carcinoma		• 68.2% tumor growth inhibition at high dose of 1000 mg/kg, *i.p.* in human pancreatic cancer xenografts • Significant delay in tumor growth at 750 mg/kg, *p.o.* dose in human mammary tumors • Significant inhibition of tumor growth and tumor volume at 750 mg/kg, *p.o.* dose in human colorectal cancer xenografts		2007; Suzuki *et al*., 2008; Tan *et al*., 2013; Yang *et al*., 2013; Ye *et al*., 2016; Yoo *et al*., 2008; You *et al*., 2012; You *et al*., 2013; You *et al*., 2014
6-tG	• Incorporates into DNA and RNA and inhibits DNA and RNA synthesis • Inhibits DNA methylation via proteasomal degradation of DNMT1	Leukemia, Kidney	1-4 µM	-	-	Hogarth *et al*., 2008; Nelson *et al*., 1975; Wang *et al*., 2009; Yuan *et al*., 2011
DHDAC	• High aqueous stability • Minimal cytotoxicity	Leukemia	50-100 µM	-	-	Agrawal *et al*., 2017; Matoušová *et al*., 2011
TdCyd **5-aza-TdCyd**	• Longer half-life • Minimal off target toxicity • Orally bioavailable	Leukemia, Lung, Ovary, Colon	TdCyd: 0.6-100 µM 5-aza-TdCyd: 0.06-58 µM	• TdCyd at 1.3 and 0.9 mg/kg and 5-aza-TdCyd at 6.7 and 10 mg/kg, *i.p.* doses caused significant tumor growth inhibition in human lung cancer xenografts	Phase 1	Thottassery *et al*., 2014

1.4. Second generation prodrugs

Despite, immense clinical development of azacytidine and decitabine in epigenetic cancer therapy, the efficacy of these nucleoside drugs is limited due to significant challenges arising from low bioavailability, metabolic instability, and reduced cellular uptake of both compounds. Based on the current mechanistic understanding about metabolization and cellular drug uptake, efforts are under way to identify novel AZN derivatives with better PK and pharmacodynamics (PD) profile, exemplified by SGI-110 and CP-4200. SGI-110, dinucleotide of decitabine with increased metabolic stability, and CP-4200, azacytidine variant affording improved cellular delivery, are recently developed second generation nucleoside analogs with enhanced therapeutic efficacy over FDA approved DNA methylation inhibitors. Apart from SGI-110 and CP-4200, other potential pro-drugs of decitabine and azacytidine, NPEOC-DAC and 2'3'5'triacetyl-5-azacytidine respectively, and a novel cytidine analog, RX-3117 have also been investigated in pre-clinical trials and/or have entered into clinical trials (Fig.1.7, Table 1.4).

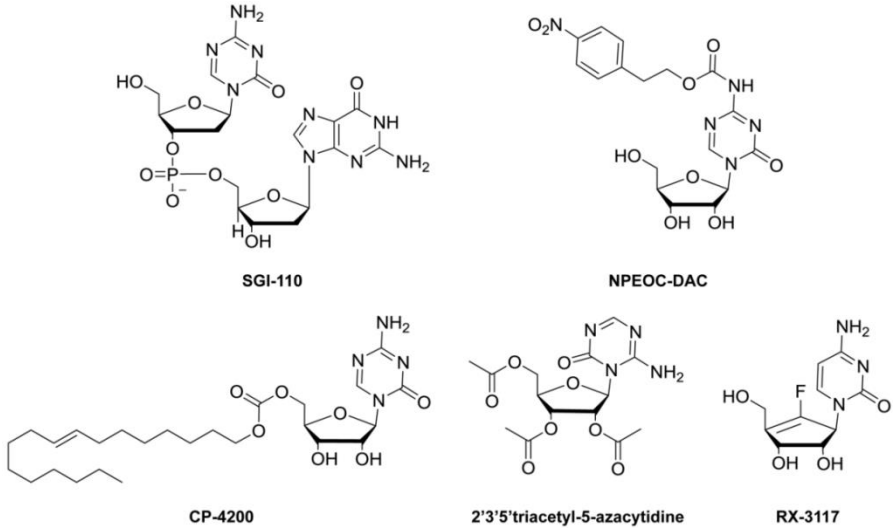

Figure 1.7 Second generation prodrugs

1.4.1. SGI-110

SGI-110 or S-110; Decitabine deoxyguanosine; Decitabine deoxyguanosine dinucleotide; Guadecitabine (Astex Pharmaceuticals, Dublin, CA, USA) is a second generation hypomethylating pro-drug of decitabine in advanced clinical development. SGI-110 is a dinucleotide of decitabine formulated by binding active decitabine with its chemically modified form, deoxyguanosine, by a natural phosphodiester linkage, fig.1.7 (Yoo *et al.*, 2007). Unlike decitabine which is susceptible to *in vivo* deamination by CDA which compromises the plasma

level of the drug resulting in low bioavailability, SGI-110 dinucleotide is highly protected from inactivation by CDA (Yoo *et al*., 2007). The mechanism of action of SGI-110 to inhibit DNA methylation via depletion of DNMT1, its aqueous stability, and cytotoxicity remains similar to the parent compound (Yoo *et al*., 2007; Stresemann & Lyko, 2008). However, the differentiated PK and PD profile of SGI-110 offers improved clinical efficacy over existing hypomethylating agents, not only in patients with hematologic malignancies, but also marks the drug useful for the treatment of solid tumors for which first generation drugs are not approved. The first biological study of SGI-110 was conducted in bladder and colon cancer cells, where, SGI-110 caused dose-dependent demethylation and increase in *p16* expression at both mRNA and protein level (Yoo *et al*., 2007). The demethylation activity of SGI-110 was also confirmed *in vivo* by its ability to reduce DNA methylation and induce *p16* expression in human bladder cancer xenografts. Also, SGI-110 retarded tumor growth of xenografts by both *i.p.* and *s.c.* deliveries, and offered less toxicity in tumor-free nude mice as compared to decitabine (Chuang *et al*., 2010). The *s.c.* administered SGI-110 further showed anti-tumor efficacy in human hepatocellular carcinoma xenografts by impeding tumor growth and inhibiting angiogenesis. The study also demonstrated the pronounced demethylation effects of SGI-110 in subset of TSGs, *CDKN2A*, *DLEC1*, and *RUNX3*. (Jueliger *et al*., 2016). In another study conducted in ovarian cancer, SGI-110 proved its demethylation potential by inducing expression of significant epithelial mesenchymal transition genes silenced by hypermethylation (Cardenas *et al*., 2014). The demethylation activity of SGI-110 was also evidenced in primates (Lavelle *et al*., 2010). Furthermore, studies investigating the immunomodulatory potential of SGI-110 revealed that SGI-110 improved the immunogenic potential and immune recognition of treated cancer cells. It was demonstrated in wide variety of human cancer cell lines that SGI-110 treated neoplastic cells showed induced expression of various methylated cancer testis antigen genes by promoter demethylation, up-regulated expression of HLA class I antigens, MHC class I, and co-stimulatory molecule expression in a dose-dependent manner, both *in vitro* and *in vivo* (Coral *et al*., 2013; Srivastava *et al*., 2014; Srivastava *et al*., 2015). Moreover, the immunomodulatory potential of SGI-110 was found to be significantly higher than azacytidine or decitabine (Srivastava *et al*., 2014). These key findings emphasize towards the clinical application of SGI-110 in cancer immunotherapies and provide strong rationale for the development of novel anti-cancer chemo-immunotherapies, utilizing SGI-110 in combination with immunotherapeutic drugs. After encouraging demethylation and anti-tumor effects in pre-clinical models, SGI-110 entered into clinical trial phases. At first, a multicenter randomized dose escalation phase 1study of SGI-110, formulated as low volume and pharmaceutically stable *s.c.* injections was conducted in previously treated relapsed or refractory,

intermediate or high-risk MDS or AML patients. The results of the study demonstrated the drastic increase in therapeutic exposure window (beyond 8 h) compared to decitabine *i.v.* infusions (3-4 h) and prolonged half-life (~2.4 h) which is 4 -fold higher than achieved by *i.v.* administered decitabine (Issa *et al*., 2015). The clinical response was observed in 31% of MDS patients and 8% of AML patients, and DNA demethylation was confirmed as PD marker for clinical response. The most common grade ≥ 3 adverse events were febrile neutropenia, pneumonia, thrombocytopenia, anemia, and sepsis and of which febrile neutropenia, pneumonia, and sepsis were recorded as serious adverse events (Issa *et al*., 2015). Two dose limiting toxicities were observed for MDS at 125 mg/m^2 daily × 5, and MTD for MDS was established as 90 mg/m^2 daily × 5, however, MTD was not attained for AML patients. Notably, optimal biologically effective dose (BED) of SGI-110, 60 mg/m^2 daily × 5 was lower than MTD of the drug in either case (Issa *et al*., 2015). The outcomes of the study warranted further phase 2 trials with the recommended dose of 60 mg/m^2 daily × 5. Presently, SGI-110 is being evaluated in phase 1/2 and/or phase 3 clinical trials in MDS/AML and in phase 1/2 clinical trials for various solid tumors. The complete list of ongoing clinical studies can be found at https://clinicaltrials.gov/ct2/results?term=SGI-110&Search=Search. Apart from its clinical progress as single agent in leukemia, SGI-110 has also gained significant interest in combinatorial therapies and as a priming agent in solid tumors (Table 1.8).

1.4.2. NPEOC-DAC

NPEOC-DAC or 2'-deoxy-N4-[2-(4-nitrophenyl)ethoxycarbonyl]-5-azacytidine is another analogue of DAC that was developed to circumvent the metabolic instability of the drug. NPEOC-DAC was synthesized by binding 2-(p-nitrophenyl)ethoxycarbonyl at N4 position of the azacytidine ring (Fig.1.7). This modification at N4 position protects the exocyclic amine of DAC from deamination by plasma CDA, rendering increased plasma half-life to the drug (Byun *et al*., 2008). In addition, unlike DAC, NPEOC-DAC is highly hydrophobic with very low aqueous solubility which further improves the PK profile of the drug, including oral bioavailability. The orally available mechanistic inhibitor of DNMT thus allows for continuous drug administration, adding to its clinical effectiveness (Byun *et al*., 2008). The demethylation activity of the pro-drug was demonstrated by the ability of NPEOC-DAC to significantly decrease global DNA methylation, reverse hypermethylation and reactivate expression of TSG, *ID4*. The DNA demethylation ability was found to be specific for the liver cancer cell lines and dependent on the activity of the carboxylesterase 1 (CES1) enzyme (Byun *et al*., 2008). While NPEOC-DAC at doses ≥ 10 μM was comparatively more effective at inhibiting DNA methylation, the potency of

the pro-drug to inhibit DNA methylation at low doses (<10 μM) was found to be significantly lower than DAC. Besides, a 3-day delay in the effect of NPEOC-DAC was also reported, along with less toxicity than observed with DAC. It is assumed that the low potency and the delayed effect could result from the inefficient or slow conversion of NPEOC-DAC to active drug, DAC. The fact that NPEOC-DAC is dependent on the activity of CES1 enzyme for its metabolization to DAC has limited the development of the prodrug, because expression of CES1 is variable in different tissues and also may not be 100% efficient in converting NPEOC-DAC to DAC (Byun *et al*., 2008). Nevertheless, it is speculated that substitution of N4-NPEOC group of NPEOC-DAC with a smaller carbon chain may lead to a molecule which can inhibit DNA methylation much more efficiently. Furthermore, the prodrug NPEOC-DAC facilitates the attachment of another epigenetic agent such as histone deacetylase inhibitors at N4 position, and release two active agents on cleavage of the carboxylester bond, thereby extending the possibility of combined epigenetic therapy (Byun *et al*., 2008).

1.4.3. CP-4200

CP-4200 or 5-azacytidine-5'-elaidate (Clavis Pharma, ASA, Oslo, Norway) is a 5-azacytidine variant with modified chemical properties, currently in pre-clinical research phase for MDS. The pro-drug is essentially an elaidic acid ester analog developed by conjugating azacytidine molecule with a fatty acid, elaidic acid (Fig.1.7). CP-4200 was designed to decrease the drug dependency on conventional nucleoside transporters involved in azacytidine uptake and to overcome transport-related drug resistance (Brueckner *et al*., 2010). An extensive study characterizing the mode of action and therapeutic efficacy of CP-4200 was conducted in a panel of human cancer cell lines. The results of the study proved that cellular uptake mechanism of CP-4200 was fundamentally different from that of azacytidine. Also, it was shown that despite extensive chemical modification CP-4200 retained its epigenetic potency. This was well evident by significant depletion of DNMT protein, genome-wide DNA demethylation, and widespread DNA demethylation of hypermethylated markers causing robust reactivation of epigenetically silenced TSGs, *TIMP-3* and *DAPK-1* in colon cancer and leukemia cells, respectively. Importantly, during *in vivo* study conducted in orthotopic ALL mouse tumor model, *i.v.* or *i.p.* administered CP-4200 demonstrated significantly higher anti-tumoral activity compared with equitoxic doses of azacytidine (Brueckner *et al*., 2010). Furthermore, it was shown during a study that inhibition of human equilibrative nucleoside transporter 1 (hENT1) resulted in strong abolishment of cytotoxic and demethylation drug effects of azacytidine, however, CP-4200 effectively retained its cellular activity, thereby explaining its effectiveness in overcoming hENT-

related resistance (Hummel-Eisenbeiss *et al*., 2013). Thus, pre-clinical studies which evidenced the low dependence of CP-4200 on nucleoside transporters combined with increased epigenetic potential have marked the pro-drug as intriguing candidate for epigenetic cancer therapy. Currently, further pre-clinical studies are ongoing but clinical trials have not been initiated yet.

1.4.4. 2',3',5'-Triacetyl-5-Azacytidine

2'3'5'triacetyl-5-azacytidine (TAC) is another potential pro-drug of 5-azacytidine with improved PK profile over parent drug. Structurally, TAC is an acetylated derivative of AZA, synthesized by condensation of trimethylsilylated-5-azacytosine and 1,2,3,5-tetra-O-acetyl-β-D-ribofuranose, fig.1.7 (Ziemba *et al*., 2011). During *in vitro* and *in vivo* characterization, TAC demonstrated favorable physio-chemical characteristics in contrast to its parent compound. *In vitro*, TAC showed higher solubility and stability across wide range of pH which confirmed efficient drug absorption in gastrointestinal tract, and increased bioavailability over AZA which is rapidly degraded in acidic environment (Ziemba *et al*., 2011). *In vivo*, the terminal phase half-life (9.2 h vs. 6.8 h) and the alpha phase half-life (0.73 h vs. 0.32 h) of *p.o.* administered TAC was longer than *i.v.* administered AZA, respectively (Ziemba *et al*., 2011). However, during *in vitro* assessment of anti-proliferative and demethylation effects, TAC showed no cellular toxicity in leukemia cells, and less effect on methylation level of *P15INK4B* as compared to AZA. The reduced *in vitro* efficacy is predicted to be due to lack of necessary esterase activity in cultured cells, required for conversion and activation of pro-drug to AZA (Ziemba *et al*., 2011). The analysis of anti-leukemic activity of *p.o.* administered TAC in human lymphocytic leukemia animal model demonstrated significantly increased survival time with minimal general toxicity, but it was less effective than AZA at improving life span. The less effectivity may be due to higher C_{max} achieved by *i.p.* administered AZA in comparison to *p.o.* administered TAC. While, the ability of *p.o.* TAC to suppress global methylation was comparable with *i.v.* AZA, further studies are required to confirm the demethylation efficacy of TAC in cancer cells (Ziemba *et al*., 2011). Altogether, higher solubility, stability, and bioavailability combined with minimal toxicity encourage further pre-clinical investigation of its mechanism of action, epigenetic modulatory effect, and possible clinical evaluation to establish it as an effective pro-drug for AZA.

1.4.5. RX-3117

RX-3117 or TV-1360; Fluorocyclopentenylcytosine (Rexahn Pharmaceuticals Inc., Rockville, MD, USA) is a next generation novel cytidine analog, currently being investigated in

phase 1/2 clinical trial in solid tumors. The synthesis of RX-3117 involves replacement of sugar moiety with a cyclopentenyl group, fig.1.7 (Zhao *et al*., 2005; Jeong *et al*., 2007). The metabolism and mechanism of action of RX-3117 is distinct from other (deoxy) cytidine analogs. Unlike existing nucleoside analogs which are phosphorylated by dCK, RX-3117 has a different activation pathway that involves phosphorylation by uCK to its monophosphate and subsequently to its diphosphate (RX-DP) and triphosphate (RX-TP) forms. RX-TP is incorporated into RNA and inhibits RNA synthesis, whereas, RX-DP is further reduced by ribonucleotide reductase to dRX-DP, converted to its triphosphate form dRX-TP, and incorporated into DNA where it inhibits DNA synthesis. Apart from exerting its cytotoxic effects by inhibition of DNA and RNA synthesis, RX-3117 also mediates down-regulation of DNMT1 (Peters *et al*., 2013). Remarkably, due to unique specificity of uCK for cancer cells in contrast to dCK which is highly expressed in both cancer and normal cells, RX-3117 has improved efficacy and safety profile in cancer patients (Peters *et al*., 2013). Moreover, a recent study evidenced significant correlation of RX-3117 phosphorylation in intact cells specifically with uCK2 expression, but not with uCK1. This may be implicated in clinic to potentially select the patients sensitive to RX-3117 (Sarkisjan *et al*., 2016). Also, RX-3117 is protected from extensive deamination by CDA and therefore has long half-life and high oral bioavailability (Peters *et al*., 2013). The potent anti-tumor activity of RX-3117 was reported *in vitro* in broad range of tumor cell lines (Zhao *et al*., 2005; Jeong *et al*., 2007; Choi *et al*., 2012), and was further correlated with *in vivo* anti-tumor effects in tumor xenograft model of human lung cancer cells, where, *i.p.* administered RX-3117 significantly inhibited the tumor growth, tumor volume, and tumor weight in a dose-dependent manner (Choi *et al*., 2012). The mechanism of action involved in potent anti-tumor activity was discovered to be dose-dependent inhibition of DNMT1, demonstrated in breast cancer cells (Choi *et al*., 2012). The *p.o.* administered RX-3117 further demonstrated high bioavailability and superior toxicity profile across wide variety of human tumor xenografts in contrast to gemcitabine, an orally unavailable chemotherapeutic drug of the same class (Yang *et al*., 2014a). RX-3117 also showed potent efficacy against human pancreatic xenograft, relatively resistant to gemcitabine. This indicated the therapeutic potential of RX-3117 for treatment of gemcitabine in-sensitive tumors (Yang *et al*., 2014a). The study also demonstrated the positive correlation between the efficacy of RX-3117 and uCK levels in xenograft models (Yang *et al*., 2014a). After the promising results of the pre-clinical studies, RX-3117 is currently being evaluated in phase 1/2 dose escalation open-label clinical trial. The study aims to evaluate the MTD of RX-3117 in patients with advanced or metastatic solid tumors in phase 1, and anti-tumor activity in patients with relapsed or refractory pancreatic or advanced bladder cancer in phase 2 (NCT02030067).

Table 1.4 Second generation DNA demethylating pro-drugs in pre-clinical or clinical development

This table presents the beneficial characteristics of second generation DNA methylation inhibitors, their in vitro cellular potency in various cancer types, in vivo anti-tumor activity, and current phase of clinical development.

Drug	Specific characteristics	Types of cancer (*In vitro*)	*In vitro* cellular potency	Pre-clinical activity	Clinical phase	References
SGI-110	• Longer *in vivo* half-life • Prolonged *in vivo* exposure to decitabine by small volume *s.c.* administrations • Improved PK and PD profile, and clinical efficacy over existing hypomethylating agents	Bladder, Colon, Melanoma, Renal cell carcinoma, Mesothelioma, Sarcoma, Leukemia, Ovary	1 µM	• Retardation in tumor growth at 10 mg/kg, *i.p.* and 12.2 mg/kg, *s.c.* doses in human bladder cancer xenografts • Reduction in tumor mass at 2 mg/kg, *s.c.* dose in human hepatocellular carcinoma xenografts • Enhanced antigen-specific CD8+ T cell anti-tumor response at 3 mg/kg, *s.c.* dose in human epithelial ovarian cancer xenografts	Phase 1/2 Phase 3	Cardenas *et al*., 2014; Chuang *et al*., 2010; Coral *et al*., 2013; Issa *et al*., 2015; Jueliger *et al*., 2016; Yoo *et al*., 2007
NPEOC-DAC	• Increased plasma half-life • Decreased cytotoxicity • Orally bioavailable	Liver	≥10 µM	-	-	Byun *et al*., 2008
CP-4200	• Low dependence on nucleoside transporters involved in drug uptake mechanisms • Increased epigenetic potential	Leukemia, Colon, Breast	2-15 µM	• Significant decrease in spleen weight at 15 and 20 mg/kg, *i.v.* or *i.p.* doses in orthotopic ALL mouse tumor model	-	Brueckner *et al*., 2010; Hummel-Eisenbeiss *et al*., 2013
TAC	• Higher solubility and stability across wide range of pH • Longer half-life • Minimal general toxicity • Orally bioavailable	Leukemia	No cellular toxicity	• 50% increased lifespan at 38 mg/kg, *p.o.* dose in human lymphocytic leukemia animal model	-	Ziemba *et al*., 2011
RX-3117	• Long half-life • Improved efficacy and safety profile in cancer patients • Orally bioavailable	Breast, Colon, Lung, Stomach, Pancreas, Prostate, Liver, Ovary, Leukemia, Kidney, Brain, Cervix, Melanoma	0.18-2.67 µM	• 31.8% and 58.1% tumor growth inhibition at 3 and 10 mg/kg, *i.p.* doses in human lung cancer xenograft model • 100%, 78%, 62%, and 66% tumor growth inhibition in human colon, non-small cell lung, small cell lung, and cervical cancer xenograft models, and 76% tumor growth inhibition in gemcitabine resistant human pancreatic xenografts by *p.o.* administration	Phase 1/2	Choi *et al*., 2012; Peters *et al*., 2013; Sarkisjan *et al*., 2016; Yang *et al*., 2014a

1.5. Mechanisms of drug resistance to azanucleosides

Drug resistance to AZN is an ongoing intractable problem which accounts for limited success and durability of AZN-based therapy. The failure of treatment with AZN drugs can be divided into two broad categories: primary resistance in which case patients do not show response to therapy for at least 4-6 cycles of treatment, and acquired resistance in which patients relapse during long-term treatment. To this end, the researches in past few years have identified some possible reasons for worst outcomes of these drugs in clinic. Since the therapeutic efficacy of AZN is largely dependent on uptake of nucleoside transporters by cells, metabolic activation, as well as degradation by cascade of enzymes (Stresemann & Lyko, 2008), each of these steps makes available a mechanism by which cells exhibit primary or secondary resistance to these agents. First indication towards the involvement of metabolic pathways in AZN resistance came from the study of native and acquired resistance towards fazarabine in a panel of tumor cell lines which suggested dCK as an important determinant of sensitivity towards fazarabine, demonstrated by markedly decreased level of dCK in resistant cells (Ahluwalia *et al*., 1986). Several years later, loss of dCK was established as mechanism behind resistance to decitabine in panel of cultured human cancer cell lines (Qin *et al*., 2009) which was further confirmed *in vivo* in a subset of MDS patients (Qin *et al*., 2011). The study suggested decreased levels of dCK (decreased phosphorylation of decitabine) and increased levels of CDA (increased deamination) as the marker of primary resistance to decitabine, demonstrated by higher CDA/dCK ratio in non-responders than responders (Qin *et al*., 2011). Similar results were obtained for azacytidine in leukemic cell lines (Sripayap *et al*., 2014) and in MDS patients treated with azacytidine in which low levels of uCK (which phosphorylates azacytidine) correlated with poor clinical outcomes (Valencia *et al*., 2014). The implication of altered expression of AZN metabolizing enzymes on modulation of response to azacytidine or decitabine therapy was further demonstrated by decreased cytidine analog half-life and worse outcomes, as a consequence of increased CDA expression in another trial with MDS patients (Mahfouz *et al*., 2013). Recently, the change in expression levels of CDA and/or dCK during acquisition of resistance to decitabine has been shown in *in vitro* developed decitabine resistant variant of colorectal cancer cells (Hosokawa *et al*., 2015). Besides enzymes involved in metabolic activation, membrane proteins involved in drug uptake are potential mediators of drug resistance. In this context the recent studies identified hENT1 expression as a key determinant of azacytidine-triggered cytotoxicity (Hummel-Eisenbeiss *et al*., 2013) and hCNT1, hCNT3, and hENT2 as the key transporters involved in

cellular uptake of zebularine (Arimany-Nardi *et al*., 2014) which suggests the significance of these transporters as useful biomarkers that may predict the therapeutic efficiency of these drugs. However, pharmacological mechanisms involved in primary resistance to these nucleoside analogs are not related with secondary resistance to these drugs, evident by no significant difference in decitabine metabolism gene expressions between diagnosis and relapse (Qin *et al*., 2011). The study further suggested that secondary resistance to AZN is also independent of DNA methylation, evident by significant hypomethylation at relapse compared to diagnosis (Qin *et al*., 2011). Instead secondary resistance to these AZN may result from genetic activation of oncogenic survival and progression pathways. In the past years studies have identified several aberrantly expressed oncogenes as predictors of response to DNA hypomethylating agents. Included in the list is DNMT3B gene amplification (Simó-Riudalbas *et al*., 2011), up-regulated expression of anti-apoptotic *BCL2L10* (Cluzeau *et al*., 2012), constitutive activation of the ATM/BRCA1 pathway (Imanishi *et al*., 2014), simultaneous DNA re-methylation due to up-regulation of DNMT1 and re-activation of tyrosine-protein kinase cascades (Yan *et al*., 2015). But so far none of these bona fide oncogenes/pathways have revealed clinical or molecular patterns that differentiate between responders and non-responders. Thus, investigation of response predicting biomarkers and mechanisms of primary and secondary resistance to hypomethylating agents is an unmet need towards the successful DNA-methylation based epigenetic therapy.

1.6. DNMTIs in rational combinations: An alternative strategy targeting drug resistance

DNA methylation is associated with silencing of various drug-response genes, and resistance of cancer cells to anti-cancer drugs. Consequently, epigenetic reprogramming via DNA methylation inhibitors could be expected to result in restoration of silenced TSGs and facilitate re-sensitization. The recent studies suggest that low concentrations of DNMTIs such as azacytidine and decitabine may act synergistically when combined with chemotherapy and contribute to overcoming intrinsic or acquired chemoresistance in several cancer types. Moreover, single-agent activities of DNA methylation inhibitors have been limited in solid tumors. Therefore rational combination of epigenetic drug with each other or with conventional agents is a promising approach which has demonstrated enhanced effectiveness in various cancer-types, especially in advanced solid tumors. Tables 1.5 - 1.8 summarizes the registered clinical trials of azacytidine (Table 1.5) and decitabine (Table 1.6), and combinatorial effects of zebularine (Table 1.7) and SGI-110 (Table 1.8) in various rational combinations.

Table 1.5 Azacytidine in combinatorial therapies

This table summarizes all registered clinical trials of azacytidine in combination with various chemotherapeutic, epigenetic or immunomodulatory agents for which study results have been posted or are available as publications.

Conditions	Phase	Study start, Status	Brief summary	NCT number (References)
➢ **Standard chemotherapy drugs: Cytarabine, Cisplatin, Docetaxel, Daunorubicin** (+ Prednisone)				
AML, MDS	Phase 1/2	2005, Completed	Randomized study of azacytidine in combination with cytarabine in patients with relapsed or refractory AML or high-risk MDS, for determining (i) MTD of azacytidine in combination, and (ii) safety and effectiveness of the combination treatment; • **Group 1: Azacytidine:** 37.5 mg/m^2, *i.v.*, 20-30 min, daily, 1-7 d + **Cytarabine:** 100 mg/m^2, c.*i.v.*, daily, 1-7 d, every 4-8 w • **Group 2: Azacytidine:** 75 mg/m^2, *i.v.*, 20-30 min, daily, 1-7 d + **Cytarabine:** 100 mg/m^2, c.*i.v.*, daily, 1-7 d, every 4-8 w • **Group 3: Azacytidine:** 37.5 mg/m^2, *i.v.*, 20-30 min, daily, 1-7 d + **Cytarabine:** 1 g/m^2, c.*i.v.*, daily, 1-4 d (age < 65 y) or 1-3 d (age ≥ 65 y), every 4-8 w • **Group 4: Azacytidine:** 75 mg/m^2, *i.v.*, 20-30 min, daily, 1-7 d + **Cytarabine:** 1 g/m^2, c.*i.v.*, daily, 1-4 d (age < 65 y) or 1-3 d (age ≥ 65 y), every 4-8 w • **Result** (Group 1 vs. Group 2 vs. Group 3 vs. Group 4): CR: 0/6 (0%) vs. 0/6 (0%), vs. 0/11 (0%) vs. 2/11 (18%), SAE: 5/6 (83%) vs. 5/6 (83%) vs. 8/11 (73%) vs. 3/11 (27%)	NCT00569010
Squamous cell carcinoma	Phase 1	2007, Terminated	Non-randomized dose-escalation study of azacytidine in combination with cisplatin in patients with recurrent or metastatic squamous cell carcinoma of the head and neck, for determining the safety and toxicity of the combination; • **Azacytidine:** 37-110 mg/m^2/day, *s.c.*, daily, 1-5 d + **Cisplatin:** 75 mg/m^2, *i.v.*, d 8, every 4 w • **Result:** SAE: 1/1 (100%)	NCT00443261
Prostate cancer	Phase 1/2	2007, Terminated	Non-randomized study of azacytidine in combination with docetaxel and prednisone in patients with previously treated hormone refractory metastatic prostate cancer, for determining (i) a safe and potentially efficacious phase 2 dose of azacytidine in combination with docetaxel and prednisone (ii) the therapeutic efficacy of the combination (iii) toxicity profile (iv) DOR, and (v) PFS and OS; • **Phase 1: Azacytidine** (*i.v.*, 30 min, daily, 1-5 d, every 3 w) + **Docetaxel** (*i.v.*, 1 h, d 6, every 3 w): 75 mg/m^2 + 60 mg/m^2 (level 1) – 75 mg/m^2 + 75 mg/m^2 (level 2) – 100 mg/m^2 + 75 mg/m^2 (level 3) – 150 mg/m^2 + 75 mg/m^2 (level 4) + **Prednisone:** 5mg, *p.o.*, twice daily, 1-21 d • **Phase 2: Azacytidine** + **Docetaxel** with 5 mg of **prednisone** at initial recommended phase 2 dose level (RPTD) • **Phase 2:** reduced dose of **Azacytidine** + **Docetaxel** with 5 mg of **prednisone** at RPTD • **Result:** [Initial and Reduced RPTD: Azacytidine: 150 and 75 mg/m^2, Docetaxel: 75 and 75 mg/m^2, Prednisone: 5 and 5 mg], [ORR: Phase 1 (Level 1): 0/2 (0%), Phase 1 (Level 2): 0/0 (0%), Phase 1 (Level 3): 1/2 (50%), Phase 1 (Level 4): 1/3 (33%), Phase 2 (initial RPTD): 1/3 (33%)], PFS: 4.9 months, OS: 19.5 months, [SAE: Level 1: 1/3 (33%), Level 2: 0/4 (0%), Level 3: 1/3 (33%), Level 4: 4/12 (33%)]	NCT00503984 (Singal *et al*., 2015)
AML	Phase 2	2009, Completed	Randomized study of the effectiveness of azacytidine added to standard primary therapy in older patients with newly diagnosed AML; • **Induction therapy: Azacytidine:** 75 or 37.5 mg/m^2/day, *i.v.*, 30 min, daily, -5 to -1 d + **Cytarabine:** 100 mg/m²/day, c.*i.v.*, daily, 1-7 d + **Daunorubicin:** 45 mg/m²/day, *i.v.*, daily, 3-5 d • **Consolidation therapy: Azacytidine:** 75 or 37.5 mg/m^2/day, *s.c.*, daily, -5 to -1 d + **Cytarabine:** 1 g/m², *i.v.*, twice a day, d 1, d 3, d 5 • **Maintenance therapy: Azacytidine:** 75 or 37.5 mg/m^2/day, *s.c.*, daily, 1-5 d, every 4 w • **Result:** CR: 7/12 (58%), OS: 8.9 months, EFS: 7.2 months	NCT00915252 (Krug *et al*., 2012)

➢ **Histone deacetylase inhibitors: Phenylbutyrate, Entinostat, Valproic Acid, Vorinostat** (+ All-Trans Retinoic Acid, Carboplatin, Gemtuzumab Ozogamicin, Lenalidomide)				
Solid tumors	Phase 1/2	2000, Completed	Study of azacytidine in combination with phenylbutyrate in patients with advanced or metastatic solid tumors, for determining (i) safety and toxicity of the combination (ii) MTD of this treatment regimen where maximal gene re-expression occurs in these patients (iii) PK, and (iv) minimal effective dose of azacytidine in combination with phenylbutyrate that elicits a biological or clinical response in these patients; • **Regimen A: Azacytidine:** 25-18.75-15-10 mg/m^2/day, *s.c.*, daily, 1-14 d + **Phenylbutyrate:** 400 mg/m^2/day, c.*i.v.*, d 6, d 13, every 5 w • **Regimen B: Azacytidine:** 75 mg/m^2/day, *s.c.*, daily, 1-7 d + **Phenylbutyrate:** 200-400 mg/m^2/day, c.*i.v.*, d 8, d 14, every 5 w • **Regimen C: Azacytidine:** 10-12.5 mg/m^2/day, *s.c.*, daily, 1-21 d + **Phenylbutyrate:** 400 mg/m^2/day, c.*i.v.*, d 6, d 13, d 20, every 6 w • **Result:** The combination of azacytidine and phenylbutyrate across three dose schedules was generally well tolerated and safe, but lacked any real evidence for clinical benefit	NCT00005639 (Lin *et al*., 2009)
MDS, CMML, AML	Phase 1	2004, Active	Study of azacytidine in combination with entinostat in patients with MDS, CMML, and AML, for determining (i) safety and toxicity of the combination (ii) MTD and optimal phase 2 dose of entinostat when combined with azacytidine (iii) therapeutic efficacy of the regimen, and (iv) correlate PK of entinostat with clinical response and laboratory correlative endpoints; • **Arm 1: Azacytidine:** 50 mg/m^2/day, *s.c.*, daily, 1-10 d, every 4 w • **Arm 2: Azacytidine:** (Arm 1) + **Entinostat:** 4 mg/m^2/day, *p.o.*, d 3, d 10, every 4 w • **Result:** (Arm 1 vs. Arm 2): ORR: 12/24 (50%) vs. 4/23 (17%), DOR: 8 months vs. 5 months, OS: 13 months vs. 6 months	NCT00101179 (Prebet *et al*., 2016)
MDS, CMML, AML	Phase 2	2006, Completed	Randomized study of azacytidine with or without entinostat in patients with *de novo* MDS, CMML (dysplastic type) or AML with multilineage dysplasia, for determining (i) ORR and the major response rate of azacytidine monotherapy versus combination (ii) toxicity of the combination (iii) to identify the changes in gene promoter methylation and expression, and (iv) the molecular mechanisms associated with response to azacytidine and entinostat such as DNA damage; • **Arm 1: Azacytidine:** 50 mg/m^2/day, *s.c.*, daily, 1-10 d, every 4 w • **Arm 2: Azacytidine:** (Arm 1) + **Entinostat:** 4 mg/m^2/day, *p.o.*, d 3, d 10, every 4 w • **Result** (Proportion of patients with clinical response; Arm A vs. Arm B): [Non-treatment induced cohort: 74 (0.32) vs. 75 (0.27)], [Treatment induced cohort: 24 (0.46) vs. 23 (0.17)], [SAE: 92/99 (93%) vs. 93/98 (95%)]	NCT00313586 (Prebet *et al*., 2016)
Colorectal cancer	Phase 2	2010, Completed	Study of azacytidine in combination with entinostat in patients with metastatic colorectal cancer, for determining (i) ORR (ii) TTP, and (iii) toxicity of the combination; • **Azacytidine:** 40 mg/m^2, *s.c.*, 1-5 d and 8-10 d + **Entinostat:** 7 mg, *p.o.*, d 3, d 10, every 4 w • **Result:** ORR: 0/22 (0%), TTP: 1.9 months, SAE: 5/22 (23%)	NCT01105377
Breast cancer	Phase 2	2011, Active	Study of azacytidine in combination with entinostat in patients with advanced breast cancer, for determining (i) ORR (ii) safety and tolerability, and (iii) PFS, OS, and clinical benefit rate of the combination; • **Azacytidine:** 40 mg/m^2, *s.c.*, 1-5 d and 8-10 d + **Entinostat:** 7 mg, *p.o.*, d 3, d 10, every 4 w • **Result:** ORR: 4%, OS: 6.6 months, PFS: 1.4 months, SAE: 2/40 (5%)	NCT01349959
MDS, AML	Phase 2	2005, Completed	Study of azacytidine in combination with valproic acid and all-trans retinoic acid in patients with high-risk MDS and AML, for determining (i) MTD of valproic acid in combination (ii) the safety and effectiveness of the combination therapy, and (iii) the *in vivo* molecular and biological effects of the combination such as analysis of changes in DNA methylation, histone modifications, and gene expression; • **Azacytidine:** 75 mg/m^2, *s.c.*, daily, 1-7 d + **Valproic Acid:** 50-62.5-75 mg/kg, *p.o.*, daily, 1-7 d + **All-Trans Retinoic Acid:** 45 mg/m^2, *p.o.*, daily (in two divided doses), 3-7 d, every 3 w • **Result:** ORR: 22/34 (65%), SAE: 31/34 (91%)	NCT00326170 (Soriano *et al*., 2007)
AML, MDS	Phase 2	2005, Completed	Randomized study of azacytidine in combination with valproic acid versus low-dose cytarabine in older patients ≥ 60 years with untreated AML or high-risk MDS not eligible for other therapies, for determining (i) EFS of either therapies, and (ii) to determine if the ability of azacytidine + valproic acid combination to induce demethylation or acetylation correlates with response;	NCT00382590

			• **Arm 1: Azacytidine:** 75 mg/m^2, *s.c.*, daily, 1-7 d + **Valproic Acid:** 50 mg/m^2, *p.o.*, daily, 1-7 d, every 4-6 w • **Arm 2: Cytarabine:** 20 mg, *s.c.*, twice daily, 1-10 d, every 4-6 w • **Result** (Arm 1 vs. Arm 2): ORR: 0/4 (0%) vs. 0/5 (0%), SAE: 4/4 (100%) vs. 6/6 (100%)	
Solid tumors	Phase 1	2007, Completed	Study of the safety and effectiveness of azacytidine in combination with carboplatin and valproic acid in patients with advanced solid tumors; • **Azacytidine:** 75 mg/m^2, *s.c.* or *i.v.*, daily, 1-5 d + **Valproic Acid:** 20-50 mg/kg, *p.o.*, daily, 5-11 d + **Carboplatin:** AUC 2-3, *i.v.*, d 3, d10 (not given in cycle 1), every 4 w • **Result:** MTD: 75 mg/m^2 (Azacytidine) + 20 mg/kg (Valproic Acid) + AUC 3.0 (Carboplatin), DLT: 6/32 (19%), Minor response or stable disease lasting ≥4 months: 6/32 (19%)	NCT00529022 (Falchook *et al*., 2013)
AML, MDS	Phase 2	2009, Active	Randomized study of the safety and effectiveness of azacytidine in combination with vorinostat as compared to azacytidine alone in patients with newly-diagnosed AML or MDS who are ineligible for other leukemia protocols; • **Azacytidine:** 75 mg/m^2/day, *i.v.*, 15-30 min, daily, 1-5 d, w/ or w/o **Vorinostat:** 200 mg, *p.o.*, thrice daily, 1-5 d, every 3-8 w • **Result** (Azacytidine vs. Azacytidine + Vorinostat): CR: 8/26 (31%) vs. 11/51 (22%), Survival-60 days: 18/27 (67%) vs. 43/51 (84%), SAE: 18/27 (67%) vs. 36/52 (69%)	NCT00948064
AML	Phase 1/2	2009, Completed	Non-randomized dose-escalation study of vorinostat in combination with azacytidine and gemtuzumab ozogamicin in older patients ≥ 50 years with relapsed or refractory AML, for determining (i) MTD and DLT of vorinostat in combination therapy (ii) CR and DFS, and (iii) *in vitro* correlative and mechanistic studies; • **Phase 1: Azacytidine:** 75 mg/m^2/day, *s.c.* or *i.v.*, 10-40 min, daily, 1-7 d + **Vorinostat:** 200-300-400 mg/day, *p.o.*, daily, 1-9 d + **Gemtuzumab Ozogamicin:** 3 mg/m^2/day, *i.v.*, 2 h, d 8 or d 4 and d 8, every 3 w • **Phase 2** (MTD defined in phase 1): **Azacytidine:** 75 mg/m^2/day, 1-7 d + **Vorinostat:** 400 mg/day, 1-9 d + **Gemtuzumab Ozogamicin:** 3 mg/m^2/day, d 4, d 8 • **Result** (Phase 1 and Phase 2): CR: 4/9 (44%) and 18/43 (42%), SAE: 6/10 (60%) and 13/43 (30%)	NCT00895934 (Walter *et al*., 2014)
MDS, CMML	Phase 2	2012, Active	Randomized study of azacytidine alone or in combination with lenalidomide or vorinostat in patients with higher-risk MDS and CMML, for determining (i) ORR for azacytidine alone versus combinations (ii) OS, RFS, cytogenetic response rate, and toxicity profile for each regimen, and (iii) association of cytogenetic abnormalities with clinical outcomes; • **Arm 1: Azacytidine:** *s.c.* or *i.v.*, 1-7 d or 1-5 d and 8-9 d, every 4 w • **Arm 2: Azacytidine (Arm 1)** + **Lenalidomide:** *p.o.*, daily, 1-21 d, every 4 w • **Arm 3: Azacytidine (Arm 1)** + **Vorinostat:** *p.o.*, twice daily, 3-9 d, every 4 w • **Result** (Arm 1 vs. Arm 2 vs. Arm 3): ORR: 35/92 (38%) vs. 46/93 (49%) vs. 25/92 (27%), OS: 15.0 months vs. 19.6 months vs. 17.6 months, RFS: 10.4 months vs. 14.5 months vs. 15.2 months, SAE: 8/91 (9%) vs. 37/89 (42%) vs. 47/91 (52%)	NCT01522976
➢ **Immunomodulatory agents: Lenalidomide, Gemtuzumab Ozogamicin, Lintuzumab, Filgrastim** (+ Darbepoetin Alfa)				
MDS	Phase 1/2	2006, Completed	Study of azacytidine in combination with linalidomide in patients with advanced MDS, for determining (i) MTD and DLT of the combination (ii) ORR (iii) TTP to AML or death (iv) DOR, and (v) to determine the effect of this regimen on hematologic status; • **Azacytidine:** 75 mg/m^2/day, *s.c.*, daily, 1-5 d or 1-5 and 8-12 d + **Lenalidomide:** 10 mg/day, *p.o.*, daily, 1-14 or 1-21 d, every 4 w • **Result:** ORR: 26/36 (72%), DOR: 17.0 months, OS: 13.6 months	NCT00352001 (Sekeres *et al*., 2012)
AML	Phase 1/2	2009, Completed	Study of azacytidine in combination with lenalidomide in older patients with previously untreated AML, for determining MTD of lenalidomide administered after azacytidine in phase 1, and the effectiveness of the combination treatment in phase 2; • **Azacytidine:** 75 mg/m^2, *s.c.* or *i.v.*, daily, 1-7 d + **Lenalidomide:** 5-10-25-50 mg, *p.o.*, daily, 8-28 d, every 4 w • **Result:** MTD of lenalidomide: 50 mg, CR: 12/43 (28%), ORR: 18/43 (42%), DOR: 1.4 months, Survival-4 weeks: 84%, OS: 4.7 months, SAE: 36/43 (84%)	NCT00890929 (Pollyea *et al*., 2012; Pollyea *et al*., 2013)
MDS, AML	Phase 1/2	2009, Completed	Study of azacytidine in combination with lenalidomide in patients with high-risk MDS and AML, for determining (i) MTD of lenalidomide in combination with azacytidine, and (ii) safety and effectiveness of the combination;	NCT01038635 (DiNardo *et al*., 2015)

			• **Azacytidine:** 75 mg/m^2/day, *i.v.*, 15-30 min, daily, 1-5 d + **Lenalidomide:** 10-15-20-25-50-75 mg, *p.o.*, daily, 6-10 or 6-15 d, every 3-8 w • **Result:** MTD of lenalidomide: 25 mg for 5 days, CR: 31/88 (35%), ORR: 27/60 (45%), SAE: 21/40 (53%)	
Multiple myeloma	-	2010, Completed	Pilot study of autologous lymphocyte (ALI) mobilization following immuno-modulatory therapy comprising azacytidine and lenalidomide in multiple myeloma, for determining (i) the feasibility of mobilizing and infusing ALI following immuno-modulatory therapy (ii) the ability to proceed with autologous stem cell transplantation in these patients (iii) CR, OS, PFS, TTP, and toxicity profile following transplant in patients treated with this regimen (iv) pre- and post-ALI immune response to cancer testis antigens (CTA), and (v) the expression of CTA in multiple myeloma before and after azacytidine therapy; • **Azacytidine:** 75 mg/m^2, *s.c.*, daily, 1-5 d + **Lenalidomide:** 15 mg, *p.o.*, daily, 6-21 d, every 4 w • **Result:** CR-6 months: 50%, OS-1 year: 93.3%, OS-2 year: 86.1%, PFS-1 year: 87.5%, PFS-2 year: 67.3%, TTP: 14.9 months, CTA-specific T cell response: 3/17 (18%), CTA up-regulation: 6/17 (35%), SAE: 9/17 (53%)	NCT01050790
AML	Phase 1/2	2010, Completed	Non-randomized study of azacytidine in combination with lenalidomide in AML, for determining (i) toxicity and feasibility of the combination in patients with relapsed or refractory AML ≥ 18 years or untreated AML ≥ 60 years in phase 1 (ii) CR and DOR (iii) ORR, OS, EFS, RFS, and TTP in untreated AML ≥ 60 years, and (iv) toxicity profile of the combination in phase 2; • **Induction regimen: Azacytidine:** 25-50-75 mg/m^2, *i.v.*, daily, 1-5 d + **Lenalidomide:** 50 mg, *p.o.*, daily, 1-28 d • **Maintenance regimen: Azacytidine:** 75 mg/m^2, *i.v.*, daily, 1-5 d + **Lenalidomide:** 10 mg, *p.o.*, daily, 1-28 d • **Result:** MTD of azacytidine: 75 mg/m^2, CR: 2/9 (22%), DOR: 12.2 months, ORR: 7/9 (78%), OS: 4.3 months, EFS: 2.9 months, RFS: 12.2 months, TTP: 3.7 months, SAE: 12/12 (100%)	NCT01016600
Lymphoma	Phase 2	2010, Terminated	Non-randomized study of the safety and effectiveness of azacytidine in combination with lenalidomide in patients with relapsed or refractory follicular or marginal zone lymphoma; • **Azacytidine:** 75 mg/m^2, *s.c.* or *i.v.*, daily, 1-5 d + **Lenalidomide:** 15 mg, *p.o.*, daily, 1-21 d, every 4 w; Arm 1: azacytidine followed by lenalidomide, Arm 2: lenalidomide followed by azacytidine • **Result** (Arm 1 vs. Arm 2): ORR: 2/4 (50%) vs. 0/1 (0%), SAE: 2/6 (33%) vs. 2/3 (67%)	NCT01121757
AML	Phase 2	2012, Active	Randomized study for comparing the safety and effectiveness of three different regimens (i) high-dose lenalidomide (ii) lenalidomide + azacytidine, and (iii) azacytidine in older patients ≥ 65 years with newly-diagnosed AML; • **Regimen A: Lenalidomide:** 50 mg (cycle 1, 2) – 25 mg (cycle 3, 4) – 10 mg (remaining cycles), *p.o.*, daily for 4 w + BSC • **Regimen B: Azacytidine:** 75 mg/m^2/day, *s.c.*, daily, 1-7 d + **Lenalidomide:** 50 mg, *p.o.*, daily, 8-28 d followed by a 14-days break + BSC • **Regimen C: Azacytidine:** 75 mg/m^2/day, *s.c.*, daily, 1-7 d followed by a 21-days break + BSC • **Result** (Regimen A vs. Regimen B vs. Regimen C): Survival-1 year: 3 months vs. 9.6 months vs. 13.7 months, SAE: 13/14 (93%) vs. 29/38 (76%) vs. 25/32 (78%)	NCT01358734
AML	Phase 2	2008, Active	Study of azacytidine in combination with gemtuzumab ozogamicin as induction and post-remission therapy in older patients ≥ 60 years with previously untreated non-M3 AML, for determining (i) Phase 3 trial justification based on outcomes (ii) toxicity profile in good- and poor-risk patients (iii) DFS and cytogenetic response rate, and (iv) the effects of cytogenetic abnormalities, promoter and global methylation changes, and multidrug resistance on OS and response to the combination therapy; • **Remission induction therapy: Azacytidine:** 75 mg/m^2, *s.c.* or *i.v.*, 10-40 min, daily, 1-7 d + **Gemtuzumab Ozogamicin:** 3 mg/m^2, *i.v.*, 2 h, d 8 • **Consolidation therapy: Azacytidine:** 75 mg/m^2, *s.c.*, daily, 1-7 d + **Gemtuzumab Ozogamicin:** 3 mg/m^2, *i.v.*, 2 h, d 8 • **Maintenance therapy:** 75 mg/m^2, *s.c.*, daily, 1-7 d, every 4 w • **Result** [Good-risk vs. Poor-risk patients: CR: 35/79 (44%) vs. 19/54 (35%), Survival-30 days: 92% vs. 87%, RFS: 8 months vs. 7 months], [SAE: Remission induction therapy: 55/133 (41%), Consolidation therapy: 1/32 (3%), Maintenance therapy: 3/27 (11%)]	NCT00658814 (Nand *et al*., 2013)
MDS	Phase 2	2009, Terminated	Study of azacytidine in combination with lintuzumab in patients with previously untreated MDS, for determining (i) CR, ORR, and toxicity profile of the combination regimen (ii) the correlation between pre-treatment and drug-induced changes in expression of *Syk* and clinical response (iii) biological activity of azacytidine as demethylating agent (iv) exploratory studies of azacytidine-triphosphate with global DNA methylation, and (vi) the biologic role of miRNA in determining clinical response and other PD endpoints;	NCT00997243

			• **Azacytidine:** 75 mg/m^2, *s.c.* or *i.v.*, daily, 1-7 d + **Lintuzumab:** 600 mg, *i.v.*, d 2, d 7, d 15, d 22, every 4 w (cycle 1) – d 7, d 22, every 4 w (subsequent cycles) • **Result:** CR: 1/7 (14%), ORR: 1/7 (14%), SAE: 7/7 (100%)	
MDS	Phase 2	2006, Terminated	Non-randomized study of azacytidine in combination with hematopoietic growth factors, darbepoetin alfa and filgrastim, for determining (i) the hematological response rate (ii) time to progression to AML or death (iii) OS and PFS, and (iv) changes in apoptotic index of bone marrow in patients treated with this regimen; • **Azacytidine:** 100 or 125 mg/m^2, *s.c.*, daily, 1-5 d, every 4 w + **Filgrastim:** 300 µg (weight < 100 kg) or 450 µg (weight ≥100 kg), *s.c.*, thrice weekly, w 2-4 + **Darbepoetin Alfa:** 500 µg, *s.c.*, d 8, every 4 w • **Result:** CR: 0/3 (0%), SAE: 1/3 (33%)	NCT00398047
MDS	Phase 2	2012, Terminated	Study of the safety and effectiveness of azacytidine in combination with filgrastim in patients with low- or intermediate-1- risk MDS; • **Azacytidine:** 40 mg/m^2, *s.c.* or *i.v.*, 15-30 min, daily, 1-4 d + **Filgrastim:** 250 mcg/m^2, *s.c.* or *i.v.*, 15 min, daily, 5-7 d, every 4-6 w • **Result:** ORR: 0/8 (0%), SAE: 3/8 (38%)	NCT01542684
➢ **Targeted therapies: Ilorasertib, Sorafenib, Midostaurin** (+ Deferasirox)				
AML, MDS, CMML	Phase 1	2010, Completed	Non-randomized study for determining the safety, PK, and MTD of ilorasertib as monotherapy and in combination with azacytidine in patients with advanced hematologic malignancies; • **Arm 1: Ilorasertib:** 10-690 mg, *p.o.*, once weekly, d 1, d 8, d 15, every 4 w • **Arm 2: Ilorasertib:** 320 or 480 mg, *p.o.*, twice weekly, d 1, d2, d 8, d 9, d 15, d 16, every 4 w • **Arm 3: Ilorasertib:** 440 mg, *p.o.*, once weekly, d 1, d 8, d 15, every 4 w + **Azacytidine:** *s.c.* or *i.v.*, daily, 1-7 d, every 4 w • **Arm 4: Ilorasertib:** 32 mg (starting dose), *i.v.*, once weekly, d 1, d 8, d 15, every 4 w • **Result:** MTD: not determined, Recommended phase 2 oral monotherapy dose: 540 mg once weekly or 480 mg twice weekly, Half-life of oral Ilorasertib: 15 h, ORR (Arm 1, 2): 3/52 (6%), TTP: 1.8 months	NCT01110473 (Garcia-Manero *et al*., 2015)
AML, MDS	Phase 1/2	2011, Completed	Study of the safety and effectiveness of azacytidine in combination with sorafenib in patients with relapsed or refractory AML and MDS; • **Azacytidine:** 75 mg/m^2, *s.c.* or *i.v.*, 10-40 min, daily, 1-7 d, every 4 w + **Sorafenib:** 200-400 mg, *p.o.*, twice daily, continuously, 12 h apart • **Result:** MTD of sorafenib: 400 mg, ORR: 25/48 (52%), SAE: 0/57 (0%)	NCT01254890 (Ravandi *et al*., 2013)
AML, MDS	Phase 1/2	2011, Completed	Study of the safety and effectiveness of azacytidine in combination with midostaurin in patients with relapsed or refractory AML and MDS; • **Azacytidine:** 75 mg/m^2/day, *s.c.* or *i.v.*, 30 min, daily, 1-7 d, every 4 w + **Midostaurin:** 25 or 50 mg, *p.o.*, twice daily, 8-21 d, every 4 w (cycle 1) – daily continuously, as of cycle 2 • **Result:** MTD of midostaurin: 50 mg, ORR: 14/54 (26%), SAE: Phase 1 (Azacytidine + 25 mg Midostaurin): 5/6 (83%), Phase 1 (Azacytidine + 50 mg Midostaurin): 5/8 (63%), Phase 2: 29/40 (73%)	NCT01202877
MDS	Phase 2	2014, Terminated	Randomized study for determining the ORR in patients with higher-risk MDS treated with azacytidine alone or in combination with deferasirox; • **Azacytidine:** 75 mg/m^2, *s.c.*, daily, 1-7 d, every 4 w, w/ or w/o **Deferasirox:** 10mg/kg/day • **Result:** SAE: 1/1 (100%)	NCT02159040

Table 1.6 Decitabine in combinatorial therapies

This table summarizes all registered clinical trials of decitabine in combination with various chemotherapeutic, epigenetic or immunomodulatory agents for which study results have been posted or are available as publications.

Conditions	Phase	Study start, Status	Brief summary	NCT number (References)
➢ **Standard chemotherapy drugs: Arsenic Trioxide, Carboplatin, Clofarabine, Cytarabine, Vincristine Sulfate, Doxorubicin Hydrochloride, PEG Asparaginase, Methotrexate** (+ Ascorbic Acid, Filgrastim, Aclacinomycin, Omacetaxine Mepesuccinate, Vorinostat, Prednisone, Imatinib Mesylate, Cytokine-induced killer cells)				
MDS	Phase 2	2007, Completed	Non-randomized pilot study of decitabine in combination with As_2O_3 and ascorbic acid in MDS for determining the safety of the combination; • **Decitabine:** 20 mg/m^2, *i.v.*, 1 h daily, 1-5 d, every 4 w + **As_2O_3:** 0.25 mg/kg, *i.v.*, daily, 1-5 d for cycle 1(4w) followed by 0.25 mg/kg, twice weekly (Mon-Thu or Tue-Fri) for all remaining cycles + **Ascorbic Acid:** 1000 mg in 100 mL solution of 5% dextrose in water, *i.v.*, 15-30 min, administered within 30 min of As_2O_3 administration • **Result:** ORR: 0/6 (0%), SAE: 4/6 (67%)	NCT00621023
MDS, AML	Phase 1	2008, Completed	Non-randomized study of the safety and effectiveness of decitabine in combination with As_2O_3 and ascorbic acid in order to improve response rate in patients with *de novo* or secondary MDS and AML; • **Decitabine:** 20 mg/m^2/day, *i.v.*, daily, 1-5 d, every 4 w + **As_2O_3:** 0.1 mg/kg/day, *i.v.*, daily, 1-5 d followed by 0.1 mg/kg, *i.v.*, weekly or : 0.2 mg/kg/day, *i.v.*, daily, 1-5 d followed by 0.2 mg/kg, *i.v.*, weekly or : 0.3 mg/kg/day, *i.v.*, daily, 1-5 d followed by 0.3 mg/kg, *i.v.*, weekly + **Ascorbic Acid:** 1000 mg, *i.v.*, following each dose of As_2O_3 • **Result:** MTD of As_2O_3 in combination: 0.2 mg/kg, CR: 1/13 (8%)	NCT00671697 (Welch *et al*., 2011)
Ovarian cancer	Phase 1/2	2007, Completed	Study of decitabine as a sensitizer to carboplatin in patients with platinum refractory or platinum resistant recurrent ovarian cancer, for determining the safety and biologic activity of the combination; • **Decitabine:** 10mg/m^2 (dose level 1) - 20mg/m^2 (dose level 2), *i.v.*, 1 h daily, 1- 5 d + **Carboplatin:** Dose ~ AUC 5, *i.v.*, 30 min, d 8, every 4 w • **Result:** MTD: 10 mg/m^2, ORR: 6/17 (35%), PFS: 10.2 months, SAE: Phase 1: 3/11 (27%), Phase 2: 4/17 (24%)	NCT00477386 (Fang *et al*., 2010; Matei *et al*., 2012)
AML, MDS	Phase 2	2008, Completed	Study of the safety and effectiveness of clofarabine in combination with low-dose cytarabine and decitabine in older patients ≥ 60 years with AML or high-risk MDS; • **Clofarabine:** 20 mg/m^2, *i.v.*, 1-2 h daily, 1-5 d + **Cytarabine:** 20 mg, *s.c.*, twice daily, 1-10 d, administered 3-6 h following the start of the clofarabine infusions + **Decitabine:** 20 mg/m^2, *i.v.*, 1-2 h daily, 1-5 d • **Result:** ORR: 73/118 (62%), OS: 11.1 months, DFS: 15.9 months, EFS: 7.7 months, SAE: 12/119 (10%)	NCT00778375
AML, MDS	Phase 2	2008, Terminated	Non-randomized study of the feasibility and toxicity of decitabine in combination with low-dose cytarabine and filgrastim in patients with high-risk MDS, refractory AML or AML patients with significant co-morbidities; • **Decitabine:** 20 mg/m^2, *i.v.*, 1 h daily, 1-5 d + **Cytarabine:** 20 mg/m^2, *s.c.*, daily, 1-5 d + **Filgrastim:** 5 mcg/kg, *s.c.*, daily, 1-5 d • **Result:** ORR: 1/9 (11%), SAE: 8/9 (89%)	NCT00740181
MDS, AML	Phase 1/2	2012, Completed	Study of the effectiveness of decitabine-based chemotherapy followed by haploidentical lymphocyte infusion (HLI) in elderly patients with intermediate-high risk MDS or AML; • **Decitabine:** 20 mg/m^2, *i.v.*, daily, 1-5 d + **Aclacinomycin:** 20mg, *i.v.*, every second day for 5 days + **Cytarabine:** 10 mg/m^2, *s.c.*, every 12 h for 5 days +	NCT01690507 (Jing *et al*., 2016)

			Filgrastim: 300 µg/day, *s.c.*, from day 0 to neutrophil recovery, every 4 w + HLI (36 h after the last dose of chemotherapy) • **Result:** CR: 21/29 (72%), OS-1 year: 72.2%, OS-2 year: 59.6%, DFS-1 year: 47.3%, DFS-2 year: 36.9%	
AML	Phase 2	2014, Terminated	Study of decitabine in combination with OAG (cytarabine, omacetaxine mepesuccinate) in older patients ≥ 65 years with newly diagnosed AML who are ineligible for intensive induction therapy, for determining (i) CR (ii) toxicity, and (iii) DFS and OS of these regimens; • **Induction chemotherapy: OAG:** *s.c.*, twice daily, 1-14 d, every 4 w • **Consolidation therapy** (alternative courses between decitabine and OAG): **Decitabine:** *i.v.*, daily, 1-5 d, every 4 w; **OAG:** *s.c.*, twice daily, 1-7 d, every 4 w • **Result:** SAE: 2/2 (100%)	NCT02029417
ALL, Lymphoblastic lymphoma	Phase 2	2009, Terminated	Study of the effectiveness of decitabine and vorinostat in combination with chemotherapy in patients with relapsed or refractory acute lymphoblastic leukemia or lymphoblastic lymphoma; • **Decitabine:** 15 mg/m^2, *i.v.*, 1 h daily, 1-4 d + **Vorinostat:** 230 mg/m^2, *p.o.*, divided twice (max dose 400 mg daily), 1-4 d + **Prednisone:** 40 mg/m^2/day, *p.o.*, divided twice, 5-33 d + **Vincristine Sulfate:** 1.5 mg/m^2 (max 2 mg), *i.v.*, d 5, d 12, d 19, d 26 + **Doxorubicin Hydrochloride:** 60 mg/m^2, *i.v.*, 15 min, d 5 + **PEG Asparaginase:** 2,500 IU/m^2, *i.m.* or *i.v.*, d 6, d 12, d 19, d 26 + **Cytarabine:** 30-70 mg (depending upon age), *i.t.*, d 5 + **Methotrexate:** 8-15 mg (depending upon age), i.t., d 12, d 33 + **Imatinib Mesylate** (for patients with Philadelphia chromosome-positive disease): 340 mg/m^2 (age <18 years) and 400 mg (age >18 years), *p.o.*, daily, 5-33 d • **Result:** ORR: 6/8 (75%), SAE: 8/13 (62%)	NCT00882206 (Burke *et al*., 2014)
Solid tumors, Lymphoma	Phase 1/2	2012, Recruiting	Study of the safety and effectiveness of low-dose decitabine alone or in combination with chemotherapy and/or autologous cytokine induced killer cells (CIK) in patients with relapsed or refractory solid tumors and B cell lymphomas; • **Decitabine:** 7 mg/m², *i.v.*, daily, 1-5 d, every 4 w or **Decitabine + Chemotherapy** or **Decitabine + CIK:** 1-5 × 10^9/L for two days in 4 w cycle • **Result** (Decitabine vs. Decitabine + Chemotherapy vs. Decitabine + CIK; 6 cycles): ORR: 1/2 (50%) vs. 7/11 (64%) vs. 4/5 (80%)	NCT01799083 (Fan *et al*., 2014)
➢ **Histone deacetylase inhibitors: Valproic Acid, Vorinostat, Panobinostat** (+ Temozolomide)				
Leukemia, MDS	Phase 1/2	2004, Completed	Study of decitabine in combination with valproic acid in patients with relapsed or refractory leukemia or MDS, for determining the MTD of the valproic acid in combination; • **Decitabine:** 15 mg/m^2, *i.v.*, 1 h daily, 1-10 d, w/ or w/o **Valproic Acid:** 20-35-50 mg/kg, *p.o.*, daily, 1-10 d • **Result:** MTD: 50 mg/kg, ORR: 12/53 (22%), DFS: 5.6 months, OS: 6 months	NCT00075010 (Garcia-Manero *et al*., 2006)
AML, Chronic lymphocytic leukemia, Small lymphocytic lymphoma	Phase 1	2004, Completed	Study of decitabine in combination with valproic acid in patients with relapsed or refractory AML or previously treated chronic lymphocytic leukemia or small lymphocytic lymphoma, for determining (i) BED of decitabine (ii) MTD and BED of valproic acid in combination with BED of decitabine (iii) toxic effects and therapeutic response of decitabine alone and in combination with valproic acid (iv) PK of the combined regimen (v) kinetics of DNMTs and re-expression of selected methylated genes, and histone deacetylase enzyme inhibition and changes in the acetylation status of histones, and (vi) correlate baseline and post-treatment changes in DNMTs expression and in histone code with disease response in these patients; • **Decitabine:** 15-20 mg/m^2/day, *i.v.*, 1 h daily, 1-5 or 1-10 d, every 4 w, w/ or w/o **Valproic Acid:** 15-20-25 mg/kg, *p.o.*, thrice daily, 5-21 d, every 4 w • **Result:** BED of decitabine: 20 mg/m^2/d (1-10 d), MTD: Decitabine; 20 mg/m^2/d (1-10 d) + Valproic Acid; 20 mg/kg/d (5-21 d), ORR: 11/21 (52%)	NCT00079378 (Blum *et al*., 2007)
MDS, AML	Phase 2	2006, Completed	Randomized study for determining the safety and effectiveness of low-dose decitabine with or without valproic acid in MDS or AML; • **Decitabine:** 20 mg/m^2, *i.v.*, 1 h daily, 1-5 d, every 4-8 w, w/ or w/o **Valproic Acid:** 50 mg/kg, *p.o.*, daily, 1-7 d, every 4-8 w • **Result** (Decitabine vs. Decitabine + Valproic Acid): ORR: 28/70 (40%) vs. 39/79 (49%), SAE: 43/71 (61%) vs. 49/79 (62%)	NCT00414310
AML, MDS	Phase 1	2007, Completed	Non-randomized study of the safety and tolerability of vorinostat in combination with decitabine, and *in vivo* molecular and biological effects of vorinostat in patients with refractory or relapsed AML and intermediate or high-risk MDS; • **Sequential: Vorinostat:** 400 mg, *p.o.*, once daily, 1-7 or 1-10 or 1-14 d + **Decitabine:** 20 mg/m^2, *i.v.*, daily, 1-5 d, every 4 w	NCT00479232 (Kirschbaum *et al*., 2014)

			• **Concurrent: Vorinostat:** 400 mg, *p.o.*, once daily, 1-7 or 1-7 and 15-21 or 1-14 d + **Decitabine:** 20 mg/m^2, *i.v.*, daily, 1-5 d, every 4 w • **Result** (sequential vs. concurrent): ORR (refractory or relapsed AML): 0/15 (0%) vs. 1/14 (7%), ORR (untreated or intermediate AML): 3/22 (14%) vs. 7/20 (35%), SAE: sequential (vorinostat; 1-7 d): 2/3 (67%), sequential (vorinostat; 1-10 d): 4/4 (100%), sequential (vorinostat; 1-14 d): 25/31 (81%), concurrent (vorinostat; 1-7 d): 3/3 (100%), concurrent (vorinostat; 1-7 and 15-21 d): 1/3 (33%), concurrent (vorinostat; 1-14 d): 21/28 (75%)	
MDS, AML	Phase 1/2	2008, Completed	Non-randomized study of the safety and effectiveness of decitabine in combination with panobinostat in older patients ≥ 60 years with high-risk MDS or AML; • **Decitabine:** 20 mg/m^2, *i.v.*, daily, 1-5 d + **Panobinostat:** 10 mg/day (Level 1) or 15 mg/day (Level 2) or 20 mg/day (Level 3) or 30 mg/day (Level 4) or 40 mg/day (Level 5), thrice weekly on nonconsecutive days or 40 mg/day (Level 5B), thrice weekly on nonconsecutive days for the first 2 w in a 4 w cycle • **Result:** MTD of panobinostat in combination: 40 mg/day (Level 5B), ORR: 6/51 (12%), DOR: 12.0 months, EFS: 3.5 months, OS: 6.4 months, SAE: Level 1: 0/4 (0%), Level 2: 0/3 (0%), Level 3: 0/6 (0%), Level 4: 0/8 (0%), Level 5: 0/10 (0%), Level 5B: 0/6 (0%), Phase 2: 0/14 (0%)	NCT00691938
Melanoma	Phase 1/2	2009, Terminated	Study of decitabine and temozolomide in combination with panobinostat for the treatment of resistant metastatic melanoma, for determining (i)safety and tolerability of the proposed schedule of decitabine, temozolomide, and panobinostat (ii) DLT and MTD of the combination (iii) OS, and (iv) TTP of patients treated with the combination in comparison to patients treated historically with the current standard of care; • **Decitabine:** 0.1-0.2 mg/kg, *s.c.*, thrice weekly for 2 w (starting on d 1) + **Panobinostat:** 10-20-30 mg, *p.o.*, every 96 h for 2 w (starting on d 8) + **Temozolomide:** 150 mg/m^2/day, *p.o.*, 9-13 d (cycle 1) -200 mg/m^2/day, *p.o.*, 9-13 d (after cycle 1, if neutropenia or thrombocytopenia had not occurred) • **Result:** DLT: 0/15, MTD: not reached, CR: 1/8 (13%), DOR: 8 months, SAE: 5/39 (13%)	NCT00925132 (Xia *et al*., 2014)
Breast cancer	Phase 1/2	2010, Terminated	Trial of tamoxifen following the epigenetic re-expression of estrogen receptor, using the combination of decitabine and panobinostat in patients with triple negative metastatic breast cancer; • **Decitabine (***i.v.*, daily, 1-5 d, every 4 w) + **Panobinostat** (*i.v.*, d 1, d 8, every 4 w)**:** 5 mg/m^2 + 10 mg/m^2 (dose level -1) – 10 mg/m^2 + 10 mg/m^2 (dose level 0) – 10 mg/m^2 + 15 mg/m^2 (dose level +1) – 10 mg/m^2 + 20 mg/m^2 (dose level +2) – 15 mg/m^2 + 20 mg/m^2 (dose level +3) – 20 mg/m^2 + 20 mg/m^2 (dose level +4) • **Result:** SAE: 4/5 (80%)	NCT01194908
➢ **Immunomodulatory agents: Romiplostim, IFNα-2b, Gemtuzumab Ozogamicin, Panitumumab, Rapamycin**				
MDS, Thrombocytopenia	Phase 2	2006, Completed	Randomized, double blind placebo controlled study for evaluation of the safety and effectiveness of romiplostim, at reducing the incidence of clinically significant thrombocytopenic events in low or intermediate risk MDS patients receiving hypomethylating agents, azacytidine or decitabine; • **Regimen A: Azacytidine:** 75 mg/m^2, *s.c.*, daily, 1-7 d + **Romiplostim:** 500 µg, *s.c.*, once weekly, every 4 w • **Regimen B: Azacytidine:** 75 mg/m^2, *s.c.*, daily, 1-7 d + **Romiplostim:** 750 µg, *s.c.*, once weekly, every 4 w • **Regimen C: Decitabine:** 20 mg/m^2, *i.v.*, 1 h daily, 1-5 d + **Romiplostim:** 750 µg, *s.c.*, once weekly, every 4 w • **Regimen D: Azacytidine:** 75 mg/m^2, *s.c.*, daily, 1-7 d, every 4 w + **Placebo:** *s.c.*, once weekly • **Regimen E: Decitabine:** 20 mg/m^2, *i.v.*, 1 h daily, 1-5 d, every 4 w + **Placebo:** *s.c.*, once weekly • **Result (A, B, C, D, E):** ORR: 1/13 (8%), 1/14 (7%), 5/15 (33%), 2/13 (15%), 3/14 (21%); Occurrence of a clinically significant thrombocytopenic event: 8/13 (62%), 10/14 (71%), 12/15 (80%), 11/13 (85%), 11/14 (79%); SAE: 4/13 (31%), 10/14 (71%), 8/15 (53%), 9/13 (69%), 8/14 (57%)	NCT00321711 (Greenberg *et al*., 2013; Kantarjian *et al*., 2010)
Renal cell carcinoma	Phase 2	2007, Terminated	Study of low-dose decitabine in combination with IFNα-2b in advanced renal cell carcinoma, for determining (i) ORR, OS, and PFS (ii) toxicity of the combination (iii) the effects on DNA methylation and gene expression, and (iv) modulation of cellular immunity in correlation with clinical outcomes; • **Decitabine:** 15 mg/m^2, *i.v.*, 1 h daily, 1-5 d, every 4 w + **IFNα-2b:** 0.5 million U, *s.c.*, twice daily continuously, d 1, as of cycle 3 • **Result:** SAE: 0/1 (0%)	NCT00561912
AML, MDS	Phase 2	2008, Completed	Study of the safety and effectiveness of decitabine in combination with gemtuzumab ozogamicin in AML or high-risk MDS; • **Decitabine:** 20 mg/m^2, *i.v.*, 1-1/2 h daily, 1-5 d + **Gemtuzumab Ozogamicin:** 3 mg/m^2, *i.v.*, 1 h, d 5, every 4-6 w	NCT00968071

			• **Result:** CR: 3/71 (4%), SAE: 15/71 (21%)	
AML, MDS, Myelofibrosis	Phase 2	2009, Completed	Study of the safety and effectiveness of decitabine in combination with gemtuzumab ozogamicin in AML, high-risk MDS or myelofibrosis; • **Decitabine:** 20 mg/m^2, *i.v.*, 1-1/2 h daily, 1-5 d + **Gemtuzumab Ozogamicin:** 3 mg/m^2, *i.v.*, 1 h, d 5, every 4-8 w • **Result:** CR: 10/40 (25%), SAE: 1/40 (3%)	NCT00882102
Colorectal cancer	Phase 1	2009, Completed	Study of the safety and feasibility of the sequential use of decitabine with panitumumab for KRAS wild-type advanced metastatic colorectal cancer, for determining (i) demethylation-induced re-expression of TSGs involved in colorectal cancer or EGFR signaling pathway, (ii) ORR, and (iii) PFS of patients with panitumumab and decitabine vs. patients treated with previous anti-EGFR therapy; • **Decitabine:** 45 mg/m^2, *i.v.*, 2 h, d 1, d 15 + **Panitumumab:** 6 mg/kg, *i.v.*, 1 h, d 8, d 22, every 4 w • **Result:** ORR: 2/20 (10%), PFS: 7 patients had a longer PFS with panitumumab and decitabine compared to their previous anti-EGFR treatment regimen	NCT00879385 (Garrido-Laguna *et al*., 2013)
AML	Phase 1	2010, Completed	Non-randomized study of the safety and feasibility of decitabine in combination with escalating doses of rapamycin in patients with relapsed or refractory AML; • **Decitabine:** 20 mg/m^2, *i.v.*, daily, 1-5 d + **Rapamycin:** 2-4-6 mg/daily, *p.o.*, daily, 6-25 d, every 4 w • **Result:** MTD: not reached, ORR: 1/13 (8%)	NCT00861874 (Liesveld *et al*., 2013)
➢ **Targeted therapy: Bortezomib**				
AML	Phase 1	2008, Completed	Study of decitabine in combination with bortezomib in AML, for determining (i) MTD of bortezomib in combination with decitabine (ii) specific toxicities and the DLT of the combination (iii) ORR and CR rate (iv) to correlate the biological activity of decitabine as demethylating agent with clinical endpoints and PK of decitabine, and intracellular concentration of decitabine triphosphate with biological endpoints and clinical response (v) to characterize the biological activity of bortezomib as a potential demethylating agent, and (vi) the biologic role of microRNAs in determining clinical response to the decitabine plus bortezomib combination and achievement of the other PD endpoints; • **Decitabine:** 20 mg/m^2, *i.v.*, 1 h daily, 1-5 d or 1-10 d + **Bortezomib:** 0.7 mg/m^2, *i.v.*, d 5, d 8 (dose level 1); 0.7 mg/m^2, *i.v.*, d 5, d 8, d 12, d 15 (dose level 2); 1.0 mg/m^2, *i.v.*, d 5, d 8, d 12, d 15 (dose level 3); 1.3 mg/m^2, *i.v.*, d 5, d 8, d 12, d 15 (dose level 4), every 4 w • **Result:** MTD of bortezomib in combination: 1.3 mg/m^2 (dose level 4), ORR: 7/19 (37%)	NCT00703300 (Blum *et al*., 2012)
AML	Phase 2	2011, Active	Randomized study of decitabine with or without bortezomib in older patients ≥ 60 years with AML, for determining (i) the effectiveness of combination therapy at improving the OS times as compared to decitabine alone (ii) CR, OS, PFS, and DFS for both regimens (iii) if ongoing treatment with these regimens prolongs OS even in the absence of CR (iv) the frequency and severity of adverse events and tolerability of both regimens; • **Arm 1 (Decitabine):** [Remission induction therapy: 20 mg/m^2, *i.v.*, 1 h daily, 1-10 d, every 4 w], [Continuation/Maintenance therapy: 20 mg/m^2, *i.v.*, 1 h daily, 1-5 d, every 4 w] • **Arm 2 (Decitabine + Bortezomib):** [Remission induction therapy: **Decitabine:** 20 mg/m^2, *i.v.*, 1 h daily, 2-11 d + **Bortezomib:** 1.3 mg/m^2, *s.c.*, d 1, d 4, d 8, d 11, every 4 w], [Continuation/Maintenance therapy: **Decitabine:** 20 mg/m^2, *i.v.*, 1 h daily, 1-5 d + **Bortezomib:** 1.3 mg/m^2, *s.c.*, d 1, every 4 w] • **Result** (Arm 1 vs. Arm 2): CR: 33/82 (40%) vs. 31/81 (38%), OS: 9.3 months vs. 8.8 months, DFS: 8.5 months vs. 15.3 months, PFS: 7.3 months vs. 8 months, SAE: 43/80 (54%) vs. 45/79 (57%)	NCT01420926

Table 1.7 Zebularine in combinatorial therapies

This table presents the combinatorial effects of zebularine with various epigenetic and chemotherapeutic agents tested so far.

Combination drug	Types of cancer	Effects of combination therapies	References
Decitabine	Leukemia	• Zeb when combined with decitabine resulted in greater inhibition of cell growth and colony formation in leukemic cell lines, as compared to either agent alone • The combination of Zeb and decitabine further produced synergistic effects at inducing demethylation and re-expression of TSG, *p57KIP2* as compared to either drug alone • *In vivo*, the combination of Zeb with decitabine resulted in increased survival of mice bearing leukemia cells as compared to either drug alone	Lemaire *et al*., 2005
Decitabine	Leukemia	• Zeb in combination with decitabine significantly enhanced the anti-neoplastic action of decitabine *in vitro* in leukemic cells expressing high levels of CDA • *In vivo*, in mice bearing leukemia cells, co-infusion of Zeb with decitabine significantly increased the plasma level of decitabine, and enhanced the survival time of mice	Lemaire *et al*., 2009
Decitabine, Vorinostat	Breast	• Low-dose Zeb in combination with decitabine or vorinostat significantly inhibited cell proliferation and colony formation in breast cancer cells, as compared with either drug alone	Billam *et al*., 2010
Vorinostat	Osteosarcoma	• Zeb in combination with vorinostat showed additive and significant cytotoxic effects in human and canine osteosarcoma cells with aggressive biological behavior	Thayanithy *et al*., 2012
Entinostat	Leukemia	• Zeb in combination with entinostat increased the effect of histone deacetylase inhibition at inducing the re-expression of TSG, *AKAP12* in leukemic cells with dense *AKAP12* methylation	Flotho *et al*., 2007
Depsipeptide	Lung	• Zeb alone or in combination with depsipeptide yielded additive or synergistic growth inhibitory effects via re-induction of silenced *CDKN2A* gene in lung cancer cell lines	Chen *et al*., 2010
Retinoic acid, Sodium phenylbutyrate, BML-210	Leukemia	• Zeb alone inhibited cell proliferation in a dose- and time-dependent manner, elicited a dose-dependent increase in growth inhibition and cell death, and in combination with retinoic acid showed additive anti-proliferative and apoptotic effects in leukemia cells • Pre-treatment with Zeb or simultaneous combination of Zeb with sodium phenylbutyrate and BML-210, and retinoic acid accelerated cell differentiation caused by retinoic acid alone • Combination of Zeb with retinoic acid resulted in greater depletion of DNMT1 and greater re-expression of TSG, *E-cadherin* at both mRNA and protein levels, as compared to treatment with either single drug	Savickiene *et al*., 2012a
Retinoic acid	Pituitary	• Pre-treatment of pituitary cells with Zeb along with trichostatin rendered retinoic acid-augmented expression of silenced genes, *BMP-4* and *D2R*, potentially involved in mediating responsiveness to drugs commonly used in this tumor type	Yacqub-Usman *et al*., 2013
Cisplatin	Ovary	• Zeb produced significant anti-proliferative effects against ovarian cancer cell lines, including cisplatin-resistant ovarian cancer cells in a dose-dependent manner, and induced demethylation and re-expression of various TSGs, *RASSF1A*, *hMLH1 ARHI*, and *BLU* • Zeb treatment significantly re-sensitized the cisplatin-resistant ovarian cancer cells to cisplatin, suggesting its potential in therapy of drug-resistant ovarian cancer	Balch *et al*., 2005
Cisplatin, 5-fluorouracil	Oral squamous cell carcinoma	• Low-dose Zeb in combination with cisplatin significantly enhanced the cisplatin-induced apoptotic cell death in oral squamous cell carcinoma cells	Suzuki *et al*., 2007
5-fluorouracil, Irinotecan,	Colorectal	• Zeb slightly potentiated the inhibitory effects of oxaliplatin and 5-fluorouracil, and the combination of Zeb with either chemotherapeutics, 5-fluorouracil, irinotecan, and oxaliplatin indicated synergistic or additive effects	Flis *et al*., 2009 Flis *et al*., 2014

Oxaliplatin		• Combination of Zeb with oxaliplatin and 5-fluorouracil increased the phosphorylation level of proteins of major signaling checkpoints in response to DNA damage, and showed augmented effects on cell cycle arrest and induction of apoptosis	Ikehata *et al*., 2014
Brostallicin	Prostate	• Pre-treatment of prostate cancer cells with Zeb enhanced the anti-proliferative activity of brostallicin, both *in vitro* and *in vivo* by inducing the re-expression of previously methylated *GST*	Sabatino *et al*., 2013
Methotrexate	Leukemia	• Zeb alone significantly inhibited cell proliferation in a dose- and time-dependent manner and colony formation in a dose-dependent manner in pediatric leukemia cell lines, and the combination of Zeb with methotrexate showed synergistic cytotoxic effects • Zeb treatment further induced and enhanced apoptotic cell death, decreased DNMT genes and protein levels, and induced *AhR* promoter demethylation and expression in pediatric leukemia cells	Andrade *et al*., 2014
Vincristine	Medulloblastoma	• Zeb combined with vincristine showed synergistic cytotoxic effects against medulloblastoma cell lines	Andrade *et al*., 2017
p53 retro-inverso peptide	Multiple myeloma	• Pre-treatment with Zeb followed by incubation with p53 retro-inverso peptide significantly reduced the cell viability, and enhanced the apoptosis as compared to singular treatment with p53 activating peptide in myeloma cell line with methylated p53	Hurt *et al*., 2006
Recombinant TRAIL	Leukemia, Breast, Prostate, Colon, Bladder	• Pre-treatment with Zeb sensitized leukemia, breast, prostate, colon, and bladder cancer cells to TRAIL-induced apoptosis by increasing the fucosylation level in a concentration dependent manner, and the expression levels of several kinds of fucosylation-related genes in these cells	Moriwaki *et al*., 2010

Table 1.8 SGI-110 as priming agent or in combinatorial therapies for solid tumors

This table presents the synergistic effects of SGI-110 as priming agent or in combinatorial therapies with epigenetic and chemotherapeutic agents in the treatment of solid tumor.

Combination drug	Types of cancer	Effects of combination therapies	References
Entinostat	Lung	• SGI-110 alone or in combination with entinostat significantly reduced the tumor burden against no effect of entinostat alone in orthotopically engrafted lung cancer model • Epigenetic therapy with SGI-110 alone or in combination with entinostat caused widespread re-programming of various genes involved in key cancer regulatory pathways such as TSG (*p21*), apoptotic gene (*BIK*), and EZH2 target genes, and various cancer testis antigen genes which could sensitize tumor cells to immunotherapy	Tellez *et al*., 2014
Cisplatin	Ovary	• Treatment with low-dose SGI-110 alone or in combination with cisplatin re-sensitized cisplatin resistant ovarian cancer cells to cisplatin by decreasing subpopulation of ALDH(+) cells, responsible for cisplatin resistance, and induced re-expression of differentiation-associated genes • SGI-110 treatment alone or in combination with cisplatin markedly inhibited the spheroid forming ability of both parental and cisplatin resistant ovarian cancer cell lines • *In vivo*, SGI-110 decreased the tumorigenesis of ovarian cancer stem cells by targeting ALDH (+) cells, and maintenance treatment with SGI-110 after carboplatin inhibited ovarian cancer stem cell growth, causing global tumor hypomethylation and decreased tumor progression	Wang *et al*., 2014
Cisplatin	Ovary	• Priming with moderate- or low-doses of SGI-110 increased the sensitivity of a wide range of parental and platinum resistant ovarian cancer cells to cisplatin, by inducing significant demethylation and re-expression of TSGs (*RASSF1A*), differentiation-associated genes (*HOXA10* and *HOXA11*), transcription factors (*STAT5B*), and putative drivers of ovarian cancer cisplatin resistance (*MLH1* and *ZIC1*) • Pre-treatment with SGI-110 significantly increased DNA damage, induced by cisplatin in parental as well as cisplatin resistant ovarian cancer cells • SGI-110 alone or in combination with cisplatin was well tolerated *in vivo*, and displayed increased antitumor effects in cisplatin resistant ovarian cancer xenografts as compared to cisplatin alone	Fang *et al*., 2014
Cisplatin	Testis	• Pre-treatment with low concentration of SGI-110 re-sensitized cisplatin resistant embryonal cancer cells (stem cells for testicular germ cell tumors) to cisplatin in a DNMT3B-dependent manner • Low concentration of SGI-110 caused transcriptional re-programming of embryonal cancer cells including induction of p53 targets genes (*GDF15*, *p21* and *GADD45A*), hypermethylation silenced genes (*RASSF1* and *SOX15*), and repression of pluripotency genes which could be responsible for the anti-proliferation and anti-survival activity of SGI-110 • As a single agent, moderate-doses of SGI-110 induced complete abrogation and regression of embryonal cancer tumor growth *in vivo*, and the combination of low-dose SGI-110 with cisplatin sensitized refractory embryonal cancer cells to cisplatin, without any evident toxicity • The *in-vivo* antitumor activity of SGI-110 was found to be associated with genome wide induction of p53 target and immune-related gene signatures	Albany *et al*., 2017
Oxaliplatin	Liver	• Pre-treatment with low-dose SGI-110 or the combination of SGI-110 and oxaliplatin showed synergistic effects yielding enhanced cytotoxicity in wide range of hepatocellular carcinoma cells, by inhibiting the expression of genes involved in WNT/EGF/IGF signaling • SGI-110 as single agent or in combination with oxaliplatin significantly delayed tumor growth in hepatocellular carcinoma xenografts as compared to oxaliplatin alone, without causing any systemic toxicity	Kuang *et al*., 2015

1.7. Specific aims of this thesis (Experimental part)

1.7.1. Aim 1: Establish DNA demethylation detection system for high throughput screening of potential hypomethylating epi-drugs

1.7.2. Aim 2: Characterize biodegradable polyanhydride microbeads formulations of azanucleoside drugs for therapeutic efficacy

1.7.3. Aim 3: Study stromal cell-induced alterations in the response of cancer cell to DNA hypomethylating agents

1.7.4. Aim 4: Investigate molecular mechanisms of drug resistance to azanucleoside drugs, and tailor alternative therapeutic regimen for overcoming resistance

Aim 1: Establish DNA demethylation detection system for high throughput screening of potential hypomethylating epi-drugs

Chapter 2

DNA demethylation detection system

This Chapter describes the development of a cell-based DNA demethylation detection system, suitable for high content screening of epigenetic drugs in two-dimensional and three-dimensional cell culture models on high-throughput platform, and *in vivo* in tumor xenografts. The described detection system facilitates the time-dependent monitoring of DNA methylation 'dynamics' as well as the induced cytostatic/cytotoxic drug effects in live cells.

2.1. Introduction

As discussed in Chapter 1, CpG island hypermethylation repressing the tumor suppressor genes is well evident in cancers. Despite major advances in field of epigenetic research, the success of DNA demethylation-based epigenetic cancer therapy remains elusive due to narrow therapeutic window. A plethora of naturally occurring epigenetic agents and synthetic molecules that can alter methylation patterns exist. These include wide variety of chemicals, certain base analogues, reactive oxygen species, and others (MacPhee, 1998). However, the usefulness of many such agents for epigenetic therapy remains unknown.

This underlines the need for a sensitive DNA demethylation detection system for large-scale screening of drug candidates with potent hypomethylation activity. The classical approaches used to study DNA methylation status include bisulfite sequencing (Frommer *et al*., 1992), methylated DNA immunoprecipitation combined with microarrays or next-generation sequencing (Clark *et al*., 2012), and immunohistochemistry (Jørgensen *et al*., 2006). However, these techniques require fixation of cells, making it impossible to study DNA methylation 'dynamics' as a function of time. Besides, they are uneconomical and not feasible for high throughput screening (HTS) of demethylating drugs. Apart from these conventional techniques, there has

been major development in the field of cell-based DNA methylation imaging. An automated imaging-based cytometrical approach, suitable for measuring DNA demethylation effects has been developed, based upon differential analysis of relevant nuclear signatures. The approach integrates segmentation of cell nuclei, homogeneity assessment of cell population, and measurement of changes in topology of low-intensity methylated CpG-dinucleotides and global DNA related sites (Gertych *et al*., 2009; Gertych *et al*., 2010; Gertych *et al*., 2013). However, the described imaging-based cytomics also requires fixation of cells, limiting its applicability for studying DNA methylation dynamics. The disadvantage of the strategies that do not permit the time-dependent analysis of DNA methylation dynamics has been circumvented by the establishment of a fluorescence-based reporter system which facilitates the monitoring of global DNA methylation status in situ under physiological conditions (Kobayakawa *et al*., 2007). The system established in mouse embryonic stem cells incorporates the methylated DNA binding domain and the nuclear localization signal sequence, coding for human methyl CpG-binding domain protein 1 (MBD1) fused with Enhanced Green Fluorescent Protein (EGFP) reporter gene. The tight correlation between the expression of MBD protein and the level of DNA methylation in cell nuclei allows visualization of majority of methylation sites in cells, and reports changes in DNA methylation status in quantitative as well as qualitative manner (Kobayakawa *et al*., 2007).

The detection system described in this Chapter is the further development of a previously established demethylation detection system (Okochi-Takada *et al*., 2004). Utilizing the *FLJ32130* gene, discovered to be silenced in HCT116 human colorectal cancer (Okochi-Takada *et al*., 2004), and additionally histone-2B gene (Kanda *et al*., 1998), a double-gene stably-transfected reporter cell line, HCT116-pFLJ-H2B was generated. The reporter cell is suitable for high content screening (HCS) of hypomethylating drug libraries on large scale in two-dimensional (2D) and three-dimensional (3D) cell cultures. The presented system takes the advantage over conventional approaches (Frommer *et al*., 1992; Clark *et al*., 2012; Jørgensen *et al*., 2006) and previously established imaging-based cytometrical approach (Gertych *et al*., 2009; Gertych *et al*., 2010; Gertych *et al*., 2013) as it allows the monitoring of DNA methylation dynamics as a function of time. The described reporter system also features advantage over MBD based experimental system (Kobayakawa *et al*., 2007) and the prior art (Okochi-Takada *et al*., 2004) by combining the additional feature which allows the monitoring of cytostatic/cytotoxic drug effects in conjunction with demethylation effects, in parallel, under same experimental setting. Furthermore, this Chapter describes the detailed stepwise cellomics work-flow at both 2D and 3D levels which can be easily adopted to process HC imaging data for analyzing induced

demethylation and cytostatic/cytotoxic drug effects, which remain undescribed in published literature.

To determine the suitability of the detection system for drug screening, the hypomethylation activity of four well-characterized DNA methyltransferase inhibitors (DNMTIs) was tested in 2D and multicellular spheroids (MCSs) of HCT116-pFLJ-H2B cells. Finally, the potential efficacy of the detection system for testing the hypomethylation activity of DNA methylation inhibitors (DMIs) is shown in tumor xenograft models of the reporter cell line.

Apart from the detection system described in this Chapter, a recent literature also presented a fluorescence-based DNA methylation reporter system for studying DNA methylation dynamics over time. The system relies on a minimal imprinted gene promoter that exhibits inherent sensitivity to DNA methylation of adjacent genomic regions resulting in transcriptional activation or silencing (Stelzer *et al*., 2015). In contrast to endogenous promoter CGI of silenced *FLJ32130* gene exploited in this study, the literature highlighted small nuclear ribonucleoprotein polypeptide N gene promoter region as an attractive candidate to generate a DNA methylation reporter system.

Also, to visualize DNA methylation dynamics in living organisms, a new experimental approach has been reported at *in vivo* level. The work describes a knock-in mouse model, MethylRO that ubiquitously expresses Red Fluorescent Protein (RFP)-fused MBD protein from the ROSA26 locus. The study provides multiple evidence, in particular RFP-mediated methylated DNA immunoprecipitation sequencing, whole-body section analysis, and live-cell imaging, to show the use of MethylRO mice in capturing the dynamic changes of the DNA methylation status, both *in vitro* and *in vivo* (Ueda *et al*., 2014).

2.2. Materials and Methods

2'-deoxy-5-azacytidine (DAC), alpha anomer of DAC (α-DAC), 5-azacytidine (AZA), and 2'-deoxy-5, 6-dihydro-5-azacytidine (DHDAC) were synthesized as described previously (Matoušová *et al*., 2011). Drugs were dissolved in DMSO and prepared fresh before each experiment. DMSO concentration was always less than 0.1% in treated wells. Unless and otherwise indicated, media, chemicals, and other reagents were purchased from Sigma-Aldrich.

2.2.1. Cell culture

The human colorectal cancer (CRC) cells, HCT116 were obtained from American Type Culture Collection (ATCC), and were maintained in McCoy's 5A growth medium, supplemented

with 10% fetal bovine serum (PAN-Biotech GmbH), 3 mM L-glutamine, 50 µg/mL streptomycin, and 100 U/mL penicillin (Biotika, a.s.) at 37°C and 5% CO_2 in a humidified incubator. Cell line authentication and routine test for mycoplasma contamination were done as described previously (Perlíková *et al*., 2016).

2.2.2. Targeting vector constructs

For assaying the demethylation potential of the epigenetic drugs, FLJ exon 3 targeting vector was used. The vector construct integrates *FLJ32130* exon 3 (Accession; AK056692) in a human bacterial artificial chromosome (BAC) clone, an internal ribosomal entry site (IRES) sequence attached to Hygromycin (Hyg^r) resistance gene fused with EGFP, and a neomycin (Neo^r) resistance cassette as a selectable marker. The underlining principle behind the vector construct was that, upon transfection into HCT116 cells, Hyg^r-EGFP fusion gene would not be expressed due to hypermethylated status of the FLJ promoter, but it would be expressed following treatment with hypomethylating drugs. The vector was a gift from Dr. T. Ushijima (National Cancer Center Research Institute, Tokyo) which was further amplified in our laboratory for the purpose of transfection and construction of reporter cell (Okochi-Takada *et al*., 2004).

For analyzing the cytostatic/cytotoxic potential of the epigenetic drugs, histone-2B (Accession; NM 021058.3) genetically fused with RFP was utilized. The rationale behind the use of fluorescently tagged histone protein was to stain the cell nuclei for cell identification during HC image analysis (Kanda *et al*., 1998).

2.2.3. Construction and selection of reporter cell line

FLJ Exon 3 targeting vector was linearized by restriction digestion with EcoRV and XhoI, and early passage HCT116 cells were transfected by electroporation, according to manufacturer's protocol (Pulse voltage; 1130 V, Pulse width; 30 ms, Pulse number; 2), using Neon Transfection System (Life Technologies). After 24 h, the cells were subjected to selection pressure of Neo^r (500 µg/mL). To pull the stably transfected reporter cell from the Neo^r resistant cell population, single cell cloning was performed in 96-well plates and about 500 single cell clones were screened. The clones with no green fluorescence or feeble EGFP expression following treatment with 1 µM DAC were discarded, whereas, the clones with positive EGFP expression were further quantified by flow cytometry. Eventually, the clone with highest EGFP intensity following treatment with 1 µM DAC was selected as the demethylation reporter cell line, HCT116-pFLJ.

The HCT116-pFLJ cells were further transduced with RFP-tagged histone (H2B) protein. Transduction was performed using Histone H2B-RFP Lentiviral Biosensor (EMD Millipore), according to manufacturer's protocol [Multiplicity of Infection (MOI) = 25]. To enhance the efficiency of lentiviral transduction, SureENTRY Transduction Reagent (Qiagen) was used at the concentration of 8 μg/mL. After 24 h, medium containing lentiviral particles was replaced with fresh growth medium, and transduced cells were visualized by fluorescence microscopy. RFP signal with varying intensity was detected in cell nuclei. After 5 days, the confluency was reached and the cells with two reporters (pFLJ + H2B) were again subjected to single cell cloning. The cell clone with highest intensity of RFP signal in nuclei was finally selected to generate the dual-reporter cell line, HCT116-pFLJ-H2B.

2.2.4. Drug treatment and cellular imaging in 2D cultures

Cells were plated at a density of 1.5×10^3 cells/well in 96-well clear bottom microplate (CellCarrier, PerkinElmer). After 24 h, DAC, α-DAC, AZA, and DHDAC were added in five different concentrations, ranging from 100 μM to 0.20 μM. Cells in control wells were treated with DMSO at concentration used in the medium with highest drug concentration (below 0.1%). Following 24 h of treatment, images were acquired at regular intervals from day 1-5, using filters for EGFP (excitation/emission: 488 nm/509 nm) and RFP (excitation/emission: 545 nm/572 nm), using Cell Voyager CV7000 High Throughput Cytological Discovery System (Yokogawa Electric Corporation). To disregard the fact that observed green fluorescence, indicative of demethylation activity was not a non-relevant side effect of drug (s) treatment, HCT116-pFLJ-H2B cells were treated with two anti-cancer drugs, cisplatin and paclitaxel which have no evidence of measurable DNA demethylation activity in published literature. Purposely, cisplatin and paclitaxel were added at their IC_{50} concentrations (determined by 72 h MTT test in HCT116 parental cells), and images were taken after 3 days of drug treatment (Fig. 2.1).

2.2.5. High content analysis of images from 2D cultures

Acquired TIFF images were imported and analyzed using Columbus Image Data Storage and Analysis System (PerkinElmer). The hypomethylation efficacy of the drugs was analyzed by quantifying the intensity of EGFP fluorescence which is directly proportional to demethylation activity, whereas, cytostatic/cytotoxic drug effects were determined by counting the cell numbers in control and treated wells (Fig. 2.1). Various parameters such as common and individual threshold, area and split factor, and contrast were fine-tuned to detect the cell nuclei utilizing RFP

channel. After selection of the cell nuclei, regions around it having intensity higher than background were detected as cytoplasm under EGFP channel (Fig. 2.1). Following detection of the cells (nuclei + cytoplasm) in region of input image, the common filter was set for removing the border objects to exclude the incompletely captured cell population, followed by filtration according to morphological properties (area, roundness, and length to width ratio) to discard the cell clumps and false discovered objects (Fig. 2.1). Each building block of image analysis was calibrated by going across several wells and several fields in each well to achieve the optimal setting. Finally, the number of objects in each image were counted to represent the number of cells in each well, reflecting cytostatic/cytotoxic effects of the drugs, whereas, mean EGFP intensity was calculated within the cell region in each image to represent mean EGFP intensity per well, reflecting demethylation efficacy of the drugs (Fig. 2.1). It is to be noted that for demethylation analysis, single cell results were exported and equal number of cells were randomly selected from each well.

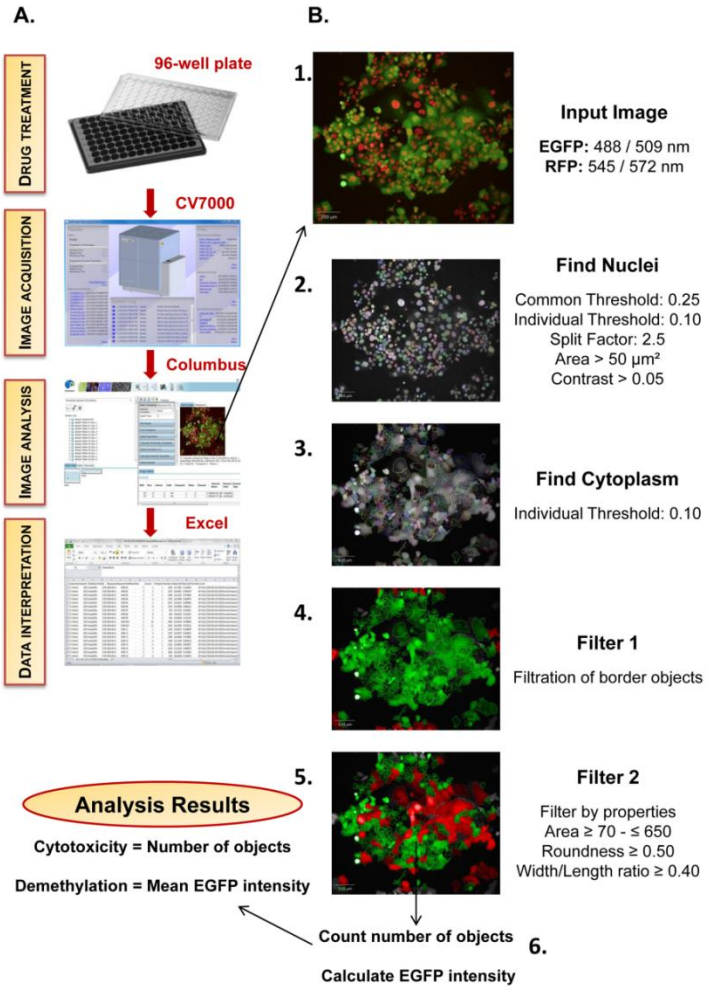

Figure 2.1 Schematic overview of cellomics workflow in 2D culture system

(A) *Assay was performed in 96-well microplates and images were acquired using HT cytological discovery system. HC images were imported and analyzed in Columbus, and analysis results were exported as excel files containing single cell results for each object in a well, for downstream processing and statistics.* ***(B)*** *Stepwise elaboration of HC image analysis: captured images (44 fields/per well, 96-well plate) under RFP and EGFP channels were defined as input for analysis* ***(B-1)***. *H2B-RFP tagged cell nuclei, and cytoplasm with EGFP expression were selected to identify the total cell population in each well* ***(B-2, 3)***. *Identified cell population was filtered by excluding the border objects and setting the morphological properties* ***(B-4, 5)***. *Number of objects and EGFP intensity were calculated in output cell population* ***(B-5)*** *for biological interpretation of the results* ***(B-6)***.

2.2.6. Multicellular spheroids culture and drug treatment

MCSs of HCT116-pFLJ-H2B cells were generated as described previously (Das *et al*., 2016). For HC imaging, MCSs were treated with DAC, α-DAC, AZA, and DHDAC in the concentration range of 100 µM to 0.20 µM for 5 days. MCSs in control wells were treated with DMSO at concentration used in the medium with highest drug concentration (below 0.1%). To monitor the extent of demethylation inside MCSs, single MCS per well were treated with 10 µM concentration of the drugs for 5 days. Following the addition of drugs, normal plate lids were replaced with MicroClime® Environmental Lid (Labcyte Inc.) to minimize the edge effect.

2.2.7. Spatial high content monitoring of demethylation in multicellular spheroids

MCSs were imaged on an Operetta High Content Screening System (PerkinElmer) using a 10× high NA objective (numerical aperture: 0.4) every 24 h for 5 days following drug treatment. Images were acquired by brightfield imaging, and with filters for EGFP (excitation/emission: 488 nm/509 nm) and RFP (excitation/emission: 545 nm/572 nm). A total of 5 z-stack images were captured at an interval of 25 µm (Fig. 2.2). Acquired images were exported in TIF Format and analyzed using an in-house image analysis algorithm developed in MatLab R2013b (MathWorks Inc.). MCSs were first selected using the brightfield channel to create a mask (Fig. 2.2). Using the mask, all channels were combined into a layered image, discarding the surrounding and background with no information (Fig. 2.2). The layered images were generated using only the sharpest z-stack image. Area normalized signal integrated density (SID) of EGFP and RFP channels were calculated from each sharpest z-stack image, and only from the MCS

region inside the mask. The obtained EGFP intensity was then normalized to the respective RFP signal of the same image (Fig. 2.2). Normalized EGFP signals from each of the 5 z-plane images per MCS were combined to obtain the total EGFP signal, and the data were processed similar to 2D data to obtain the EGFP intensity. Drug effect on MCS size was measured by determining the change in MCS area from the brightfield images. MCS were maintained at 37^{o}C and 5% CO_2 in a live-cell chamber throughout the experiment.

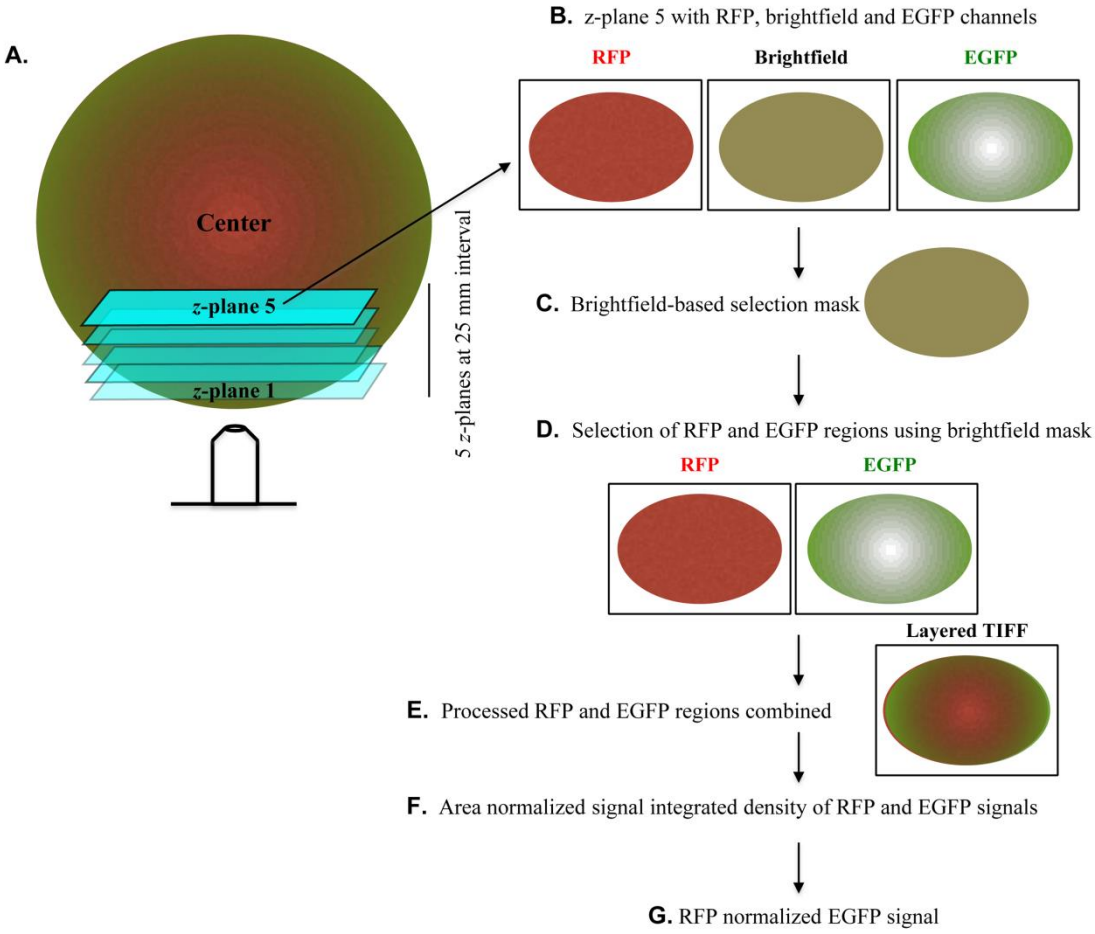

Figure 2.2 Schematic overview of demethylation studies in 3D culture system

Drug treated MCS were imaged in xyz plane at an interval of 25 µm and 5 z-stack images were captured in RFP, EGFP, and brightfield channels ***(A, B)****. Using the brightfield image, a mask was created comprising only the MCS region* ***(C)****. RFP and EGFP regions of MCS were selected based on the brightfield mask, and majority of the surrounding and background was discarded* ***(D)****. Processed RFP and EGFP images from one z-plane were combined to form a single layered TIF* ***(E)****. Area normalized SID of RFP and EGFP channels were estimated* ***(F)*** *and the EGFP signal was normalized to RFP intensity of the respective z-plane image.*

2.2.8. Monitoring of demethylation in interior of multicellular spheroids

For monitoring demethylation in MCS interior, z-stack images of MCS were acquired following drug treatment in a CSU-X1 Spinning Disk inverted confocal microscope (Axio Observer.Z1, Carl Zeiss Microscopy) using a 'Plan-Neofluar' 10×/0.30 Ph1 M27 objective. MCSs were treated with only one drug concentration and imaged on the 5^{th} day following treatment. A total of 20-30 z-planes were acquired at an interval of 5 µm, image aspect ratio of 500 × 500 pixel, and 50 ms exposure time. At least 4-5 MCS were imaged for each drug per experiment. The images were saved in .CZI format and analyzed using NIH ImageJ image analysis software (version 1.47v). Area normalized SID of RFP and EGFP signals were determined, and EGFP intensity was then normalized to RFP signal for respective z-planes. Only the first 16 z-planes were used to calculate SIDs of EGFP and RFP fluorescence, and the rest were discarded due to the lack of focus.

2.2.9. In vivo fluorescence imaging

To further validate the efficacy of the detection system for *in vivo* studies, xenografts of reporter cells were established in 11-12 weeks-old female SCID mice, inoculated with 0.5×10^7 cells, *s.c.* on both sides of the chest. After 2 weeks, tumors were palpable (average tumor volume 200 mm^3) and mice were assigned into three groups (4 mice/group) - group I: vehicle control (90% PBS + 10% DMSO), group II: DAC, 2.5 mg/kg, *i.p.*, day 1-3 (3 doses), and group III: DAC, 1 mg/kg, *i.p.*, day 1 (single dose). On day 5, mice were euthanized and tumors were extracted for imaging. The fluorescence signals of isolated tumors were captured immediately using small animal In-Vivo MS FX Pro (Bruker) optical imaging system with appropriate settings of monochromatic filters for EFGP (excitation/emission: 460 nm/535 nm) and RFP (excitation/emission: 530 nm/600 nm). The fluorescence signals were quantified using MI software (Bruker), and expressed as mean intensity of each tumor in $P/s/mm^2$. Animal care and experiments were approved by the Animal Ethics Committee of the Faculty of Medicine and Dentistry, Palacky University.

2.2.10. Biological interpretation of data and statistical analysis

Number of cells and mean EGFP intensity from HC image analysis of 2D cultures were biologically interpreted as time-course cytostatic/cytotoxic and demethylation drug effects, respectively. The area under the curve (AUC) was calculated for each drug concentration over 5 days, to represent the cumulative cytotoxic and demethylation drug effects. The total number of

cells in control and treated wells from day 1-5 were integrated to calculate the AUC for cytotoxicity, for each drug concentration separately. Likewise, EGFP intensities derived from day 1-5 were integrated to calculate the AUC for demethylation. AUCs for both, cytotoxicity and demethylation were normalized against control and presented as % control. In addition, number of cells at the end of day 5 was used to calculate equitoxic drug concentrations at two levels, IC_{50} and IC_{10}.

Similar to 2D cultures, cytostatic/cytotoxic drug effects in 3D cultures were inferred using change in MCS area, and demethylation was inferred using total EGFP intensity in MCSs. AUCs for each drug over 5 days were evaluated for MCSs area and EGFP intensity, to determine cumulative drug cytotoxicity and demethylation, respectively. MCS area was further used to calculate IC_{50} and IC_{10} at the end of day 5, similar to 2D. All statistical analyses were performed using GraphPad Prism statistical software (version 7), and differences were considered significant at $P < 0.05$.

2.3. Results

2.3.1. High content screening of DNMTIs in 2D reporter cell model

2D cultures of reporter cells were treated with DAC, α-DAC, AZA, and DHDAC at 100 µM, 20 µM, 4 µM, 0.8 µM, and 0.16 µM concentrations, and the cytostatic/cytotoxic and demethylation effects of the drugs were monitored every 24 h for 5 days. The time-dependent increase in cytostatic/cytotoxic effects was observed (Fig. 2.3A, C), accompanied by increase in EGFP fluorescence until day 5, which indicated an increase in demethylation effects (Fig. 2.3A, D).

On comparing the AUC of each drug for cell survival, AZA was found to be the most cytotoxic drug at high concentrations (100-20 µM), and DAC with the highest cytotoxicity at low concentrations (4-0.16 µM) followed by α-DAC (Fig. 2.3F). The cytotoxicity of drugs was also compared by calculating equitoxic drug concentrations at two levels, IC_{50} and IC_{10} at the end of 5 days. The result was in agreement with AUC comparison, identifying DAC as more cytotoxic than α-DAC and AZA, and DHDAC with least cytotoxicity (Fig. 2.3E).

On comparing the AUC for demethylation, the results established DAC with the highest demethylation activity at all tested concentrations. The second most active demethylating drug was found to be α-DAC which showed similar demethylation activity as DAC at high concentrations (100-4 µM), and significantly higher demethylation activity than AZA or DHDAC

at low concentrations (0.8-0.16 µM). DHDAC comparatively showed least demethylation activity at all tested concentrations (Fig. 2.3F).

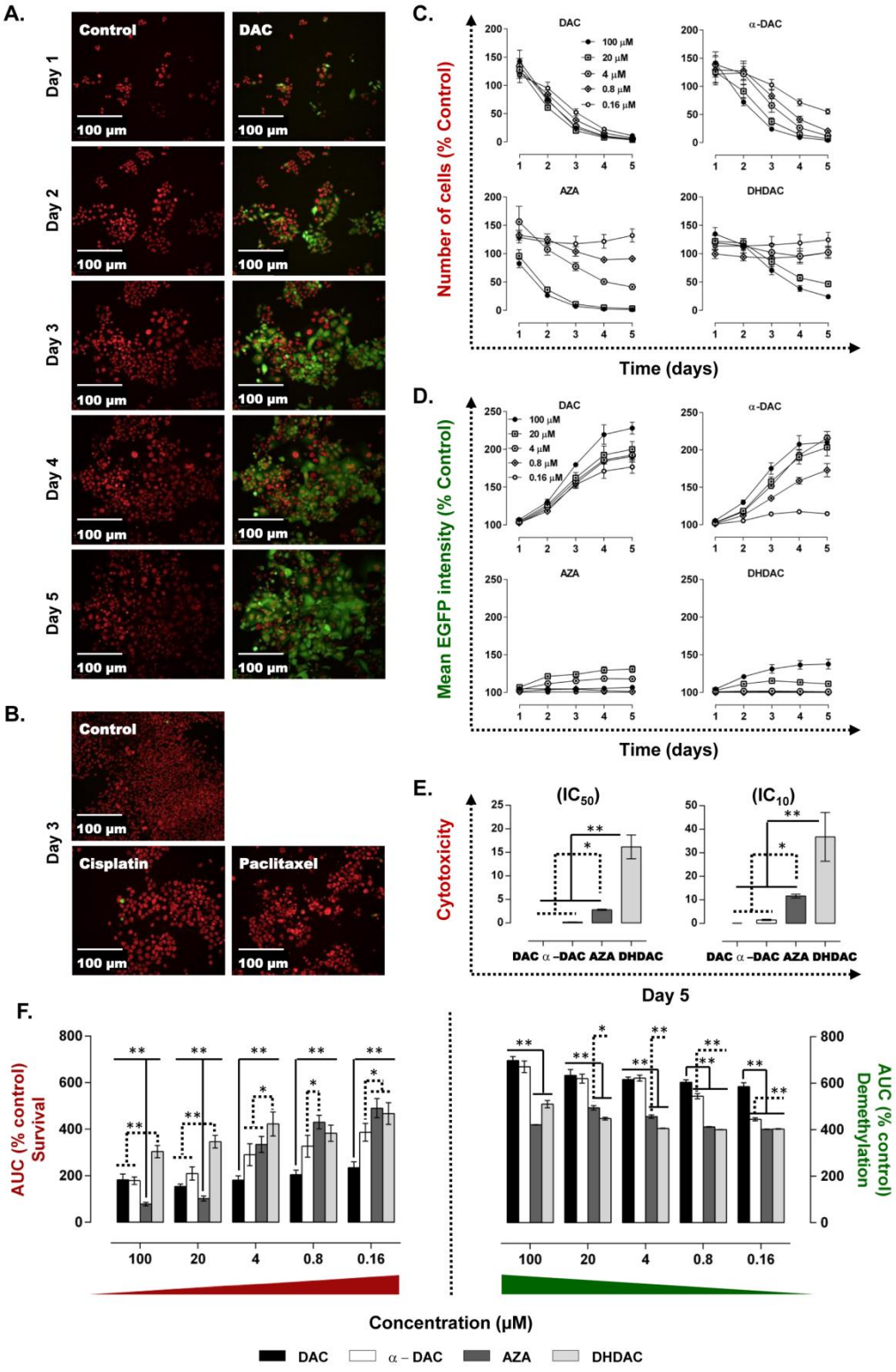

Figure 2.3 High content screening of DNMTIs in 2D cultures

(A) *HC cellular images acquired during time course measurement, exemplifying the time dependent increase in cytotoxicity and demethylation (DAC; 0.8 μM).* ***(B)*** *HC cellular images acquired after 3 days of treatment with cisplatin and paclitaxel, showing no measurable DNA demethylation activity.* ***(A,B)*** *20× objective, Scale bar – 100 μm.* ***(C,D)*** *Time course plots (% control) show time and concentration dependent increase in cytotoxicity and demethylation following treatment with DAC, α-DAC, AZA, and DHDAC for 5 days.* ***(E)*** *Cytotoxicity plots comparing the IC_{50} and IC_{10} values of drugs at the end of 5 days.* ***(F)*** *AUC plots (% control) showing cumulative cytostatic/cytotoxic and demethylation drug effects.* ***(E,F)*** *Data are the mean ± S.D., n = 5. **p < 0.0001, *p < 0.05, one-way Anova with Tukey's multiple comparisons test.*

2.3.2. High content screening of DNMTIs in multicellular spheroids cultures

MCSs were treated with DAC, α-DAC, AZA, and DHDAC at concentrations 100 μM, 25 μM, 3.13 μM, 0.78 μM, and 0.20 μM, and change in MCS size and demethylation was monitored every 24 h for 5 days. There was a significant reduction in MCS area by day 5 at 25 μM DAC, and 100 μM DAC, α-DAC, AZA, and DHDAC (Fig. 2.4A, B). Similar to 2D data, there was a time-dependent increase in EGFP intensity in MCSs treated with DAC, α-DAC, and AZA (Fig. 2.4A, C).

To determine the cytotoxic effects of drugs, AUC for growth over 5 days and IC_{50} and IC_{10} of MCS area on day 5 were calculated. AZA significantly affected MCS growth at 100 μM compared to DAC, α-DAC, and DHDAC, and at 25 μM compared to DHDAC (Fig. 2.4D). The IC_{50} and IC_{10} of DAC, α-DAC, and AZA were significantly low compared to DHDAC (Fig. 2.4E). Although α-DAC had the lowest IC_{50} and IC_{10} compared to DAC and AZA, there was no statistically significant difference (Fig. 2.4E). Interestingly, α-DAC showed higher demethylation activity compared to AZA and DHDAC at 100 μM and 100-25 μM, respectively (Fig. 2.4F). However, at low concentrations (3.13-0.20 μM), DAC was comparatively most active demethylating drug (Fig. 2.4F). DHDAC showed no significant demethylation effect in MCSs over 5 days, possibility indicating poor penetration of the drug.

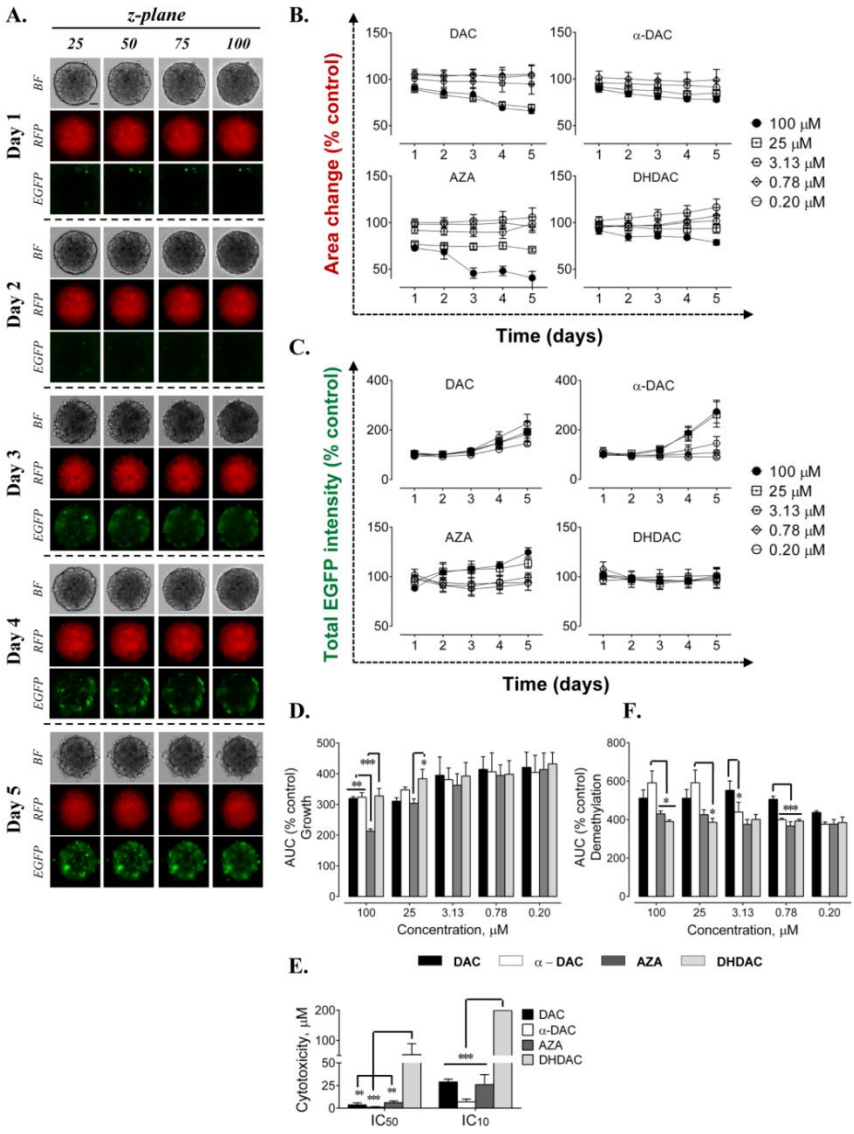

Figure 2.4 High content screening of DNMTIs in multicellular spheroids

(A) *Images showing an increase in EGFP intensity in 25 μM DAC-treated MCS over 5 days at 25, 50, 75 and 100 μm z-plane heights. DAC does not affect RFP fluorescence over 5 days of treatment. Brightfield images of MCS for each z plane heights are presented to show that 25 μM DAC results in decrease in MCS size on day 5, albeit non-significant. 40× objective, Scale bar – 200 μm.* ***(B, C)*** *Graphs are presented to show change in MCS area* ***(B)*** *and total EGFP intensity* ***(C)*** *following treatment with DAC, α-DAC, AZA, and DHDAC for 5 days.* ***(D)*** *AUC for growth calculated from change in MCS area for each drug concentration is presented.* ***(E)*** *A comparison of IC_{50} and IC_{10} values of drugs on day 5 is shown.* ***(F)*** *AUC for demethylation calculated from change in EGFP intensity for each drug concentration. Data are the mean ± S.D., n = 4. ***p < 0.001, **p < 0.01, *p < 0.05, one-way Anova with Tukey's multiple comparisons test.*

2.3.3. Reporter cell multicellular spheroids for drug penetration studies

To monitor the potential tissue penetration and changes in EGFP signal towards MCS center, reporter cell MCSs were treated with 10 µM DAC, α-DAC, AZA, and DHDAC, and *z*-stack confocal imaging was performed. There was no significant difference in the extent of demethylation caused by DAC, α-DAC, and AZA inside MCS (Fig. 2.5A-C, E). However, DHDAC was significantly less potent in its demethylation activity within MCS compared to DAC, α-DAC, and AZA (Fig. 2.5D, E).

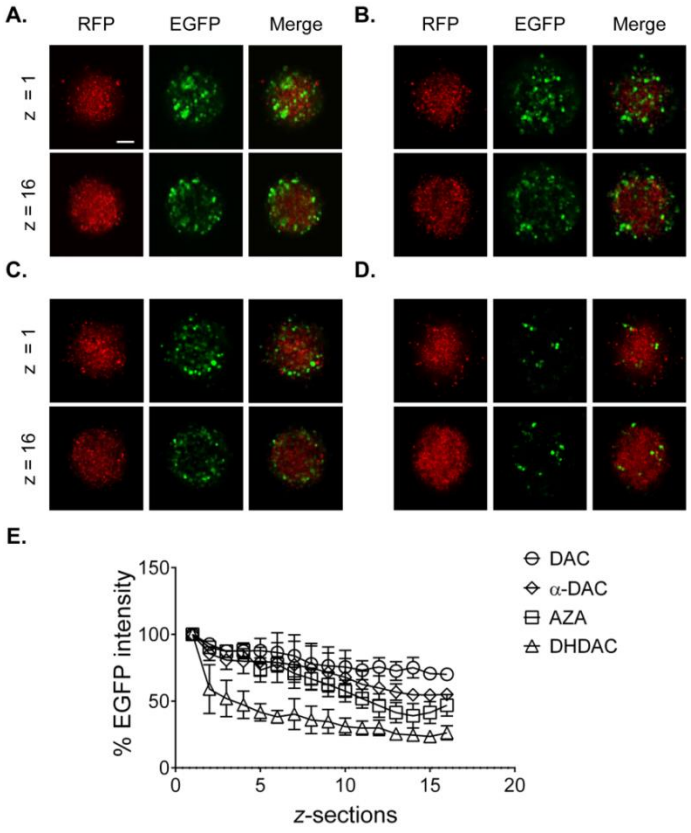

Figure 2.5 Demethylation of multicellular spheroids interior

RFP, EGFP, and merged images of z-sections of spheroids on day 5 of treatment with 10 µM DAC ***(A)****, α-DAC* ***(B)****, AZA* ***(C)*** *and DHDAC* ***(D)*** *are shown. The first and the last z-sections are shown, taken at an interval of 2.5 µm spacing. 10× objective, Scale bar – 100 µm. Graphs are presented to show EGFP intensity from z-sections 1-16 in MCSs treated with 10 µM DAC, α-DAC, AZA, and DHDAC for 5 days. EGFP intensities from 2-16 z-sections are normalized to the EGFP intensity of the 1st z-section for respective drugs. Data are the mean ± S.D., n = 3. ***p < 0.001 (DAC and α-DAC vs. DHDAC), *p < 0.05 (AZA vs. DHDAC), one-way Anova with Tukey's multiple comparisons test.*

2.3.4. Reporting demethylation in tumor xenografts

To examine the utility of the detection system in *in vivo* setting, HCT116-pFLJ-H2B-xenografted mice were treated with two-dose schedules of DAC, schedule 1: 2.5 mg/kg, day 1-3 and schedule 2: single-dose of DAC at 1 mg/kg on day 1, and EGFP and RFP fluorescence signals were measured in isolated tumors. On comparing with tumors in control group, a significant increase in EGFP fluorescence signals was observed in both the treatment groups (Fig. 2.6A). However, RFP fluorescence signals remained constant with no significant difference between control and treated (Fig. 2.6B). There was no loss of tumorigenicity of HCT116-pFLJ-H2B cells due to double transfection.

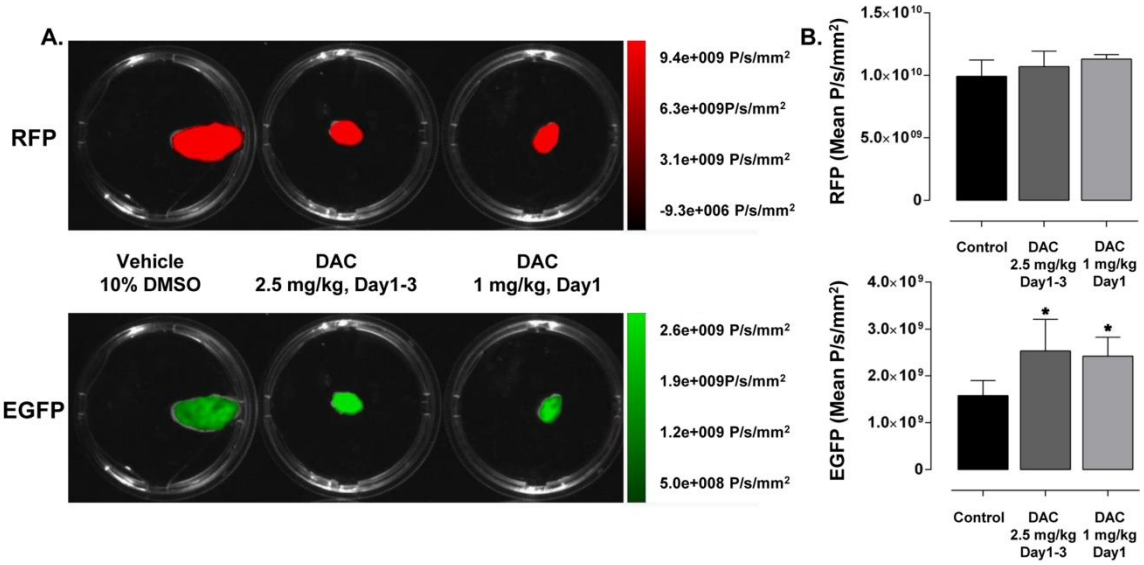

Figure 2.6 *In vivo* fluorescence imaging of reporter cell tumorgrafts

(A) *Representative images of vehicle and DAC-treated tumors are presented to show increase in EGFP fluorescence but constant RFP signal in treated tumors.* ***(B)*** *Graphs of EGFP and RFP fluorescence intensities are shown. Data are the mean ± S.D., n = 8. $p < 0.05$ (control vs. DAC: 2.5 mg/kg, Day 1-3 and DAC: 1 mg/kg, Day 1), one-way Anova with Dunnett's test.*

2.4. Discussion

This Chapter presents the development of double-gene stably-transfected cell-based detection system for effective characterization of potent DNA hypomethylating drugs in 2D, 3D, and xenograft models. To demonstrate the potential of the described detection system for screening of DMIs, clinically approved DAC and AZA, and other well-characterized DNMTIs, α-

DAC and DHDAC were used. The results established DAC with highest demethylation activity in both cell culture types, followed by α-DAC (Fojtova *et al*., 2007). AZA and DHDAC comparatively displayed low demethylation activity in both 2D and 3D cultures. Likewise, AZA at high concentrations was most cytotoxic in both 2D and 3D cultures compared to other tested drugs, however, at low concentrations, DAC showed highest cytotoxicity. DHDAC displayed least cytotoxicity in both culture types. These results are similar to previously conducted study that compared the tested drugs for their demethylation activity and cytotoxicity using a different approach, confirming the validity of the described detection system (Matoušová *et al*., 2011).

Next, to determine the suitability of reporter cell MCS cultures for drug tissue penetration studies, the changes in EGFP signals in MCSs were monitored from the surface to an approximate depth of 80 µm towards the center. DAC, α-DAC, and AZA caused significant demethylation than DHDAC in the inner regions of MCSs. This is in accordance with the results from the HCS of the drugs in 2D and MCS cultures (see above), where DHDAC displayed the least demethylation activity compared to other drugs.

Xenograft models of tumors are important tools for assessing the efficacy of potential anticancer drugs in pre-clinical stages of cancer drug discovery. Therefore, the applicability of the detection system for monitoring demethylation was next confirmed in tumor xenografts of reporter cells, using DAC. Similar to 2D and MCSs, a significant increase in EGFP fluorescence was observed in DAC-treated tumors compared to untreated controls.

In conclusion, the study presents the development of a cell-based detection system for screening of DMIs in 2D, 3D and xenograft models of colorectal cancer. The described work will provide the researchers with an efficient tool for epigenetic drug screens on a high throughput platform and would therefore benefit academic and industrial drug discovery. The potential applicability of the described detection system is evident from the results of screening of known DNMTIs in 2D and 3D cultures, and in *in vivo* tumors.

While, the detection system has significant potential for screening of epigenetic drugs, a few issues require attention for reliable screening of drugs on a routine basis. One of the limitations with optical imaging of thick biological samples is the inability of light to penetrate deep into the tissue, and lack of high throughput-compatible deep-tissue imaging techniques for 3D cultures (Das *et al*., 2016). This is also evident in this study from the lack of clarity of MCS images beyond 50 µm *z*-plane height (Fig. 2.5A). Additionally, MCS size can potentially affect the penetration of laser, resulting in bias between MCS of different sizes. For example, MCS treated with high drug concentrations that result in decrease in MCS size may allow better laser penetration than MCS treated with low concentrations of drugs or untreated controls. Although

the potential bias that may result due to difference in MCS size cannot be completely ruled out, the use of area-normalized SIDs to calculate EGFP intensities in MCSs might overcome the issue.

Besides, 10 µM DAC and AZA used in this study is beyond the physiological range, however, many other epigenetic drugs do not show significant demethylation activity at 10 µM or lower concentrations. Zebularine, a mechanism based inhibitor of DNA methylation has low cytotoxicity and show significant demethylation activity only at higher doses (Champion *et al*., 2010). Laccaic acid, an anthraquinone natural DNMTI with mild toxicity was shown to induce the expression of specific hypermethylation silenced genes at 200 µM or higher concentrations (Fagan *et al*., 2013). A previously conducted study that demonstrated DHDAC as less toxic alternative of DAC implemented 100 µM concentration as standard for drugs with low or no detectable cytotoxic effects (Matoušová *et al*., 2011). Since, this study compared the demethylation activity of drugs at each individual concentration, irrespective of their cytotoxicity, therefore, the higher concentrations for DAC and AZA were also included.

Aim 2: Characterize biodegradable polyanhydride microbeads formulations of azanucleoside drugs for therapeutic efficacy

Chapter 3

Biodegradable polyanhydride drug delivery system

This Chapter describes a conceptually new system of drug delivery which may increase the plasma circulation time of the hydrolytically labile azanucleoside drugs that are subjected to irreversible chemical decomposition in aqueous solution.

3.1. Introduction

As discussed in Chapter 1, cytosine analogues, 5-azacytidine (AZA) and 2'-deoxy-5-azacytidine (DAC) have been established as efficient therapeutics for the treatment of myeloid malignancies. The therapeutic efficacy of these drugs is determined by their ability to inhibit the expression of *de novo* DNA methyltransferases (DNMTs), and reactivate the tumor suppressor genes silenced by aberrant DNA methylation (Bryan *et al*., 2013; Gnyszka *et al*., 2013; Singh *et al*., 2013). The effect on DNMTs is based on the nucleophilic attack of the azanucleosides (AZN) on the carbon-6 atom of the cytosine ring, resulting in covalent bond formation between azacytosine and the active site of the enzyme (Stresemann & Lyko, 2008). This covalent trapping of DNMTs is stable and inhibition is therefore practically irreversible. However, the susceptibility of the carbon 6 of the azacytidine ring in the presence of other nucleophiles including water causes rapid and reversible opening of the 5-azacytosine ring, followed by irreversible decomposition. This hydrolytic lability renders the chemical instability of the azanucleoside drugs, thereby compromising the plasma circulation time (Rogstad *et al*., 2009). Often, long-term cooled infusions are necessary. This underlines the paramount importance for the AZA and DAC formulations that may overcome this hydrolytic lability.

Biodegradable polymeric implants are well established delivery devices for various drugs. Drug release may be driven either by diffusion of the drug from the polymeric depot,

cleavage of the chemical bond between polymeric carrier and the drug, degradation of the polymeric implant, or by combination of these mechanisms (Kim *et al*., 2014b; Doppalapudi *et al*., 2014; Parent *et al*., 2013). Besides, controlled chemical degradation of the implant forming polymer (desirable for many *in vivo* applications) may proceed in whole volume, e.g., hydrazone based hydrogels (Lu *et al*., 2014), from the surface only, e.g., polyanhydrides (Jain *et al*., 2005; Jain *et al*., 2008; Pereira *et al*., 2014), or by combination of both, e.g., polylactides (Parent *et al*., 2013; Lu *et al*., 2014; Jain *et al*., 2005; Jain *et al*., 2008; Pereira *et al*., 2014; Casalini & Perale, 2002).

Polyanhydrides such as poly(sebacic acid) are relatively hydrophobic polymers that degrade in aqueous milieu, by hydrolysis of carboxylic acid anhydride bond into low molecular weight water-soluble dicarboxylic acids which are further metabolized or excreted (Jain *et al*., 2005; Jain *et al*., 2008; Casalini & Perale, 2002). Since, hydrolysis of polyanhydrides strictly begin at the surface so the inner volume of the implant remains dry, until the hydrolytic zone on the surface reaches completely to the core. Rate of hydrolysis is inversely proportional to the hydrophobicity of the monomer (increased hydrophobicity decreases degradation rate), and can be controlled upon modification with highly hydrophobic fatty acids (Teomim & Domb, 1999), or with use of monomeric composition that increases crystallinity, such as conformationally rigid cyclic diacid comonomers (eg., 1,4-cyclohexanedicarboxylic acid), or aromatic diacid monomers (Jain *et al*., 2005; Jain *et al*., 2008; Pereira *et al*., 2014).

This Chapter describes a conceptually new system exploiting the ability of the polyanhydrides to hydrolyze from the surface only, to release the hydrolytically labile drugs, AZA and DAC. Instead of hydrophobic polyanhydride, the injectable/implantable polymeric microbeads are biodegradable, containing dispersed microcrystals of hydrophilic AZA or DAC, insoluble in anhydride. With the time-course degradation of the polyanhydride, the degradation zone/aqueous milieu proceeds from the surface to the core of the beads, resulting in dissolution of microcrystals and sustained release of the drugs into outer environment. The underlining principle is based on the packing of microcrystals in a dry environment protected from hydrolysis, until the hydrolytic zone reaches the core, thus circumventing the hydrolytic lability (Fig. 3.1).

For preparation of the drug loaded microbeads, Poly(sebaccic acid-co-1,4-cyclohexanedicarboxylic acid), PSA-co-PCH was used as the starting polymer. Since, microbeads may cause local irritation resulting in inflammation, nonsteroidal anti-inflammatory drug, diclofenac (DIC) was added to the polymeric matrix (Llinàs *et al*., 2007). DIC is hydrophobic and is soluble in polymeric matrix.

This biodegradable model of micro-particulate dual drug delivery system was characterized *in vitro* for physical, chemical, and biological properties. The therapeutic efficacy of the formulations was confirmed by monitoring the induced demethylation and cytostatic/cytotoxic effects of continuous drug release from the time-course dissolution of the microbeads, using cell-based DNA demethylation detection system described in Chapter 2.

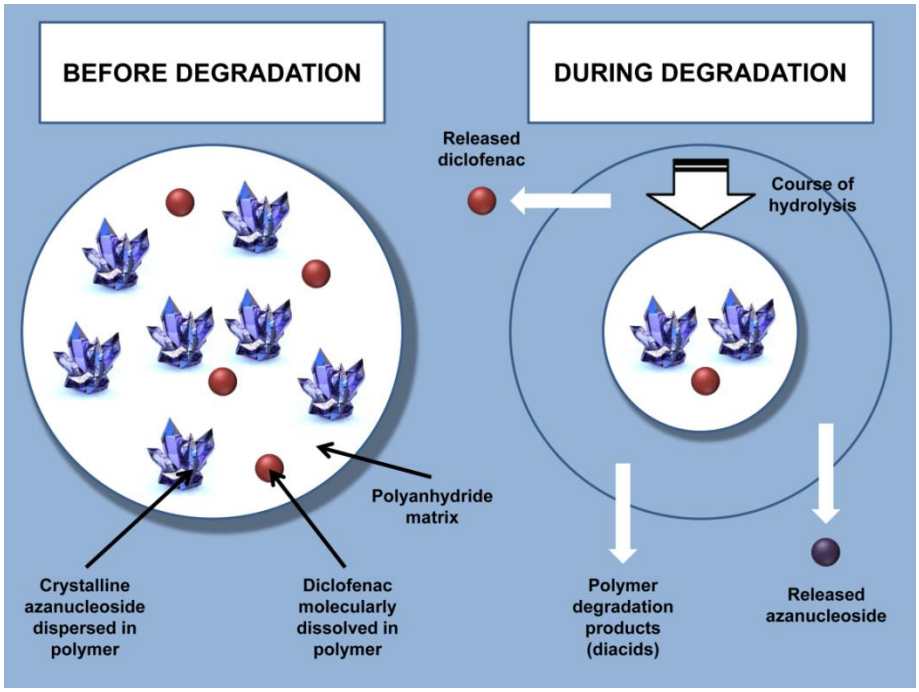

Figure 3.1 Scheme of the microbead system

3.2. Materials and Methods

All chemicals were obtained from Sigma-Aldrich, unless otherwise indicated.

3.2.1. Preparation of polymeric beads

For the preparation of PSA-co-PCH (70:30 mol/mol), a modified procedure described previously (Kipper *et al*., 2002) was used.

Sebaccic acid (8.40 g, 41.5 mmol), 1,4-cyclohexanedicarboxylic acid (3.06 g, 17.8 mmol) and acetic anhydride (115 mL, 124 g, 1210 mmol) were refluxed for 30 min, and the reaction mixture was evaporated *in vacuo*. Subsequently, the residues of acetic acid and acetic anhydride were azeotropically removed by evaporation with toluene (2x), and the solid residue was dissolved in chloroform, followed by precipitation with diethyl ether – petroleum ether mixture (1:1 v/v). The precipitated pre-polymer was then filtered off, air-dried, and heated on magnetic

stirrer at 180°C for 90 min *in vacuo* (10 Pa), and cooled. Finally, the solidified melt was dissolved in dichloromethane and precipitated with petroleum ether, yielding 7.79 g (75%) of purified PSA-co-PCH [Weight-average molecular weight (Mw): 12.1 kDa, according to gel permeation chromatography], refer solid state NMR characterization of the beads.

AZA and DAC, or uridine (model compound for *in vitro* release experiment) were homogenized in acetonitrile suspension, using IKA T25 Ultra Turrax® dispersing instrument (Thermo Fisher Scientific), filtered off, air-dried, and milled using Pulverisette 23® Mini Mill (ILABO, spol. s r. o.). PSA-co-PCH (420 mg) was dissolved in anhydrous acetonitrile (1.78 mL) at 60°C and milled AZA, DAC or uridine (180 mg) were added subsequently. For dispersions containing DIC, the amount of PSA-co-PCH was reduced to 360 mg and DIC (60 mg) was added. The suspension (58°C) was emulsified with 50 mL of polyisobutylene thickened mineral oil (58°C) by vigorous stirring at 2000 rpm, and the resulting emulsion was stirred at 60°C for 30 min, until complete evaporation of the acetonitrile. The suspension was cooled to room temperature with stirring, and filtered. Finally, the beads were collected and washed several times with hexane to get rid of mineral oil and polyisobutylene, air-dried, and washed again quickly with H_2O to remove surface- bound drug crystals, and immediately dried in vacuo. Bead size distribution, weighted by volume fraction was determined by Mie scattering, using Mastersizer 3000 instrument (Malvern Instruments).

3.2.2. In vitro drug release

Uridine was used as a model compound for release of AZA or DAC from the beads due to chemical stability, structural similarity, and analytical simplicity. Beads with 10, 20 and 30 wt. % uridine (absorbance ca A_{max} = 1.000 for 100% release, extinction coefficient $\varepsilon_{261\ nm}$ =1.197 x 104 L $mol^{-1}cm^{-1}$) were suspended in 200 mL PBS (pH 7.4), and incubated with shaking at 37°C. Samples (aa 0.5 mL) were filtered and absorbance *A* was measured at 261 nm against PBS at selected time points. Relative release was calculated by assuming uridine as the only UV-absorbing component (verified by experiment with "empty" PSA-co-PCH beads without uridine), and neglecting sampling volume change (aa 0.5 mL vs 200 mL), according to equation, $R = (A/A_{max}) *100\%$.

3.2.3. Solid state-NMR characterization of the beads

All solid state nuclear magnetic resonance (ss NMR) spectra were measured at 11.7 T, using Bruker Avance III HD 500 US/WB NMR spectrometer (Bruker) in 3.2-mm ZrO2 rotors, at

spinning frequency of 20 kHz. The ^{13}C cross-polarization magic angle spinning NMR spectra (^{13}C CP/MAS NMR) were measured with CP contact time of 2 ms, repetition delay of 5 s, and number of scans ranging from 1024 to 2048, to reach acceptable signal to noise ratio. However, the ^{13}C MAS NMR spectra with direct excitation of ^{13}C magnetization were recoded using an excitation of 90 degree, ^{13}C pulse of 2 µs, repetition delay of 10 s and 3600 scans, to reach the acceptable signal to noise ratio. During the detection of ^{13}C NMR signal, the high power dipolar decoupling, SPINAL-64 was applied, and the frictional heating of the spinning samples was mitigated by active cooling (Brus, 2000). The temperature calibrations were performed with $Pb(NO3)_2$, and glycine was used as an external standard to calibrate the ^{13}C scale (176.03 ppm – low-field carbonyl signal).

3.2.4. In vitro biological evaluation

The demethylation and cytostatic/cytotoxic effects of the drug loaded microbeads were characterized *in vitro*, using the DNA demethylation reporter cell line, HCT116-pFLJ-H2B, described in Chapter 2.

Cell Culture and Drug Treatment: The culturing of reporter cell line, HCT116-pFLJ-H2B, cell line authentication and routine test for mycoplasma contamination were done as described in Chapter 2. On day 0, the cells were plated at the density of 2.0×10^4 cells per 3.8 cm^2 well on 6 well glass bottom plate (P06-1.5H-N, In vitro Scientific). After 24 h, drugs in powder formulations or microbeads were added in three different concentrations, viz. 25 µmol/L, 50 µmol/L, and 100 µmol/L. For powdered formulation of the drugs, 50 mM solution was freshly prepared in DMSO (the final concentration of DMSO was below 0.1%), however, in case of drugs loaded in microbeads, weight equivalents of the solid microbeads were directly added to well plates, and volume of the culture medium was adjusted to maintain the required drug concentration. Untreated wells were marked as control for the baseline measurement.

High Content Cellular Imaging and Data Analysis: For monitoring the induced effects of the continuous drug release from the time-course dissolution of the microbeads in culture medium, cellular images were acquired at every 24 h intervals following treatment, from day 1-6, using filters for Enhanced Green Fluorescent Protein, EGFP (excitation/emission: 458 nm/525 nm) and Red Fluorescent protein, RFP (excitation/emission: 555 nm/584 nm), using Operetta High-Content Imaging System (PerkinElmer). Acquired TIFF images were imported and similarly analyzed using Columbus Image Data Storage and Analysis System, as described in Chapter 2.

Briefly, for reporting demethylation, the analysis was interpreted as mean EGFP intensity per cell, calculated by dividing mean EGFP intensity per well with total number of cells in each well. However, the total number of cells counted under RFP channel was used to report the cytostatic/cytotoxic drug effects. At the end, EGFP fluorescence intensities measured from day 1 to day 6 were integrated to calculate area under the curve (AUC) for demethylation, for each drug concentration separately. Similarly, total number of cells counted from day 1 to day 6 was integrated to calculate the AUC for cytotoxicity. All statistical analyses were performed using GraphPad Prism statistical software (version 7), and differences were considered significant at $P < 0.05$.

3.3. Results

3.3.1. Preparation of microbeads and characterization of in vitro release rate

The beads were prepared by solvent evaporation method. The polyanhydride, and/or DIC were dissolved in dry acetonitrile, and finely milled AZA or DAC (nearly insoluble in acetonitrile) were suspended subsequently. The suspension was emulgated in mineral oil thickened with polyisobutylene, to suppress the microparticle aggregation, which is immiscible with acetonitrile and does not dissolve AZA, DAC, DIC or polyanhydride. The solvent (acetonitrile) was evaporated and droplets were formed into beads with desired inner architecture of microcrystals embedded in spherical matrix, formed by polymer or polymer with dissolved DIC. The average size of the microparticles was 300 µmol/L in each case. The typical micrograph is shown in Fig. 3.2A.

Different formulations of AZN prepared in microbeads were 5% DAC, 5% AZA, 30% DAC, and 30% DAC + 10% DIC.

To characterize the *in vitro* release rate of AZN, uridine was used as the model, due to its similar physical and chemical properties with AZA and DAC, and chemical stability, unlike hydrolytically labile AZA and DAC (Rogstad *et al*., 2009). Besides, at 261 nm, uridine is only UV-absorbing component in uridine-polyanhydride system, both before and after degradation.

Initially, beads were incorporated with five different loadings of uridine viz., 10, 20, 30, 40 and 50 wt. % of beads respectively. However, maximal loading to keep the microparticles cohesive was 30 wt. %, and loadings of 40 and 50 wt. % were not coherent, so only beads with 10, 20 and 30 wt. % uridine were tested for release.

Further, as seen in Fig. 3.2B, formulations with 10 and 20 wt. % loading showed relatively fast release within first 5 h, until the release of ca 80% uridine, followed by significant

slower release. Adversely, beads with 30 wt. % loading released uridine more slowly amongst all with zero order kinetics (R^2 = 0.984 for linear regression), and the release rate of 10.0 %/h within first 5 h, followed by significant slower release. The beads with 30 wt. % loading were therefore able to maintain the level of drugs in outer environment, considerably longer than the typical plasma half-life of free AZN.

Surface of the microparticles (Fig. 3.2C) as well as their size distribution (Fig. 3.2D), both may have influence on the release rate. In accordance with the release data, surface of the microparticles is smoothly and continuously covered with polymer, sufficient to provide defined release rate from the beginning. On the other hand, the microparticles are somehow polydisperse in size (Fig. 3.2D), but with negligible effect on the release rate (Fig. 3.2B).

Release of DIC from the beads was also confirmed by the test (data not shown), but experiment was complicated by the limited solubility of DIC in the concentrations suitable for "100% release" of AZN (Llinàs *et al.*, 2007).

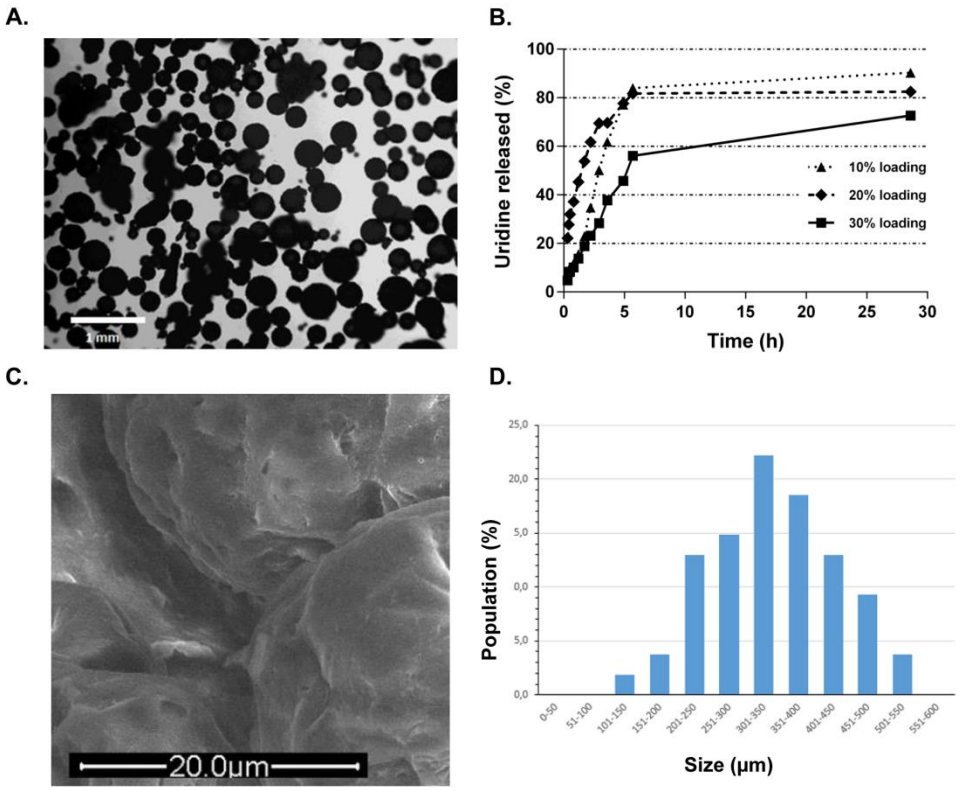

Figure 3.2 Characterization of the *in vitro* release rate of microbeads

(A) *The polymer beads with embedded AZA crystals. 10× objective, Scale bar – 1 mm.* ***(B)*** *In vitro release of 10, 20, and 30 wt. % uridine loadings from the beads into PBS (pH 7.4) at 37ºC.*

(C) *Surface of the microparticles under scanning electron microscopy.* ***(D)*** *Typical histogram of the size distribution of the microparticles,weighted by volume fraction (Mie scattering).*

3.3.2. Structural solid state-NMR analysis

For structural confirmation of the particles, dispersion with 30 wt % DAC and 10 wt. % DIC was chosen for further study by solid state NMR spectroscopy. Interpretation of the recorded data is based on previous comprehensive structural ss-NMR analyses of various polymeric solid dispersions of active compounds (Policianova *et al*., 2014; Urbanova *et al*., 2013). Chemical structures are presented in Fig. 3.3.

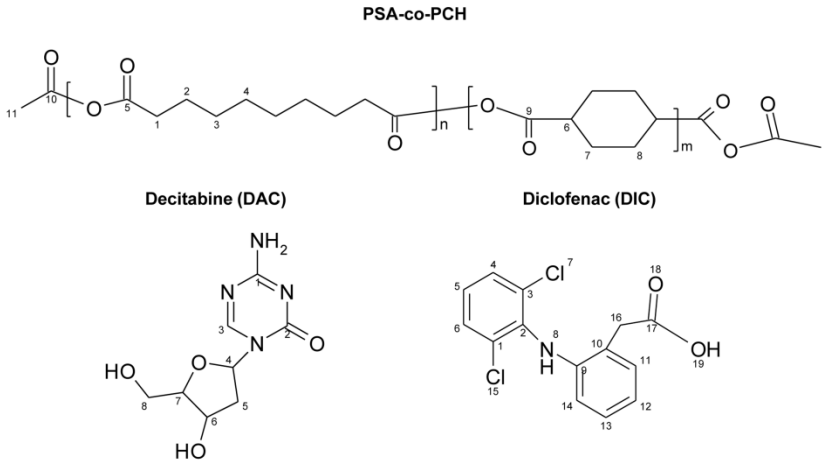

Figure 3.3 Chemical structures of the pure components

The copolymer, PSA-co-PCH and the active pharmaceutical ingredients, DAC and DIC.

The narrow well-resolved signals detected in ^{13}C CP/MAS NMR spectra of powdered DAC and DIC (Fig. 3.4A and 3.4B respectively) indicated a single-phase highly crystalline character of the active pharmaceutical ingredients (APIs), used for the preparation of solid dispersions. In contrast, the structure of PSA-co-PCH copolymer matrix was far complicated, as followed from the comparison of ^{13}C CP/MAS and ^{13}C MAS NMR spectra (Fig. 3.4C and 3.4D respectively), optimized for selective measurements of rigid (crystalline), and mobile (amorphous) phases respectively. While the ^{13}C CP/MAS NMR spectrum of PSA-co-PCH copolymer was dominated by the set of strong narrow lines at 168, 36, 34, 33 and 25 ppm, attributed to highly crystalline PSA block (carbons 5, 1, 4, 3, 2 respectively), the 13C MAS NMR spectrum consisted of the narrow signals at 170, 35, 29, 28 and 24 ppm, corresponding to highly mobile PSA segments in amorphous phase (carbons 5, 1, 4, 3, 2 respectively). Furthermore, the

presence of immobilized amorphous PSA blocks was indicated by a weak broad signal at ca. 29 ppm, and presence of amorphous PCH segments was indicated by the weak signals at ca. 41 and 27 ppm, corresponding to the carbons 6 and 7, 8 respectively, recorded in ^{13}C CP/MAS NMR spectrum (Fig. 3.4C). Besides, the weak signals, particularly detected in ^{13}C MAS NMR spectrum (Fig. 3.4D) correspond to monomer units that couple PSA and PCH blocks. These spectra thus clearly reflect the heterogeneous character of the PSA-co-PCH copolymer that consists of both, rigid (crystalline) and mobile (amorphous) phase of PSA blocks, and PCH segments that are spread in both phases (rigid and mobile). Overall, it is clear that structure of the prepared solid dispersions, DAC/PSA-co-PCH, DIC/PSA-co- PCH, and DAC+DIC/PSA-co-PCH are hardly predictable.

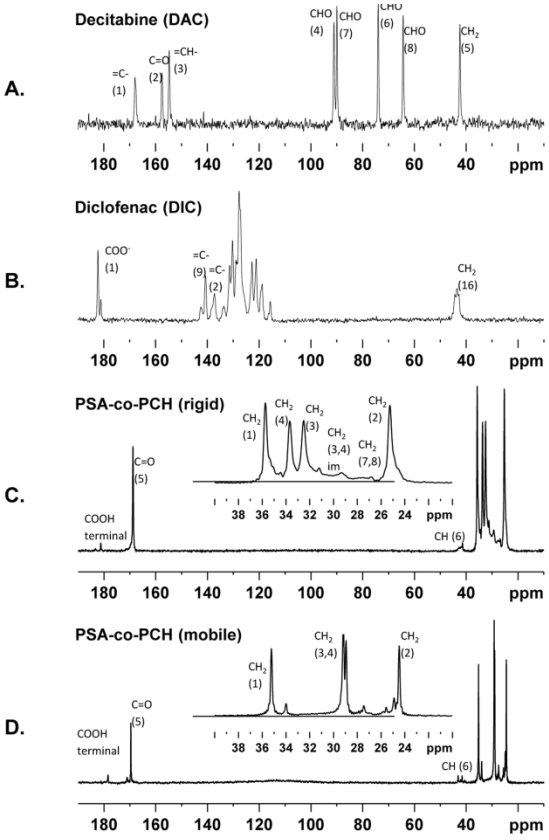

Figure 3.4 NMR spectra of the pure components and copolymer matrix

*The ^{13}C CP/MAS NMR spectra of **(A)** Decitabine **(B)** Diclofenac **(C)** PSA-co-PCH copolymer, and **(D)** the ^{13}C MAS NMR spectrum of the PSA-co-PCH copolymer.*

3.3.3. Solid state-NMR, characterizing the distribution of active pharmaceutical ingredients in copolymer matrix

The recorded ^{13}C CP/MAS and ^{13}C MAS NMR spectra of the solid dispersions further revealed the considerable differences in the distribution of DIC and DAC in the copolymer matrix.

Specifically, the set of narrow and well-resolved signals of DAC were clearly detected in ^{13}C CP/MAS NMR spectrum. The resonance frequencies of these signals were identical with the resonance frequencies recorded for pure, crystalline DAC, indicating unchanged polymorphic form of DAC. In contrast, DAC signals were absent in corresponding ^{13}C MAS NMR spectrum, measured with a relatively short repetition period. These facts indicated that in DAC/PSA-co-PCH solid dispersion, the molecules of DAC were partly phase-separated, forming nano crystalline domains. Moreover, preliminary ^{13}C detected $T_1(^1H)$ relaxation experiments showed incomplete ^1H polarization transfer between crystalline DAC and crystalline fraction of PSA, indicating the close contact of these fractions. Thus, crystallites of decitabine are probably surrounded by the crystalline fraction of PSA-co-PCH copolymer, Fig. 3.5A.

In contrast to DAC/PSA-co-PCH solid dispersion, the signals of the active compound (DIC) in DIC/PSA-co-PCH system were detected only in single-pulse ^{13}C MAS NMR spectrum, while in ^{13}C CP/MAS NMR spectrum, only the signals of crystalline rigid fraction of PSA blocks were identified. Thus, the presence of extremely narrow signals of DIC (<35 Hz) in ^{13}C MAS NMR spectrum, and the absence of the corresponding signals in ^{13}C CP/MAS NMR spectrum, confirmed nearly unrestricted molecular motion of DIC molecules in DIC/PSA-co-PCH solid dispersion. Consequently, it can be assumed that the active compound (DIC) is molecularly dispersed (dissolved) in highly mobile, amorphous fraction of PSA-co-PCH matrix (Fig. 3.5B).

However, the most complicated spectra were recorded for the triple-component solid dispersion, DAC+DIC/PSA-co-PCH, where both the active compounds incorporated in PSA- co-PCH copolymer matrix were detected in ^{13}C MAS NMR spectrum (red line) as broad unresolved signals, whereas, the corresponding signals were not detected in ^{13}C CP/MAS NMR spectrum (blue line). The observed broadening of the signals in ^{13}C MAS NMR spectrum, and the absence of the signals in ^{13}C CP/MAS NMR spectrum thus indicated considerably disordered and

amorphous character of both APIs. In consistence with the molecular mobility, the molecules of DAC and DIC probably exhibit restricted high- amplitude motions. On one hand, the motion is sufficiently fast to destroy the static ^{1}H-^{13}C dipolar couplings, disallowing the detection of the cross-polarization signals. On other hand, the motion is too slow to completely remove the signal broadening, resulting from the conformational and orientational non-equivalence of the molecules of APIs in amorphous phase. This further indicates the weak interactions between APIs and the polymer matrix. Thus, molecules of APIs are either dispersed in the amorphous, semi-flexible phase of PSA, and/or form nano-size clusters. For discrimination of these possibilities, more extensive experimentation is required. However, the detailed structural analysis of the prepared multicomponent systems, currently under progress, is beyond the scope of this literature (Fig. 3.5C).

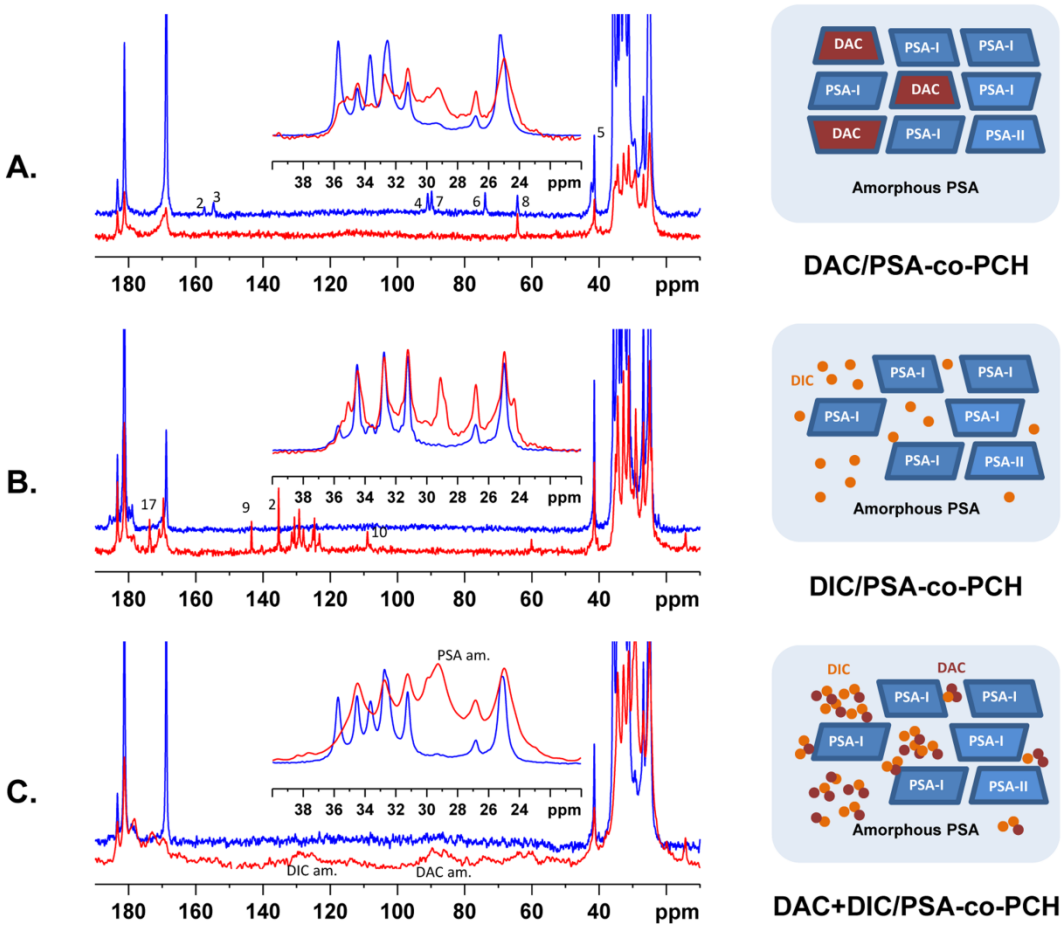

Figure 3.5 NMR spectra and schematic structural representation of the solid dispersions

The ^{13}C CP/MAS (blue lines) and ^{13}C MAS (red lines) NMR spectra, and the schematic structural representation of ***(A)*** *DAC/PSA-co-PCH* ***(B)*** *DIC/PSA-co-PCH* ***(C)*** *DAC+DIC/PSA-co-PCH.*

In conclusion, solid-state ^{13}C NMR experiments, optimized for domain-selective detection of the rigid, and/or mobile fractions, enabled the primary characterization of the multicomponent solid dispersions of DAC and DIC, in semi-crystalline PSA-co-PCH copolymer matrix. Noticeably, three types of solid dispersions (DAC/PSA-co-PCH, DIC/PSA-co-PCH, and DAC+DIC/PSA-co-PCH), each exhibiting different molecular structures were analyzed. While, the DAC/PSA-co-PCH solid dispersion was distinguished as a partially phase-separated system with crystalline domains of DAC probably surrounded by the crystalline fraction of PSA blocks, the DIC/PSA-co-PCH system was basically homogenous with highly mobile molecules of DIC dispersed in flexible amorphous fractions of PSA chains. Whereas, the three-component solid dispersion, DAC+DIC/PSA-co-PCH exhibit far complicated structure in which both active compounds form amorphous semi- flexible phase dispersed in the copolymer matrix. Also, clustering of the molecules of APIs can be assumed.

3.3.4. Biological interpretation of the therapeutic efficacy

The time-course analysis of the observed biological effects of various formulated solid dispersions with different loadings of APIs viz., 5% DAC, 5% AZA, 30% DAC, 30% DAC + 10% DIC, and powder formulations of the respective drugs (DAC and AZA), clearly demonstrated the exponential increase in the demethylation activity, in a time dependent manner until day 5, after which begin the gradual decrease. Parallel was observed for cytotoxicity. On comparing the powder drugs with microbeads for demethylation activity, microbeads were less effective at 25 µM concentration with low significant differences which started reducing at higher concentrations, and effect of microbeads was nearly equivalent or higher at 100 µmol/L concentration. In case of cytotoxicity, the differences between powder drugs and microbeads were almost negligible at 25 µM and at higher concentrations, comparatively better results were observed for microbeads.

However, formulation with additional diclofenac (30% DAC + 10% DIC) showed least demethylation and cytotoxic effects, indicating decreased drug efficacy for additional diclofenac. The decrease in hypomethylation efficacy in the presence of diclofenac may probably be a pharmacological interaction on cell- biochemical level, since the two molecules differ significantly in their physico-chemical interactions, under relevant conditions. However, after further optimization of the ratio (DAC:DIC), the effect of the anti- inflammatory drug, diclofenac is expected to remain local to the application site, as intended, while the effect of the hypomethylation drug, decitabine would be systemic (Fig. 3.6).

At last, considering the fact that the polymeric microbeads used for loading drugs may exhibit auto fluorescence or significant cytotoxicity, resulting in false interpretation of the results, beads without loaded DAC or AZA was also incorporated during the experiment (100% polymer, 30% DIC, 5% uridine), but the values obtained were similar to the untreated cells (data not shown).

Besides, the present study was performed in cell culture system and it was difficult to analyze the demethylation profile after day 6, due to increasing number of dead cells in experimental wells because of high drug concentrations used, and the confluency attained in control wells. Also, it was not suitable to perform the experiment using drug concentration lower than 25 µmol/L due to difficulty in weighing low amount of beads, and the concentrated molar solutions were not possible for this type of experiment. However, on the basis of microscopic observations, it is assumed that if the experiment is prolonged, the effects of microbeads will overcome the powder drug formulation, which is subjected to rapid chemical decomposition in aqueous solution after a short life span.

Moreover, the hypomethylation efficacy may also be influenced by the fact that the inhibition of DNMTs by azacytidine nucleosides is irreversible, and the turnover of the enzyme in a cell is relatively slow, so even a short exposition to free AZN may have effect *in vitro* due to high concentrations, causing immediate distribution of the drug within the cultivation well. On contrary, sufficiently long exposition is required *in vivo* for proper exposition of all malignant cells within the organism.

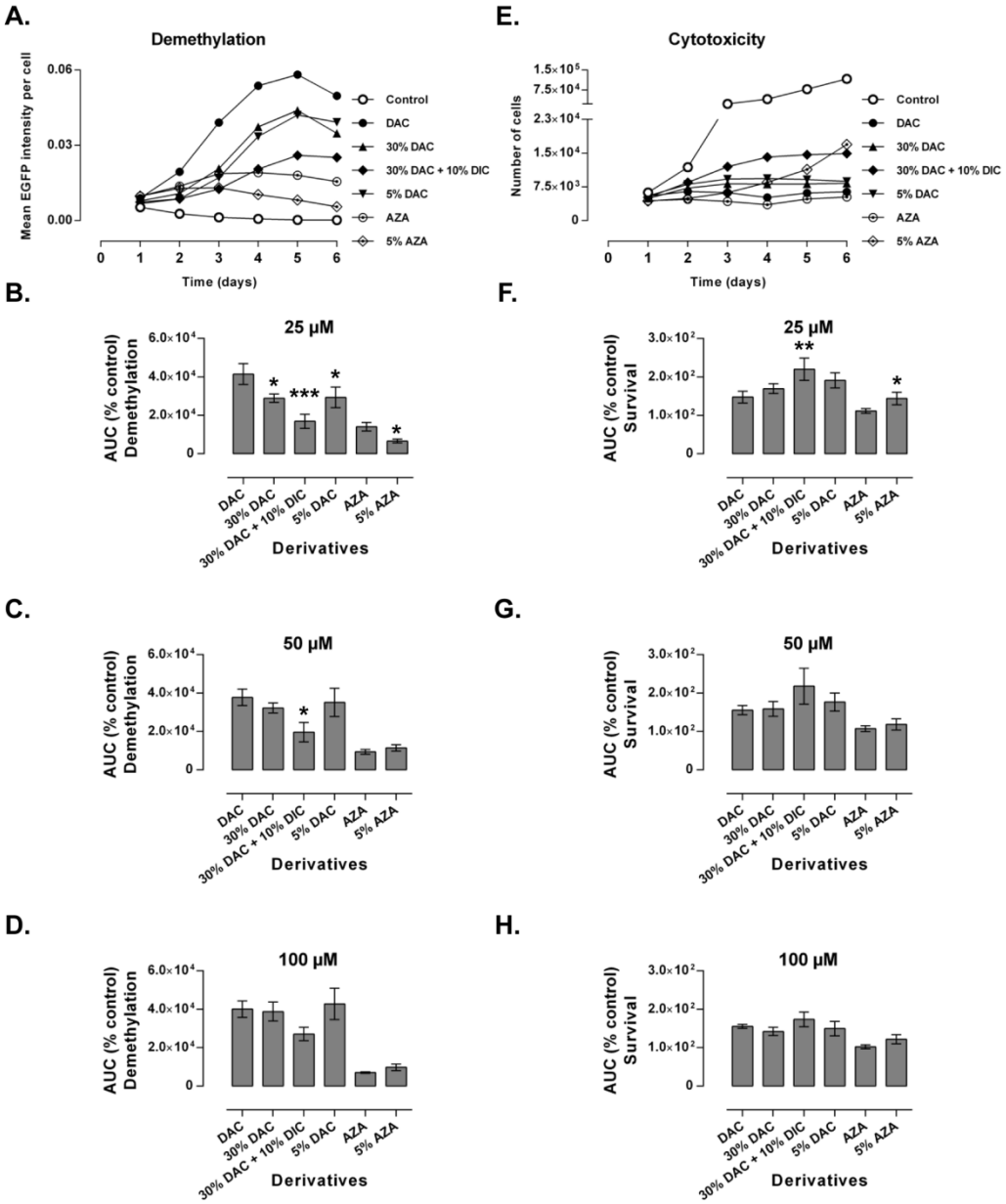

Figure 3.6 Characterization of the therapeutic efficacy of azanucleosides: powder drug formulation versus microbeads

*Demethylation **(A)** and Cytotoxicity **(E)** represent schematic plot for calculation of AUC at 25 µM. AUC for demethylation was calculated from the mean EGFP intensity per cell, quantified from day 1-6, and AUC for cytotoxicity was similarly calculated using number of cells from day 1-6. **(B-D)**, show AUC plots for demethylation, and **(F- H)**, show AUC plots for cytotoxicity. Values are means ± S.D, n = 3. Statistical significance, *p<0.05, **p<0.005, ***p <0.0005, was determined by comparing DAC, powder drug with its various formulations in microbeads, likewise, AZA, powder drug with its formulation in microbeads.*

3.4. Discussion

The characterization of *in vitro* release rate of microbeads indicated that PSA-co-PCH containing 30 wt. % drug showed zero-order release (R^2= 0.984 for linear regression), and release rate of 10.0 %/h within the first 5 h, and subsequent slower release of the remaining drug, thus maintaining the level of drugs in the outer environment considerably longer than the typical plasma half-life of free AZN.

The biodegradable microbeads were than characterized for the therapeutic efficacy. For the purpose the induced demethylation and cytotoxic effects of DAC and AZA loaded in microbeads was evaluated in comparison with the powder formulations, using the DNA demethylation detection system described in Chapter 2. The study reported almost negligible or no differences between powder drug formulations and microbeads, at lower concentration, instead, at higher concentrations, equivalent or increasing effects of the drugs loaded in microbeads was discovered.

Besides, on comparing the microbeads formulations with different loadings of azanucleoside drug (DAC), no significant difference was observed. Therefore, it may be advantageous (as in most cases) to achieve as high drug loading as possible, without compromising the physico-chemical and biological properties. This will significantly reduce the amount of additional excipients and adjuvants (which should be eliminated from the organism after use), and also reduce the application volume for injection.

In conclusion, this study predicts that the substitution of the powder drug formulations of DAC and AZA, for injections, with drugs loaded microbeads, may increase the plasma circulation time of these hydrolytically labile drugs, and release the patients from the painful treatment therapy by reducing the number of *i.v.* injections per cycle of the treatment, on account of the chemical decomposition of the powder drug in aqueous solution.

To our knowledge, this is the first demonstration of the comparative effects of the powder and the biodegradable microbeads formulations for the studied drugs *in vitro*, however, the complex pre-clinical data still needs to be determined.

Aim 3: Study stromal cell-induced alterations in the response of cancer cell to DNA hypomethylating agents

Chapter 4

Stromal cell-induced effects on demethylation therapy

This Chapter describes the effects of the stromal cells of the tumor-microenvironment on the response of colorectal cancer cells to DNA methyltransferase inhibitors, in 2-dimensional and 3-dimensional cultures, using DNA demethylation detection system described in Chapter 2.

4.1. Introduction

The cellular heterogeneity in the tumor microenvironment plays a key role in tumor progression, invasion, metastasis, and the outcome of anti-cancer therapy (Li *et al*., 2007). While the tumor stroma does not have metastatic potential per se, stromal cells acquire abnormal phenotype through crosstalk with tumor parenchyma and support the growth and progression of cancer (Li *et al*., 2007; Coussens & Werb, 2002; Tlsty & Hein, 2001; Liotta & Kohn, 2001). Therefore, there is a growing interest in the role of tumor-stroma interactions to understand how tumor cells respond to different classes of anti-cancer drugs (McMillin *et al*., 2013).

Colorectal cancer (CRC) is one of the most common cancers with heterogeneous treatment outcomes (Guinney *et al*., 2015; Linnekamp *et al*., 2015), and recent evidence indicate the key role of the stroma in CRC invasion, metastasis, and resistance to chemo- and radiotherapy (Conti & Thomas, 2011; Lotti *et al*., 2013; Isella *et al*., 2015). An image-based quantitative study suggested the abundance of cancer-associated fibroblasts in tumor-stroma as an indicator of disease recurrence after curative CRC surgery (Tsujino *et al*., 2007). In poor-prognosis CRC subtypes that are characterized by epithelial-to-mesenchymal transition, elevated expression of mesenchymal genes is mainly contributed by tumor-associated stroma (Calon *et al*., 2015). High Wnt signaling activity in tumor cells located close to stromal myofibroblasts further indicates that stemness of colon cancer cells is partly regulated by the tumor-microenvironment (Vermeulen *et*

al., 2010). Besides tumor-stroma crosstalk, the colonic fibroblast secretome plays a crucial role in regulating the proliferation of colon cancer cells (Chen *et al*., 2014). Moreover, soluble and insoluble factors released by stromal cells following irradiaiton has also been suggested to contribute to tumorigenesis and drug resistance (Barcellos-Hoff *et al*., 2005).

DNA methyltransferase inhibitors (DNMTIs), such as 2'-deoxy-5-azacytidine (DAC) and 5-azacitidine (AZA) have shown promising activity in the treatment of solid tumors in early clinical trials (Tsimberidou *et al*., 2015; Brown *et al*., 2014; Li *et al*., 2015a). Furthermore, DNMTIs have been reported to work synergistically in combination with various other anti-cancer therapies (Blum *et al*., 2012; Chiappinelli *et al*., 2015; Garcia-Manero *et al*., 2006; Kirschbaum *et al*., 2014; Li *et al*., 2014; Matei *et al*., 2012; Wrangle *et al*., 2013) and radiotherapy (Son *et al*., 2016; Gravina *et al*., 2010; Kim *et al*., 2014a). Although the effects of DAC alone or in combination with various combinatorial therapies are well-reported, it is not known how stromal cells of the tumor-microenvironment influence the response of cancer cells to DNMTIs. In this study, the influence of irradiated and non-irradiated fibroblasts, and of the conditioned medium (CM) from the two culture types on the response of CRC cells to DNMTIs was evaluated, in 2-dimensional and multicellular spheroids (MCS) cultures, using DNA demethylation detection system described in Chapter 2.

4.2. Materials and Methods

Unless and otherwise indicated, media, chemicals, and other reagents were purchased from Sigma-Aldrich.

4.2.1. Chemicals and cell lines

DAC, alpha anomer of DAC (α-DAC), AZA, and 2'-deoxy-5, 6-dihydro-5-azacytidine (DHDAC) were synthesized as described previously (Matoušová *et al*., 2011). Drugs were dissolved in DMSO and prepared fresh before each experiment. DMSO concentration was always less than 0.1% in treated wells.

DNA demethylation reporter cells, HCT116-pFLJ-H2B, henceforth referred to as HCT116, were generated and maintained as described in Chapter 2. Human BJ fibroblasts were maintained as described elsewhere (Das *et al*., 2016). Human mesenchymal stromal cells (MESCs) with or without Red Fluorescent Protein (RFP) were generated and maintained as described previously (Skolekova *et al*., 2016).

4.2.2. X-ray irradiation, conditioned medium and viability assay

BJ cells, at 70-80% confluency were exposed to 10 Gy X-ray irradiation in an X-Ray irradiator (Model: RS225; Xstrahl) at a dose rate of 2.3 Gy/min. Irradiated BJ (irBJ) were then maintained for 7 additional days before the collection of CM and use of cells for co-cultures. The collected CM from irBJ culture was filtered using a 0.2 µm filter and stored at -80ºC for later use. In parallel, CM was also collected from 7-day old non-irradiated BJ cells. CM was diluted to 25-100% in complete medium prior to experiments.

HCT116 cells were seeded in 96-well plates and exposed to X-ray irradiation as described above (irHCT116). After 8 h following irradiation, cells were treated with DAC either in CM from irBJ or complete medium for 72 h, and cell viability was determined using standard 3-(4,5-dimethylthiazol-2-yl)-2,5-diphenyltetrazolium bromide (MTT) assay.

4.2.3. Demethylation bystander experiments in 2D cultures

Co-cultures were established by seeding HCT116 and BJ or irBJ cells at a ratio of 7:3 to 3:7 in clear-bottom Cell Carrier 96-well plates (PerkinElmer) at a total density of 3×10^3 cells per well. The plate also included wells containing monocultures of HCT116. All co-cultures were established in Eagle's Minimum Essential Medium (EMEM) which support the normal growth of both cell types. For CM culture experiments, the old medium was replaced with CM from BJ or irBJ. Cells were treated with DNMTIs diluted in appropriate medium for 72 h, and imaged in a CellVoyager™ CV7000 High-throughput Cytological Discovery System (Yokogawa Electric Corporation) as described in Chapter 2. Acquired images were analyzed to evaluate the intensity of Enhanced Green Fluorescent Protein (EGFP) signals as described in Chapter 2. The rate of HCT116 cell proliferation (Day 3/Day 1) in different culture types was determined by counting total number of RFP-H2B-tagged cell nuclei (representative of HCT116).

4.2.4. Multicellular spheroids, drug treatment and imaging

MCSs were generated according to the MCS generation protocol described previously (Das *et al*. 2016). Co-culture MCSs of HCT116 and BJ or irBJ were established only at a single ratio of 3:7. To study the effect of CM, monotypic HCT116 MCSs were transferred to new culture plates containing CM with or without drugs. MCSs were allowed to grow for 7 days before the start of any treatment, and all drug treatments were carried out for 96 h. Imaging of MCSs was done using Operetta High Content Screening System (PerkinElmer), and images were

analyzed to quantity EGFP intensity as described in Chapter 2. The change in MCS size following drug treatment was determined as described previously (Das *et al*., 2017).

4.2.5. Hoechst dye diffusion assay, imaging and flow cytometry of Hoechst-stained multicellular spheroids

Hoechst dye diffusion assay: Prior to the end of drug treatment, MCSs were stained with 10-20 µM Hoechst 33342 (Molecular Probes™, Invitrogen) at 37^{o}C for 2 h. Hoechst-stained MCSs were than either processed for light-sheet fluorescence microscopy or flow cytometry as described below.

Imaging: Following the Hoechst dye diffusion assay, images of drug-treated MCSs were acquired in a Zeiss Lightsheet Z.1 microscope (Carl Zeiss). Briefly, drug-treated Hoechst-stained MCSs were collected, washed 1× with PBS and mounted in 1.5% (w/v) low-melting agarose maintained at 40ºC. MCS-embedded agarose was drawn into a 0.5 mm glass capillary tube (Carl Zeiss) with a metal plunger (Carl Zeiss) and allowed to polymerize for 5 min at room temperature. The capillary tube was then vertically mounted on a sample holder, and immersed in a sample chamber filled with phenol-red free EMEM. The polymerized agarose containing the embedded MCS was then extruded into the sample chamber using the plunger, and multi-directional z-stack images were acquired using a 5× detection optics and two 10× illumination optics. Captured images were processed using Zen Blue image processing software (Carl Zeiss).

Flow cytometry: To determine the extent of demethylation in sub-regions of MCSs, flow cytometric analysis was performed following the methods described previously (Haass *et al*., 2014) with some modifications. Briefly, 25-30 Hoechst-stained MCSs were collected in a 15 mL Falcon® tube, washed thoroughly with PBS, and disaggregated into single cell, using Accutase® cell detachment solution. Disaggregated cells were resuspended in PBS containing 1% FBS and analyzed in a BD Influx™ cell sorter (BD Biosciences).

4.2.6. Western blot analysis of colorectal cancer cells from mono- and co-cultures

HCT116 in complete medium and 25% irBJ CM, and 3:7 co-cultures of HCT116:BJ or irBJ were treated with 1 µM DAC for 72 h. HCT116 cells from monocultures were immediately lysed and processed for western blot analysis as described previously (Das *et al*., 2012). To analyze the effect of DAC on HCT116 only in co-cultures, RFP stained HCT116 cells were isolated by sorting in a BD FACSAria II cell sorter (BD Biosciences). Briefly, following drug treatment, co-cultures were trypsinized and harvested into a 15 mL Falcon® tube, and a uniform

single-cell suspension was prepared by passing cells through a sterile Falcon® 100-µm cell strainer (Corning Inc.,). Cells were resuspended in 1% FBS-containing PBS and sorted based on RFP-tagged nuclei (excitation/emission: 488 nm/572 nm) into a new Falcon® tube filled with complete growth medium. Sorted cells were resuspended in cell lysis buffer for western blot analysis as described above.

Primary antibody against DNA methyltransferase 1 (DNMT1) was purchased from Cell Signaling Technology (Danvers), whereas, those against cytidine deaminase (CDA), deoxycytidine kinase (DCK), and TET methylcytosine dioxygenase 1 (TET1) were purchased from Bio-Techne (Abingdon). Secondary blots were developed using goat anti-mouse or anti-rabbit Alexa Fluor® 488-conjugated secondary antibodies (Life Technologies).

4.2.7. Determination of NFκB activity and cytokines

Human lung carcinoma A549 cells (ATCC) were transduced with lentiviral particles (Cignal Lenti NFkB Reporter, Qiagen) expressing the firefly luciferase gene under the control of a minimal CMV promoter and tandem repeats of the *NFκB* transcriptional response element according to manufacturer's protocol [Multiplicity of Infection = 20]. To enhance the efficiency of transduction, SureENTRY Transduction Reagent (Qiagen) was used at a concentration of 8 µg/mL. Transduced A549 cells were subjected to selection pressure of puromycin (3 µM) followed by single cell cloning using FACS to generate the stably transfected A549-*NFκB* reporter cells.

For determining *NFκB* activity, A549-*NFκB* cells were seeded at a density of 2×10^3 cells/well in Ham's F-12 medium in white opaque 96-well plates (PerkinElmer) and allowed to attach for 24 h. The following day, the old medium was replaced with CM (100%) from BJ and irBJ, and the cells were incubated for 48 h. At every 24 h, 100 µL of Britelite plus luminescent reagent (PerkinElmer) was added per well, the plate contents were mixed in a plate shaker, and the luminescent signal was measured using EnVision Multilabel Plate Reader (PerkinElmer).

The cytokines in CM were assayed using a Cytokine Human Magnetic 25-Plex Panel Luminex™ kit (Life Technologies), following manufacturer's protocol.

4.2.8. Statistical analysis

All statistical analyses were performed using GraphPad Prism statistical software (version 7), and differences were considered significant at $P < 0.05$.

4.3. Results

4.3.1. Co-culturing with stromal cells makes colorectal cancer cells susceptible to hypomethylating agents

To examine the bystander effect of irradiation on HCT116 response to DNMTIs, irBJ cells were co-cultured with HCT116 at 7:3 and 3:7 ratios. A comparison of EGFP intensities between monoculture and co-cultures showed a culture-dependent increase in the effect of DAC, α-DAC, and AZA on HCT116 in the order of 3:7 > 7:3 > monoculture (Fig. 4.1A). To examine if the effect of irBJ was limited only to bystander effect, a similar comparison of EGFP intensity was performed following treatment of HCT116 in co-culture with BJ (Fig. 4.1A, B). Similar to irBJ co-cultures, there was a significant effect of BJ on DAC- and α-DAC-induced demethylation of HCT116 (Fig. 4.1A). Remarkably, the altered response was more pronounced when HCT116 were co-cultured with irBJ than BJ.

To examine if the effects of irBJ and/or BJ cells were due to secreted factors, HCT116 cells were treated with DNMTIs in CM from both irBJ and BJ cells. There was a concentration-dependent effect of irBJ CM on DAC- and α-DAC-induced demethylation of HCT116 (Fig. 4.1C). In contrast, there was no effect of BJ CM on EGFP intensity (data not shown).

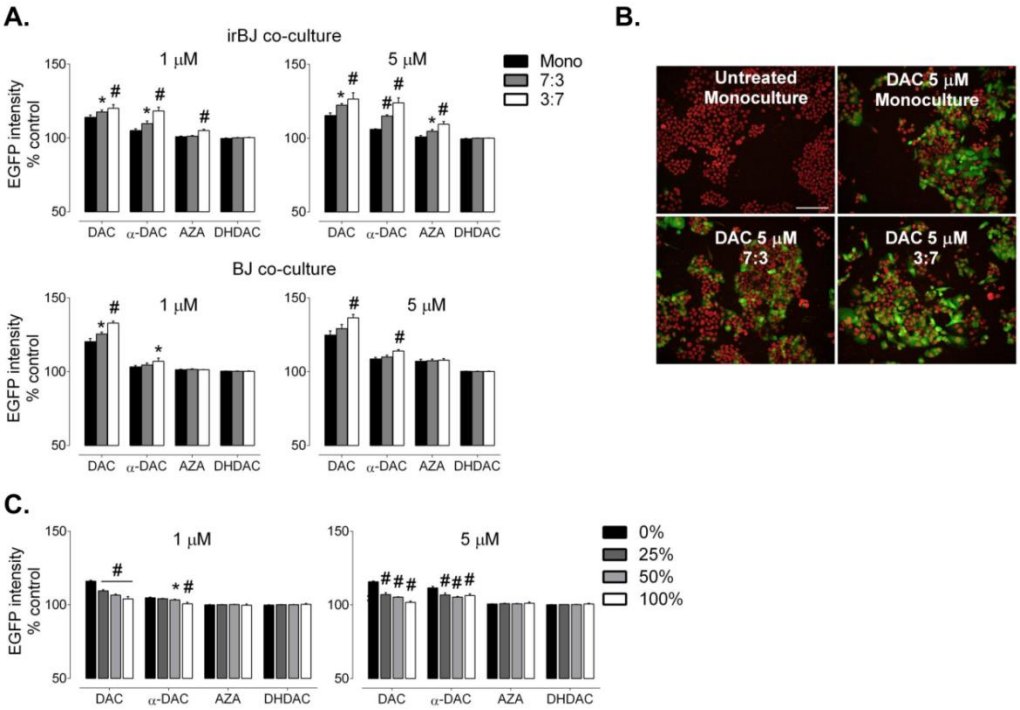

Figure 4.1 Effect of irradiated fibroblast cells on colorectal cancer demethylation by DNMTIs

(A) *Graphs are presented to show the change in EGFP intensity following 72 h of treatment with 1 µM and 5 µM DNMTIs in different culture types. Data are mean ± SEM, n = 4, #p < 0.001, *p < 0.01 comparing 7:3 and 3:7 to monocultures, one-way Anova with Dunnett's multiple comparisons test.* ***(B)*** *High-content cellular images showing RFP (red) nuclear fluorescence but no EGFP fluorescence in untreated control, and varying EGFP (green) fluorescence following 72 h of treatment with 5 µM DAC. 20× objective, Scale bar: 100 µm.* ***(C)*** *Graphs showing the effect of CM from 7-day old cultures of irBJ on EGFP fluorescence in monocultures of HCT116 following treatment with 1 µM and 5 µM DNMTIs. Data are mean ± SEM, n = 4. #p < 0.001, *p < 0.01, comparing 0% CM to others, one-way Anova with Dunnett's multiple comparisons test.*

4.3.2. Conditioned medium from irradiated fibroblasts increased colorectal cancer cell proliferation

Since the demethylation effects of DAC is more pronounced in actively proliferating cells (Yang *et al*., 2010), the effect of BJ and irBJ co-cultures and irBJ CM on the proliferation of drug-untreated HCT116 was examined. Compared to monocultures, the proliferation of HCT116 was markedly increased in BJ and irBJ co-cultures (Fig. 4.2A). Likewise, there was an increase in HCT116 proliferation in cultures supplemented with 25-50% but not 100% irBJ-derived CM compared to 0% CM (Fig. 4.2B).

If irradiation-associated factors from stromal cells are responsible for increased proliferation of HCT116 and their susceptibility to DAC and α-DAC, then it can be speculated that DAC will be more effective in inhibiting the proliferation of HCT116 in CM. Accordingly, an increased anti-proliferative activity of DAC in HCT116 was observed when the treatment was done in irBJ CM than cell-free irradiated medium (Fig. 4.2 C). However, irradiating HCT116, which is known to result in G2 arrest (Moran *et al*., 2008), significantly abrogated anti-proliferative effects of DAC even under irBJ CM culture condition (Fig. 4.2C).

To understand the mechanism behind increased proliferation of HCT116 cells in CM, the *NFκB* activity, and pro-inflammatory and immunomodulatory cytokines and chemokines were analyzed in CM. The findings showed a significant (2-fold) activation of *NFκB*, and subsequent induction of *IFN-α* and pro-inflammatory chemokines, *IL-6*, *IL-8* and *MCP-1* in CM from irBJ than BJ cells (Fig. 4.2D).

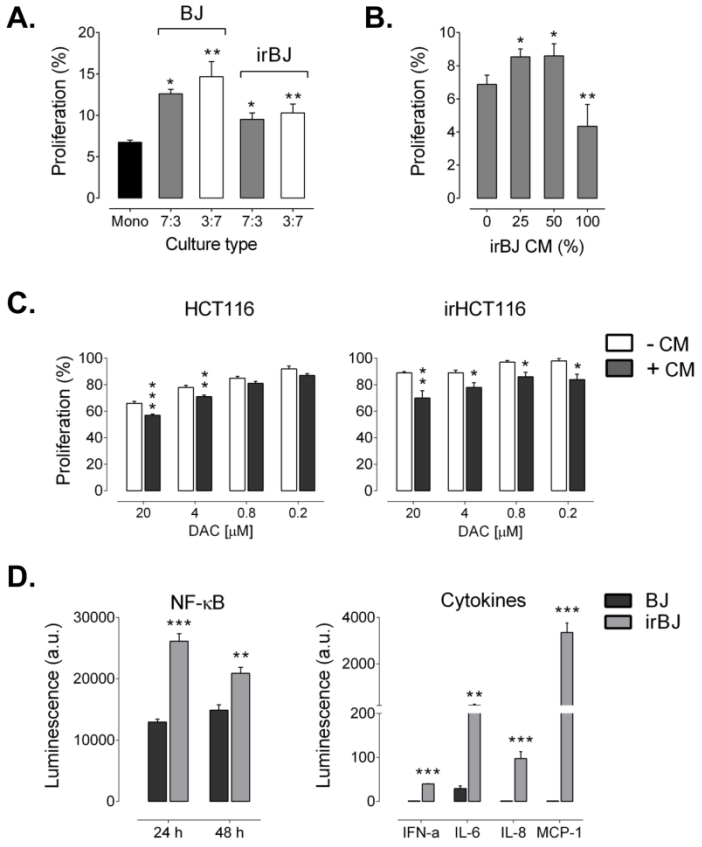

Figure 4.2 Proliferation of colorectal cancer cells, and pro-inflammatory cytokines in irradiated fibroblasts conditioned medium

(A, B) *HCT116 proliferation in monoculture, and BJ and irBJ co-cultures* ***(A)*** *and the effect of irBJ CM on HCT116 proliferation* ***(B)****. Data are mean ± SEM, n = 4, **p < 0.01, *p < 0.05 comparing 7:3 and 3:7 to monoculture or comparing 0% CM to others, one-way Anova with Dunnett's multiple comparisons test.* ***(C)*** *Graphs showing the anti-proliferative activity of DAC treatment (72 h) on HCT116 and irHCT116 in the absence (-CM) and presence (+CM) of 25% irBJ CM. Data are mean ± SEM, n = 4, ***p < 0.001, **p < 0.01, *p < 0.05 comparing –CM to +CM, Student's t-test, unpaired.* ***(D)*** *The levels of NF-kB and cytokines in CM from 7-day old non-irBJ and irBJ cultures. Data are mean ± SEM, n = 3, ***p < 0.001, **p < 0.01, comparing BJ to irBJ, Student's t-test, unpaired.*

4.3.3. Increased demethylation of colorectal cancer cells in multicellular spheroids co-culture

To study the co-culture- and CM-induced alterations under more physiologically relevant growth conditions, the effect of DAC and α-DAC was investigated in co-culture MCSs of

HCT116 and BJ. Similar to 2D culture, high ratio of BJ and irBJ significantly increased HCT116 demethylation in co-cultures compared to monoculture following treatment with DAC and α-DAC at 5 μM (Fig. 4.3A, B). There was no major difference between BJ or irBJ effects on drug-induced HCT116 demethylation. However, in contrast to 2D CM cultures, CM from irBJ did not affect DNMTI-induced demethylation (Fig. 4.3C). Only the effect of 25% irBJ CM was investigated since the maximum effect was observed at this concentration in 2D cultures (Fig. 4.1C).

Because there was no difference between BJ and irBJ effects, it was determined if increased demethylation activity of DAC and α-DAC translated into anti-tumor effect in co-culture MCSs of HCT116 and non-irBJ cells. The untreated co-culture MCSs showed a significant growth compared to monotypic HCT116 MCSs after 7 days in culture (Fig. 4.3D). However, DAC and α-DAC at 1 μM significantly decreased the growth of 3:7 co-culture MCSs compared to monotypic MCSs (Fig. 4.3E). This effect was evident only at lower doses of drugs and in 3:7 co-cultures only.

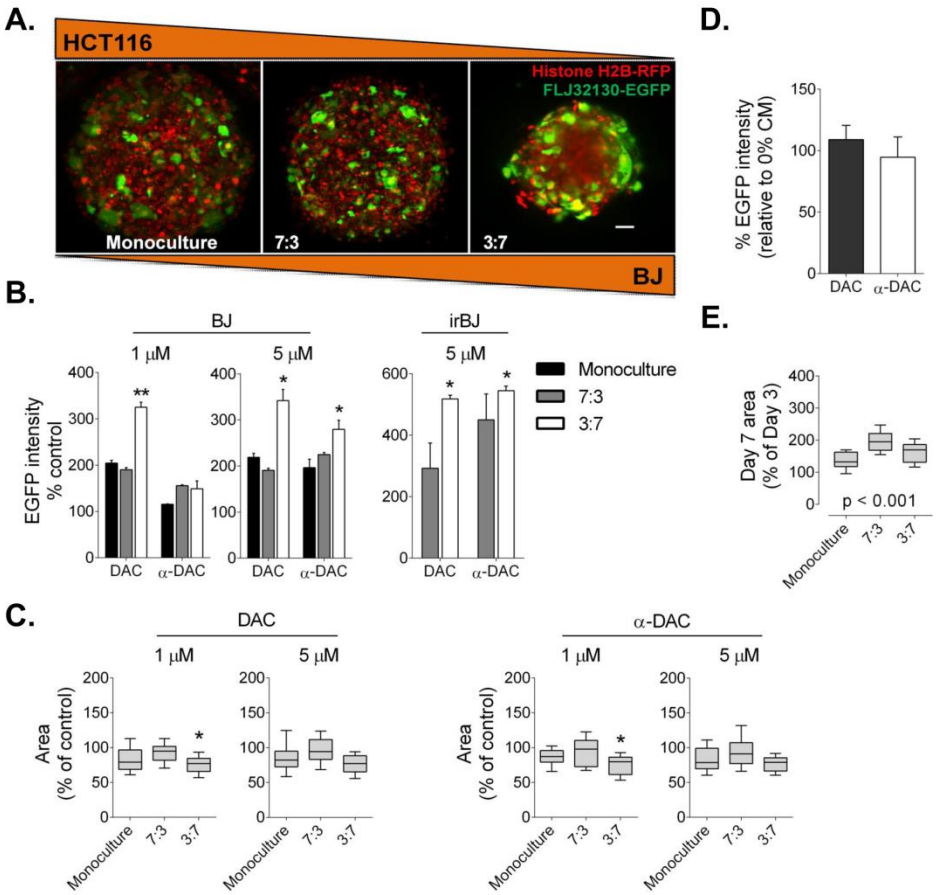

Figure 4.3. Co-culture and conditioned medium effects on colorectal cancer demethylation in multicellular spheroids

(A) *Images showing the effect of altered HCT116 to BJ ratio on demethylation following 1 μM DAC treatment for 96 h. 5× objective, Scale bar: 50 μm.* ***(B)*** *The quantification of EGFP intensity in monoculture MCSs, and 7:3 and 3:7 co-culture MCSs of HCT116 and BJ (left) or irBJ (right) following treatment with the indicated concentrations of DAC and α-DAC. Data are mean ± SEM, n = 3, **p < 0.01, *p < 0.05, comparing 7:3 and 3:7 to monocultures, one-way Anova with Dunnett's multiple comparisons test.* ***(C)*** *Graph showing no effect of 25% irBJ CM on demethylation by DAC and α-DAC in MCSs. Data are mean ± SEM, n = 4.* ***(D)*** *An increase in the growth of co-cultured (7:3 and 3:7) MCSs following 7 days in culture. The co-cultures were established between HCT116 and non-irBJ cells. The P-value of the Kruskal–Wallis test is shown in the graph.* ***(E)*** *The effect of DAC and α-DAC on monoculture and co-culture MCS size following 96 h of treatment. Co-culture MCSs are of HCT116 and normal BJ cells. In* ***(D)*** *and* ***(E)*** *data are shown for n > 20 spheroids per group from 3-4 independent experiments, Kruskal–Wallis test with Dunnet's multiple comparisons test. The boxes and horizontal bar within the boxes in the boxplots in* ***(D)*** *and* ***(E)*** *represent the 25th and 75th percentiles and median, respectively. The whiskers represent the 10th and 90th percentiles.*

4.3.4. Co-culturing with mesenchymal cells increased colorectal cancer demethylation

To examine if the high stroma-induced increased response of HCT116 to epigenetic drugs is reproducible with other stromal cell type and in a different experimental setting, the effect of DAC on co-culture MCSs of HCT116 and MESCs at a ratio of 3:7 was examined by flow cytometry. Light sheet fluorescence microscopic analysis revealed that the MESCs were present at the center of MCSs surrounded by HCT116, and were visible only after a depth of approximately 100 μm (Fig. 4.4A). Therefore, MCSs were stained with Hoechst for 2 h which created a diffusion depth of 80 μm, resulting in Hoechst high (0-80 μm) and Hoechst low (> 80 μm) sub-regions (Fig. 4.4B, C).

Next, the flow cytometric analysis of DAC-treated Hoechst-stained MCSs was performed to understand the extent of demethylation in sub-regions of MCSs, demarcated by Hoechst staining. A comparison of cells in Hoechst high region demonstrated an increased effect of 5 μM DAC on HCT116 in BJ co-cultures compared to HCT116 only MCSs (Fig. 4.4D). Interestingly, this effect was significantly pronounced when HCT116 were co-cultured with MESCs (Fig. 4.4D). Although, HCT116 were demethylated following DAC treatment compared to untreated

cells in Hoechst low region, there was no difference in the effect of DAC between culture types (Fig. 4.4D).

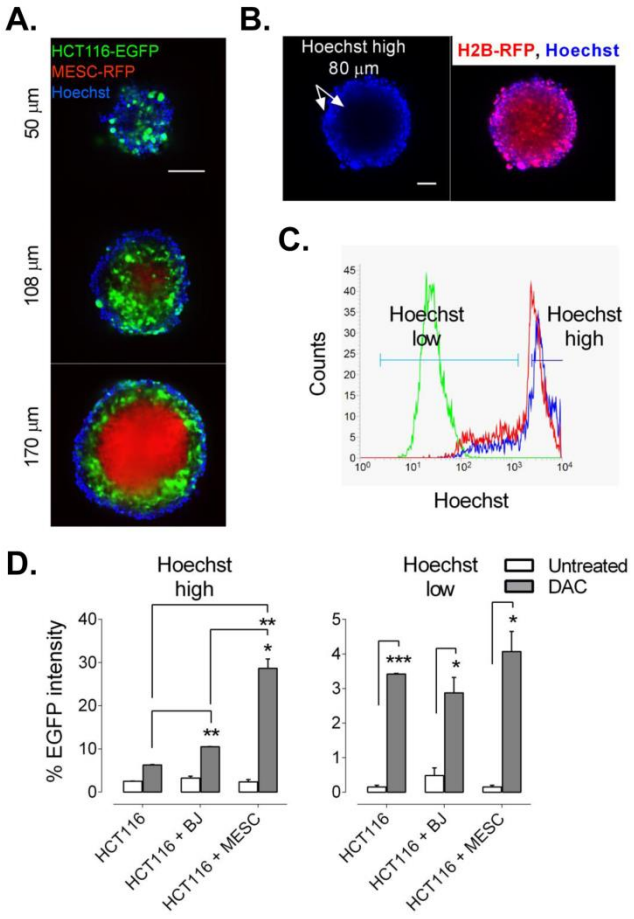

Figure 4.4. Flow cytometric analysis of demethylation in multicellular spheroids co-culture

(A) *Images showing the distribution of HCT116 (green) and MESCs (red) in MCSs at 50, 108, and 170 µm z-plane height. Outer layer of MCS is stained blue with Hoechst nuclear staining dye. 5× objective, Scale bar: 50 µm.* ***(B)*** *An image of MCS after 2 h of staining with 20 µM Hoechst showing the penetration of Hoechst to a depth of 80 µm demarcated as Hoechst high region. 5× objective, Scale bar: 20 µm.* ***(C)*** *Representative overlay histogram showing the gating of Hoechst low (green) and Hoechst high (blue) regions of MCSs. Red denotes an overlay of treated samples.* ***(D)*** *Bar graphs showing the % of EGFP intensity with Hoechst high and Hoechst low regions in monotypic HCT116 MCSs and co-culture MCSs of HCT116 and normal BJ fibroblast or MESCs at a ratio of 3:7. Data are mean ± SEM of 3-4 independent experiments. **p < 0.01, *p < 0.05, one-way Anova with Dunnett's multiple comparisons test when comparing HCT116 to HCT116 + BJ and HCT116 + MESCs in Hoechst* high. ***p < 0.001, *p < 0.05, comparing untreated to DAC, Student's *t*-test, unpaired.

4.3.5. Co-culturing with irradiated fibroblasts, and irradiated fibroblasts conditioned medium altered DAC-induced inhibition of DNMT1

To elucidate the potential mechanism that resulted in enhanced DAC effect under co-culture and in CM, the level of DNMT1 and TET1 in HCT116 was analyzed from different culture conditions. DAC resulted in down-regulation of DNMT1 in HCT116 in all culture types, however, this down-regulation was significantly greater in irBJ co-cultures (Fig. 4.5A). Additionally, the expression level of DNMT1 was markedly reduced in untreated HCT116 from both BJ and irBJ co-cultures. While DAC significantly inhibited DNMT1 when the treatment was carried out in BJ CM, this inhibition was abrogated when HCT116 were treated with DAC in irBJ CM (Fig. 4.5B). There was no statistically significant difference in TET1 levels in HCT116 under different culture conditions following DAC treatment.

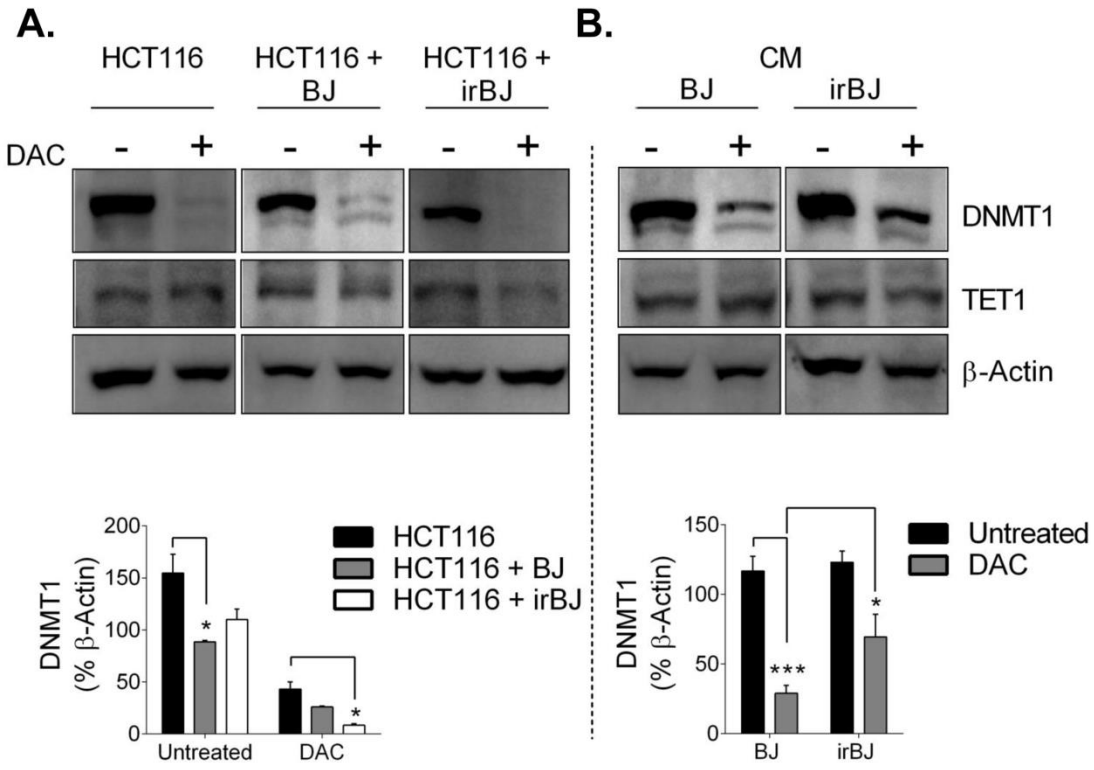

Figure 4.5. Changes in the expression of DNMT1 and TET1

*Representative western blots and densitometry analysis of DNMT1 and TET1 levels in DAC-untreated- and -treated HCT116 cells in **(A)** monocultures and co-culture with BJ and irBJ cells at a ratio of 3:7 and, **(B)** CM from 7-day old cultures of BJ and irBJ cells. DNMT1 and TET1 blots in **(A)** and **(B)** are taken from different gels. Data are mean ± SEM, n = 3, **p < 0.01, *p < 0.05, one-way Anova with Dunnett's multiple comparisons test.*

4.4. Discussion

DNMTIs are approved interventions for hematological malignances and have shown promising outcome for the treatment of solid tumors in the clinic. Although the radiosenitizing effects of DNMTIs are well-reported (Son *et al*., 2016; Kim *et al*., 2014a), the effect of irradiated and/or non-irradiated stromal cells on tumor cell response to DNMTIs remains elusive. Using the demethylation detection system described in Chapter 2, it is shown that irradiated, perhaps senescent BJ cells increase the susceptibility of HCT116 to DNMTIs. This effect is not limited to just bystander effect of irradiated cells as non-irradiated BJ cells induced a similar effect on HCT116 in both 2D and MCS cultures. Moreover, the increase in HCT116 demethylation in the order of 3:7 > 7:3 > monocultures suggests that HCT116 in a higher stroma environment are more susceptible to hypomethylating agents. This is also evident from the significant effect of low concentrations of DAC and α-DAC on co-culture MCSs with higher ratio of BJ cells compared to HCT116 only MCSs. Tumor-stroma ratio has been suggested to have prognostic significance in different cancer types (de Kruijf *et al*., 2011; Panayiotou *et al*., 2015; Yoshihara *et al*., 2013). The increased activity of DAC and α-DAC in high stromal cell co-cultures suggests the potential of tumor-stroma ratio for predicting the outcome of epigenetic therapy in CRC or other cancer types.

The stroma has been reported to regulate the growth of tumor cells, increasing their invasive and metastatic characteristics (Tlsty & hein, 2001). In this study, BJ-induced increase in the proliferation of HCT116 in 2D co-cultures, and a higher growth of co-culture MCSs compared to monotypic MCSs of HCT116 was observed. Since DAC is reported to have greater effects in actively proliferating cells (Yang *et al*., 2010), the increased proliferation of HCT116 in co-cultures potentially increases the activity of DAC. This is partly indicated by the decreased anti-proliferative activity of DAC in irradiated HCT116 that result in cell cycle arrest. Additionally, a marked decrease in DNMT1 levels in co-cultures presumably facilitate the DNMT1 inhibitory effect of DAC in HCT116 cells. This is evident from the significant effect of DAC on DNMT1 level in HCT116 from co-cultures than monocultures. Exposing cancer cells to gamma irradiation has been reported to decrease the protein level of DNMT1 and DNMT3B (Bae *et al*., 2015; Antwih *et al*., 2013). The data indicate that bystander effect and tumor-stroma cross-talk in non-irradiated BJ co-cultures decrease DNMT1 levels and regulate epigenetic changes in tumor cells.

Previous studies have shown that the CM from non-irradiated normal fibroblasts does not affect the proliferation of breast cancer cell (Heylen *et al*., 1998; Samoszuk *et al*., 2005).

Similarly, an increased proliferation of HCT116 was evident only when the cells were cultured in CM from irBJ. Interestingly, despite increasing the proliferation of HCT116, irBJ CM resulted in a concentration-dependent decrease in DNMTI-induced demethylation in 2D cultures. These findings were unexpected presuming that increased proliferation makes HCT116 susceptible to DNMTIs and suggest the role of other factors in altering the effect of DAC. Analysis of irBJ and non-irBJ CM shows a marked increase in *NFkB* activity and up-regulation of pro-inflammatory cytokine and chemokine levels in irBJ CM. A recent study shows that an increase in the *NFkB* activity downregulates the level of DNMT1 (Rajabi *et al*., 2016). Although any direct effect of irBJ CM on DNMT1 was not observed, the inability of DAC to significantly reduce DNMT1 levels in treated cells suggests the negative effect of pro-inflammatory cytokines on DNA demethylation (Winfield *et al*., 2016).

Aim 4: Investigate molecular mechanisms of drug resistance to azanucleoside drugs, and tailor alternative therapeutic regimen for overcoming resistance

Chapter 5

Drug resistance and alternative therapeutics

This Chapter describes the study of the molecular mechanisms of drug resistance to azanucleosides, represented by 2'-deoxy-5-azacytidine. The Chapter presents the biomarker genes which may be used to differentiate between sensitivity and resistance to azanucleosides, and proposes an alternative therapeutics for use in combinatorial therapy with azanucleosides.

5.1. Introduction

As presented in Chapter 1, the therapeutic potential of prototypal hypomethylating agent, 2'-deoxy-5-azacytidine (DAC) in treatment of hematological malignancies, mainly high-risk myelodysplastic syndrome (MDS) and acute myeloid leukemia (AML) has been constantly demonstrated through numerous clinical trials (Lyons *et al.*, 2003; Kihslinger & Godley, 2007; Robak, 2011). But the clinical success in MDS patients is highly variable with every second patient having no clinical benefit (Gore *et al*., 2013). While a number of patients exhibit primary resistance to DAC and do not respond to initial therapy, at least until 4-6 cycles, the others develop secondary resistance and eventually relapse despite continued DAC therapy (Qin *et al*., 2011). Thus, mechanisms of both primary and secondary resistance to DAC have been a topic of intense research. The previous study conducted *in vitro* in panel of cancer cell lines reported insufficient intracellular triphosphate resulting from mutations or aberrant expression of membrane transporter, deoxycytidine kinase (dCK) as the mechanism of primary resistance to DAC (Qin *et al*., 2009). The following study conducted *in vivo* in a subset of MDS patients validated the *in vitro* findings, and suggested high cytidine deaminase (CDA), responsible for rapid deamination of DAC, and decrease dCK levels as the marker of primary resistance (Qin *et al*., 2011). However, the study eliminated the likelihood of pharmacological mechanisms

involved in secondary resistance to DAC, demonstrated by no significant differences in CDA/dCK or expression of other relevant genes involved in DAC metabolism, between diagnosis and relapse (Qin *et al*., 2011). Thus secondary resistance to DAC, not entirely dependent on initial drug disposition remains somewhat elusive. Furthermore, the clinical resistance of patients to DAC therapy is complicated by the requirement of at least 4-6 cycles before treatment failure becomes apparent (Gore *et al*., 2013). This identifies the unmet requirement for the development of response predicting biomarkers to enable the selection of patients at early stage, thereby preventing them from the drug-related side-effects, and for designing better therapeutic options in time.

Apart from blood malignancies, DAC is presently being tested in phase 1/2 clinical trials for the treatment of patients with advanced solid tumors, mainly colorectal cancer (CRC), small-cell lung carcinomas, ovarian cancer, and breast cancer (Cowan *et al*., 2010; Nervi *et al*., 2015). But so far experience in early clinical trials with DAC as single agent therapy for solid tumors reported fewer responses which indicate towards the reduced efficacy of DAC in solid tumors (Cowan *et al*., 2010; Nervi *et al*., 2015). One of the causes behind low therapeutic efficacy of DAC in solid tumors is the specificity of DAC for S-phase of the cell cycle required for its selective and effective incorporation into DNA of rapidly proliferating cells, but lack of dividing cells in solid tumors (Yang *et al*., 2010). But previous studies have reported abundance of stable epigenetic alterations in solid tumors which support the potential activity of DAC against solid tumors (Cowan *et al*., 2010; Qiu *et al*., 2010). Even though the effectiveness of DAC in solid tumors remains controversial, the combinatorial therapy with DAC and cytotoxic anti-cancer drugs is likely to improve clinical response (Azad *et al*., 2013; Flis *et al*., 2014). A recent clinical trial of low-dose DAC in combination with cytotoxic drugs in patients with advanced solid tumors showed encouraging results (Fan *et al*., 2014).

In this study research was conducted to understand the molecular mechanisms of secondary resistance to DAC and to reveal the predictive biomarkers which may differentiate between DAC-sensitivity and resistance, using CRC cell line, representative of solid tumors. In addition, the efforts were emphasized to propose alterative therapeutic regimen to overcome DAC resistance.

5.2. Materials and Methods

Unless and otherwise indicated, media, chemicals, and other reagents were purchased from Sigma-Aldrich.

The stock solution of DAC was freshly prepared in DMSO before each experiment. DMSO concentration was always less than 0.1% in treated wells. DAC was replenished every 24 h without changing medium for all experiments with DAC.

5.2.1. Cell culture and development of DAC-resistant colorectal cancer cell lines

The culturing of HCT116 human CRC cells, cell line authentication, and routine test for mycoplasma contamination were done as described in Chapter 2.

DAC-resistant CRC cell lines were developed through long-term treatment with increasing concentrations of DAC (100 nM - 1 μM). Early passage HCT116 cells were initially seeded at a density of 1×10^6 cells in 100-mm dish and treated with 100 nM DAC. Medium with > 20-25% of dead cells was regularly replaced by fresh medium with DAC, and remaining attached cells were allowed to grow until they reached ~80% confluency, at which point they were sub-cultured. DAC-free intervals were included in between if required for the recovery of surviving cells. Concentration of DAC was gradually increased every 14 days with adaptation of resistance. After long-term treatment, when the bulk-population was determined to be resistant to 1 μM DAC, single cell cloning was performed in 96-well plate and 3 resistant clones were isolated to generate DAC-resistant CRC cell lines for further studies.

5.2.2. Cytotoxicity assay

Single-agent growth inhibitory activities of a panel of 22 therapeutic candidates for DAC-resistant tumors (Supplemental Table S5.1), and effect of two-drug combinations were determined using 3-(4,5-dimethylthiazol-2-yl)-2,5-diphenyl tetrazolium bromide (MTT) cytotoxicity assay. Parental and DAC-resistant CRC cell lines were plated at a density of 3.0×10^3 cells and 1.5×10^3 cells per well in 96-well plates for 72 and 120 h assay respectively. After plating, cells were allowed to recover for 3 h, and then exposed to serial concentrations of drugs [decitabine & azacytidine (Matoušová *et al*., 2011), guadecitabine (AdooQ BioScience), other epigenetic inhibitors (Tocris Bioscience), 5-fluorouracil, oxaliplatin (Ebewe Pharma), irinotecan, gemcitabine, roscovitine, palbociclib, cycloheximide (Sigma-Aldrich), actinomycin D (ApexBio)] for 72 or 120 h. For DAC, treatment was replenished every 24 h without changing medium. After incubation with drugs for indicated time points, 10 μL MTT (5 mg/mL in 1× PBS) was added to each well including blank and untreated control, and incubated at 37 °C for another 3 h until the purple formazan crystals were visible, after which 100 μL of detergent (10% SDS,

pH: 5.5) was added and the plates were incubated overnight to solubilize the formazan and the cellular material. MTT absorbance was read at 540 nM using Labsystems iEMS Reader MF.

The half maximal inhibitory concentration (IC_{50}) determining drug-induced cell growth inhibition or cytotoxicity of single-agents were evaluated using an in-house developed Chemorezist software (IMTM, Palacky University, Olomouc, Czech Republic) based on Hill's equation. For two-drug combination screening, dose-response curves for each individual drug and the combination index (CI), indicative of synergism, additive effects or antagonism for all combinations were calculated, using CompuSyn 1.0 software (Chou & Martin, 2004) based on Chou-Talalay method.

5.2.3. Cell cycle analysis

Cells were plated in 100-mm dishes at density of 2.5×10^6 cells and treated with drugs as indicated. After incubation, the cells were harvested by trypsin release, washed 1× with PBS, and resuspended in 1 mL of ice cold 70% ethanol and fixed for a minimum of 16 h at 4°C. Fixed cells were then washed 1× with PBS followed by 1× wash with citrate buffer (1.14 mg/mL sodium citrate tribasic monohydrate in deionized H_2O), and finally stained by incubating in dark for 15 min in water bath at 37°C with 600 µL of propidium iodide (PI) solution [PI (50 µg/mL), 0.2% Triton X-100 in citrate buffer] followed by addition of 500 µL of RNase solution (2 mg/mL in citrate buffer) for another 15 min. After incubation and before measurement, samples were stabilized at 4°C for 1 h.

For flow cytometric analysis, 20,000 cells were acquired using a BD FACSCalibur flow cytometer and CellQuest 3.3 (linear fluorescence signals, area and width were assessed with dye excitation by 15-mw, 488-nm laser light), and DNA histograms were analyzed by using ModFit LT 2.0 Software (Verity Software House).

5.2.4. Drug efficacy study in xenografts

Parental and DAC-resistant CRC xenografts were established in 11-12 weeks-old female SCID mice (ENVIGO), inoculated with 5×10^6 cells, *s.c.* on both sides of the chest. After 2 weeks, tumors were palpable (average tumor volume = 20 mm^3) and mice were assigned into four groups (8 mice/group) each for parental and DAC-resistant xenografts. Group I: vehicle control for DAC (10:90, DMSO: PBS) and Group II: DAC, 2.5 mg/kg by *i.p.* injection once a day for 14 days (5 d on, 2 d off), total 10 doses. Group III: vehicle control for (+)-JQ1 (5:95, DMSO: 10% 2-Hydroxypropyl-β-cyclodextrin) and Group IV: (+)-JQ1, 50 mg/kg by *i.p.* injection once a day for

28 days (5 d on, 2 d off), total 20 doses. Body weights of the animals were measured daily and tumor volume data were collected twice a week. Tumor volume was calculated from caliper measurements by using the formula: L × H × H/2. Mice were killed when the body weight decreased >20% of initial weight or under poor health conditions as established in the protocol. All animal work was performed according to protocols approved by Central Commission for Animal Welfare in Czech Republic.

For determining the efficacy of the drugs, tumor volume was compared between parental and DAC-resistant CRC xenografts treated with DAC or (+)-JQ1. At first, tumor volume data for different time points for each mice in a group were transformed into relative tumor volumes (tumor volume of the mice divided by mean tumor volume of the group on day 1), followed by computation of treatment to control ratio (T/C ratio) for each time point. Statistical significance of the data was determined by calculating bootstrap p-value, n=10,000, one-sided test of H_0: T/C ratio = 1, H_1: T/C ratio <1 (Wu, 2010). T/C ratios for day 0-21 were then used to calculate adjusted area under the curve (aAUC) for each drug (Wu & Houghton, 2010). aAUC values thus obtained were used to define *in vivo* resistance or sensitivity towards the drugs for DAC-resistant CRC xenografts as compared to parental tumorgrafts. Statistical significance of aAUC was determined by calculating bootstrap p-value, n=10,000, one-sided test of H_0: aAUC T/C ratio = 1, H_1: aAUC T/C ratio <1 (Wu, 2010). After day 21, statistical significance cannot be measured accurately due to decreased survival of animals in control group.

5.2.5. Transcriptomics sequencing

Total RNA from treated and untreated cells was isolated using Ambion RiboPure Kit (Life Technologies) according to manufacturer's protocol. The integrity of the extracted RNA samples was analyzed using Agilent RNA 6000 Nano Kit (Agilent Technologies) and Agilent 2100 Bioanalyzer. 0.1-4 µg of total RNA was then used to construct the cDNA library for sequencing, using TruSeq Stranded mRNA Sample Prep Kit (Illumina) following standard manufacturer's protocol. The indexed cDNA library of 12 samples (4 samples × 3 replicates) was validated and quantified using Agilent High Sensitivity DNA Kit (Agilent Technologies), and the pooled library was sequenced using Illumina HiSeq 2500 Sequencing System in 50 cycles single-end run mode. About 44-158 million assigned reads were obtained per sample, and the reads generated were aligned to annotated human reference genome (hg38), using Tophat 2 (Langmead *et al.*, 2009). For the quantification of gene expression, featureCounts (Liao *et al.*, 2014) was used, and differential expressions were reported after data normalization and statistical evaluation

using DESeq2 (Love *et al.*, 2014). Statistical significance was determined by the binomial test and threshold for significance was set to 0.05.

5.2.6. Bisulfite sequencing

Genomic DNA from treated and untreated cells was isolated using DNeasy Blood & Tissue Kit (Qiagen) according to manufacturer's protocol. The concentration was measured using Qubit™ dsDNA BR Assay Kit (ThermoFisher), and total of 1.5 µg of genomic DNA was converted with the EZ DNA methylation-gold kit (Zymo Research) following standard manufacturer's protocol. Universal Methylated Human DNA Standard (Zymo Research) was used as a control to assess the efficiency of bisulfite-mediated conversion, and bisulfite-converted Universal Methylated Human DNA Standard (Zymo Research) was used as control to check the methylation rates of fully methylated CpGs (expected rates ≥ 80%). Bisulfite-converted DNA was then amplified with specific primer sets designed in the region of gene promoter and transcription start site (TSS), using MethPrimer software (Li & Dahiya, 2002). The promoter area and TSS was localized using EPDnew, the Homo sapiens (human) curated promoter database (Dreos *et al.*, 2015) implemented on hg19 - UCSC Genome Browser. Primer sequences are presented in Supplemental Table S5.3. PCR mixtures contained 1× KAPA2G buffer A, 2.5 mM $MgCl_2$, 0.5 U KAPA2G Robust DNA Polymerase, 0.2 mM of each dNTP (all from Kapa Biosystems), 0.5× EvaGreen dye (Biotium), 0.4 µM of each primer, and 20 ng of bisulfite-modified DNA in a total volume of 20 µL. Cycling parameters were 3 min at 95 °C, followed by 50 amplification cycles of 15 s at 95 °C, 30 s at 59 °C, and 45 s at 60 °C with a subsequent extension for 5 min at 72 °C on a BIO-RAD CFX96 Touch™ Real-Time PCR Detection System. For each sample, 2 µL of each amplicon were pooled together, and mixture was purified using QIAquick PCR Purification Kit (Qiagen). 1 ng of purified DNA from each sample was then used to prepare sequencing library, using Nextera XT DNA Library Prep Kit (Illumina), and indexed library of 12 samples (4 samples × 3 replicates) was purified using Agencourt SPRIselect (Beckman Coulter), and the pooled library was sequenced using Illumina MiSeq Next Generation Sequencer.

Generated demultiplexed fastq files were aligned using Bismark Bisulfite Mapper 0.15.0 (Babraham Institute), and obtained bam files were sorted and indexed using SAMtools (Li *et al.*, 2009). Contex-dependent CpG methylation data was extracted using Bismark Methylation Extractor (Babraham Institute), and extracted data was imported and processed using SeqMonk 0.33.0 (Babraham Institute), where genomic coordinates of amplicons and/or separate CpG coordinates were used as quantitation features. Quantification pipeline, "Bisulphite methylation

over features" was used for data processing, and quantified data table was exported using Feature Report Tool. Statistical significance was determined by the t-test and threshold for significance was set to 0.05.

5.2.7. Determination of NFκB activity

NFκB activity in conditioned medium (CM) isolated from 3 days cultures of parental and DAC-resistant CRC cells was determined using in-house developed *NFκB* reporter cell line described in Chapter 4. The data was normalized using total cell count for each sample.

5.2.8. Statistical analysis

All statistical analyses were performed using GraphPad Prism statistical software (version 7), and differences were considered significant at $P < 0.05$.

5.3. Results

5.3.1. BET inhibitor sensitized DAC-resistant colorectal cancer cells

DAC-resistant CRC cell lines developed through long-term treatment with increasing concentrations of DAC exhibited > 100 fold resistance (IC_{50} > 100 µM) as compared to their normal counter parts (IC_{50} = 0.11 µM) in 5 days MTT cell-survival assay. The acquired DAC resistance was similar to the previously published study (Hosokawa *et al*., 2015). Resistant cell lines were then screened against a panel of therapeutic candidates (Fig. 5.1A) which included epigenetic modifiers, viz. inhibitors of epigenetic 'writers' – DNA methyltransferase (DNMT) inhibitors (Bestor, 2000); histone acetyltransferase (HAT) inhibitors (Lee & Workman, 2007); histone methyltransferase (HMT) inhibitors (Trievel *et al*., 2004), inhibitors of epigenetic 'erasers' – histone deacetylase (HDAC) inhibitors (Glozak & Seto, 2007); histone demethylase (HDM) inhibitors (Højfeldt *et al*., 2013), inhibitors of epigenetic 'readers' – bromodomain and extra terminal (BET) inhibitors (Owen *et al*., 2000), and additionally chemotherapeutic agents which included conventional chemotherapeutics used for CRC (Pardini *et al*., 2011; Fuchs *et al*., 2006; Mayer, 2012; Saif *et al*., 2011), cyclin-dependent kinase (CDK) inhibitors (Harper & Adams, 2001), and inhibitors of transcription (Bensaude, 2011) and protein synthesis (Baliga *et al*., 1969). The results of the study revealed that all DAC-resistant cell lines exhibited cross-resistance to other tested epigenetic inhibitors (Fig. 5.1A). For chemotherapeutic agents, no significant difference was observed in IC_{50} values between parental and DAC-resistant cell lines

for any tested drugs except gemcitabine which showed high levels of cross-resistance (Fig. 5.1A), Interestingly, only the tested BET inhibitors were found to significantly sensitize the DAC-resistant CRC cells amongst the panel of 21 therapeutic agents screened in this study (Fig. 5.1A).

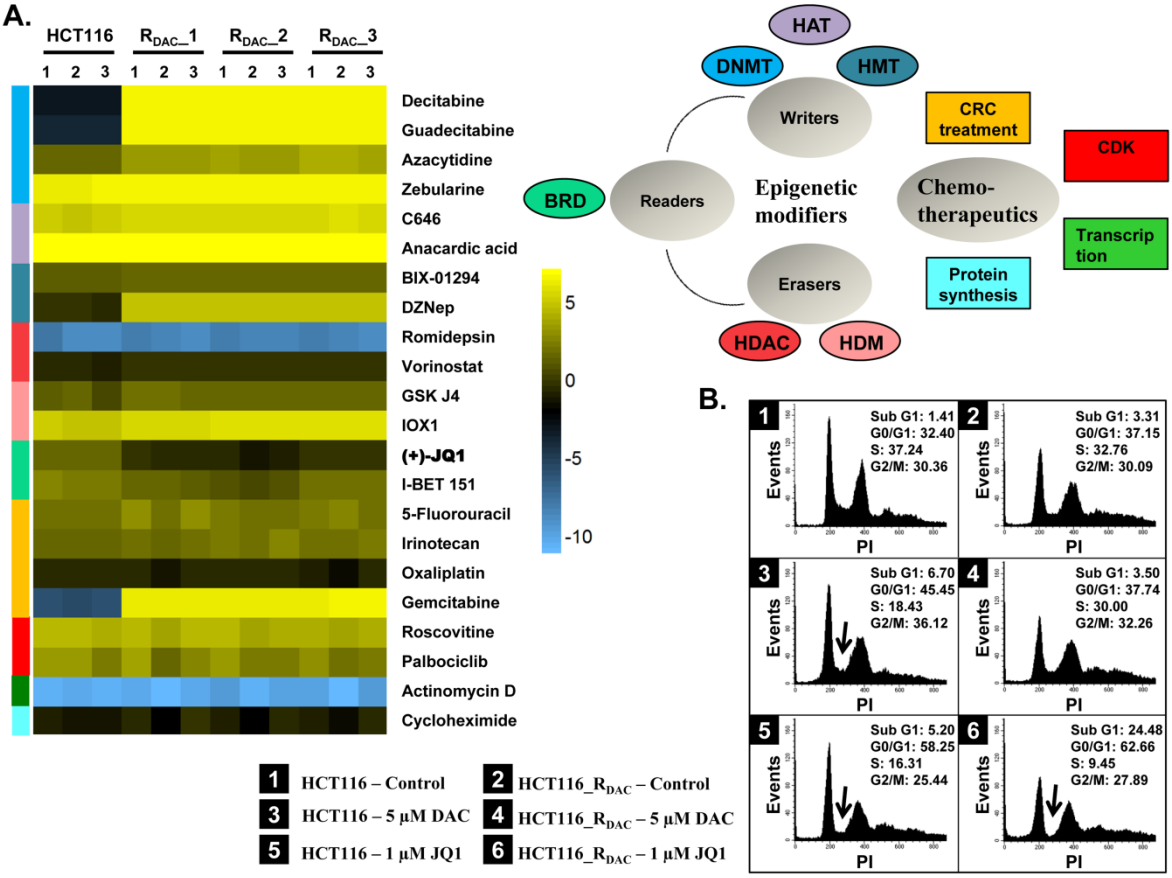

Figure 5.1 Screening of DAC-resistant colorectal cancer cell lines against a panel of therapeutic agents, and flow-cytometric analysis

(A) *Heatmap showing IC_{50} values (log2) of DAC, and epigenetic-and chemo-therapeutics in parental CRC cell line (HCT116) and 3 DAC-resistant CRC cell lines (R_{DAC}_1, R_{DAC}_2, R_{DAC}_3). IC_{50} values are representative of 3 independent experiments. Statistical significance of the data (parental vs. each DAC-resistant cell line) was determined by calculating P-value, one-way Anova with Dunnett's multiple comparisons test, and data were considered significant at $p < 0.05$. IC_{50} of drugs (Mean ± S.D., n = 3) and P-values are presented in Supplemental Table S5.1.* ***(B)****. Cell cycle profiles of parental and DAC-resistant CRC cells after treatment with DAC (5 µM) or (+)-JQ1 (1 µM) for 48 h. Data are representative of 3 independent experiments. Arrow shown in DNA histograms indicate towards decreasing S-phase following accumulation of cells in G_0/G_1.*

5.3.2. BET inhibitor mediated augmented response on cell cycle phases of DAC-resistant colorectal cancer cells

Consistent with the sensitizing effects of BET inhibitors on DAC-resistant CRC cell lines (Fig. 5.1A), the effect of DAC and (+)-JQ1 was assessed on cell cycle profile of parental and one selected DAC-resistant CRC cell line. Assessment of cell cycle revealed that DAC-resistant CRC cells displayed no significant changes in phases of cell cycle versus G_0/G_1 blockage and increase in sub-G_1 population in DAC-sensitive parental cells on 48 h treatment with 5 µM DAC, however, (+)-JQ1 conversely showed augmented effects in DAC-resistant CRC cells (Fig. 5.1B). 48 h exposure to 1 µM (+)-JQ1 caused 25.5% increase in the accumulation of cells in G_0/G_1 in DAC-resistant cells which was similar to percentage arrested in parental cells, but exposure of DAC-resistant cells to (+)-JQ1 increased the population of apoptotic cells by 21.2% which was significantly higher as compared to 3.8% increase in DAC-sensitive parental cells (Fig. 5.1B). Therefore BET bromodomain inhibitor induced cell-cycle arrest and apoptosis with increased sensitivity in DAC-resistant CRC cells. These data are in line with higher cytotoxic effects of (+)-JQ1 observed in DAC-resistant cell lines as compared to DAC-sensitive parental cells (Fig. 5.1A).

5.3.3. BET inhibitor displayed increased anti-proliferative effects in xenograft models of DAC-resistant colorectal cancer

To further investigate the anti-tumor effects of DAC and BET inhibitor, the xenograft models of parental and *in vitro* developed DAC-resistant CRC cells were explored. Tumors were grown *s.c.* in immunocompromised mice, and DAC; 2.5 mg/kg or (+)-JQ1; 50 mg/kg was administered *i.p.* for 2-weeks and 4-weeks respectively in a schedule with 2 days drug-free intervals in each week (Fig. 5.2A). As shown in Fig. 5.2B, DAC-sensitive CRC tumors grew significantly slower in DAC-treated mice compared with vehicle-treated control. In this model, the relative tumor volume (RTV) was 65.2% smaller in the DAC-treated group at day 21. However, the RTV of DAC-resistant CRC tumors at day 21 was only 22.1% smaller in DAC treated group (Fig. 5.2B). Alternatively, both DAC-sensitive and DAC-resistant CRC xenografts were observed to be sensitive to (+)-JQ1, but 39.4% regression of (+)-JQ1-dosed DAC-resistant tumorgrafts was slightly higher than 36.7% regression of (+)-JQ1-dosed DAC-sensitive tumorgrafts, each compared to vehicle controls (Fig. 5.2B). In addition to RTV, the *in vivo* efficacy of the drugs was also determined by calculating aAUC for day 0-21 (Fig. 5.2D). The lesser effectiveness of DAC in xenograft models of *in vitro* developed DAC-resistant CRC cells

confirmed DAC resistance under *in vivo* conditions (Fig. 5.2C). Concomitantly, the higher effectiveness of (+)-JQ1 seen in DAC-resistant CRC xenografts (Fig. 5.2C) is consistent with the *in vitro* findings (Fig. 5.1A,B) which highlights the increased sensitivity of (+)-JQ1 towards DAC-resistant CRC cells. Therefore, these data demonstrating the significant anti-tumor activity of (+)-JQ1 in DAC-resistant tumors suggest potential therapeutic efficacy for small molecule inhibitors of BET for the treatment of DAC-resistant tumors.

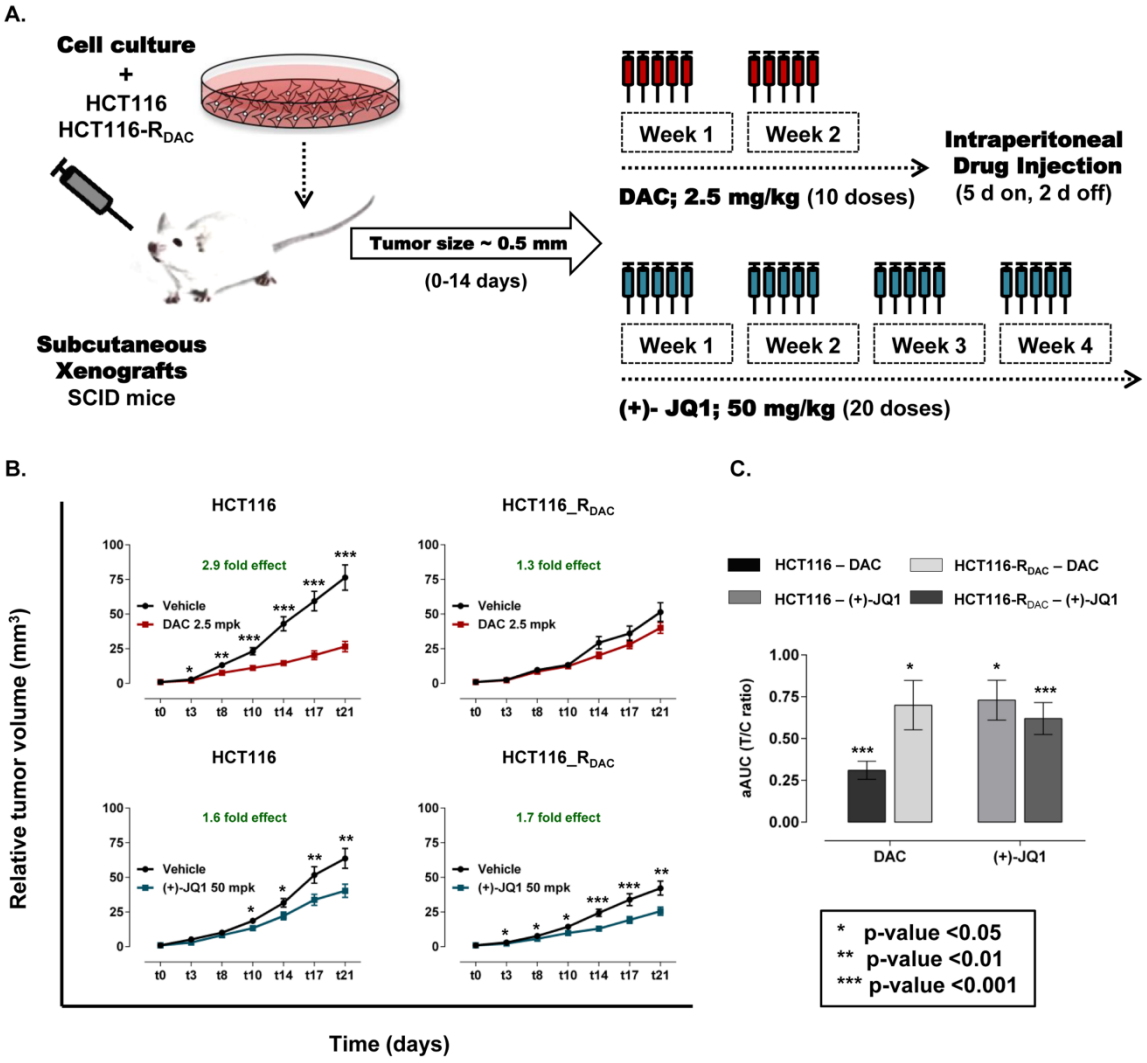

Figure 5.2 BET inhibitor decreased DAC-resistant tumor load *in vivo*

(A) *Schematic representation of xenograft transplantation, dosing regimens and treatment schedules of drugs.* ***(B)*** *Mice bearing parental (HCT116) and DAC-resistant (HCT116-R$_{DAC}$) CRC xenografts were treated with DAC [2.5 mg/kg (mpk)] or (+)-JQ1 (50 mg/kg) or volume equivalent of vehicle for each drug as indicated in A. Error bars represent SEM. Statistical significance for each time interval for difference in tumor growth rate (relative tumor volume)*

was determined by calculating bootstrap P-value, n=10,000, one-sided test of H_0: T/C ratio = 1, H_1: T/C ratio <1. ***(C)*** *Graph showing aAUC plots were calculated using T/C ratio for 0-21 days. Error bars represent S.D., calculated by delta method. Bootstrap P-value, n=10,000, one-sided test of H_0: aAUC T/C ratio = 1, H_1: aAUC T/C ratio <1 compares aAUC T/C ratio for each drug and for both, parental and DAC-resistant CRC xenografts.*

5.3.4. BET inhibitor combined with DAC showed synergistic effects

After persistent single-agent anti-proliferative effects of BET inhibitor were observed during *in vitro* experiments, and animal models of DAC-resistant CRC cells, DAC and (+)-JQ1 was tested in all permutations of two-drug combinations to define synergistic effects of this novel combination (Fig. 5.3). The combinations were analyzed for two different orders of drug application, concurrent drug application for 5 days and sequential application of (+)-JQ1 after 3 days of DAC application. To identify synergy, 5 × 5 checker-board matrix format that assessed the two agents at 5 serial drug concentrations with the dilution factor of 1: 2.5 and multiple drug ratios was used. Full dose-response curves for each individual drug, "effect oriented" CI values (Fig. 5.3A), and "dose oriented" normalized isobolograms (Fig. 5.3B) for all combinations were obtained, using CompuSyn 1.0 software based on the Chou-Talalay method. For concurrent drug application, the combinations continued to demonstrate synergistic or additive effects in case of both DAC-sensitive and DAC-resistant CRC cells. Interestingly, the synergistic effects were better defined in DAC-resistant CRC cells in which case all tested combinations were synergistic or showed additive effects (Fig. 5.3A). For sequential drug combinations, the synergistic effects were demonstrated in DAC-sensitive CRC cells, while most of the tested combinations produced antagonistic effects in DAC-resistant cells (Fig. 5.3A). Additionally, normalized isobologram for non-constant ratio combinations, further yielded identical conclusion of synergism, additive effects or antagonism, as observed with CI method (Fig. 5.3B). No synergistic effects observed in DAC-resistant cells on sequentially combining (+)-JQ1 with DAC might be due to complete resistance of cells towards DAC which means no active drug in combination wells for first 3 days compared to 5 days of (+)-JQ1 alone. The diagonal (highlighted) of the 5 × 5 checker-board matrix represents the effects of the drug combinations at constant 1:1 ratio (Fig. 5.3A). Graphs presented in Fig. 5.3C compare the anti-proliferative effects of each individual drug and the constant 1:1 combinations. These data demonstrate additive/synergistic cytotoxic effects of (+)-JQ1 combined concurrently or sequentially with DAC, and suggests the potential application of DAC and BET inhibitor as combinatorial regimen for anti-cancer therapy or the concurrent application of BET inhibitor and DAC to sensitize DAC-resistant cancer cells.

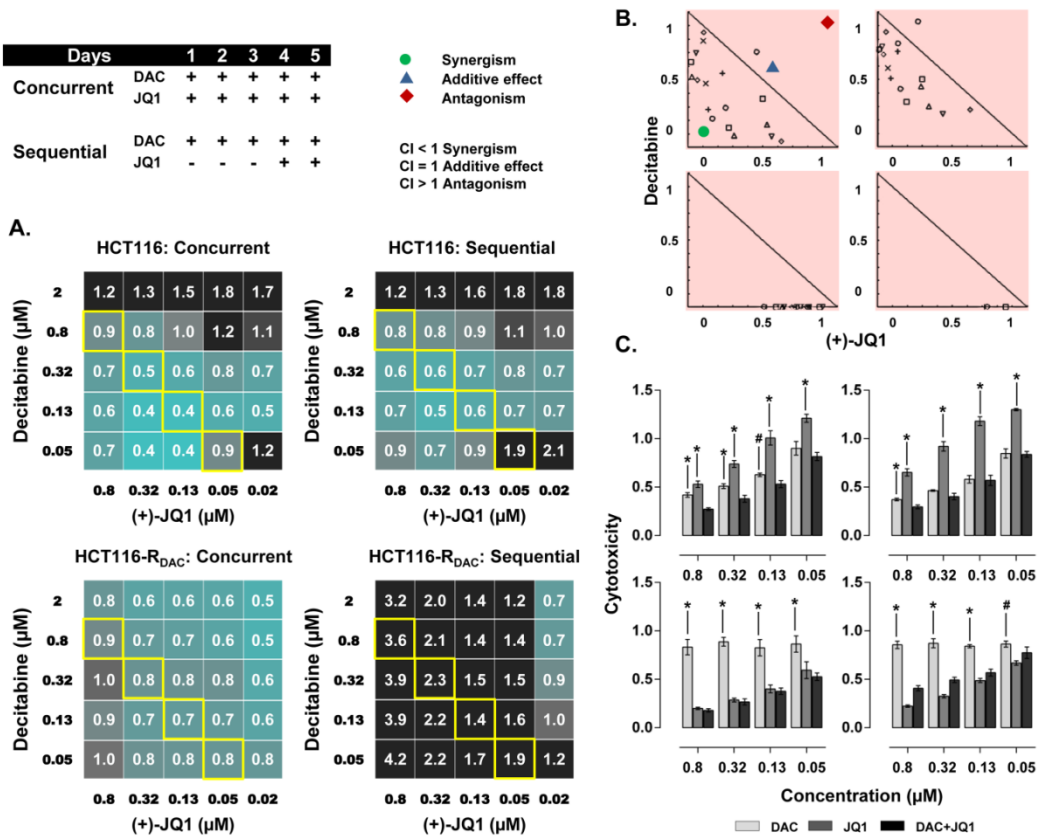

Figure 5.3 Screening results of the novel combination of hypomethylating agent with BET inhibitor

(A) *5 × 5 checker-board matrix showing CI of the DAC and (+)-JQ1 concurrent and sequential combinations in parental (HCT116) and DAC-resistant (HCT116-R_{DAC}) CRC cells, using non-constant ratio CI method.* ***(B)*** *Normalized isobolograms for non-constant ratio drug combinations.* ***(C)*** *Graphs comparing the anti-proliferative effects of each individual drug and constant combinations at 1:1 ratio (highlighted in yellow). Data are mean ± S.D., n = 4. **p < 0.005, $^{\#}p < 0.05$, one-way Anova with Dunnett's multiple comparisons test.*

5.3.5. Gene expression profiling and supervised clustering

In order to identify genes that are altered during acquisition of resistance to DAC, and alteration of genes on treatment with BET inhibitor, the mRNA expression profiles were assessed using RNA sequencing. The normalized expression levels obtained for parental and DAC-resistant CRC cells, untreated and treated with 1 μM DAC or 1 μM (+)-JQ1 for 48 h were analyzed by supervised clustering. Initial analysis of expression levels revealed that significant expression signals across all experiments were recorded for 1805 genes: these were then

compared between samples and log fold changes were calculated. Results are displayed in a color-coded matrix (Fig. 5.4) where samples are ordered on the horizontal axis and genes on the vertical axis. First column (black) of the cluster represents log fold changes in DAC-treated CRC cells as compared to parental cells, second column (yellow) represents expression levels of genes in DAC-resistant CRC cells as compared to parental cells, and third column (blue) represents the gene expression changes in (+)-JQ1-treated DAC-resistant CRC cells as compared to DAC-resistant CRC cells. Genes on the vertical axis are ordered on the basis of the expression levels (high to low) in DAC-resistant CRC as compared to parental cells. The cluster clearly indicates that the three groups exhibit noticeable differences in global gene expression profiles. In general the expression of genes was slightly increased on treatment with DAC and these genes were then overexpressed (up-regulated cluster) in DAC-resistant CRC cells and down-regulated on treatment with (+)-JQ1. In other case, the expression of genes were up-regulated on treatment with DAC but their expressions were decreased again (down-regulated cluster) in DAC-resistant CRC cells and either marginally increased or remained same on treatment with (+)-JQ1. Expectedly, these data are in agreement with the previously established hypothesis. The gene expression patterns in down-regulated cluster fits to the fact that tumor suppressor genes which are re-activated on treatment with hypomethylating agents are re-silenced again leading to resistance (Hesson *et al*., 2013), and overexpression of genes in up-regulated cluster indicates the likelihood of activation of oncogenes involved in survival and progression pathways which might contribute to secondary resistance towards DAC, in a manner that is independent of CpG island methylation (Qin *et al*., 2011).

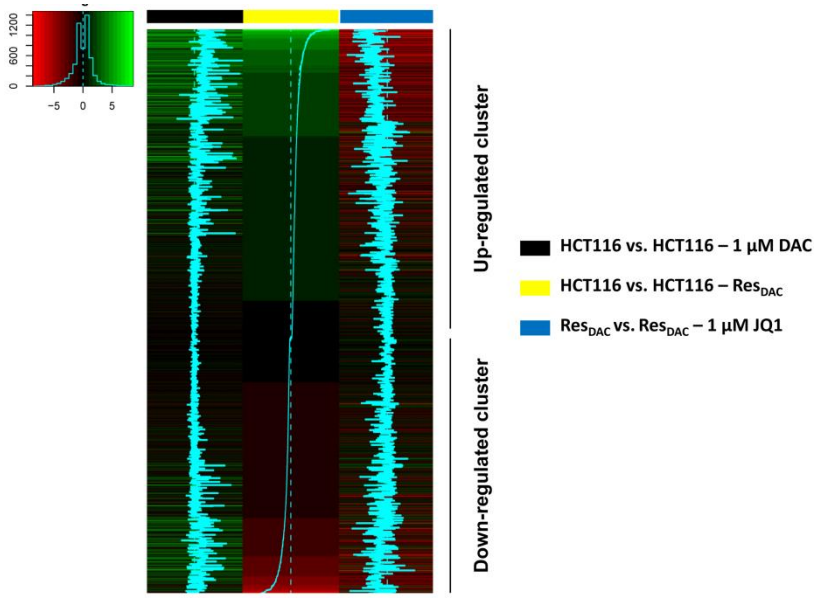

Figure 5.4 Hierarchical supervised clustering of gene expression profiles

Clustering of 1805 genes based on their significant expressions across all experiments. Parental vs. DAC-treated (black), Parental vs. DAC-resistant (yellow), DAC-resistant vs. (+)-JQ1-treated DAC-resistant (blue) CRC cells. Each column represents mean of fold changes (log2) calculated from 3 independent experiments. P-value ≤ 0.05, binomial test. Up-regulated and down-regulated clusters respectively represents genes overexpressed and down-regulated in DAC-resistant CRC as compared to parental CRC cells.

5.3.6. Functional clustering of differentially expressed genes

In order to unveil the signature genes that might be involved in mechanisms of secondary resistance to DAC or might serve as surrogate biomarkers that differentiate between DAC sensitivity and resistance, and to expose those candidate genes, the alteration of which might be responsible for increased sensitivity of DAC-resistant CRC cells towards BET inhibitor, the genes were clustered according to functional categories (Fig. 5.5). For up-regulated cluster, all genes whose expressions were at least ≥ 4 folds (log fold change ≥ 2, p-value ≤ 0.05) in DAC-resistant CRC cells as compared to parental cells were considered overexpressed (201 genes). These 201 genes were then subjected to supervised clustering where the genes were filtered according to their expression levels in DAC-treated CRC cells as compared to parental cells, and only those genes were included in the cluster, the expression of which was ≤ 2 folds (log fold change ≤ 1) in DAC-treated CRC cells, and in last column the expressions of filtered genes in (+)-JQ1-treated DAC-resistant cells were included (Fig. 5.5). Conversely, for down-regulated cluster, all genes whose expressions were ≤ 0.30 (70% down-regulated; log fold change ≤ -1.74, p-value ≤ 0.05) were sorted as down-regulated (487 genes). These 487 genes were then subjected to supervised clustering, where, the genes were again filtered according to their expression levels in DAC-treated CRC cells as compared to parental cells, and only those genes were included in the cluster, the expression of which was ≥ 2 folds (log fold change ≥ 1, p-value ≤ 0.05) in DAC-treated CRC cells, and in last column the expressions of filtered genes in (+)-JQ1-treated DAC-resistant cells were included, similarly as up-regulated cluster (Fig. 5.5). The supervised clustering identified 89 genes that were significantly and differentially overexpressed and 152 genes that were significantly and differentially down-regulated in DAC-resistant CRC cells (Fig. 5.5). These differentially regulated genes were then clustered according to their functional categories based on published information about their involvement in adhesion/migration, cell-proliferation/apoptosis, differentiation, drug resistance, immune response/inflammation,

metabolic process, metastasis/progression, signaling pathways, and transcription factor (Fig. 5.5). The genes which lacked the clear-cut evidence of oncogenic or tumor suppressor functions in literature or genes which remain uncharacterized, and other genes including pseudogenes, anti-sense RNA genes, and non-protein coding genes (Supplemental Table S5.2) were excluded from the functional clusters.

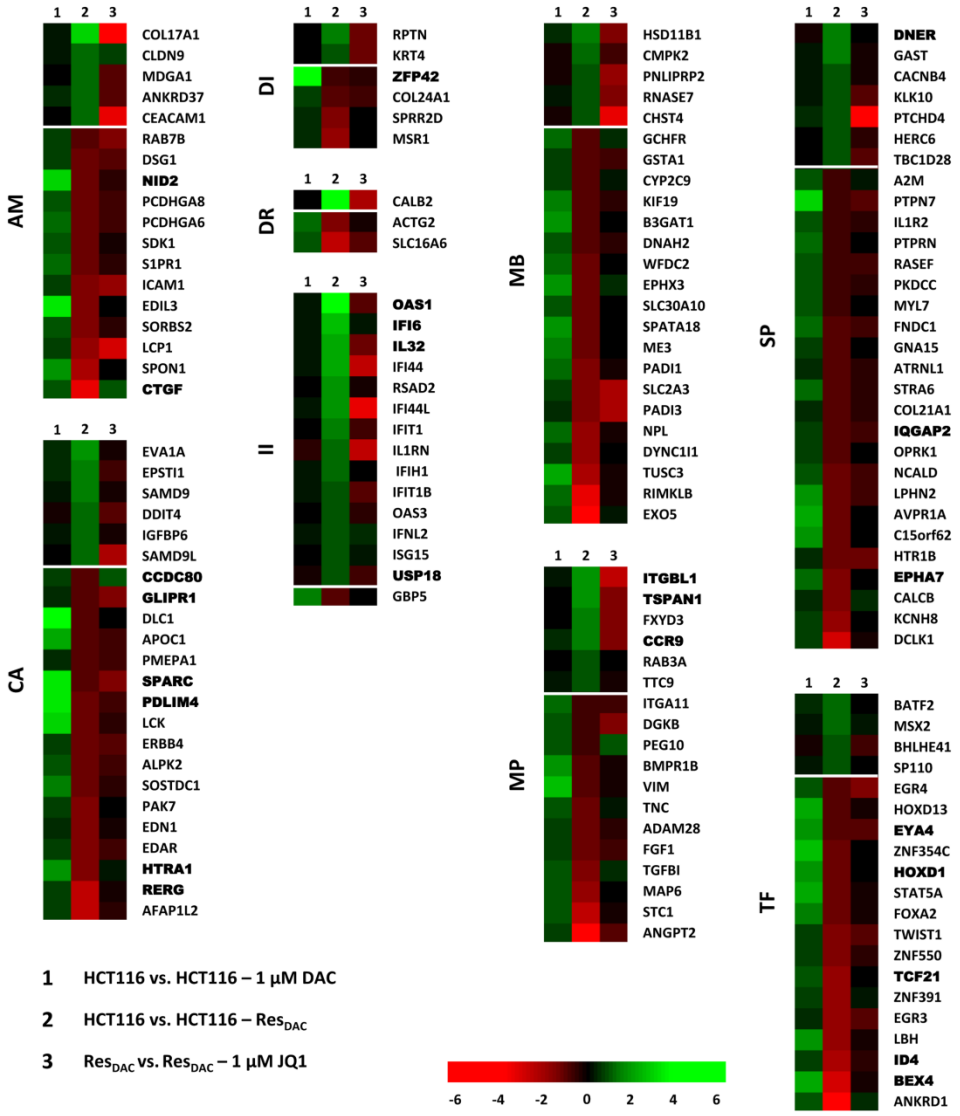

Figure 5.5 Gene expression profiles according to the functional categories

Genes were assigned to the functional categories based on published information about their performance (AM: Adhesion/Migration, CA: Cell-proliferation/Apoptosis, DI: Differentiation, DR: Drug resistance, II: Immune response/Inflammation, MB: Metabolic process, MP: Metastasis/progression, SP: Signaling pathways, TF: Transcription factor). Horizontal white line separates up-regulated cluster [HCT116 vs.HCT116-1 µM DAC (log fold change ≤ 1), *HCT116*

*vs.HCT116-Res$_{DAC}$ (*log fold change ≥ 2, p-value ≤ 0.05)] *and down-regulated cluster [HCT116 vs.HCT116-1 μM DAC* (log fold change ≥ 1, p-value ≤ 0.05), *HCT116 vs.HCT116-Res$_{DAC}$ (*log fold change ≤ -1.74, p-value ≤ 0.05]. *Genes marked in bold were selected for CpG methylation analysis of promoter regions based on their biological relevance*.

5.3.7. CpG Methylation analysis of promoter regions of signature genes

To address DNA methylation changes underlying the differential mRNA expressions of genes in up- and down-regulated clusters, methylation levels were determined. Based on altered expression profiles and biological relevance, 24 genes (8 up-regulated, 16 down-regulated) were selected for bisulfite sequencing (Supplemental table S5.3). These genes were further classified as CpG island or non-CpG island genes using a standard criterion that identifies CpG islands. A gene was considered as CpG island gene if G + C content was at least 50% and if CpG (obs)/CpG(exp) ≥ 0.6 in a 200-bp window length, and the sequence length was at least 500-bp (Bird, 1986; Takai and Jones, 2002). Based on this classification, 6/8 genes: *OAS1, IFI6, IL32, ITGBL1, TSPAN1, CCR9* in up-regulated cluster were classified as non-CpG island genes and only 2 genes: *DNER* and *USP18* were classified as CpG island genes. Whereas, in down-regulated cluster 13/16 genes: *BEX4, CTGF, ID4, RERG, TCF21, EPHA7, HTRA1, IQGAP2, HOXD1, EYA4, PDLIM4, ZFP42, NID2* were identified as CpG island genes and only 3 genes: *SPARC, GLIPR1,* and *CCDC80* were identified as non-CpG island genes. The methylation levels of these genes obtained by promoter analysis were then paired with their RNA expressions (Fig. 5.6).

On comparing the methylation and expression levels for each individual gene, it was found that the methylation levels of genes in up-regulated cluster did not correspond with their RNA expression profiles except for *IL-32* (Fig. 5.6A,B). This was well-expected as majority of genes in up-regulated cluster were identified as non-CpG island genes. Based on the published literature, these genes in the up-regulated cluster have oncogenic functions and are involved in survival and progression pathways. *OAS1* was found to be overexpressed in individuals with disseminated cancer (Merritt *et al*., 1985) and node-positive breast cancer (Huang *et al*., 2003), and lymph node status and metastatic relapse are inter-related events. *IFI6* has been discovered as inhibitor of apoptosis via mitochondrial-dependent pathway in vascular endothelial cells (Qi *et al*., 2015) and by antagonizing TRAIL-induced apoptosis in human myeloma cells (Cheriyath *et al*., 2007). *IL-32* was found to promote breast cancer cell growth and invasiveness (Wang *et al*., 2015), increase gastric cancer cell invasion, associated with tumor progression and metastasis (Tsai *et al*., 2014), was found to be implicated in pathogenesis of most lung cancer histotypes

(Sorrentino *et al*., 2009), and in induction of metastasis in CRC patients (Yang *et al*., 2015). *ITGBL1* was found to promote breast cancer bone metastasis by activating the TGFβ signaling pathway (Li *et al*., 2015b), stimulate ovarian cancer cell migration and adhesion through Wnt/PCP signaling and FAK/SRC pathway (Sun *et al*., 2016). *TSPAN1* has been found to play important role in colon cancer progression (Chen *et al*., 2010), gastric carcinogenesis (Lu *et al*., 2015), poor prognosis in lung cancer and CRC (Huang *et al*., 2015; Chen *et al*., 2009; Zhang *et al*., 2015). *CCR9* has been found to be associated with small intestinal metastasis (Letsch *et al*., 2004), mediate key steps of metastasis in non-small cell lung cancer (Gupta *et al*., 2014), cell migration, invasion, and matrix metalloproteinase expression, together affecting metastasis in prostate cancer (Singh *et al*., 2004). *DNER*, an epigenetically modulated gene (Sun *et al*., 2009), classified as CpG island gene in this study, is the activator of the NOTCH1 pathway which is independent predictor of poor-prognosis in CRC (Chu *et al*., 2011), promotes stemness and epithelial to mesenchymal transition in CRC (Fender *et al*., 2016), and positively regulates the growth of colon cancers (Zhang *et al*., 2010). *USP18* has been found to be inhibitor of extrinsic apoptotic pathway triggered by IFN-alpha and TRAIL (Potu *et al*., 2010; Manini *et al*., 2013), creates a tumour-progressive micro-environment by downregulating interferon-λ signaling (Burkart *et al*., 2013), has been found to positively regulate EGFR, involved in development and progression of many human cancers (Duex *et al*., 2011), and has been identified as poor-prognostic marker in bladder cancer (Kim *et al*., 2014c). The overexpression of these oncogenic signatures in a manner independent of DNA methylation fits to the previously proposed hypothesis which suggests that methylation independent genetic activation of oncogenic survival and progression pathways may contribute to secondary resistance towards DAC (Qin *et al*., 2011). Interestingly, the overexpression of all these genes was significantly inhibited on treatment of DAC-resistant CRC cells with (+)-JQ1 (Fig. 5.5). This means that BET inhibitor reversed the oncogenic survival and progression pathway active in DAC-resistant cells, and therefore DAC-resistant CRC cells exhibited high sensitivity towards (+)-JQ1 during *in vitro* and *in vivo* anti-proliferation studies (Fig. 5.1, 5.2). The correlation between the down-regulation of these oncogenic signatures on treatment with BET inhibitor and sensitizing effect of BET inhibitor on DAC-resistant CRC cells indicate towards the role of these genes in mechanism of secondary resistance to DAC.

Conversely, the changes in methylation status of all genes in down-regulated cluster, majority of them identified as CpG island genes, corresponds to their differential RNA expressions. Based on the published results, the genes in down-regulated cluster have tumor-suppressor functions. *BEX4* has been reported as a cell death regulatory protein inactivated in

ovarian cancer (Chien *et al*., 2005) and oral squamous cell carcinoma (Gao *et al*., 2016) due to CpG hypermethylation of the promoter. *CTGF* expression has been significantly correlated with higher overall survival and a disease-free advantage in stage II and stage III CRC patients, and down-regulation of *CTGF* has been reported to regulate CRC invasion and metastasis (Lin *et al*., 2005). *ID4* has been reported as a potential tumor suppressor gene (TSG), silenced by aberrant methylation in gastric adenocarcinoma (Chan *et al*., 2003), breast cancer (Noetzel *et al*., 2008), CRC (Gómez Del Pulgar *et al*., 2008), AML (Xu *et al*., 2011), and its epigenetic inactivation has been correlated with poor differentiation and unfavorable prognosis in CRC (Umetani *et al*., 2004), and high risk of leukemic transformation in MDS patients (Wang *et al*., 2010). *RERG* expression has been correlated with longer breast cancer specific survival and distant metastasis free interval (Habashy *et al*., 2011), and its decreased expression has been correlated with poor clinical-prognosis in primary breast cancer (Finlin *et al*., 2001). *TCF21* hypermethylation and downregulation has been frequently reported in majority of head and neck squamous cell carcinomas (Smith *et al*., 2006), non-small cell lung cancer (Smith *et al*., 2006; Richards *et al*., 2011), metastatic melanoma (Arab *et al*., 2011), and gastric cancer (Yang *et al*., 2014), and hypermethylation has been correlated with decreased survival in metastatic melanoma and gastric cancer (Arab *et al*., 2011; Yang *et al*., 2014b), and increased cell proliferation, migration and invasion in CRC (Dai *et al*., 2016). *EPHA7* has been reported as TSG, and its downregulation by hypermethylation has been found in CRC (Wang *et al*., 2005), gastric carcinoma (Wang *et al*., 2007), prostate cancer (Guan *et al*., 2009), and follicular lymphoma (Oricchio *et al*., 2011). *HTRA1* has been reported as potential TSG that works by inhibiting epithelial-mesenchymal transition, mediating ATM DNA damage response pathways (Wang *et al*., 2012), and inhibiting TGF-β signaling pathway (Zurawa-Janicka *et al*., 2012). Its lower expression has been positively correlated with lymph node metastasis in esophageal cancer (Yu *et al*., 2012), and high-grade endometrioid tumors (Bowden *et al*., 2006; Mullany *et al*., 2011). *IQGAP2* inactivation through aberrant promoter methylation has been reported to induce invasiveness in gastric cancer cells (Jin *et al*., 2008). It has also been reported as a candidate TSG that suppresses tumorigenesis in hepatocellular carcinoma by activating Wnt/beta-catenin signaling pathway (Schmidt *et al*., 2008), and prostate cancer tumorigenesis by up-regulation of E-cadherin (Xie *et al*., 2012). *HOXD1* has been found to be epigenetically silenced by hypermethylation in colon cancer (Jacinto *et al*., 2007), and at high frequency in early stage breast cancer (Jeschke *et al*., 2012). *EYA4* expression has been found to be regulated by CpG methylation in CRC (Kim *et al*., 2011; Kim *et al*., 2015) and frequently in Barrett's esophagus and esophageal adenocarcinoma (Zou *et al*., 2005). It has been reported as a putative TSG in CRC that works by inhibiting Wnt-signaling

pathway (Kim *et al*., 2015), displays TSG-like properties with a role in modulating apoptosis and DNA repair in non-small cell lung cancer (Wilson *et al*., 2014). Its decreased expression has been correlated with poor survival in sporadic lung cancers (Wilson *et al*., 2014). *PDLIM4* has been reported as TSG silenced by hypermethylation in prostate cancer (Vanaja *et al*., 2009; Vanaja *et al*., 2006), and renal cell carcinoma (Morris *et al*., 2010). *ZFP42* expression has been found to be epigenetically regulated by aberrant promoter methylation (Dansranjavin *et al*., 2009). *NID2* promoter is aberrantly methylated in gastrointestinal cancer (Ulazzi *et al*., 2007), bladder cancer (Yegin *et al*., 2013) and squamous cell carcinoma (Guerrero-Preston *et al*., 2011), and its loss has been correlated with invasion and metastasis (Ulazzi *et al*., 2007). *SPARC* has been found to be inactivated by promoter hypermethylation in colon or CRC (Yang *et al*., 2007; Cheetham *et al*., 2008) and its loss has been associated with poor prognosis and aggressive clinicopathological features in colon or CRC (Liang *et al*., 2010; Liu *et al*., 2015), and has been further identified as putative resistance-reversal gene in CRC (Tai *et al*., 2005). *GLIPR1* has been reported as TSG in prostate cancer (Tabata *et al*., 2011; Li *et al*., 2011; Karantanos *et al*., 2014), and AML (Xiao *et al*., 2011) that function by targeting oncoprotein destruction (Li *et al*., 2011), increasing production of reactive oxygen species, apoptosis, decreasing c-Myc protein levels, and increasing cell cycle arrest (Karantanos *et al*., 2014), mediating proapoptotic reactive oxygen species-c-Jun-NH2 kinase signaling (Li *et al*., 2008), and its expression has been found to be regulated by methylation in AML (Xiao *et al*., 2011). *CCDC80* has been reported as TSG in CRC (Herbst *et al*., 2011; Grill *et al*., 2014) and thyroid cancer (Ferraro, *et al*., 2013) that functions by sensitizing cells to receptor-mediated apoptosis (Herbst *et al*., 2011), through mechanism involving ERK phosphorylation (Grill *et al*., 2014) or by increasing expression of E-cadherin (Ferraro, *et al*., 2013).

The correlation between CpG island hypermethylation and down-regulation of these TSGs in DAC-resistant CRC cells observed in this study is according to the previously published finding which established the role of re-silencing of TSGs in development of dug resistance (Hesson *et al*., 2013). Therefore, these hypermethylation silenced TSGs exposed in this study might be used to differentiate between resistance and sensitivity to DAC. However, there validation in clinical samples is a pre-requisite for their development as response predicting biomarkers in clinic. Besides, unlike genes in up-regulated clusters whose expressions were reversed on treatment with BET inhibitor, there was no significant change in expression of these TSGs on exposing DAC-resistant CRC cells to (+)-JQ1. The observation is true as BET proteins play a critical role in gene activation by recruitment of the factors necessary for transcription

(Josling *et al*., 2012). This also means that sensitizing effects of (+)-JQ1 is independent of DNA methylation.

5.3.8. BET inhibitor sensitized DAC-resistant colorectal cancer cells by inducing degradation of elevated NF-kB

The connection between inflammation and CRC tumorigenesis has long been established. The recent studies suggested the role of distinct immune cells, inflammatory cytokines, and other immune modulators in regulation of CRC tumorigenesis (Terzić *et al*., 2010), and the involvement of immune activation machineries in clinical responses to DNA hypomethylating drugs (Qin *et al*., 2011). In line of these findings, functional clustering of differentially expressed gene signatures in this study revealed the overexpression of various immunomodulatory cytokines in DAC-resistant CRC cells, which were down-regulated on exposure of cells to BET inhibitor (Fig. 5.5). Amongst the group of various cytokines, the high differential expression was recorded for pro-inflammatory cytokine, *IL-32* which was further selected for CpG methylation analysis (Fig 5.5). Intrestingly, amongst the panel of up-regulated genes analyzed for CpG island methylation, the methylation level of only *IL-32* correlated with the RNA expression. The methylation levels (Fig. 5.6A,B) and RNA expressions (Fig. 5.6A) of this gene in parental and DAC-resistant CRC cells treated or untreated with DAC or BET inhibitor is shown. While no published litreture indicate the epigenetic regulation of *IL-32*, this is the first study suggesting the epigenetic regulation of this gene by 2nd promoter. The results demonstrate that the *IL-32* was marginally increased on treatment with DAC following promoter demethylation, was overexpressed with increase in hypomethylation in DAC-resistant CRC cells, and was down-regulated again on treatment with BET inhibitor (Fig. 5.6A,B).

Furthermore, it is known from the published literature (Yousif *et al*., 2013) that *IL-32* expression modulates *NFkB* actvity which is connected with multiple aspects of oncogenesis, including the regulation of cell proliferation, migration, cell cycle progression, and apoptosis (Piva *et al*., 2006). Moreover, the activation of *NFκB* in cancer cells by chemotherapy has been known to be associated with the acquisition of resistance to apoptosis (Piva *et al*., 2006). Therefore, activity of *NFκB* was analyzed in conditioned medium from parental and DAC-resistant CRC cell cultures, using in-house developed *NFκB* reporter system at 24, 48, 72, and 96 h (Fig. 5.6C). Intrestingly, *NFκB* pathway was found to be significantly up-regulated in DAC-resistant CRC cells as compared to parental cells (Fig.5.6C). In congruency with these findings, a recent study published the role of *Brd4* in maintenance of constitutive *NFkB,* and role of BET inhibitor (+)-JQ1 in ubiquitination-mediated degradation of *NFκB* (Zou *et al*., 2014). The study

elucidated that *BRD4* binds to acetylated lysine-310 of *RelA* and prevents the ubiquitination and degradation of nuclear *RelA;* this interaction plays potential role in the maintenance of constitutively active *NF-κB* and in tumor formation, whereas treatment of cells with (+)-JQ1 induces the ubiquitination and degradation of the constitutively active nuclear form of *RelA* (Fig. 5.5D). Based on the previous finding (Zou *et al*., 2014) and the observed results, this study proposes up-regulation of *NFκB* as the mechanism responsible for secondary resistance to DAC, and degradation of active *NF-κB* in DAC-resistant CRC cells upon exposure to (+)-JQ1 as the mechanism responsible for observed sensitivity of DAC-resistant cells to BET inhibitor. However, further validation is clearly required to prove this hypothesis.

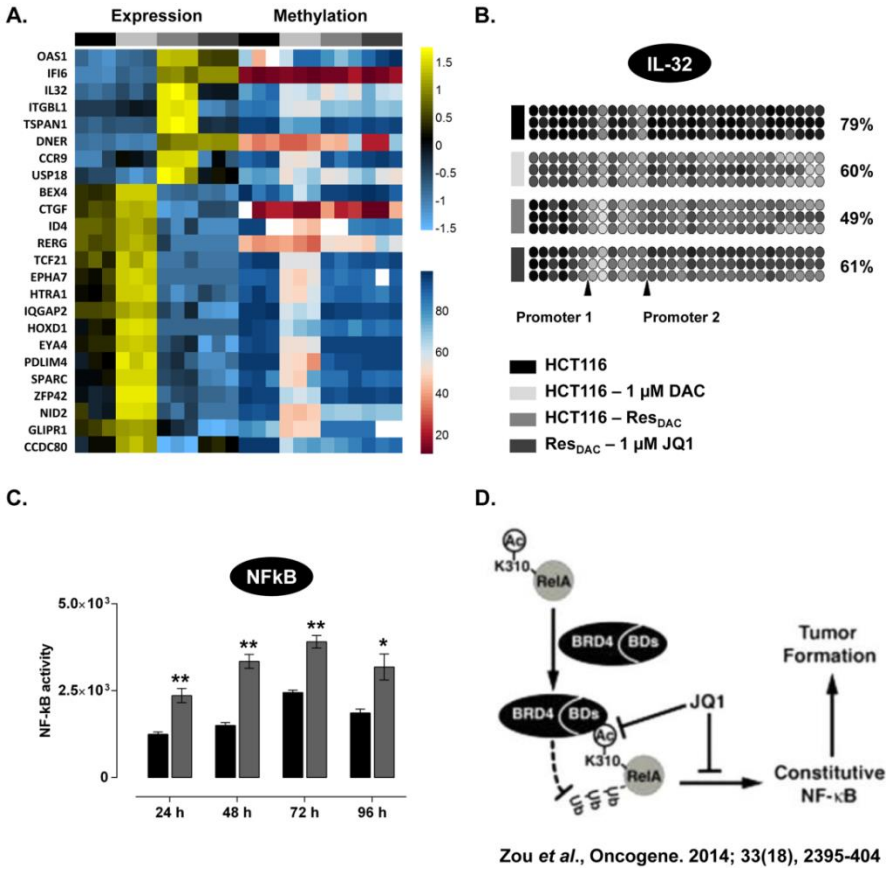

Zou *et al*., Oncogene. 2014; 33(18), 2395-404

Figure 5.6 Gene signatures differentiating DAC-sensitivity and resistance, and *NF-κB* activity and proposed mechanism of sensitivity induced by BET inhibitor

(A) *Gene expression and methylation levels of selected genes in parental and DAC-resistant CRC cells, treated or untreated with 1μM DAC or 1μM (+)-JQ1 for 48 h is shown.* ***(B)*** *CpG methylation analysis of IL-32* ***(C)*** *NFκB activity in parental and DAC-resistant CRC cells.* Data are mean ± *S.D., n = 3. **p < 0.001, *p < 0.005, Student's t-test, unpaired* ***(D)*** *Schematic re-presentation showing mechanism behind maintenance of constitutive NFκB by BRD4.*

5.4. Discussion

In this study secondary resistance to DAC was investigated using HCT116 CRC cells which showed highest sensitivity to DAC among 4 human CRC cell lines examined previously (Baylin & Ohm, 2006). DAC-resistant CRC cell lines were developed through long-term treatment with DAC and > 100 fold difference was observed in IC_{50} value of DAC between parent and resistant cell lines. In order to determine if DAC-resistant CRC cells acquired cross-resistance to other epigenetic modulators and chemotherapeutic agents, their cell growth inhibitory effects were investigated in parental and DAC-resistant CRC cells. The results of the study revealed that all DAC-resistant cell lines are cross-resistant to other tested DNMT inhibitors (Fig. 5.1A). The observed results are contrary to the previously published results which demonstrated no cross-resistance against DNMT inhibitors (Hosokawa *et al*., 2015). The inconsistency might be due to different mechanisms of drug resistance than up-regulation of CDA and down-regulation of dCK as demonstrated in the previous study (Hosokawa *et al*., 2015). This is proven by the observed cross-resistance towards guadecitabine (Fig. 5.1A), a second generation pro-drug of decitabine which is protected from deamination by CDA (Yoo *et al*., 2007). Moreover, another drug zebularine did not display cross-resistance in previous studies because zebularine is a potent inhibitor of CDA (Kim *et al*., 1986). No cross-resistance towards azacytidine was seemed in previous study because uridine cytidine kinase (uCK) instead of dCK is mainly responsible for phosphorylation of azacytidine (Valencia *et al*., 2014). Moreover, unlike previous study which demonstrated absence of cross-resistance towards HDAC inhibitors, the results of this study showed increase in IC_{50} of HDAC inhibitors (Fig.5.1A), but only marginally (Hosokawa *et al*., 2015). The cross-resistance was also demonstrated for all tested HAT, HMT, and HDM inhibitors (Fig.5.1A). For chemotherapeutic agents, the difference in IC_{50} values between parental and DAC-resistant cell lines were not significant for any tested drugs except gemcitabine which showed high levels of cross-resistance (Fig. 5.1A), similar to previous study (Hosokawa *et al*., 2015). Interestingly, only the tested BET inhibitors were discovered to significantly sensitize the DAC-resistant CRC cells amongst the panel of 21 therapeutic agents screened in this study (Fig. 5.1A). This observation was further corroborated by *in vitro* cell cycle analysis of parental and DAC-resistant CRC cells, following exposure of these cells to DAC and BET inhibitor (Fig. 5.1B), and anti-tumor study of these drugs in xenograft models of parental and DAC-resistant CRC cells (Fig. 5.2). The results were congruent with the sensitizing effects of (+)-JQ1 in DAC-resistant CRC cells, seen in cytotoxicity assay (Fig. 5.1, 5.2). As, this is the first study of BET inhibitor in combination with DAC, it was necessary to rule out the antagonistic

effects of the two drugs in combination. Therefore, the novel combination of DAC and BET inhibitor was tested in both parental and DAC-resistant CRC cell lines, and the results demonstrated the synergistic/additive cytotoxic effects of the two drugs in combination (Fig. 5.3).

After promising anti-proliferative synergistic effects were seen for BET inhibitor with or without combination with DAC, the mechanism behind the secondary resistance towards DAC and observed sensitivity towards BET inhibitor was investigated by transcriptomics and bisulfite sequencing (Fig. 5.4, 5.5, 5.6). The RNA expression and methylation profiling revealed the overexpressed oncogenic candidates in DAC-resistant CRC cells, the expressions of which were regulated independent of DNA methylation, and abrogated on treatment with BET inhibitor (Fig. 5.5). These data confer with the previously published hypothesis which suggests the likelihood of secondary resistance to be independent of DNA methylation and pharmacologic pathways, and the genetic activation of oncogenic survival and progression pathways during secondary resistance to DAC (Qin *et al*., 2011). However, the reversal of the oncogenic signatures of DAC resistance by BET inhibitor is the novel finding of this study. Alternatively, the transcriptomics and methylation analysis revealed a set of hypermethylation-silenced TSGs, the expression of which was differentially regulated between DAC-sensitive and resistant cell lines but was not affected on exposure of cells to BET inhibitor. The study proposes these epigenetically regulated genes as the response predictors which may differentiate between DAC-resistance and sensitivity. But their potential as surrogate biomarkers that differentiate between responders and non-responders is contradicted by the results of the two independent studies. One line of evidence suggests absence of hypermethylation at relapse (Qin *et al*., 2011) whereas, another line of evidence states that re-silencing of TSGs that were re-activated by promoter demethylation leads to resistance (Hesson *et al*., 2013) as observed in this study. Also, several other studies have correlated hypermethylation marks with resistance to azanucleosides, but so far none of the studies revealed the clear-cut molecular patterns to identify non-responders (Diesch *et al*., 2016). Therefore, clinical validation of hypermethylation marks revealed in this study is a prerequisite for the development of these genes as diagnostic tools. Towards the end, the preliminary results of this study proposes the role of *IL-32* mediated activation of oncogenic *NFκB* in DAC-resistant cells, and ubiquitination-mediated degradation of *NFκB* by BET inhibitors as the possible mechanism behind the observed sensitization.

Supplemental Table S5.1 Epigenetic- and chemo-therapeutics screened against parental and 3 decitabine resistant colorectal cancer cell lines

Mean ± S.D. represents IC_{50} of drugs ([a] - 5 days MTT test, others - 3 days), calculated from 3 independent experiments. P-value, one-way Anova with Dunnett's multiple comparisons test compares HCT116 vs. each resistant cell line.

Drugs		Mechanism	HCT116	$Resistant_{DAC}\_1$		$Resistant_{DAC}\_2$		$Resistant_{DAC}\_3$	
			Mean ± S.D.	Mean ± S.D.	P-value	Mean ± S.D.	P-value	Mean ± S.D.	P-value
Epigenetic inhibitors	[a] Decitabine	DNA methyltransferase	0.11 ± 0.01	100.00 ± 0.00	< 0.0001	100.00 ± 0.00	< 0.0001	100.00 ± 0.00	< 0.0001
	[a] Guadecitabine		0.08 ± 0.00	100.00 ± 0.00		100.00 ± 0.00		100.00 ± 0.00	
	Azacytidine		3.03 ± 0.22	10.15 ± 1.16	0.0001	11.45 ± 1.35	< 0.0001	15.33 ± 1.23	< 0.0001
	Zebularine		82.71 ± 3.42	100.00 ± 0.00	< 0.0001	100.00 ± 0.00	< 0.0001	100.00 ± 0.00	< 0.0001
	C646	Histone acetyltransferase	30.91 ± 2.79	43.55 ± 3.33	0.0064	47.08 ± 4.12	0.0014	50.38 ± 3.91	0.0004
	Anacardic acid		120.70 ± 4.08	128.05 ± 8.15	0.3794	124.23 ± 6.49	0.8242	120.77 ± 5.07	> 0.9999
	BIX-01294	Histone methyltransferase	2.46 ± 0.17	3.01 ± 0.09	0.0013	2.94 ± 0.08	0.0031	3.02 ± 0.11	0.0012
	DZNep		0.78 ± 0.07	25.00 ± 0.00	< 0.0001	25.00 ± 0.00	< 0.0001	25.00 ± 0.00	< 0.0001
	Romidepsin	Histone deacetylase	0.003 ± 0.00	0.003 ± 0.00	0.9547	0.003 ± 0.00	0.9547	0.003 ± 0.00	0.9547
	Vorinostat		0.64 ± 0.06	0.82 ± 0.03	0.0005	0.86 ± 0.01	0.0002	0.92 ± 0.02	< 0.0001
	GSK J4	Histone demethylase	2.17 ± 0.64	3.48 ± 0.23	0.0052	3.18 ± 0.05	0.0206	3.05 ± 0.21	0.0404
	IOX1		30.10 ± 3.52	45.54 ± 2.40	0.0005	56.00 ± 2.96	< 0.0001	60.31 ± 2.72	< 0.0001
	(+)-JQ1	Bromodomain	2.79 ± 0.16	0.79 ± 0.15	< 0.0001	0.52 ± 0.10	< 0.0001	0.88 ± 0.07	< 0.0001
	I-BET 151		5.08 ± 0.75	2.64 ± 0.26	0.0003	1.75 ± 0.22	< 0.0001	3.64 ± 0.26	0.0089
Chemotherapeutics	5-Fluorouracil	Colorectal cancer treatment	3.55 ± 0.08	6.81 ± 2.78	0.0954	4.09 ± 0.97	0.957	4.97 ± 1.40	0.6014
	Irinotecan		2.90 ± 0.18	3.78 ± 0.45	0.2764	4.76 ± 1.07	0.0172	4.12 ± 0.44	0.1051
	Oxaliplatin		0.71 ± 0.02	0.55 ± 0.13	0.1779	0.67 ± 0.02	0.9104	0.49 ± 0.15	0.0706
	Gemcitabine		0.02 ± 0.00	69.00 ± 2.82	< 0.0001	72.36 ± 1.46	< 0.0001	84.31 ± 4.03	< 0.0001
	Roscovitine	Cyclin-dependent kinase	19.12 ± 4.01	17.65 ± 4.94	0.944	16.89 ± 4.04	0.8426	15.07 ± 3.09	0.5123
	Palbociclib		8.73 ± 3.00	6.86 ± 4.40	0.8383	6.81 ± 3.31	0.8268	5.96 ± 2.51	0.6394
	Actinomycin D	Transcription	0.001 ± 0.00	0.001 ± 0.00	> 0.9999	0.001 ± 0.00	> 0.9999	0.001 ± 0.00	0.4044
	Cycloheximide	Protein synthesis	0.46 ± 0.09	0.57 ± 0.29	0.8567	0.49 ± 0.23	0.9958	0.50 ± 0.14	0.9887

Supplemental Table S5.2 Gene expression profiles according to the functional categories

Positive values indicate up-regulation and negative values indicate down-regulation. Up and Down clusters genes significantly overexpressed and down-regulated respectively in DAC-resistant colorectal cancer cells compared to parental cells. LogFC represents fold changes calculated from 3 biological replicates; [a]LogFC – HCT116 vs. HCT116-1 µM DAC, [b]LogFC – HCT116 vs. HCT116-Resistant$_{DAC}$, [c]LogFC – HCT116-Resistant$_{DAC}$ vs. HCT116-Resistant$_{DAC}$-1 µM JQ1. P-value (adjusted P-value) ≤ 0.05 indicates statistical significance.

Ensembl ID	Gene	Protein name	HCT116-1 µM DAC		HCT116-Res$_{DAC}$		Res$_{DAC}$-1 µM JQ1		Function	
			[a]LogFC	P-value	[b]LogFC	P-value	[c]LogFC	P-value		
ENSG00000065618	COL17A1	Collagen Type XVII Alpha 1	0.38	0.0163	4.26	9.83E-273	-5.12	0	Up	Adhesion / Migration
ENSG00000213937	CLDN9	Claudin 9	0.53	0.3202	2.15	1.91E-09	1.23	0.0002		
ENSG00000112139	MDGA1	MAM Domain Containing Glycosylphosphatidylinositol Anchor 1	-0.08	0.8212	2.14	2.94E-39	-1.58	2.11E-22		
ENSG00000186352	ANKRD37	Ankyrin Repeat Domain 37	0.73	0.1147	2.12	8.44E-09	-1.46	7.12E-05		
ENSG00000079385	CEACAM1	Carcinoembryonic Antigen Related Cell Adhesion Molecule 1	0.09	0.7848	2.09	1.45E-39	-4.55	3.05E-127		
ENSG00000276600	RAB7B	RAB7B, Member RAS Oncogene Family	1.03	3.75E-05	-1.84	2.21E-12	-2.62	7.91E-12	Down	
ENSG00000134760	DSG1	Desmoglein 1	1.28	0.0208	-1.86	0.0020	-1.51	0.0347		
ENSG00000087303	NID2	Nidogen 2	4.01	7.59E-20	-1.89	0.0039	-0.71	0.4029		
ENSG00000253767	PCDHGA8	Protocadherin Gamma Subfamily A, 8	1.57	0.0020	-1.90	0.0011	-1.36	0.0517		
ENSG00000253731	PCDHGA6	Protocadherin Gamma Subfamily A, 6	1.95	1.22E-10	-1.96	5.20E-07	-1.43	0.0067		
ENSG00000146555	SDK1	Sidekick Cell Adhesion Molecule 1	1.65	0.0211	-2.11	0.0064	-0.22	0.8500		
ENSG00000170989	S1PR1	Sphingosine-1-Phosphate Receptor 1	2.22	3.82E-06	-2.12	0.0006	-1.02	0.1917		
ENSG00000090339	ICAM1	Intercellular Adhesion Molecule 1	1.09	1.92E-09	-2.27	1.76E-35	-2.95	1.20E-35		
ENSG00000164176	EDIL3	EGF Like Repeats And Discoidin Domains 3	4.59	4.68E-31	-2.46	0.0001	0.20	0.8563		
ENSG00000154556	SORBS2	Sorbin And SH3 Domain Containing 2	1.45	0.0002	-2.66	9.76E-08	-1.02	0.1484		
ENSG00000136167	LCP1	Lymphocyte Cytosolic Protein 1	1.19	4.51E-08	-2.72	1.45E-30	-3.95	1.30E-17		
ENSG00000262655	SPON1	Spondin 1	2.68	6.94E-12	-3.28	5.78E-08	0.18	0.8756		

ENSG00000118523	CTGF	Connective Tissue Growth Factor	1.79	5.25E-33	-4.49	8.25E-195	1.62	1.35E-25		
ENSG00000115363	EVA1A	Eva-1 Homolog A, Regulator Of Programmed Cell Death	0.86	7.59E-05	3.40	2.20E-86	-0.43	0.0021	Up	Cell proliferation / Apoptosis
ENSG00000133106	EPSTI1	Epithelial Stromal Interaction 1	0.75	0.0005	3.02	2.50E-69	-1.21	1.76E-17		
ENSG00000205413	SAMD9	Sterile Alpha Motif Domain Containing 9	0.35	0.0777	2.75	9.51E-72	-0.54	0.0012		
ENSG00000168209	DDIT4	DNA Damage Inducible Transcript 4	-0.57	0.0348	2.49	7.23E-30	-1.93	1.40E-18		
ENSG00000167779	IGFBP6	Insulin Like Growth Factor Binding Protein 6	0.44	0.1421	2.21	2.44E-22	-0.30	0.2859		
ENSG00000177409	SAMD9L	Sterile Alpha Motif Domain Containing 9 Like	0.04	0.9760	2.21	5.90E-07	-3.81	7.58E-16		
ENSG00000091986	CCDC80	Coiled-Coil Domain Containing 80	1.30	3.13E-11	-1.79	1.93E-15	1.99	2.35E-20	Down	
ENSG00000139278	GLIPR1	GLI Pathogenesis Related 1	1.14	0.0010	-1.82	8.92E-08	-2.60	1.50E-10		
ENSG00000164741	DLC1	DLC1 Rho GTPase Activating Protein	5.87	9.41E-40	-1.84	0.0127	0.23	0.8384		
ENSG00000130208	APOC1	Apolipoprotein C1	3.96	8.41E-50	-1.87	6.33E-06	-1.61	0.0059		
ENSG00000124225	PMEPA1	Prostate Transmembrane Protein, Androgen Induced 1	1.04	0.0005	-1.94	1.22E-10	-1.53	3.55E-05		
ENSG00000113140	SPARC	Secreted Protein Acidic And Cysteine Rich	5.29	7.73E-149	-2.10	1.10E-19	-2.63	1.26E-16		
ENSG00000131435	PDLIM4	PDZ And LIM Domain 4	5.17	1.15E-51	-2.12	5.51E-06	-1.41	0.0211		
ENSG00000182866	LCK	LCK Proto-Oncogene, Src Family Tyrosine Kinase	4.88	1.91E-95	-2.16	8.65E-08	-1.08	0.0670		
ENSG00000178568	ERBB4	Erb-B2 Receptor Tyrosine Kinase 4	1.24	0.0011	-2.22	4.88E-07	-1.72	0.0044		
ENSG00000198796	ALPK2	Alpha Kinase 2	2.07	7.65E-13	-2.28	2.49E-11	-1.51	0.0009		
ENSG00000171243	SOSTDC1	Sclerostin Domain Containing 1	2.99	6.80E-13	-2.34	0.0001	-0.72	0.3982		
ENSG00000101349	PAK7	P21 Protein (Cdc42/Rac)-Activated Kinase 7	1.64	0.0089	-2.83	6.45E-05	0.00	1		
ENSG00000078401	EDN1	Endothelin 1	1.11	2.95E-09	-2.90	3.42E-41	-0.30	0.3690		
ENSG00000135960	EDAR	Ectodysplasin A Receptor	1.37	1.39E-05	-2.96	1.49E-13	-1.45	0.0141		
ENSG00000166033	HTRA1	HtrA Serine Peptidase 1	3.21	1.18E-18	-3.04	1.65E-07	0.48	0.5832		
ENSG00000134533	RERG	RAS Like Estrogen Regulated Growth Inhibitor	1.60	4.11E-06	-4.09	1.06E-14	-0.54	0.5470		
ENSG00000169129	AFAP1L2	Actin Filament Associated Protein 1 Like 2	1.19	1.18E-14	-4.41	1.04E-68	-1.12	0.0076		
ENSG00000215853	RPTN	Repetin	-0.21	0.8828	3.62	4.74E-07	-3.20	3.09E-06		

ENSG00000170477	KRT4	Keratin 4	0.04	0.9827	2.40	0.0007	-3.03	4.83E-06	Up	Differentiation
ENSG00000179059	ZFP42	ZFP42 Zinc Finger Protein	8.11	3.70E-255	-1.93	4.23E-06	-1.02	0.0878	Down	
ENSG00000171502	COL24A1	Collagen Type XXIV Alpha 1	1.99	1.13E-13	-2.59	3.93E-14	-2.02	8.89E-05		
ENSG00000163216	SPRR2D	Small Proline Rich Protein 2D	1.37	0.0090	-3.65	1.17E-08	0.22	0.8463		
ENSG00000038945	MSR1	Macrophage Scavenger Receptor 1	1.14	0.0045	-4.73	1.88E-17	-0.18	0.8717		
ENSG00000172137	CALB2	Calbindin 2	0.06	0.8621	3.87	6.82E-150	-2.50	2.72E-67	Up	Drug resistance
ENSG00000163017	ACTG2	Actin, Gamma 2, Smooth Muscle, Enteric	1.69	0.0020	-1.85	0.0034	-0.26	0.7864	Down	
ENSG00000108932	SLC16A6	Solute Carrier Family 16 Member 6	1.34	1.17E-18	-2.74	8.36E-74	-1.16	3.17E-13		
ENSG00000089127	OAS1	2'-5'-Oligoadenylate Synthetase 1	0.62	0.0256	6.66	3.72E-250	-2.21	8.56E-44	Up	Immune response / Inflammation
ENSG00000126709	IFI6	Interferon Alpha Inducible Protein 6	0.65	0.0019	4.66	5.61E-150	0.27	0.2352		
ENSG00000008517	IL32	Interleukin 32	0.44	0.0675	4.14	1.88E-122	-2.91	2.83E-67		
ENSG00000137965	IFI44	Interferon Induced Protein 44	0.73	0.0015	4.10	5.10E-109	-4.79	3.07E-143		
ENSG00000134321	RSAD2	Radical S-Adenosyl Methionine Domain Containing 2	0.24	0.7331	3.81	1.46E-33	-0.49	0.0807		
ENSG00000137959	IFI44L	Interferon Induced Protein 44 Like	0.38	0.7159	3.67	1.00E-12	-5.67	1.20E-22		
ENSG00000185745	IFIT1	Interferon Induced Protein With Tetratricopeptide Repeats 1	0.15	0.3760	3.29	2.54E-213	-1.66	6.45E-56		
ENSG00000136689	IL1RN	Interleukin 1 Receptor Antagonist	-0.95	0.0183	2.91	8.64E-29	-4.53	7.49E-51		
ENSG00000115267	IFIH1	Interferon Induced With Helicase C Domain 1	0.40	0.0072	2.74	3.94E-114	0.06	0.7479		
ENSG00000204010	IFIT1B	Interferon Induced Protein With Tetratricopeptide Repeats 1B	0.72	0.5210	2.38	0.0025	-2.01	0.0085		
ENSG00000111331	OAS3	2'-5'-Oligoadenylate Synthetase 3	0.06	0.7082	2.35	4.78E-159	-0.81	9.81E-20		
ENSG00000183709	IFNL2	Interferon, Lambda 2	0.75	0.4508	2.30	0.0004	1.16	0.0349		
ENSG00000187608	ISG15	ISG15 Ubiquitin-Like Modifier	0.14	0.8588	2.16	7.97E-08	0.76	0.0860		
ENSG00000184979	USP18	Ubiquitin Specific Peptidase 18	-0.60	0.0159	2.09	3.28E-25	-1.49	7.39E-14		
ENSG00000154451	GBP5	Guanylate Binding Protein 5	3.08	1.97E-14	-2.38	6.75E-05	-0.15	0.8952	Down	

ENSG00000117594	HSD11B1	Hydroxysteroid (11-Beta) Dehydrogenase 1	0.81	0.4545	3.09	3.32E-05	-3.26	4.70E-06	Up	Metabolic process
ENSG00000134326	CMPK2	Cytidine/Uridine Monophosphate Kinase 2	-0.41	0.0411	2.58	1.39E-74	-1.46	5.77E-28		
ENSG00000266200	PNLIPRP2	Pancreatic Lipase Related Protein 2	-0.56	0.6046	2.25	0.0003	-3.63	2.15E-09		
ENSG00000165799	RNASE7	Ribonuclease A Family Member 7	0.66	0.5524	2.12	0.0032	-3.16	2.27E-06		
ENSG00000140835	CHST4	Carbohydrate Sulfotransferase 4	-0.39	0.3560	2.07	7.86E-16	-5.35	7.64E-55		
ENSG00000137880	GCHFR	GTP Cyclohydrolase I Feedback Regulator	2.40	5.29E-26	-1.78	5.59E-12	0.93	0.0006	Down	
ENSG00000243955	GSTA1	Glutathione S-Transferase Alpha 1	1.32	0.0160	-1.88	0.0022	-1.36	0.0637		
ENSG00000138109	CYP2C9	Cytochrome P450 Family 2 Subfamily C Member 9	1.39	0.0328	-1.99	0.0044	0.41	0.6576		
ENSG00000196169	KIF19	Kinesin Family Member 19	3.10	2.30E-25	-2.03	1.98E-06	-1.07	0.0673		
ENSG00000109956	B3GAT1	Beta-1,3-Glucuronyltransferase 1	3.48	4.40E-10	-2.06	0.0070	0.00	1		
ENSG00000183914	DNAH2	Dynein Axonemal Heavy Chain 2	1.89	1.45E-59	-2.11	8.66E-49	-0.97	4.07E-07		
ENSG00000101443	WFDC2	WAP Four-Disulfide Core Domain 2	2.40	3.84E-07	-2.27	0.0002	0.01	1		
ENSG00000105131	EPHX3	Epoxide Hydrolase 3	3.73	6.53E-27	-2.40	1.19E-05	0.82	0.2147		
ENSG00000196660	SLC30A10	Solute Carrier Family 30 Member 10	2.00	0.0006	-2.56	0.0003	0.04	0.9949		
ENSG00000163071	SPATA18	Spermatogenesis Associated 18	3.46	9.26E-18	-2.66	1.78E-05	-0.19	0.8643		
ENSG00000151376	ME3	Malic Enzyme 3	3.13	2.85E-13	-2.69	9.43E-06	-0.15	0.8951		
ENSG00000142623	PADI1	Peptidyl Arginine Deiminase 1	2.61	6.42E-23	-2.77	2.09E-11	-0.32	0.6556		
ENSG00000059804	SLC2A3	Solute Carrier Family 2 Member 3	1.64	7.71E-11	-2.94	1.40E-32	-3.78	7.68E-38		
ENSG00000142619	PADI3	Peptidyl Arginine Deiminase 3	1.04	0.0001	-2.99	3.14E-31	-3.88	1.35E-25		
ENSG00000135838	NPL	N-Acetylneuraminate Pyruvate Lyase	2.60	4.06E-12	-3.39	5.20E-09	-0.38	0.6982		
ENSG00000158560	DYNC1I1	Dynein Cytoplasmic 1 Intermediate Chain 1	1.45	0.0069	-3.52	6.74E-08	0.00	1		
ENSG00000104723	TUSC3	Tumor Suppressor Candidate 3	3.92	6.89E-76	-4.20	1.27E-19	-0.62	0.4448		
ENSG00000166532	RIMKLB	Ribosomal Modification Protein RimK-Like Family Member B	2.73	5.08E-40	-5.38	1.45E-35	-0.68	0.3691		
ENSG00000164002	EXO5	Exonuclease 5	1.90	6.28E-25	-6.27	1.35E-40	0.64	0.3962		
ENSG00000198542	ITGBL1	Integrin Subunit Beta Like 1	0.45	0.0630	3.60	1.40E-104	-4.52	6.40E-147		

ENSG00000117472	TSPAN1	Tetraspanin 1	0.05	0.8261	3.44	7.58E-235	-2.87	7.93E-169	Up	Metastasis / Progression
ENSG00000089356	FXYD3	FXYD Domain Containing Ion Transport Regulator 3	0.13	0.6027	3.31	9.15E-130	-2.89	6.56E-104		
ENSG00000173585	CCR9	C-C Motif Chemokine Receptor 9	0.98	0.3374	3.27	3.27E-06	-3.07	3.26E-06		
ENSG00000105649	RAB3A	RAB3A, Member RAS Oncogene Family	-0.22	0.4143	2.19	1.94E-39	0.02	0.9496		
ENSG00000133985	TTC9	Tetratricopeptide Repeat Domain 9	0.61	1.16E-05	2.18	1.08E-70	-0.71	4.33E-09		
ENSG00000137809	ITGA11	Integrin Subunit Alpha 11	2.39	2.78E-11	-1.75	0.0003	-1.54	0.0139	Down	
ENSG00000136267	DGKB	Diacylglycerol Kinase Beta	2.02	1.16E-14	-1.77	7.19E-09	-3.33	6.73E-12		
ENSG00000242265	PEG10	Paternally Expressed 10	2.07	1.21E-95	-1.78	9.82E-69	2.24	2.05E-109		
ENSG00000138696	BMPR1B	Bone Morphogenetic Protein Receptor Type 1B	3.63	6.44E-21	-1.90	0.0014	-0.27	0.7840		
ENSG00000026025	VIM	Vimentin	4.87	0	-1.98	1.45E-57	-0.68	7.94E-07		
ENSG00000041982	TNC	Tenascin C	1.82	0.0071	-2.42	0.0012	0.45	0.6540		
ENSG00000042980	ADAM28	ADAM Metallopeptidase Domain 28	1.31	0.0061	-2.67	8.68E-07	-1.08	0.1406		
ENSG00000113578	FGF1	Fibroblast Growth Factor 1	1.37	0.0001	-2.74	1.21E-14	-1.80	3.13E-05		
ENSG00000120708	TGFBI	Transforming Growth Factor Beta Induced	2.31	2.03E-11	-3.24	3.74E-13	1.12	0.0308		
ENSG00000171533	MAP6	Microtubule Associated Protein 6	1.89	3.49E-05	-3.50	3.45E-08	0.24	0.8284		
ENSG00000159167	STC1	Stanniocalcin 1	2.14	1.84E-21	-4.44	1.39E-22	-0.41	0.6323		
ENSG00000091879	ANGPT2	Angiopoietin 2	1.37	4.92E-23	-6.48	1.68E-123	-1.83	0.0004		
ENSG00000187957	DNER	Delta/Notch Like EGF Repeat Containing	-0.31	0.0781	3.39	1.53E-158	0.29	0.0370	Up	Signaling pathways
ENSG00000184502	GAST	Gastrin	0.56	0.4224	3.22	3.38E-14	-0.80	0.0497		
ENSG00000182389	CACNB4	Calcium Voltage-Gated Channel Auxiliary Subunit Beta 4	0.41	0.0542	2.51	2.67E-53	-0.74	1.05E-05		
ENSG00000129451	KLK10	Kallikrein Related Peptidase 10	0.38	0.1752	2.41	3.60E-31	-2.10	3.14E-24		
ENSG00000244694	PTCHD4	Patched Domain Containing 4	0.91	5.17E-05	2.23	3.36E-28	-7.29	2.47E-100		
ENSG00000138642	HERC6	HECT And RLD Domain Containing E3 Ubiquitin Protein Ligase Family Member 6	-0.05	0.8291	2.18	9.93E-85	-1.09	1.28E-22		
ENSG00000189375	TBC1D28	TBC1 Domain Family Member 28	0.16	0.9147	2.12	0.0036	-2.23	0.0008		
ENSG00000175899	A2M	Alpha-2-Macroglobulin	2.05	0.0006	-1.77	0.0161	0.61	0.4841		

ENSG00000143851	PTPN7	Protein Tyrosine Phosphatase, Non-Receptor Type 7	5.57	2.91E-176	-1.80	1.42E-09	-2.30	1.76E-06		
ENSG00000115590	IL1R2	Interleukin 1 Receptor Type 2	2.22	2.98E-07	-1.81	0.0013	-1.37	0.0465		
ENSG00000054356	PTPRN	Protein Tyrosine Phosphatase, Receptor Type N	3.09	2.99E-11	-1.88	0.0045	-0.15	0.8958		
ENSG00000165105	RASEF	RAS And EF-Hand Domain Containing	2.29	2.61E-08	-1.89	0.0004	-1.48	0.0261		
ENSG00000162878	PKDCC	Protein Kinase Domain Containing, Cytoplasmic	2.43	3.58E-07	-2.00	0.0011	-1.20	0.1097		
ENSG00000106631	MYL7	Myosin Light Chain 7	2.06	0.0023	-2.01	0.0096	-0.23	0.8404		
ENSG00000164694	FNDC1	Fibronectin Type III Domain Containing 1	2.79	4.39E-16	-2.12	1.47E-06	-1.95	0.0011		
ENSG00000060558	GNA15	G Protein Subunit Alpha 15	1.80	7.35E-11	-2.22	3.96E-11	-0.02	0.9948		
ENSG00000107518	ATRNL1	Attractin Like 1	1.14	4.32E-06	-2.35	1.27E-16	-1.17	0.0027		
ENSG00000137868	STRA6	Stimulated By Retinoic Acid 6	2.74	8.50E-22	-2.35	1.79E-09	-1.41	0.0109		
ENSG00000124749	COL21A1	Collagen Type XXI Alpha 1	1.08	0.0031	-2.46	1.34E-09	-1.21	0.0291		
ENSG00000145703	IQGAP2	IQ Motif Containing GTPase Activating Protein 2	1.49	1.50E-09	-2.48	8.53E-23	-1.86	8.43E-10	Down	
ENSG00000082556	OPRK1	Opioid Receptor Kappa 1	1.70	0.0137	-2.51	0.0008	0.00	1		
ENSG00000104490	NCALD	Neurocalcin Delta	2.09	1.24E-14	-2.66	8.13E-13	-1.71	0.0021		
ENSG00000117114	LPHN2	Adhesion G Protein-Coupled Receptor L2	3.82	2.87E-71	-2.73	1.41E-13	-1.83	0.0020		
ENSG00000166148	AVPR1A	Arginine Vasopressin Receptor 1A	4.55	2.71E-32	-2.73	1.30E-05	-0.20	0.8616		
ENSG00000188277	C15orf62	Chromosome 15 Open Reading Frame 62	3.91	1.17E-42	-2.77	1.82E-09	0.25	0.7594		
ENSG00000135312	HTR1B	5-Hydroxytryptamine Receptor 1B	1.40	1.61E-17	-2.80	6.80E-41	-3.04	1.77E-13		
ENSG00000135333	EPHA7	EPH Receptor A7	2.92	2.27E-12	-3.26	3.06E-07	0.00	1		
ENSG00000175868	CALCB	Calcitonin Related Polypeptide Beta	1.35	0.0116	-3.49	4.41E-08	1.09	0.1618		
ENSG00000183960	KCNH8	Potassium Voltage-Gated Channel Subfamily H Member 8	1.53	0.0005	-3.93	1.78E-10	0.00	1		
ENSG00000133083	DCLK1	Doublecortin Like Kinase 1	1.49	9.08E-27	-6.03	4.73E-83	-0.55	0.3384		
ENSG00000168062	BATF2	Basic Leucine Zipper ATF-Like Transcription factor 2	0.99	6.05E-08	2.52	2.87E-51	-0.12	0.6077		
ENSG00000120149	MSX2	Msh Homeobox 2	0.60	3.52E-06	2.48	1.31E-102	0.29	0.0254		
ENSG00000123095	BHLHE41	Basic Helix-Loop-Helix Family Member E41	-0.39	0.1150	2.15	1.00E-32	-1.26	2.06E-12	Up	

ENSG00000135899	SP110	SP110 Nuclear Body Protein	0.60	1.27E-07	2.12	8.18E-95	0.17	0.1737		
ENSG00000135625	EGR4	Early Growth Response 4	1.98	1.40E-07	-1.82	1.03E-05	-2.89	3.10E-08		
ENSG00000128714	HOXD13	Homeobox D13	3.98	1.25E-17	-1.86	0.0087	-0.42	0.6699		
ENSG00000112319	EYA4	EYA Transcriptional Coactivator And Phosphatase 4	3.32	1.92E-45	-2.17	1.12E-10	-2.17	3.78E-05		
ENSG00000177932	ZNF354C	Zinc Finger Protein 354C	4.41	1.60E-29	-2.29	0.0003	-0.20	0.8586		
ENSG00000128645	HOXD1	Homeobox D1	3.36	3.38E-11	-2.33	0.0013	0.00	1		
ENSG00000126561	STAT5A	Signal Transducer And Activator Of Transcription 5A	3.94	1.03E-31	-2.36	1.33E-05	-0.74	0.3440		
ENSG00000125798	FOXA2	Forkhead Box A2	2.97	3.15E-14	-2.50	1.41E-05	-0.64	0.4451		
ENSG00000122691	TWIST1	Twist Family BHLH Transcription Factor 1	1.67	1.08E-15	-2.94	1.00E-23	-2.08	2.44E-05		
ENSG00000251369	ZNF550	Zinc Finger Protein 550	1.67	4.67E-27	-3.02	8.36E-48	-0.89	0.0034	Down	Transcription factor
ENSG00000118526	TCF21	Transcription Factor 21	1.94	7.96E-05	-3.36	1.04E-07	-0.20	0.8653		
ENSG00000124613	ZNF391	Zinc Finger Protein 391	1.31	8.15E-12	-3.42	1.57E-37	0.58	0.1065		
ENSG00000179388	EGR3	Early Growth Response 3	1.22	5.56E-07	-3.59	5.10E-53	-1.97	8.47E-14		
ENSG00000213626	LBH	Limb Bud And Heart Development	3.43	1.08E-45	-3.62	9.19E-25	-0.62	0.2687		
ENSG00000172201	ID4	Inhibitor Of DNA Binding 4, HLH Protein	1.37	4.73E-06	-4.21	1.56E-21	-1.17	0.0921		
ENSG00000102409	BEX4	Brain Expressed X-Linked 4	4.20	1.32E-158	-4.77	3.11E-33	-0.58	0.4278		
ENSG00000148677	ANKRD1	Ankyrin Repeat Domain 1	2.13	5.14E-15	-6.20	3.29E-61	0.75	0.1493		
ENSG00000237975	FLG-AS1	FLG Antisense RNA 1	0.84	0.0225	3.03	1.31E-27	-1.19	3.94E-07	Up	Antisense RNA genes
ENSG00000237836	PHKA2-AS1	PHKA2 Antisense RNA 1	6.60	1.43E-76	-1.75	0.0040	0.00	1.0000		
ENSG00000246145	RRS1-AS1	RRS1 Antisense RNA 1	1.01	0.0236	-1.81	8.05E-05	-1.07	0.0619		
ENSG00000229124	VIM-AS1	VIM Antisense RNA 1	1.59	9.06E-21	-2.32	1.65E-27	-0.64	0.0312	Down	
ENSG00000203706	SERTAD4-AS1	SERTAD4 Antisense RNA 1	1.07	0.0472	-3.28	6.78E-08	0.51	0.5664		
ENSG00000224189	HAGLR	HOXD Antisense Growth-Associated Long Non-Coding RNA	2.05	4.84E-15	-4.73	2.93E-19	-0.19	0.8658		
ENSG00000249306	LINC01411	Long Intergenic Non-Protein Coding RNA 1411	0.72	0.2188	3.11	1.73E-16	-2.09	2.10E-11		
ENSG00000185847	LINC01405	Long Intergenic Non-Protein Coding RNA 1405	0.39	0.1249	2.97	1.83E-56	-3.99	7.64E-99		

ENSG00000250337	LINC01021	Long Intergenic Non-Protein Coding RNA 1021	0.81	0.0002	2.88	1.39E-53	-0.49	0.0128	Up	Non-protein coding genes
ENSG00000214145	LINC00887	Long Intergenic Non-Protein Coding RNA 887	-0.29	0.6979	2.60	1.41E-11	-3.14	5.25E-17		
ENSG00000258689	LINC01269	Long Intergenic Non-Protein Coding RNA 1269	-0.42	0.7325	2.27	0.0004	-3.50	2.07E-08		
ENSG00000251191	LINC00589	Long Intergenic Non-Protein Coding RNA 589	0.54	0.6319	2.23	0.0009	-2.71	1.50E-05		
ENSG00000221949	LINC01465	Long Intergenic Non-Protein Coding RNA 1465	1.25	0.0184	-1.89	0.0009	0.95	0.1162	Down	
ENSG00000215515	IFIT1P1	Interferon Induced Protein With Tetratricopeptide Repeats 1 Pseudogene 1	0.35	0.5178	3.32	1.58E-31	-1.79	8.64E-14	Up	Pseudogenes
ENSG00000215559	ANKRD20A11P	Ankyrin Repeat Domain 20 Family Member A11, Pseudogene	-0.07	0.9684	2.64	2.88E-05	-1.29	0.0274		
ENSG00000220563	PKMP3	Pyruvate Kinase, Muscle Pseudogene 3	-0.54	0.5812	2.03	0.0002	-0.24	0.7016		
ENSG00000214544	GTF2IRD2P1	GTF2I Repeat Domain Containing 2 Pseudogene 1	1.71	0.0010	-2.05	0.0008	-0.13	0.9070	Down	
ENSG00000251348	HSPD1P11	Heat Shock Protein Family D (Hsp60) Member 1 Pseudogene 11	1.05	0.0017	-2.32	2.20E-12	0.98	0.0059		
ENSG00000185031	SLC2A3P2	Solute Carrier Family 2 Member 3 Pseudogene 2	1.82	1.55E-08	-2.38	1.80E-08	-1.49	0.0128		
ENSG00000254088	SLC2A3P4	Solute Carrier Family 2 Member 3 Pseudogene 4	1.57	1.95E-08	-2.73	1.53E-13	-1.23	0.0229		
ENSG00000189089	RIMKLBP1	Ribosomal Modification Protein RimK-Like Family Member B Pseudogene 1	2.48	2.98E-06	-2.76	7.20E-05	0.00	1.0000		
ENSG00000210100	MT-TI	Mitochondrially Encoded TRNA Isoleucine	-0.20	0.4808	3.77	3.72E-120	0.78	1.70E-06	Up	Unknown function
ENSG00000227744	FLJ43879	FLJ43879 Protein	0.63	0.5917	3.37	9.06E-07	-3.06	1.82E-06		
ENSG00000203985	LDLRAD1	Low Density Lipoprotein Receptor Class A Domain Containing 1	-0.25	0.6444	2.92	3.22E-25	-2.81	9.64E-25		
ENSG00000210112	MT-TM	Mitochondrially Encoded TRNA Methionine	-0.38	0.6011	2.66	1.72E-10	-0.30	0.5868		
ENSG00000119703	ZC2HC1C	Zinc Finger C2HC-Type Containing 1C	0.26	0.4498	2.22	1.30E-32	0.07	0.7841		
ENSG00000233198	RNF224	Ring Finger Protein 224	0.76	0.1013	2.17	1.39E-09	3.69	2.90E-32		
ENSG00000182795	C1orf116	Chromosome 1 Open Reading Frame 116	0.08	0.7016	2.08	5.74E-91	-0.78	1.07E-13		
ENSG00000213171	LINGO4	Leucine Rich Repeat And Ig Domain Containing 4	0.97	0.3516	2.02	0.0134	-2.10	0.0052		
ENSG00000223601	EBLN1	Endogenous Bornavirus-Like Nucleoprotein 1	4.52	2.85E-22	-1.88	0.0098	-0.22	0.8464	Down	
ENSG00000178033	FAM26E	Family With Sequence Similarity 26 Member E	1.19	7.23E-10	-1.93	3.45E-20	-3.85	2.02E-22		

ENSG00000159784	FAM131B	Family With Sequence Similarity 131 Member B	1.15	1.58E-05	-1.99	2.69E-12	-0.01	1.0000		
ENSG00000280303	ERICD	E2F1-Regulated Inhibitor Of Cell Death	1.06	7.48E-05	-2.11	5.46E-12	2.15	2.23E-13		
ENSG00000164588	HCN1	Hyperpolarization Activated Cyclic Nucleotide Gated Potassium Channel 1	1.15	3.23E-05	-2.19	5.92E-12	-3.06	1.09E-08		
ENSG00000169067	ACTBL2	Actin, Beta-Like 2	1.95	2.85E-12	-2.32	2.55E-10	-1.53	0.0036		
ENSG00000114405	C3orf14	Chromosome 3 Open Reading Frame 14	3.67	1.96E-18	-2.35	0.0003	0.00	1.0000		
ENSG00000196376	SLC35F1	Solute Carrier Family 35 Member F1	3.05	1.99E-19	-2.41	1.51E-06	-0.61	0.4124		
ENSG00000151572	ANO4	Anoctamin 4	1.00	1.70E-05	-2.42	7.32E-22	-2.88	4.03E-12		
ENSG00000033122	LRRC7	Leucine Rich Repeat Containing 7	1.48	0.0449	-2.43	0.0014	0.00	1.0000		
ENSG00000145945	FAM50B	Family With Sequence Similarity 50 Member B	3.43	1.44E-30	-2.59	9.60E-13	-2.52	1.98E-06		
ENSG00000188883	KLRG2	Killer Cell Lectin Like Receptor G2	1.48	0.0002	-2.73	1.08E-09	-1.35	0.0244		
ENSG00000152580	IGSF10	Immunoglobulin Superfamily Member 10	4.61	1.04E-55	-2.76	2.20E-07	-0.67	0.4150		
ENSG00000177614	PGBD5	PiggyBac Transposable Element Derived 5	1.80	0.0002	-2.87	2.33E-06	-0.15	0.8985		
ENSG00000102445	KIAA0226L	KIAA0226-Like	2.11	9.08E-21	-3.51	1.64E-20	-1.66	0.0071		
ENSG00000197872	FAM49A	Family With Sequence Similarity 49 Member A	1.50	2.07E-13	-3.54	2.07E-33	-1.58	0.0009		
ENSG00000174899	PQLC2L	PQ Loop Repeat Containing 2-Like	2.83	1.29E-16	-3.56	1.10E-09	-0.20	0.8586		
ENSG00000162755	KLHDC9	Kelch Domain Containing 9	1.15	0.0002	-4.34	1.45E-19	-0.80	0.3075		
ENSG00000214107	MAGEB1	MAGE Family Member B1	3.10	1.54E-140	-7.04	1.34E-82	-0.09	0.9285		

Supplemental Table S5.3 Genes selected for CpG methylation analysis based on differential RNA expressions and biological relevance

A minimum of 2 primer pairs was designed for each gene. The table represents only those primer pairs for which results were obtained.

Ensembl ID	Gene	F_primer	R_primer	Chr	Start	End	Size (bp)
Up-regulated CpG island genes							
ENSG00000187957	DNER_1	5'-TTTATTTTTTAGGAGTGGGT-3'	5'-CAAAAAACCAAAAATAACTACTAC-3'	2	230579440	230579688	248
	DNER_2	5'-TTTTTTTTAAAGTGGGAAAGTTTGT-3'	5'-ACCTAACTACAACTACACCTACCCC-3'	2	230578738	230578915	177
ENSG00000184979	USP18	5'-GGGATTATAGGTGTGAGTTAT-3'	5'-TTTAAAATCCTTACAATTAACC-3'	22	18632162	18632391	229
Up-regulated Non-CpG island genes							
ENSG00000089127	OAS1	5'-GGGAGTTTTAAAATTGGGATAT-3'	5'-TTCTAAATAACCTACCCTTAATTTACAC-3'	12	113343388	113343683	295
ENSG00000126709	IFI6_1	5'-GTATTTTTATTTGTTTTTATTTTATTGTAAG-3'	5'-AAAATCCTAAATTCCATTCACC-3'	1	27995716	27996010	294
	IFI6_2	5'-GGAGTTTGTTGATAGATGGGTATA-3'	5'-CCAACAAACAACACACAAATATT-3'	1	27998644	27998934	290
ENSG00000008517	IL32_1	5'-GTTTAGAAGGGTTAGAAGGATTTG-3'	5'-CCCTATCCTTACATAAAATATACCC-3'	16	3114986	3115276	290
	IL32_2	5'-AGGGAGTAGGGGTTTAGTTAGG-3'	5'-CCACTAAAACAATCACCTTCTACA-3'	16	3115405	3115698	293
	IL32_3	5'-GTAGAAGGTGATTGTTTTAGTGGAG-3'	5'-ATCTATTTTCAAACATACCCACAA-3'	16	3115626	3115901	275
	IL32_4	5'-TTGTGGGTATGTTTGAAAATAGAT-3'	5'-CTCCTAAAACAAATACTCCCTCTC-3'	16	3115829	3116086	257
	IL32_5	5'-TGGATGAGAGGGAGTATTTGTT-3'	5'-CTCCCTAAAAAATATAATAAACCTAACATT-3'	16	3116011	3116312	301
ENSG00000198542	ITGBL1_1	5'-GTTGTGTTTGTTAGATTTTTTTGTTT-3'	5'-AAATATCCTATTCACAAATTTCAAATAC-3'	13	102104614	102104906	292
	ITGBL1_2	5'-TATTAAAGAGTAGGGTAGTTTATTTTTGTT-3'	5'-CCAATATCCCCTCCAAATAC-3'	13	102105932	102106157	225
ENSG00000117472	TSPAN1	5'-ATTTTAGGGGGTTAGGTTATTAAAG-3'	5'-TTTTCCATTTAAATTTCTAAATATATACTC-3'	1	46640138	46640433	295
ENSG00000173585	CCR9	5'-GTGTTGTTTAGGAAGAGAATTTG-3'	5'-TCTACCTAAAATAAAAAACAAACTTTA-3'	3	45927790	45928069	279
Down-regulated CpG island genes							
ENSG00000102409	BEX4_1	5'-GTGTAGAAAATGGTGGTTAGTTTG-3'	5'-TCCTTACAATCTCCTCCTCC-3'	X	102470139	102470441	302
	BEX4_2	5'-GGTTTTTGGGGTTGGTGT-3'	5'-CACCATTTTCTACACCAAAAAATAC-3'	X	102470383	102470682	299
ENSG00000118523	CTGF	5'-GTAGTAGTTGGAGAAAGAAATTTAGTT-3'	5'-CACAAAAACCTATTCTATCACTTC-3'	6	132271774	132271996	222
ENSG00000172201	ID4	5'-TTTTTAAGGTATTGGAATTTTA-3'	5'-AAACTAATATATACCCAAAAAAAA-3'	6	19837038	19837265	227
ENSG00000134533	RERG	5'-GTAGAAGTAAGTGTTAGTGGTT-3'	5'-CTACCCCCAATAAAAAAC-3'	12	15374257	15374462	205
ENSG00000118526	TCF21_1	5'-GTGTAGGTGGAAGGTTTAGAAAGAGT-3'	5'-CAACCACCTTCTCCCAACTATAA-3'	6	134209904	134210064	160
	TCF21_2	5'-TATTTGAGGTAGATTTTGGTTAA-3'	5'-TCCCTAAAAACTCTAAACCC-3'	6	134210922	134211134	212

ENSG00000135333	EPHA7	5'-AGTTTGAAAAATTATGGTGTATGAG-3'	5'-AAAACTTACAAACAACAAACA-3'	6	94129044	94129265	221
ENSG00000166033	HTRA1_1	5'-GAAAAATTAAAAGAGGGGAAAATTTT-3'	5'-CCCAAACCCACAATAAAATAATAAA-3'	10	124220297	124220503	206
	HTRA1_2	5'-GTGGAATGGAGTAATGTTTAATTTTTT-3'	5'-CCCTATACCCCTCTCCTAACACTAC-3'	10	124222451	124222680	229
ENSG00000145703	IQGAP2_1	5'-TTTTTGAAATTTTTTAATTTTTTTT-3'	5'-ACTCTAAACTCTACACATAAAACCAC-3'	5	75699991	75700211	220
	IQGAP2_2	5'-ATTTTTATTTTGTTTTTTTTAAGTTGTGTA-3'	5'-CAACCCCCACCTAATAATATTAAAC-3'	5	75903278	75903523	245
ENSG00000128645	HOXD1	5'-AGTAAATAAAATTATATTATTAAGGGAAAGA-3'	5'-CTTTCTAAAAAACTAACACAAACACC-3'	2	177052280	177052581	301
ENSG00000112319	EYA4_1	5'-GTTGAGAGAATTTTTAAATTTTT-3'	5'-TCTTCTAAAACAAAAAACACC-3'	6	133562939	133563131	192
	EYA4_2	5'-GGGGATGTTTTGTTTTTATTAGAG-3'	5'-TAAAAATTCTCTCAACTCAAACTCC-3'	6	133562743	133562955	212
ENSG00000131435	PDLIM4_1	5'-TGGTTTTTATAAATTAGTTTGAGGATTTT-3'	5'-CCAACTCAAATACCTCCTCATAAAC-3'	5	131592801	131593001	200
	PDLIM4_2	5'-GTTTGTGTTTGTTTGTGTGTGTTAT-3'	5'-TCAACTCCAAACAAAACTATTACTACTACT-3'	5	131594867	131595116	249
ENSG00000179059	ZFP42_1	5'-ATTTAGGTTGGAGTTTAGTGG-3'	5'-ACAAAAATTAACCAAACATAATAATACT-3'	4	188916238	188916373	135
	ZFP42_2	5'-GTTTAAAAGGGTAAATGTGATTAT-3'	5'-CTAATCAAACTACAACCACCCATC-3'	4	188916497	188916862	365
ENSG00000087303	NID2	5'-GATTATGAAATATTATTGTGTGTGATT-3'	5'-ATAAATAAAATTCCCCTTCTCCTAC-3'	14	52536501	52536746	245
Down-regulated Non-CpG island genes							
ENSG00000113140	SPARC_1	5'-TTTGAAAAGTAATAGGTAGATAGGAT-3'	5'-TACCACTAAAATATATATAACCCCC-3'	5	151066241	151066435	194
	SPARC_2	5'-TTTTGGTTAATTGTAATTTTTATTTTT-3'	5'-ATCCCTATAATCCTTTAAAAAACC-3'	5	151053637	151053847	210
ENSG00000139278	GLIPR1	5'-GTTATTGAAAATTATTGAAAAGATAGGG-3'	5'-AAACCATCCAAACTATTATAACAAATA-3'	12	75874428	75874697	269
ENSG00000091986	CCDC80_1	5'-TTGTTATAAGGATTTAATGGAGAAG-3'	5'-CAAAACAAAATAAAACTAATCAAAAC-3'	3	112360673	112360950	277
	CCDC80_2	5'-TTTTTAGAGTGGATTTTTTAATTT-3'	5'-TTTCACTATACTATTAACCATATAACTAATA-3'	3	112358446	112358680	234

Supplemental Table S5.4 Methylation levels and RNA expressions of selected genes

Methylation – data indicate % methylation, Expression – data show normalized (log2) mRNA expressions.

Ensembl ID	Gene	Methylation												Expression											
		HCT116			HCT116-1 µM DAC			HCT116-Res$_{DAC}$			Res$_{DAC}$-1 µM JQ1			HCT116			HCT116-1 µM DAC			HCT116-Res$_{DAC}$			Res$_{DAC}$-1 µM JQ1		
		1	2	3	1	2	3	1	2	3	1	2	3	1	2	3	1	2	3	1	2	3	1	2	3
ENSG00000089127	OAS1	67	42	NA	61	87	88	79	71	78	88	95	99	6.2	5.4	5.1	6.0	6.2	6.5	12.5	12.4	12.2	10.2	10.1	10.1
ENSG00000126709	IFI6	14	11	14	15	14	12	14	14	20	11	13	18	10.7	10.6	10.5	11.4	11.1	11.3	15.5	15.6	14.8	15.7	15.6	15.6
ENSG00000008517	IL32	76	82	88	57	61	64	53	61	54	73	61	61	7.5	7.2	7.4	7.9	7.4	8.0	11.6	11.8	11.3	8.6	8.7	8.7
ENSG00000198542	ITGBL1	84	85	85	58	57	57	70	69	70	74	69	70	6.2	6.3	6.2	6.6	6.8	6.7	9.9	9.8	9.9	5.0	5.0	5.6
ENSG00000117472	TSPAN1	95	95	97	74	78	77	94	93	92	94	93	94	10.1	9.9	10.2	10.1	10.0	10.2	13.5	13.7	13.5	10.6	10.6	10.7
ENSG00000187957	DNER	42	34	37	31	30	35	44	43	65	21	21	69	8.9	8.8	8.9	8.6	8.6	8.5	12.0	12.5	12.4	12.6	12.6	12.6
ENSG00000173585	CCR9	87	91	94	55	54	57	93	85	92	94	96	94	0.0	0.0	0.9	2.0	1.7	1.2	4.1	4.0	4.1	0.0	1.8	0.6
ENSG00000184979	USP18	73	78	75	53	62	68	54	57	66	73	57	53	8.4	8.2	8.2	7.7	7.4	7.7	10.7	10.5	9.9	8.7	9.1	8.9
ENSG00000102409	BEX4	98	84	92	81	60	74	94	95	97	98	96	89	6.5	6.3	6.6	10.7	10.7	10.8	0.9	1.5	1.8	1.0	1.1	0.0
ENSG00000118523	CTGF	NaN	15	21	22	14	15	40	21	26	11	11	42	12.9	13.4	13.2	15.1	14.9	15.0	8.4	8.9	8.7	10.4	10.3	10.2
ENSG00000172201	ID4	94	94	NA	NA	48	45	NA	NA	82	84	86	85	6.2	6.2	5.8	7.5	7.7	7.1	1.5	0.0	2.4	0.0	0.0	0.0
ENSG00000134533	RERG	44	37	39	41	36	30	53	52	52	47	67	56	5.5	4.9	5.0	6.6	7.1	6.6	1.9	0.0	0.0	0.0	0.0	0.0
ENSG00000118526	TCF21	92	96	97	57	56	56	91	87	92	93	92	94	3.8	4.6	3.3	6.2	5.5	6.2	0.0	0.0	0.7	0.0	0.0	0.0
ENSG00000135333	EPHA7	90	90	91	52	47	55	88	85	88	86	NA	89	3.4	3.1	4.0	6.5	6.6	6.3	0.0	0.0	0.0	0.0	0.0	0.0
ENSG00000166033	HTRA1	92	96	92	52	50	58	86	89	90	86	82	92	3.6	3.4	4.4	7.1	7.0	7.3	0.9	0.0	0.7	1.9	1.1	0.6
ENSG00000145703	IQGAP2	96	97	98	58	63	60	96	94	95	93	93	95	8.5	8.6	8.7	9.9	10.3	10.1	6.0	5.2	6.6	4.2	4.1	4.0
ENSG00000128645	HOXD1	96	95	93	61	70	74	86	87	79	88	85	87	2.1	2.9	2.5	5.8	6.0	5.9	0.0	0.0	0.0	0.0	0.0	0.0
ENSG00000112319	EYA4	93	94	93	53	53	56	94	95	94	95	94	94	5.2	5.6	5.6	8.7	9.0	8.8	2.4	3.2	3.7	0.0	1.8	0.0
ENSG00000131435	PDLIM4	96	96	96	52	49	37	89	94	92	95	95	95	3.6	5.2	4.8	10.4	9.5	10.1	2.4	3.2	1.5	0.0	0.0	1.0
ENSG00000113140	SPARC	93	95	81	51	47	75	85	86	93	87	86	88	7.7	7.9	8.4	13.4	13.4	13.4	5.4	5.9	6.2	3.6	3.2	2.3
ENSG00000179059	ZFP42	97	95	95	63	57	64	92	91	94	94	93	95	4.6	3.9	4.2	12.2	12.4	12.4	0.9	2.5	2.6	1.0	1.1	0.6
ENSG00000087303	NID2	93	91	93	46	44	49	69	66	67	70	69	68	4.1	2.1	2.5	7.2	7.1	7.0	0.9	0.0	1.5	0.0	0.0	0.0
ENSG00000139278	GLIPR1	81	77	68	46	50	49	86	85	86	86	NA	NA	6.8	7.2	7.8	8.5	8.6	8.5	6.1	5.2	4.7	2.5	2.2	2.8
ENSG00000091986	CCDC80	96	97	97	61	75	77	74	77	82	90	84	87	6.5	7.0	7.0	8.2	8.3	8.0	5.0	5.2	5.0	7.1	7.2	6.9

Summary

Aberrant DNA methylation that results in transcriptional silencing of tumor suppressor genes is a major hallmark in all cancer types. This has greatly emphasized the development of anti-cancer therapies that work by inhibiting DNA methylation, and restore normal epigenetic landscape by reprogramming of genes involved in disease mechanisms. This dissertation is focussed on the four main objectives related with the study of DNA hypomethylating agents, as summarized below:

Aim 1: Establish DNA demethylation detection system for high throughput screening of potential hypomethylating epi-drugs

Despite major advances in the field of epigenetics, the success of DNA demethylation based anti-cancer therapy is limited due to narrow therapeutic window. A wide variety of naturally occurring epigenetic agents and synthetic molecules that can alter methylation patterns exist, however, their usefulness in epigenetic therapy remains unknown. This underlines the need for effective tumor models for large-scale screening of drug candidates with potent hypomethylation activity. Chapter 2 describes the development of a cell-based DNA demethylation detection system, which is suitable for high content screening of epigenetic drugs in two-dimensional and three-dimensional cell culture models. Additionally, the detection system also supports the *in vivo* monitoring of demethylation efficacy of potential lead compounds from *in vitro* screens in tumor xenografts. The described detection system not only permits the continuous monitoring of demethylation but also of the induced cytostatic/cytotoxic drug effects in live cells, as a function of time. The detection system is fluorescence based and exploits the dominant ability of DNA methylation to inhibit gene transcription, and utilizes *FLJ32130* gene, which is silenced on account of promoter hypermethylation in human colorectal cancer (CRC). The described work will provide the researchers with an efficient tool for epigenetic drug screens on a high throughput platform and would therefore benefit academic and industrial drug discovery.

Aim 2: Characterize biodegradable polyanhydride microbeads formulations of azanucleoside drugs for therapeutic efficacy

The cytosine analogues, 5-azacytidine (AZA) and 2'-deoxy-5-azacytidine (DAC) are established therapies for human malignancies. However, the administration of these prototypal hypomethylating agents is confounded by their hydrolytic lability which renders the chemical instability of these drugs, thereby compromising their plasma circulation time. Often, long-term cooled infusions are necessary. This underlines the importance for the AZA and DAC

formulations that may overcome this hydrolytic lability. Chapter 3 describes a new biodegradable, polyanhydride formulation for drug delivery that circumvents this drawback. Injectable/implantable polymeric microbeads containing dispersed microcrystals of hydrophilic AZA or DAC packed in a dry environment are protected from hydrolysis, until the hydrolytic zone reaches the core. Diclofenac is embedded into the formulation to decrease any local inflammation. The efficacy of the formulations was confirmed by monitoring the induced demethylation, and cytostatic/cytotoxic effects of continuous drug release from the time-course dissolution of the microbeads, using DNA demethylation detection system described in Chapter 2. Poly(sebaccic acid-co-1,4-cyclohexanedicarboxylic acid) containing 30 wt. % drug showed zero-order release (R^2= 0.984 for linear regression), and release rate of 10.0 %/h within the first 5 h, and subsequent slower release of the remaining drug, thus maintaining the level of drugs in the outer environment considerably longer than the typical plasma half-life of free azanucleosides. At lower concentrations, the differences between powder drug formulations and microbeads were very low or negligible, however, at higher concentrations, the equivalent or increasing effects of the drugs loaded microbeads were discovered. The study provides evidence that microbead formulations of the hydrolytically labile azanucleoside drugs could prevent their chemical decomposition in aqueous solution, and effectively increase plasma circulation time.

Aim 3: Study stromal cell-induced alterations in the response of cancer cell to DNA hypomethylating agents

The stromal cells in the tumor-microenvironment play a key role in the outcome of anti-cancer therapy. Moreover, soluble and insoluble factors released by stromal cells have also been suggested to contribute to tumorigenesis and drug resistance. Recently, hypomethylating agents, AZA and DAC have shown promising activity in the treatment of solid tumors in early clinical trials. While, the effects of these hypomethylating agents on solid tumors are well-reported, it is not known how stromal cells of the tumor-microenvironment affect the response of cancer cells to hypomethylating agents. Chapter 4 describes the influence of stromal cells on the response of CRC cells to hypomethylating agents in 2-dimensional and multicellular spheroids cultures. Using the demethylation detection system described in Chapter 2, it is shown that both irradiated and non-irradiated stromal cells increase the susceptibility of CRC cells to hypomethylating agents, and the increase in CRC demethylation was relative to increasing stromal environment. The increased activity of hypomethylating agents in high stromal cell co-cultures further suggests the potential of tumor-stroma ratio for predicting the outcome of epigenetic therapy in CRC or other cancer types. Further, in this study, stromal cell-induced increase in the proliferation of CRC cells was observed in both culture systems. Since DAC is reported to have greater effects in

actively proliferating cells, the increased proliferation of CRC in co-cultures potentially increases the activity of DAC. This is also evident from the significant effect of DAC on DNA methyltransferase 1 (DNMT1) level in CRC cells from co-cultures than monocultures.

Furthermore, an increased proliferation of CRC was observed when the cells were cultured in conditioned medium (CM) from irradiated stromal cells. Evidently, despite increasing the proliferation of CRC cells, irradiated stromal cell CM resulted in a concentration-dependent decrease of demethylation in 2 dimensional cultures. These findings were unexpected presuming that increased proliferation makes CRC cells susceptible to hypomethylating agents. This suggested the role of other factors in altering the effect of DAC. Analysis of irradiated and non-irradiated stromal cell CM showed a marked increase in *NFkB* activity and up-regulation of pro-inflammatory cytokines and chemokines levels in irradiated stromal cell CM. Although no direct effect of irradiated stromal cell CM was observed on DNMT1, the inability of DAC to significantly reduce DNMT1 levels in treated cells suggests the negative effect of pro-inflammatory cytokines on DNA demethylation.

Aim 4: Investigate molecular mechanisms of drug resistance to azanucleoside drugs, and tailor alternative therapeutic regimen for overcoming resistance

The clinical success of the prototypal hypomethylating agent DAC is highly variable due to acquisition of primary and secondary resistance in patients. While the published literature describes the pharmacological mechanisms involved in primary resistance to DAC, the secondary resistance to this drug which is not entirely dependent on initial drug disposition remains elusive. Moreover, failure of treatment to DAC is apparent only after 4-6 cycle of therapy. Therefore, the investigation of the molecular mechanisms of secondary resistance to this drug, and identification of response predicting biomarkers is an unmet need. Chapter 5 presents the study of the secondary mechanism of resistance to DAC using CRC cells. The study revealed the response predicting biomarkers which may differeniate between DAC sensitivity and resistance, and proposes alternative therapeutics to overcome DAC resistance.

At first, DAC-resistant CRC cells were developed through long-term culturing of cells under selection pressure of DAC. The DAC-resistant cell lines were then screened against a panel of epigenetic- and chemotherapeutic agents to check the cross-resistance or sensitivity towards these agents. The results of the study demonstrated the cross-resistance or no significant change in the half-maximal inhibitory concentration of all tested epigenetic and chemotherapeutic agents except bromodomain and extra terminal (BET) inhibitors which significantly sensitized the DAC resistant cells in culture. The sensitizing effect of BET inhibitor was further validated by cell cycle analysis which demonstrated augmented response of BET inhibitor on cell cycle phases of

DAC-resistant cells. The sensitivity of *in vitro* developed DAC-resistant cells towards BET inhibitor was then examined in xenograft models in which BET inhibitor significantly reduced tumor load, while DAC showed resitance under *in vivo* conditions, as compared to parental cells. The novel combination of DAC and BET inhibitor, combined concurrently or sequentially was then analyzed for synergistic, additive or antagonistic effects. The results demonstrated additive/synergistic cytotoxic effects of BET inhibitor combined concurrently or sequentially with DAC in parental CRC cells, and synergistic effects of concurrent application in DAC-resistant CRC cells. These results suggests the potential application of DAC and BET inhibitor as combinatorial regimen for anti-cancer therapy or the concurrent application of BET inhibitor and DAC to sensitize DAC-resistant cancer cells.

Further, to identify the differentially expressed genes in parental and DAC-resistant CRC cells, and genes altered on treatment of DAC-resistant CRC cells with BET inhibitor, RNA expression of parental and DAC-resistant CRC cells, treated or untreated with DAC or BET inhibitor was accessed. Based on differential expressions between parental and DAC-resistant CRC cells, and biological relevance, genes were selected for CpG island methylation analysis. The pairing of RNA expressions and methylation levels of validated genes revealed epigenetically regulated tumor suppressor genes silenced by hypermethylation in DAC-resistant CRC cells, and DNA-methylation independent oncogenic candidates overexpressed in DAC-resistant cells. Intrestingly, the expressions of overexpressed genes were reversed on treatment with BET inhibitor. The correlation between down-regulation of oncogenes and sensitizing effect of BET inhibitor on DAC-resistant CRC cells suggest the involvement of these genes in secondary resistance to DAC. However, expression of hypermethylation-silenced tumor suppressor genes in DAC-resistant CRC cells remained unchanged. This means that BET inhibitor-induced effects are independent of DNA methylation status. Nevertheless, the hypermethylation-silenced genes might be used as response predicting biomarkers to differentiate between DAC resistance and sensitivity. However, the validation of these genes in clinical samples is a pre-requisite for their development as surrogate biomarkers which may differentiate between responders and non-responders.

Besides, preliminary results of this study propose the inhibition of *IL-32* mediated activation of *NFkB* in DAC-resistant CRC cells as the partial mechanism for sensitivity of DAC-resistant CRC cells by BET inhibitor.

Souhrn

Aberantně zvýšená methylace DNA, která má za následek utlumení transkripce tumor-supresorových genů je významným znakem všech typů rakovinných buněk. Toto zjištění velmi urychlilo vývoj protirakovinných léčiv, jež inhibují DNA methylaci a obnovují tak normální epigenetický stav buňky. Dochází pak k normální expresi genů, jejichž utlumení souvisí se vznikem onemocnění. Tato disertační práce je zaměřena na studium snížené DNA methylace, konkrétně byly definovány tyto čtyři cíle studia:

Cíl 1: Vývoj systému pro detekci snížené DNA methylace umožňující testování velkého množství potenciálních látek snižujících methylaci DNA, tzv. high-throughtput screening

Navzdory výrazným pokrokům, kterých bylo dosaženo v oblasti studia epigenetiky je využití látek modifikujících DNA methylaci značně limitováno jejich úzkým terapeutickým oknem. Existuje však velké množství přírodních i syntetických molekul modifikujících methylaci DNA a jejich možné terapeutické využití není zatím prostudováno. Je tedy velmi žádoucí mít k dispozici nástroje pro efektivní testování velkého množství látek s potenciálním účinkem na methylaci DNA v modelových buněčných liniích reprezentujících různé typy rakovinných buněk. V kapitole 2 je popsán vývoj systému pro detekci snížené methylace DNA v jednotlivých buňkách, který je vhodný pro vysoce propustné testování látek s potenciálním účinkem na epigenetické procesy v 2D a 3D buněčných modelech *in vitro*. Tento systém je adaptabilní také pro *in vivo* monitoring snížené methylace DNA, neboť buňky mohou být transplantovány a sledovány jako xenografty. Popsaný detekční systém umožňuje kromě kontinuálního sledování demethylace také monitoring dalších průvodních jevů, např. cytostatický nebo cytotoxický efekt použitých látek v závislosti na čase. Detekční systém je založen na kvantifikaci fluorescenčního signálu a využívá schopnosti DNA methylace inhibovat transkripci genů. Systém využívá gen FLJ32130, který je umlčen hypermethylací svého promoteru v buňkách nádoru tlustého střeva (colorectal cancer, CRC). Tento detekční systém poskytuje efektivní nástroj pro vysoce propustné testování látek a přináší tak značné výhody pro primární i aplikovaný výzkum nových léčiv.

Cíl 2: Charakterizace terapeutické účinnosti biodegradabilních polyanhydridových modifikací azanukleosidových léčiv

Analoga cytosinu 5-azacytidine (AZA) a 2'-deoxy-5-azacytidine (DAC) jsou běžně používanými terapeutiky pro léčbu lidských maligních onemocnění. Nicméně podávání těchto léčiv snižujících methylaci DNA je komplikováno jejich nestabilitou ve vodném prostředí, čímž se snižuje jejich setrvání v krevní plazmě a tím jejich účinnost. Často je nutné léčiva podávat ve formě dlouhotrvajících chlazených infuzí. Tato komplikace zvýrazňuje potřebu stabilnějších AZA

a DAC derivátů. Kapitola 3 popisuje nové biodegradabilní polyanhydridové deriváty, které tento problém eliminují. Polymerní mikrokuličky vhodné k podávání formou injekcí nebo implantátů obsahují mikrokrystaly hydrofilního AZA nebo DAC. Modifikace AZA a DAC probíhá v suchém prostředí, čímž jsou látky chráněny před hydrolýzou až do té doby než je mikrokulička, pozvolna rozpuštěna a látka je tak kontinuálně uvolňována do prostředí. Substance dále obsahuje léčivo Diclofenac pro snížení vzniku lokálního zánětu. Efektivita takto modifikovaných látek byla potvrzena měřením indukované demethylace DNA a evaluací cytostatického a cytotoxického účinku. Pro monitoring byl využit detekční systém, jehož vývoj je popsán v kapitole 2. Derivát "Poly(sebaccic acid-co-1,4-cyclohexanedicarboxylic acid)" obsahující 30 hm. % léčiva vykázal tzv. „zero-order release" (R^2= 0.984, lineární regrese) a uvolňoval se rychlostí 10.0 %/h během prvních 5 h. Zbylé léčivo bylo uvolňováno pomaleji. Bylo tak dosaženo signifikantně delšího setrvání látky ve vnějším prostředí než je typický poločas setrvání volných azanukleosidů v krevní plazmě. Při nižších koncentracích byl rozdíl mezi klasickým podáním nukleosidů a podáním léčiva v mikrokuličkách nepatrný až žádný, naopak při vyšších koncentracích bylo pozorováno stejné nebo výraznější setrvání látek ve vnějším prostředí. Studie tak podává důkaz o schopnosti polymerních mikrokuliček zvýšit stabilitu azanukleosidů ve vodném prostředí a tím také umožnit delší setrvání těchto látek v krevní plazmě.

Cíl 3: Studium vlivu buněk nádorového stromatu na odpověď nádorových buněk při podání látek snižujících methylaci DNA

Buňky nádorového stromatu jsou součástí mikroprostředí nádoru a hrají klíčovou roli v nádorové terapii. Buňky nádorového stromatu vylučují rozpustné i nerozpustné faktory a je možné, že tyto molekuly přispívají k tumorogenezi a lékové rezistenci. Nedávné studie prokázaly, že látky snižující methylaci DNA, AZA a DAC vykazují slibnou aktivitu při léčbě solidních nádorů v raných fázích klinických zkoušek. Zatímco efekt AZA a DAC na solidní nádory byl velmi dobře popsán, není známo, zda buňky nádorového stromatu ovlivňují odpověď rakovinných buněk na tyto látky. V kapitole 4 je adresován vliv buněk stromatu na odpověď CRC buněk na látky způsobující demethylaci DNA v 2D a 3D buněčných směsných kulturách. K měření byl využit detekční reportérový systém popsaný v kapitole 2 a bylo prokázáno, že ozářené i neozářené buňky nádorového stromatu zvyšují citlivost CRC buněk k látkám zvyšujícím hypomethylaci DNA. Vyšší podíl buněk nádorového stromatu způsoboval výraznější demethylaci DNA v CRC buňkách. Studie ukázala také zvýšenou aktivitu látek a tedy zvýšení demethylace DNA v nádorových buňkách kultivovaných společně s velkým množstvím buněk nádorového stromatu ve směsné kultuře. Studie tak poukazuje na možnost predikce efektivity léčby látkami ovlivňujícími epigenetické procesy na základě zhodnocení poměrného zastoupení

buněk stromatu a nádorových buněk, jak u CRC, tak i u dalších typů nádorů. Byl také pozorován vliv stromatu na zvýšenou proliferaci CRC buněk v 2D i 3D kulturách. Zvýšený efekt DAC byl již dříve pozorován u aktivně proliferujících buněk a zvýšená proliferace CRC buněk ve směsné kultuře tak potenciálně zvyšuje aktivitu DAC. Tento efekt byl také pozorován při detekci množství DNA methyltransferázy 1 (DNMT1) v CRC buňkách, které je vyšší u směsných kultur než u monokultur. Zvýšená proliferace CRC buněk byla také pozorována, pokud byly buňky vystaveny kondiciovanému mediu (conditioned medium, CM) z ozářených buněk nádorového stromatu.

Překvapivě navzdory zvýšené proliferaci CRC buněk vystavených CM z ozářených buněk stromatu, byla ve 2D kulturách pozorována snížená míra demethylace. Toto zjištění poukazuje na fakt, že zvýšená proliferace CRC buněk je dělá citlivějšími k látkám snižujícím demethylaci a poukazuje tak na možnost, že další faktory mohou ovlivňovat efekt DAC. Analýza CM z ozářených a neozářených buněk stromatu vykazuje zvýšení aktivity jaderného proteinu *Kappa-B (NFkB)*, což indikuje vyšší sekreci pro-zánětlivých cytokinů a chemokinů z ozářených buněk do CM. Přestože nebyl pozorován přímý efekt CM z ozářených buněk stromatu na množství DNMT1 proteinu v CRC buňkách, DAC zároveň nebyl schopen signifikantně snížit množství DNMT1 proteinu. Toto pozorování ukazuje na možný negativní efekt zánětlivých cytokinů na demethylaci DNA.

Cíl 4: Studium molekulárních mechanismů lékové rezistence k azanukleosidovým léčivům a návrh alternativních terapeutických postupů pro překonání rezistence

Úspěšná léčba pomocí typické látky snižující DNA methylaci DAC je silně závislá na vzniku primární a sekundární rezistence u pacientů. Mechanismus vzniku primární rezistence k DAC již byl detailně popsán. Zatímco vznik sekundární rezistence zatím zůstává neobjasněn. K rezistenci a tedy nutnému přerušení léčby navíc často dochází už po 4-6 cyklech terapie. Výzkum molekulárních mechanismů zodpovědných za sekundární rezistenci tohoto léčiva a identifikace biomarkerů, které by umožnily monitoring probíhající léčby je tedy velmi žádoucí. V kapitole 5 je prezentována studie mechanismů zodpovědných za vznik sekundární lékové rezistence k DAC v CRC buňkách. Studie identifikuje biomarkery umožňující rozlišit mezi sensitivitou k DAC a rezistencí a navrhuje alternativní terapeutické přístupy vedoucí k překonání DAC resistence. Nejprve byly generovány DAC-rezistentní CRC buňky dlouhodobou kultivací v DAC. Tato buněčná linie pak byla vystavena panelu látek s vlivem na epigenetické procesy nebo dalších chemoterapeutikům. Byla testována rezistence a sensitivita mezi těmito látkami. Výsledky studie ukazují, že testované látky v koncentracích IC50 (50%-ní inhibiční efekt) nevykazují žádný efekt nebo vykazují rezistenci. Výjimku tvořila skupina inhibitorů s účinky na bromodomény a tzv.

extra-terminální (BET) inhibitory, které signifikantně zvýšily sensitivitu DAC-rezistentních buněk. Sensitizující efekt BET inhibitorů byl dále validován. Byla provedena analýza buněčného cyklu, která ukázala vliv BET inhibitorů na průběh buněčného cyklu u DAC-rezistentních buněk. Citlivost DAC-rezistentních buněk (vyvinutých *in vitro*) k BET inhibitorům byla dále testována pomocí xenograftových modelů. BET inhibitory signifikantně snížily velikosti tumorů a DAC rezistence byla *in vivo* srovnatelná jako u parentální buněčné linie.

Poprvé byla také testována kombinovaná léčba DAC společně s BET inhibitory. Látky byly podány sekvenčně i současně a testován byl synergní, aditivní a antagonistický efekt. Výsledky ukazují, že pokud je DAC podán sekvenčně nebo současně s BET inhibitory dochází k aditivnímu příp. synergnímu efektu u CRC parentální buněčné linie. U DAC-rezistentní buněčné linie byl pozorován synergní efekt při současném podání obou látek. Tyto výsledky poukazují na možnost podávání DAC a BET inhibitorů v kombinačním režimu u protirakovinných terapií nebo na možnost podávat látky současně a sensitizovat tak DAC-rezistenení nádorové buňky k DAC. Dále byly identifikovány geny s rozdílnou expresí u parentální a DAC-rezistentní CRC linie, a také geny, jejichž exprese byla ovlivněna v DAC-rezistentních buňkách pomocí BET inhibitorů. Za tímto účelem byla hodnocena exprese RNA v parentálních a DAC-rezistentních buňkách ovlivněných DAC a/nebo BET inhibitory. Geny vybrané na základě rozdílné exprese (mezi parentální a DAC-rezistentní CRC linií) a biologické relevance byly dále podrobeny analýze stavu methylace v rámci CpG sekvencí. Spojením výsledků RNA exprese a úrovně methylace validovaných genů byl vytvořen seznam tumorových supresorů umlčených methylací a také seznam potenciálních onkogenů nezávislých na methylaci, které jsou overexprimované v DAC-rezistentních CRC buňkách. Zvýšená exprese některých genů byla potlačena BET inhibitory. Korelace mezi utlumením exprese onkogenů a sensitizujícím efektem BET inhibitorů v DAC-rezistentních CRC buňkách ukazuje na jejich možnou roli v mechanismu rozvoje získané sekundární rezistence k DAC. Avšak exprese hypermethylovaných a tedy umlčených tumor supresorových genů v DAC-rezistentních CRC buňkách zůstala nezměněna. To by mohlo znamenat, že mechanismus účinku BET inhibitorů je nezávislý na úrovni DNA methylace. Nicméně geny umlčené hypermethylací by mohly být použity jako biomarkery k predikci DAC sensitivity nebo rezistence. Jako prerekvizita musí být nejdříve provedena validace těchto genů v pacientských vzorcích. Dále budou moci být vybrány geny – biomarkery na základě kterých bude možné rozlišit pacienty dobře respondující a nerespondujících na zvolenou léčbu. Předběžné výsledky této studie ukazují na možnost inhibice *Interleukin-32* zprostředkované aktivace *NFkB* v DAC-rezistentních CRC buňkách jako možného mechanismu k sensitizaci DAC-rezistentních buněk k BET inhibitorům.

References

Agrawal, A., Murphy, R.F., Agrawal, D.K. **(2007)**. DNA methylation in breast and colorectal cancers. *Mod Pathol.* **20**(7), 711-21.

Agrawal, K., Das, V., Otmar, M., Krečmerová, M., Džubák, P., Hajdúch, M. **(2017)**. Cell-based DNA demethylation detection system for screening of epigenetic drugs in 2D, 3D, and xenograft models. *Cytometry A.* **91**(2), 133-43.

Ahluwalia, G.S., Cohen, M.B., Kang, G.J., Arnold, S.T., McMahon, J.B., Dalai, M., Wilson, Y.A., Cooney, D.A., Balzarini, J., Johns, D.G. **(1986)**. Arabinosyl-5-a/acytosine: Mechanisms of Native and Acquired Resistance. *Cancer Res.* **46**, 4479-85.

Aimiuwu, J., Wang, H., Chen, P., Xie, Z., Wang, J., Liu, S., Klisovic, R., Mims, A., Blum, W., Marcucci, G., Chan, K.K. **(2012)**. RNA-dependent inhibition of ribonucleotide reductase is a major pathway for 5-azacytidine activity in acute myeloid leukemia. *Blood.* **119**(22), 5229-38.

Albany, C., Hever-Jardine, M.P., von Herrmann, K.M., Yim, C.Y., Tam, J., Warzecha, J.M., Shin, L., Bock, S.E., Curran, B.S., Chaudhry, A.S., Kim, F., Sandusky, G.E., Taverna, P., Freemantle, S.J., Christensen, B.C., Einhorn, L.H., Spinella, M.J. **(2017)**. Refractory testicular germ cell tumors are highly sensitive to the second generation DNA methylation inhibitor guadecitabine. *Oncotarget.* **8**(2), 2949-59.

Amato, R., Ho, D., Schmidt, S., Krakoff, I.H., Raber, M. **(1992)**. Phase I trial of a 72-h continuous-infusion schedule of fazarabine. *Cancer Chemother Pharmacol.* **30**(4), 321-4.

Andrade, A.F., Borges, K.S., Castro-Gamero, A.M., Silveira, V.S., Suazo, V.K., Oliveira, J.C., Moreno, D.A., de Paula Queiroz, R.G., Scrideli, C.A., Tone, L.G. **(2014)**. Zebularine induces chemosensitization to methotrexate and efficiently decreases AhR gene methylation in childhood acute lymphoblastic leukemia cells. *Anticancer Drugs.* **25**(1), 72-81.

Andrade, A.F., Borges, K.S., Suazo, V.K., Geron, L., Corrêa, C.A., Castro-Gamero, A.M., de Vasconcelos, E.J., de Oliveira, R.S., Neder, L., Yunes, J.A., Dos Santos Aguiar, S., Scrideli, C.A., Tone, L.G. **(2017)**. The DNA methyltransferase inhibitor zebularine exerts antitumor effects and reveals BATF2 as a poor prognostic marker for childhood medulloblastoma. *Invest New Drugs.* **35**(1), 26-36.

Antonsson, B.E., Avramis, V.I., Nyce, J., Holcenberg, J.S. **(1987)**. Effect of 5-azacytidine and congeners on DNA methylation and expression of deoxycytidine kinase in the human lymphoid cell lines CCRF/CEM/0 and CCRF/CEM/dCk-1. *Cancer Res.* **47**(14), 3672-8.

Antwih, D.A., Gabbara, K.M., Lancaster, W.D., Ruden, D.M., Zielske, S.P. **(2013)**. Radiation-induced epigenetic DNA methylation modification of radiation-response pathways. *Epigenetics.* **8**(8), 839-48.

Arab, K., Smith, L.T., Gast, A., Weichenhan, D., Huang, J.P., Claus, R., Hielscher, T., Espinosa, A.V., Ringel, M.D., Morrison, C.D., Schadendorf, D., Kumar, R., Plass, C. **(2011)**. Epigenetic deregulation of TCF21 inhibits metastasis suppressor KISS1 in metastatic melanoma. *Carcinogenesis.* **32**(10), 1467-73.

Arimany-Nardi, C., Errasti-Murugarren, E., Minuesa, G., Martinez-Picado, J., Gorboulev, V., Koepsell, H., Pastor-Anglada, M. **(2014)**. Nucleoside transporters and human organic cation transporter 1 determine the cellular handling of DNA-methyltransferase inhibitors. *Br J Pharmacol.* **171**(16), 3868-80.

Avramis, V.I., Powell, W.C., Mecum, R.A. **(1989)**. Cellular metabolism of 5,6-dihydro-5-azacytidine and its incorporation into DNA and RNA of human lymphoid cells CEM/0 and CEM/dCk(-). *Cancer Chemother Pharmacol.* **24**(3), 155-60.

Azad, N., Zahnow, C.A., Rudin, C.M., Baylin, S.B. **(2013)**. The future of epigenetic therapy in solid tumours-lessons from the past. *Nat Rev Clin Oncol.* **10**(5), 256-66.

Bae, J.H., Kim, J.G., Heo, K., Yang, K., Kim, T.O., Yi, J.M. **(2015)**. Identification of radiation-induced aberrant hypomethylation in colon cancer. *BMC Genomics*. **16**, 56.

Bailey, H., Tutsch, K.D., Arzoomanian, R.Z., Tombes, M.B., Alberti, D., Bruggink, J., Wilding, G. **(1991)**. Phase I Clinical Trial of Fazarabine as a Twenty-four-Hour Continuous Infusion. *Cancer Res.* **51**(4), 1105-8.

Balch, C., Yan, P., Craft, T., Young, S., Skalnik, D.G., Huang, T.H., Nephew, K.P. **(2005)**. Antimitogenic and chemosensitizing effects of the methylation inhibitor zebularine in ovarian cancer. *Mol Cancer Ther.* **4**(10), 1505-14.

Baliga, B.S., Pronczuk, A.W., Munro, H.N. **(1969)**. Mechanism of cycloheximide inhibition of protein synthesis in a cell-free system prepared from rat liver. *J Biol Chem.* **244**(16), 4480-9.

Barcellos-Hoff, M.H., Park, C., Wright, E.G. **(2005)**. Radiation and the microenvironment - tumorigenesis and therapy. *Nat Rev Cancer.* **5**(11), 867-75.

Barchi, J.J., Cooney, D.A., Ahluwalia, G.S., Gharehbaghi, K., Covey, J.M., Hochman, I., Paull, K.D., Jayaram, H.N. **(1996)**. Studies on the mechanism of action of 1-beta-D-arabinofuranosyl-5-azacytosine (fazarabine) in mammalian lymphoblasts. *J Exp Ther Oncol.* **1**(3), 191-203.

Baylin, S.B., Esteller, M., Rountree, M.R., Bachman, K.E., Schuebel, K., Herman, J.G. **(2001)**. Aberrant patterns of DNA methylation, chromatin formation and gene expression in cancer. *Hum Mol Genet.* **10**(7), 687-92.

Baylin, S.B., Ohm, J.E. **(2006)**. Epigenetic gene silencing in cancer - a mechanism for early oncogenic pathway addiction? *Nat Rev Cancer.* **6**(2), 107-16.

Beisler, J.A., Abbasi, M.M., Driscoll, J.S. **(1979)**. Synthesis and antitumor activity of 5-azacytosine arabinoside. *J Med Chem.* **22**(10), 1230-4.

Beisler, J.A., Abbasi, M.M., Kelley, J.A., Driscoll, J.S. **(1977)**. Synthesis and antitumor activity of dihydro-5-azacytidine, a hydrolytically stable analogue of 5-azacytidine. *J Med Chem.* **20**(6), 806-12.

Ben-Baruch, N., Denicoff, A.M., Goldspiel, B.R., O'Shaughnessy, J.A., Cowan, K.H. **(1993)**. Phase II study of fazarabine (NSC 281272) in patients with metastatic colon cancer. *Invest New Drugs.* **11**(1), 71-4.

Ben-Kasus, T., Ben-Zvi, Z., Marquez, V.E., Kelley, J.A., Agbaria, R. **(2005)**. Metabolic activation of zebularine, a novel DNA methylation inhibitor, in human bladder carcinoma cells. *Biochem Pharmacol.* **70**(1), 121-33.

Bensaude, O. **(2011)**. Inhibiting eukaryotic transcription: Which compound to choose? How to evaluate its activity? *Transcription.* **2**(3), 103-8.

Bernstein, M.L., Whitehead, V.M., Grier, H., Dubowy, R., Land, V., Devine, S., Murphy, S., Kung, F. **(1993)**. A phase I trial of fazarabine in refractory pediatric solid tumors. A Pediatric Oncology Group study. *Invest New Drugs.* **11**(4), 309-12.

Bestor, T.H. **(2000)**. The DNA methyltransferases of mammals. *Hum Mol Genet.* **9**(16), 2395-402.

Bestor, T., Laudano, A., Mattaliano, R., Ingram, V. **(1988)**. Cloning and sequencing of a cDNA encoding DNA methyltransferase of mouse cells. The carboxyl-terminal domain of the mammalian enzymes is related to bacterial restriction methyltransferases. *J Mol Biol.* **203**(4), 971-83.

Beumer, J.H., Eiseman, J.L., Parise, R.A., Joseph, E., Holleran, J.L., Covey, J.M., Egorin, M.J. **(2006)**. Pharmacokinetics, metabolism, and oral bioavailability of the DNA methyltransferase inhibitor 5-fluoro-2'-deoxycytidine in mice. *Clin Cancer Res.* **12**(24), 7483-91.

Beumer, J.H., Parise, R.A., Newman, E.M., Doroshow, J.H., Synold, T.W., Lenz, H.J., Egorin, M.J. **(2008)**. Concentrations of the DNA methyltransferase inhibitor 5-fluoro-2'-

deoxycytidine (FdCyd) and its cytotoxic metabolites in plasma of patients treated with FdCyd and tetrahydrouridine (THU). *Cancer Chemother Pharmacol.* **62**(2), 363-68.

Billam, M., Sobolewski, M.D., Davidson, N.E. **(2010)**. Effects of a novel DNA methyltransferase inhibitor zebularine on human breast cancer cells. *Breast Cancer Res Treat.* **120**(3), 581-92.

Bird, A.P. **(1986)**. CpG-rich islands and the function of DNA methylation. *Nature.* **321**, 209-13.

Blum, W., Garzon, R., Klisovic, R.B., Schwind, S., Walker, A., Geyer, S., Liu, S., Havelange, V., Becker, H., Schaaf, L., Mickle, J., Devine, H., Kefauver, C., Devine, S.M., Chan, K.K., Heerema, N.A., Bloomfield, C.D., Grever, M.R., Byrd, J.C., Villalona-Calero, M., Croce, C.M., Marcucci, G. **(2010)**. Clinical response and miR-29b predictive significance in older AML patients treated with a 10-day schedule of decitabine. *Proc Natl Acad Sci U S A.* **107**(16), 7473-8.

Blum, W., Klisovic, R.B., Hackanson, B., Liu, Z., Liu, S., Devine, H., Vukosavljevic, T., Huynh, L., Lozanski, G., Kefauver, C., Plass, C., Devine, S.M., Heerema, N.A., Murgo, A., Chan, K.K., Grever, M.R., Byrd, J.C., Marcucci, G. **(2007)**. Phase I study of decitabine alone or in combination with valproic acid in acute myeloid leukemia. *J Clin Oncol.* **25**(25), 3884-91.

Blum, W., Sanford, B.L., Klisovic, R., DeAngelo, D.J., Uy, G., Powell, B.L., Stock, W., Baer, M.R., Kolitz, J.E., Wang, E.S., Hoke, E., Mrózek, K., Kohlschmidt, J., Bloomfield, C.D., Geyer, S., Marcucci, G., Stone, R.M., Larson, R.A., Alliance for Clinical Trials in Oncology. **(2017)** Maintenance therapy with decitabine in younger adults with acute myeloid leukemia in first remission: a phase 2 Cancer and Leukemia Group B Study (CALGB 10503). *Leukemia.* **31**(1), 34-9.

Blum, W., Schwind, S., Tarighat, S.S., Geyer, S., Eisfeld, A.K., Whitman, S., Walker, A., Klisovic, R., Byrd, J.C., Santhanam, R., Wang, H., Curfman, J.P., Devine, S.M., Jacob, S., Garr, C., Kefauver, C., Perrotti, D., Chan, K.K., Bloomfield, C.D., Caligiuri, M.A., Grever, M.R., Garzon, R., Marcucci, G. **(2012)**. Clinical and pharmacodynamic activity of bortezomib and decitabine in acute myeloid leukemia. *Blood.* **119**(25), 6025-31.

Bogdanović, O., Veenstra, G.J. **(2009)**. DNA methylation and methyl-CpG binding proteins: developmental requirements and function. *Chromosoma.* **118**(5), 549-65.

Bowden, M.A., Di Nezza-Cossens, L.A., Jobling, T., Salamonsen, L.A., Nie, G. **(2006)**. Serine proteases HTRA1 and HTRA3 are down-regulated with increasing grades of human endometrial cancer. *Gynecol Oncol.* **103**(1), 253-60.

Braun, T., Itzykson, R., Renneville, A., de Renzis, B., Dreyfus, F., Laribi, K., Bouabdallah, K., Vey, N., Toma, A., Recher, C., Royer, B., Joly, B., Vekhoff, A., Lafon, I., Sanhes, L., Meurice, G., Oréar, C., Preudhomme, C., Gardin, C., Ades, L., Fontenay, M., Fenaux, P., Droin, N., Solary, E; Groupe Francophone des Myélodysplasies. **(2011)**. Groupe Francophone des Myélodysplasies Molecular predictors of response to decitabine in advanced chronic myelomonocytic leukemia: a phase 2 trial. *Blood.* **118**(14), 3824-31.

Brown, R., Curry, E., Magnani, L., Wilhelm-Benartzi, C.S., Borley, J. **(2014)**. Poised epigenetic states and acquired drug resistance in cancer. *Nat Rev Cancer.* **14**(11), 747-53.

Brueckner, B., Rius, M., Markelova, M.R., Fichtner, I., Hals, P.A., Sandvold, M.L., Lyko, F. **(2010)**. Delivery of 5-azacytidine to human cancer cells by elaidic acid esterification increases therapeutic drug efficacy. *Mol Cancer Ther.* **9**(5), 1256-64.

Brus, J. **(2000)**. Heating of samples induced by fast magic-angle spinning. *Solid State Nucl Magn Reson.* **16**(3), 151-60.

Bryan, J., Kantarjian, H., Jabbour, E. **(2013)**. Decitabine for the treatment of acute myeloid leukemia. *Expert Opin Orphan Drugs*. **1**(8), 661-73.

Burchenal, J.H., Ciovacco, K., Kalaher, K., O'Toole, T., Kiefner, R., Dowling, M.D., Chu, C.K., Watanabe, K.A., Wempen, I., Fox, J.J. **(1976)**. Antileukemic effects of pseudoisocytidine, a new synthetic pyrimidine C-nucleoside. *Cancer Res.* **36**(4), 1520-3.

Burkart, C., Arimoto, K., Tang, T., Cong, X., Xiao, N., Liu, Y.C., Kotenko, S.V., Ellies, L.G., Zhang, D.E. **(2013).** Usp18 deficient mammary epithelial cells create an antitumour environment driven by hypersensitivity to IFN-λ and elevated secretion of Cxcl10. *EMBO Mol Med.* **5**(7), 967-82.

Burke, M.J., Lamba, J.K., Pounds, S., Cao, X., Ghodke-Puranik, Y., Lindgren, B.R., Weigel, B.J., Verneris, M.R., Miller, J.S. **(2014)**. A therapeutic trial of decitabine and vorinostat in combination with chemotherapy for relapsed/refractory acute lymphoblastic leukemia. *Am J Hematol.* **89**(9), 889-95.

Byun, H.M., Choi, S.H., Laird, P.W., Trinh, B., Siddiqui, M.A., Marquez, V.E., Yang, A.S. **(2008)**. 2'-Deoxy-N4-[2-(4-nitrophenyl)ethoxycarbonyl]-5-azacytidine: a novel inhibitor of DNA methyltransferase that requires activation by human carboxylesterase 1. *Cancer Lett.* **266**(2), 238-48.

Calon, A., Lonardo, E., Berenguer-Llergo, A., Espinet, E., Hernando-Momblona, X., Iglesias, M., Sevillano, M., Palomo-Ponce, S., Tauriello, D.V., Byrom, D., Cortina, C., Morral, C., Barceló, C., Tosi, S., Riera, A., Attolini, C.S., Rossell, D., Sancho, E., Batlle, E. **(2015)**.

Stromal gene expression defines poor-prognosis subtypes in colorectal cancer. *Nat Genet.* **47**(4), 320-9.

Calvisi, D.F., Ladu, S., Gorden, A., Farina, M., Conner, E.A., Lee, J.S., Factor, V.M., Thorgeirsson, S.S. **(2006)**. Ubiquitous activation of Ras and Jak/Stat pathways in human HCC. *Gastroenterology.* **130**(4), 1117-28.

Cardenas, H., Vieth, E., Lee, J., Segar, M., Liu, Y., Nephew, K.P., Matei, D. **(2014)**. TGF-β induces global changes in DNA methylation during the epithelial-to-mesenchymal transition in ovarian cancer cells. *Epigenetics.* **9**(11), 1461-72.

Casalini, T., Perale, G. **(2002)**. Types of bioresorbable polymers for medical applications. In: Stamboulis A, Jenkins M, editors. Durability and Reliability of Medical Polymers. *Cambridge: Woodhead Publ Ltd.* p. 3-29.

Casper, E.S., Schwartz, G.K., Kelsen, D.P. **(1992)**. Phase II trial of fazarabine (arabinofuranosyl-5-azacytidine) in patients with advanced pancreatic adenocarcinoma. *Invest New Drugs.* **10**(3), 205-9.

Champion, C., Guianvarc'h, D., Sénamaud-Beaufort, C., Jurkowska, R.Z., Jeltsch, A., Ponger, L., Arimondo, P.B., Guieysse-Peugeot, A.L. **(2010)**. Mechanistic insights on the inhibition of c5 DNA methyltransferases by zebularine. *PLoS One.* **5**(8), e12388.

Chan, A.S., Tsui, W.Y., Chen, X., Chu, K.M., Chan, T.L., Chan, A.S., Li, R., So, S., Yuen, S.T., Leung, S.Y. (2003). Downregulation of ID4 by promoter hypermethylation in gastric adenocarcinoma. *Oncogene.* **22**(44), 6946-53.

Cheetham, S., Tang, M.J., Mesak, F., Kennecke, H., Owen, D., Tai, I.T. **(2008)**. SPARC promoter hypermethylation in colorectal cancers can be reversed by 5-Aza-2'deoxycytidine to increase SPARC expression and improve therapy response. *Br J Cancer.* **98**(11), 1810-9.

Cheng, J.C., Matsen, C.B., Gonzales, F.A., Ye, W., Greer, S., Marquez, V.E., Jones, P.A., Selker, E.U. **(2003)**. Inhibition of DNA methylation and reactivation of silenced genes by zebularine. *J Natl Cancer Inst.* **95**(5), 399-409.

Cheng, J.C., Weisenberger, D.J., Gonzales, F.A., Liang, G., Xu, G.L., Hu, Y.G., Marquez, V.E., Jones, P.A. **(2004a)**. Continuous zebularine treatment effectively sustains demethylation in human bladder cancer cells. *Mol Cell Biol.* **24**(3), 1270-8.

Cheng, J.C., Yoo, C.B., Weisenberger, D.J., Chuang, J., Wozniak, C., Liang, G., Marquez, V.E., Greer, S., Orntoft, T.F., Thykjaer, T., Jones, P.A. **(2004b)**. Preferential response of cancer cells to zebularine. *Cancer Cell.* **6**(2), 151-8.

Chen, L., Yuan, D., Zhao, R., Li, H., Zhu, J. **(2010)**. Suppression of TSPAN1 by RNA interference inhibits proliferation and invasion of colon cancer cells in vitro. *Tumori.* **96**(5), 744-50.

Chen, L., Zhu, Y.Y., Zhang, X.J., Wang, G.L., Li, X.Y., He, S., Zhang, J.B., Zhu, J.W. **(2009)**. TSPAN1 protein expression: a significant prognostic indicator for patients with colorectal adenocarcinoma. *World J Gastroenterol.* **15**(18), 2270-6.

Chen, M., Shabashvili, D., Nawab, A., Yang, S.X., Dyer, L.M., Brown, K.D., Hollingshead, M., Hunter, K.W., Kaye, F.J., Hochwald, S.N., Marquez, V.E., Steeg, P., Zajac-Kaye, M. **(2012)**. DNA methyltransferase inhibitor, zebularine, delays tumor growth and induces apoptosis in a genetically engineered mouse model of breast cancer. *Mol Cancer Ther.* **11**(2), 370-82.

Chen, M., Voeller, D., Marquez, V.E., Kaye, F.J., Steeg, P.S., Giaccone, G., Zajac-Kaye, M. **(2010)**. Enhanced growth inhibition by combined DNA methylation/HDAC inhibitors in lung tumor cells with silenced CDKN2A. *Int J Oncol.* **37**(4), 963-71.

Chen, S.X., Xu, X.E., Wang, X.Q., Cui, S.J., Xu, L.L., Jiang, Y.H., Zhang, Y., Yan, H.B., Zhang, Q., Qiao, J., Yang, P.Y., Liu, F. **(2014)**. Identification of colonic fibroblast secretomes reveals secretory factors regulating colon cancer cell proliferation. *J. Proteomics.* **110**, 155-71.

Cheriyath, V., Glaser, K.B., Waring, J.F., Baz, R., Hussein, M.A., Borden, E.C. **(2007)**. G1P3, an IFN-induced survival factor, antagonizes TRAIL-induced apoptosis in human myeloma cells. *J Clin Invest.* **117**(10), 3107-17.

Chiappinelli, K.B., Strissel, P.L., Desrichard, A., Li, H., Henke, C., Akman, B., Hein, A., Rote, N.S., Cope, L.M., Snyder, A., Makarov, V., Budhu, S., Slamon, D.J., Wolchok, J.D., Pardoll, D.M., Beckmann, M.W., Zahnow, C.A., Merghoub, T., Chan, T.A., Baylin, S.B., Strick, R. **(2015)**. Inhibiting DNA Methylation Causes an Interferon Response in Cancer via dsRNA Including Endogenous Retroviruses. *Cell.* **162**(5), 974-86.

Chien, J., Staub, J., Avula, R., Zhang, H., Liu, W., Hartmann, L.C., Kaufmann, S.H., Smith, D.I., Shridhar, V. **(2005)**. Epigenetic silencing of TCEAL7 (Bex4) in ovarian cancer. *Oncogene.* **24**(32), 5089-100.

Choi, W.J., Chung, H.J., Chandra, G., Alexander, V., Zhao, L.X., Lee, H.W., Nayak, A., Majik, M.S., Kim, H.O., Kim, J.H., Lee, Y.B., Ahn, C.H.., Lee, S.K., Jeong, L.S. **(2012)**. Fluorocyclopentenyl-cytosine with broad spectrum and potent antitumor activity. *J Med Chem.* **55**(9), 4521-5.

Chou, T.C., Martin, N. **(2004)**. CompuSyn for Drug Combinations: PC Software and User's Guide: A Computer Program for Quantitation of Synergism and Antagonism in Drug Combinations, and the Determination of IC50 and ED50 and LD50 Values, *ComboSyn, Inc.*

Chuang, J.C., Warner, S.L., Vollmer, D., Vankayalapati, H., Redkar, S., Bearss, D.J., Qiu, X., Yoo, C.B., Jones, P.A. **(2010)**. S110, a 2'-deoxy-5-azacytidine-containing dinucleotide, is an effective DNA methylation inhibitor in vivo and can reduce tumor growth. *Mol Cancer Ther*. **9**(5), 1443-50.

Chu, C.K., Watanabe, K.A., Kyoichi, A., Fox, J.J. **(1975)**. Nucleosides XXCII: A Facile Synthesis of 5-(β-D-Ribofuranosyl)-isocytosine (Pseudoisocytidine). *J Heterocyclic Chem.* **12**(4), 817-8.

Chu, D., Zhou, Y., Zhang, Z., Li, Y., Li, J., Zheng, J., Zhang, H., Zhao, Q., Wang, W., Wang, R., Ji, G. **(2011)**. Notch1 expression, which is related to p65 Status, is an independent predictor of prognosis in colorectal cancer. *Clin Cancer Res.* **17**(17), 5686-94.

Cihák, A. **(1974)**. Biological effects of 5-azacytidine in eukaryotes. *Oncology.* **30**(5), 405-22.

Clark, C., Palta, P., Joyce, C.J., Scott, C., Grundberg, E., Deloukas, P., Palotie, A., Coffey, A.J. **(2012)**. A comparison of the whole genome approach of MeDIP-seq to the targeted approach of the Infinium HumanMethylation450 BeadChip(®) for methylome profiling. *PLoS One.* **7**(11), e50233.

Cluzeau, T., Robert, G., Mounier, N., Karsenti, J.M., Dufies, M., Puissant, A., Jacquel, A., Renneville, A., Preudhomme, C., Cassuto, J.P., Raynaud, S., Luciano, F., Auberger, P. **(2012)**. BCL2L10 is a predictive factor for resistance to Azacytidine in MDS and AML patients. *Oncotarget.* **3**(4), 490-501.

Conti, J., Thomas, G. **(2011)**. The Role of Tumour Stroma in Colorectal Cancer Invasion and Metastasis. *Cancers.* **3**(2), 2160-8.

Coral, S., Parisi, G., Nicolay, H.J., Colizzi, F., Danielli, R., Fratta, E., Covre, A., Taverna, P., Sigalotti, L., Maio, M. **(2013)**. Immunomodulatory activity of SGI-110, a 2'-deoxy-5-azacytidine-containing demethylating dinucleotide. *Cancer Immunol Immunother.* **62**(3), 605-14.

Costanzi, S., Vilar, S., Micozzi, D., Carpi, F.M., Ferino, G., Vita, A., Vincenzetti, S. **(2011)**. Delineation of the molecular mechanisms of nucleoside recognition by cytidine deaminase through virtual screening. *Chem Med Chem.* **6**(8), 1452-8.

Coussens, L.M., Werb, Z. **(2002)**. Inflammation and cancer. *Nature*. **420**(6917), 860-7.

Cowan, L.A., Talwar, S., Yang, A.S. **(2010)**. Will DNA methylation inhibitors work in solid tumors? A review of the clinical experience with Azacytidine and decitabine in solid tumors. *Epigenomics.* **2**(1), 71-86.

Creagan, E.T., Schaid, D.J., Hartmann, L.C., Loprinzi, C.L. **(1993)**. A phase II study of 5,6-dihydro-5-azacytidine hydrochloride in disseminated malignant melanoma. *Am J Clin Oncol.* **16**(3), 243-4.

Curt, G.A., Kelley, J.A., Fine, R.L., Huguenin, P.N., Roth, J.S., Batist, G., Jenkins, J., Collins, J.M. **(1985)**. A phase I and pharmacokinetic study of dihydro-5-azacytidine (NSC 264880). *Cancer Res.* **45**(7), 3359-63.

Dai, Y., Duan, H., Duan, C., Zhou, R., He, Y., Tu, Q., Shen, L. (2016). Down-regulation of TCF21 by hypermethylation induces cell proliferation, migration and invasion in colorectal cancer. *Biochem Biophys Res Commun.* **469**(3), 430-6.

Dalai, M., Plowman, J., Breitman, T.R., Schuller, H.M., Campo, A.D., Vistica, D.T., Driscoll, J.S., Cooney, D.A., Johns, D.G. **(1986)**. Arabinofuranosyl-5-azacytosine: Antitumor and Cytotoxic Properties. *Cancer Res.* **46**(2), 831-8.

Dansranjavin, T., Krehl, S., Mueller, T., Mueller, L.P., Schmoll, H.J., Dammann, R.H. **(2009)**. The role of promoter CpG methylation in the epigenetic control of stem cell related genes during differentiation. *Cell Cycle.* **8**(6), 916-24.

Dario, L.S., Rosa, M.A., Mariela, E., Roberto, G., Caterina, C. **(2008)**. Chromatin remodeling agents for cancer therapy. *Rev Recent Clin Trials.* **3**(3), 192-203.

Das, V., Fürst, T., Gurská, S., Džubák, P., Hajdúch, M. **(2016)**. Reproducibility of Uniform Spheroid Formation in 384-Well Plates: The Effect of Medium Evaporation. *J Biomol Screen.* **21**(9), 923-30.

Das, V., Fürst, T., Gurská, S., Džubák, P., Hajdúch, M. **(2017)**. Evaporation-reducing Culture Condition Increases the Reproducibility of Multicellular Spheroid Formation in Microtiter Plates. *J Vis Exp.* **121**, e55403.

Das, V., Miller, J.H. **(2012)**. Non-taxoid site microtubule-stabilizing drugs work independently of tau overexpression in mouse N2a neuroblastoma cells. *Brain Res.* **1489**, 121-32.

de Kruijf, E.M., van Nes, J.G., van de Velde, C.J., Putter, H., Smit, V.T., Liefers, G.J., Kuppen, P.J., Tollenaar, R.A., Mesker, W.E. **(2011)**. Tumor–stroma ratio in the primary tumor is a prognostic factor in early breast cancer patients, especially in triple-negative carcinoma patients. *Breast Cancer Res. Treat.* **125**(3), 687-96.

Dhingra, H.M., Murphy, W.K., Winn, R.J., Raber, M.N., Hong, W.K. **(1991)**. Phase II trial of 5,6-dihydro-5-azacytidine in pleural malignant mesothelioma. *Invest New Drugs.* **9**(1), 69-72.

Diesch, J., Zwick, A., Garz, A.K., Palau, A., Buschbeck, M., Götze, K.S. **(2016)**. A clinical-molecular update on azanucleoside-based therapy for the treatment of hematologic cancers. *Clin Epigenetics.* **8**, 71.

DiNardo, C.D., Daver, N., Jabbour, E., Kadia, T., Borthakur, G., Konopleva, M., Pemmaraju, N., Yang, H., Pierce, S., Wierda, W., Bueso-Ramos, C., Patel, K.P., Cortes, J.E., Ravandi, F., Kantarjian, H.M., Garcia-Manero, G. **(2015)**. Sequential azacytidine and lenalidomide in patients with high-risk myelodysplastic syndromes and acute myeloid leukaemia: a single-arm, phase 1/2 study. *Lancet Haematol.* **2**(1), e12-20.

Dombret, H., Seymour, J.F., Butrym, A., Wierzbowska, A., Selleslag, D., Jang, J.H., Kumar, R., Cavenagh, J., Schuh, A.C., Candoni, A., Récher, C., Sandhu, I., Bernal del Castillo, T., Al-Ali, H.K., Martinelli, G., Falantes, J., Noppeney, R., Stone, R.M., Minden, M.D., McIntyre, H., Songer, S., Lucy, L.M., Beach, C.L., Döhner, H. **(2015)**. International phase 3 study of Azacytidine vs conventional care regimens in older patients with newly diagnosed AML with >30% blasts. *Blood.* **126**(3), 291-9.

Doppalapudi, S., Jain, A., Khan, W., Domb, A.J. **(2014)**. Biodegradable polymers-an overview. *Polym Adv Technol.* **25**(5), 427-35.

Dreos, R., Ambrosini, G., Périer, R.C., Bucher, P. **(2015)**. The Eukaryotic Promoter Database: expansion of EPDnew and new promoter analysis tools. *Nucleic Acids Res.* **43**(Database issue), D92-6.

Duex, J.E., Comeau, L., Sorkin, A., Purow, B., Kefas, B. **(2011)**. Usp18 regulates epidermal growth factor (EGF) receptor expression and cancer cell survival via microRNA-7. *J Biol Chem.* **286**(28), 25377-86.

Eidinoff, M.L., Rich, M.A., Perez, A.G. **(1959)**. Growth inhibition of a human tumor cell strain by 5-fluorocytidine and 5-fluoro-2'-deoxycytidine: reversal studies. *Cancer Res.* **19**(6), 638-42.

Fabre, C., Grosjean, J., Tailler, M., Boehrer, S., Adès, L., Perfettini, J.L., de Botton, S., Fenaux, P., Kroemer, G. **(2008)**. A novel effect of DNA methyltransferase and histone deacetylase inhibitors: NFkappaB inhibition in malignant myeloblasts. *Cell Cycle.* **7**(14), 2139-45.

Fagan, R.L., Cryderman, D.E., Kopelovich, L., Wallrath, L.L., Brenner, C. **(2013)**. Laccaic acid A is a direct, DNA-competitive inhibitor of DNA methyltransferase 1. *J Biol Chem.* **288**(33), 23858-67.

Falchook, G.S., Fu, S., Naing, A., Hong, D.S., Hu, W., Moulder, S., Wheler, J.J., Sood, A.K., Bustinza-Linares, E., Parkhurst, K.L., Kurzrock, R. **(2013)**. Methylation and histone deacetylase inhibition in combination with platinum treatment in patients with advanced malignancies. *Invest New Drugs.* **31**(5), 1192-200.

Fang, F., Balch, C., Schilder, J., Breen, T., Zhang, S., Shen, C., Li, L., Kulesavage, C., Snyder, A.J., Nephew, K.P., Matei, D.E. **(2010)**. A phase 1 and pharmacodynamic study of decitabine in combination with carboplatin in patients with recurrent, platinum-resistant, epithelial ovarian cancer. *Cancer.* **116**(17), 4043-53.

Fang, F., Munck, J., Tang, J., Taverna, P., Wang, Y., Miller, D.F., Pilrose, J., Choy, G., Azab, M., Pawelczak, K.S., VanderVere-Carozza, P., Wagner, M., Lyons, J., Matei, D., Turchi, J.J., Nephew, K.P. **(2014)**. The novel, small-molecule DNA methylation inhibitor SGI-110 as an ovarian cancer chemosensitizer. *Clin Cancer Res.* **20**(24), 6504-16.

Fan, H., Lu, X., Wang, X., Liu, Y., Guo, B., Zhang, Y., Zhang, W., Nie, J., Feng, K., Chen, M., Zhang, Y., Wang, Y., Shi, F., Fu, X., Zhu, H., Han, W. **(2014)**. Low-dose decitabine-based chemoimmunotherapy for patients with refractory advanced solid tumors: a phase I/II report. *J Immunol Res.* **2014**, 371087.

Fenaux, P., Mufti, G. J., Hellstrom-Lindberg, E., Santini, V., Finelli, C., Giagounidis, A., Schoch, R., Gattermann, N., Sanz, G., List, A., Gore, S.D., Seymour, J.F., Bennett, J.M., Byrd, J., Backstrom, J., Zimmerman, L., McKenzie, D., Beach, C., Silverman, L.R; International Vidaza High-Risk MDS Survival Study Group. **(2009)**. Efficacy of azacitidine compared with that of conventional care regimens in the treatment of higher-risk myelodysplastic syndromes: a randomised, open-label, phase III study. *Lancet Oncol.* **10**(3), 223-32.

Fender, A.W., Nutter, J.M., Fitzgerald, T.L., Bertrand, F.E., Sigounas, G. **(2015)**. Notch-1 promotes stemness and epithelial to mesenchymal transition in colorectal cancer. *J Cell Biochem.* **116**(11), 2517-27.

Ferraro, A., Schepis, F., Leone, V., Federico, A., Borbone, E., Pallante, P., Berlingieri, M.T., Chiappetta, G., Monaco, M., Palmieri, D., Chiariotti, L., Santoro, M., Fusco, A. **(2013)**. Tumor suppressor role of the CL2/DRO1/CCDC80 gene in thyroid carcinogenesis. *J Clin Endocrinol Metab.* **98**(7), 2834-43.

Finlin, B.S., Gau, C.L., Murphy, G.A., Shao, H., Kimel, T., Seitz, R.S., Chiu, Y.F., Botstein, D., Brown, P.O., Der, C.J., Tamanoi, F., Andres, D.A., Perou, C.M. **(2001)**. RERG is a novel

ras-related, estrogen-regulated and growth-inhibitory gene in breast cancer. *J Biol Chem.* **276**(45), 42259-67.

Flesner, B.K., Kumar, S.R., Bryan, J.N. **(2014)**. 6-Thioguanine and zebularine down-regulate DNMT1 and globally demethylate canine malignant lymphoid cells. *BMC Vet Res.* **10**, 290.

Flis, S., Gnyszka, A., Flis, K. **(2014)**. DNA methyltransferase inhibitors improve the effect of chemotherapeutic agents in SW48 and HT-29 colorectal cancer cells. *PLoS One.* **9**(3), e92305.

Flis, S., Gnyszka, A., Misiewicz-Krzemińska, I., Spławiński, J. **(2009)**. Decytabine enhances cytotoxicity induced by oxaliplatin and 5-fluorouracil in the colorectal cancer cell line Colo-205. *Cancer Cell Int.* **9**, 10.

Flotho, C., Paulun, A., Batz, C., Niemeyer, C.M. **(2007)**. AKAP12, a gene with tumour suppressor properties, is a target of promoter DNA methylation in childhood myeloid malignancies. *Br J Haematol.* **138**(5), 644-50.

Fojtova, M., Piskala, A., Votruba, I., Otmar, M., Bartova, E., Kovarik, A. **(2007)**. Efficacy of DNA hypomethylating capacities of 5-aza-2′-deoxycytidine and its alpha anomer. *Pharmacol Res.* **55**(1), 16-22.

Frommer, M., McDonald, L.E., Millar, D.S., Collis, C.M., Watt, F., Grigg, G.W., Molloy, P.L., Paul, C.L. **(1992)**. A genomic sequencing protocol that yields a positive display of 5-methylcytosine residues in individual DNA strands. *Proc Natl Acad Sci U S A.* **89**(5), 1827-31.

Fuchs, C., Mitchell, E.P., Hoff, P.M. **(2006)**. Irinotecan in the treatment of colorectal cancer. *Cancer Treat Rev.* **32**(7), 491-503.

Futterman, B., Derr, J., Beisler, J.A., Abbasi, M.M., Voytek, P. **(1978)**. Studies on the cytostatic action, phosphorylation and deamination of 5-azacytidine and 5,6-dihydro-5-azacytidine in HeLa cells. *Biochem Pharmacol.* **27**(6), 907-9.

Gao, W., Li, J. Z-H., Chen, S.Q., Chu, C.Y., Chan, J. Y-W., Wong, T.S. **(2016)**. Decreased brain-expressed X-linked 4 (BEX4) expression promotes growth of oral squamous cell carcinoma. *J Exp Clin Cancer Res.* **35**, 92.

Garcia-Manero, G., Gore, S.D., Cogle, C., Ward, R., Shi, T., Macbeth, K.J., Laille, E., Giordano, H., Sakoian, S., Jabbour, E., Kantarjian, H., Skikne, B. **(2011)**. Phase I study of oral azacitidine in myelodysplastic syndromes, chronic myelomonocytic leukemia, and acute myeloid leukemia. *J Clin Oncol.* **29**(18), 2521-7.

Garcia-Manero, G., Jabbour, E., Borthakur, G., Faderl, S., Estrov, Z., Yang, H., Maddipoti, S., Godley, L.A., Gabrail, N., Berdeja, J.G., Nadeem, A., Kassalow, L., Kantarjian, H. **(2013)**. Randomized open-label phase II study of decitabine in patients with low- or intermediate-risk myelodysplastic syndromes. *J Clin Oncol.* **31**(20), 2548-53.

Garcia-Manero, G., Kantarjian, H.M., Sanchez-Gonzalez, B., Yang, H., Rosner, G., Verstovsek, S., Rytting, M., Wierda, W.G., Ravandi, F., Koller, C., Xiao, L., Faderl, S., Estrov, Z., Cortes, J., O'brien, S., Estey, E., Bueso-Ramos, C., Fiorentino, J., Jabbour, E., Issa, J.P. **(2006)**. Phase 1/2 study of the combination of 5-aza-2'-deoxycytidine with valproic acid in patients with leukemia. *Blood.* **108**(10), 3271-9.

Garcia-Manero, G., Tibes, R., Kadia, T., Kantarjian, H., Arellano, M., Knight, E.A., Xiong, H., Qin, Q., Munasinghe, W., Roberts-Rapp, L., Ansell, P., Albert, D.H., Oliver, B., McKee, M.D., Ricker, J.L., Khoury, H.J. **(2015)**. Phase 1 dose escalation trial of ilorasertib, a dual Aurora/VEGF receptor kinase inhibitor, in patients with hematologic malignancies. *Invest New Drugs.* **33**(4), 870-80.

Garrido-Laguna, I., McGregor, K.A., Wade, M., Weis, J., Gilcrease, W., Burr, L., Soldi, R., Jakubowski, L., Davidson, C., Morrell, G., Olpin, J.D., Boucher, K., Jones, D., Sharma, S. **(2013)**. A phase I/II study of decitabine in combination with panitumumab in patients with wild-type (wt) KRAS metastatic colorectal cancer. *Invest New Drugs.* **31**(5), 1257-64.

Gertych, A., Farkas, D.L., Tajbakhsh, J. **(2010)**. Measuring topology of low-intensity DNA methylation sites for high-throughput assessment of epigenetic drug-induced effects in cancer cells. *Exp Cell Res.* **316**(19), 3150-60.

Gertych, A., Oh, J.H., Wawrowsky, K.A., Weisenberger, D.J., Tajbakhsh, J. **(2013)**. 3-D DNA methylation phenotypes correlate with cytotoxicity levels in prostate and liver cancer cell models. *BMC Pharmacol Toxicol.* **14**, 11.

Gertych, A., Wawrowsky, K.A., Lindsley, E., Vishnevsky, E., Farkas, D.L., Tajbakhsh, J. **(2009)**. Automated quantification of DNA demethylation effects in cells via 3D mapping of nuclear signatures and population homogeneity assessment. *Cytometry A.* **75**(7), 569-83.

Glazer, R.I., Knode, M.C. **(1984)**. 1-beta-D-arabinosyl-5-azacytosine. Cytocidal activity and effects on the synthesis and methylation of DNA in human colon carcinoma cells. *Mol Pharmacol.* **26**(2), 381-7.

Glozak, M.A., Seto, E. **(2007)**. Histone deacetylases and cancer. *Oncogene.* **26**, 5420-32.

Gnyszka, A., Jastrzebski, Z., Flis, S. **(2013)**. DNA Methyltransferase Inhibitors and Their Emerging Role in Epigenetic Therapy of Cancer. *Anticancer Res.* **33**(8), 2989-96.

Goldberg, R.M., Reid, J.M., Ames, M.M., Sloan, J.A., Rubin, J., Erlichman, C., Kuffel, M.J., Fitch, T.R. **(1997)**. Phase I and Pharmacological Trial of Fazarabine (Ara-AC) with Granulocyte Colony-stimulating Factor. *Clin Cancer Res.* **3**(12 Pt 1), 2363-70.

Gómez Del Pulgar, T., Valdés-Mora, F., Bandrés, E., Pérez-Palacios, R., Espina, C., Cejas, P., García-Cabezas, M.A., Nistal, M., Casado, E., González-Barón, M., García-Foncillas, J., Lacal, J.C. **(2008)**. Cdc42 is highly expressed in colorectal adenocarcinoma and downregulates ID4 through an epigenetic mechanism. *Int J Oncol.* **33**(1), 185-93.

Gore, S.D., Fenaux, P., Santini, V., Bennett, J.M., Silverman, L.R., Seymour, J.F., Hellström-Lindberg, E., Swern, A.S., Beach, C.L., List, A.F. **(2013)**. A multivariate analysis of the relationship between response and survival among patients with higher-risk myelodysplastic syndromes treated within azacitidine or conventional care regimens in the randomized AZA-001 trial. *Haematologica.* **98**(7), 1067-72.

Gowher, H., Liebert, K., Hermann, A., Xu, G., Jeltsch, A. **(2005)**. Mechanism of stimulation of catalytic activity of Dnmt3A and Dnmt3B DNA-(cytosine-C5)-methyltransferases by Dnmt3L. *J Biol Chem.* **280**(14), 13341-8.

Grant, S. **(2009)**. Targeting Histone Demethylases in Cancer Therapy. *Clin Cancer Res.* **15**(23), 7111-3.

Gravina, G.L., Festuccia, C., Marampon, F., Popov, V.M., Pestell, R.G., Zani, B.M., Tombolini, V. **(2010)**. Biological rationale for the use of DNA methyltransferase inhibitors as new strategy for modulation of tumor response to chemotherapy and radiation. *Mol. Cancer.* **9**, 305.

Greenberg, P.L., Garcia-Manero, G., Moore, M., Damon, L., Roboz, G., Hu, K., Yang, A.S., Franklin, J. **(2013)**. A randomized controlled trial of romiplostim in patients with low- or intermediate-risk myelodysplastic syndrome receiving decitabine. *Leuk Lymphoma.* **54**(2), 321-8.

Grill, J.I., Neumann, J., Herbst, A., Hiltwein, F., Ofner, A., Marschall, M.K., Wolf, E., Kirchner, T., Göke, B., Schneider, M.R., Kolligs, F.T. **(2014)**. DRO1 inactivation drives colorectal carcinogenesis in ApcMin/+ mice. *Mol Cancer Res.* **12**(11), 1655-62.

Guan, M., Xu, C., Zhang, F., Ye, C. **(2009)**. Aberrant methylation of EphA7 in human prostate cancer and its relation to clinicopathologic features. *Int J Cancer.* **124**(1), 88-94.

Guerrero-Preston, R., Soudry, E., Acero, J., Orera, M., Moreno-López, L., Macía-Colón, G., Jaffe, A., Berdasco, M., Ili-Gangas, C., Brebi-Mieville, P., Fu, Y., Engstrom, C., Irizarry, R.A., Esteller, M., Westra, W., Koch, W., Califano, J., Sidransky, D. **(2011)**. NID2 and HOXA9 promoter hypermethylation as biomarkers for prevention and early detection in

oral cavity squamous cell carcinoma tissues and saliva. *Cancer Prev Res (Phila).* **4**(7), 1061-72.

Guinney, J., Dienstmann, R., Wang, X., de Reyniès, A., Schlicker, A., Soneson, C., Marisa, L., Roepman, P., Nyamundanda, G., Angelino, P., Bot, B.M., Morris, J.S., Simon, I.M., Gerster, S., Fessler, E., De Sousa, E., Melo, F., Missiaglia, E., Ramay, H., Barras, D., Homicsko, K., Maru, D., Manyam, G.C., Broom, B., Boige, V., Perez-Villamil, B., Laderas, T., Salazar, R., Gray, J.W., Hanahan, D., Tabernero, J., Bernards, R., Friend, S.H., Laurent-Puig, P., Medema, J.P., Sadanandam, A., Wessels, L., Delorenzi, M., Kopetz, S., Vermeulen, L., Tejpar, S. **(2015)**. The Consensus Molecular Subtypes of Colorectal Cancer. *Nat. Med.* **21**(11), 1350-6.

Gupta, P., Sharma, P.K., Mir, H., Singh, R., Singh, N., Kloecker, G.H., Lillard, J.W. Jr, Singh, S. **(2014)**. CCR9/CCL25 expression in non-small cell lung cancer correlates with aggressive disease and mediates key steps of metastasis. *Oncotarget.* **5**(20), 10170-9.

Haass, N.K., Beaumont, K.A., Hill, D.S., Anfosso, A., Mrass, P., Munoz, M.A., Kinjyo, I., Weninger, W. **(2014)**. Real-time cell cycle imaging during melanoma growth, invasion, and drug response. *Pigment Cell Melanoma Res.* **27**(5), 764-76.

Habashy, H.O., Powe, D.G., Glaab, E., Ball, G., Spiteri, I., Krasnogor, N., Garibaldi, J.M., Rakha, E.A., Green, A.R., Caldas, C., Ellis, I.O. **(2011)**. RERG (Ras-like, oestrogen-regulated, growth-inhibitor) expression in breast cancer: a marker of ER-positive luminal-like subtype. *Breast Cancer Res Treat.* **128**(2), 315-26.

Han, S., Kim, Y.J., Lee, J., Jeon, S., Hong, T., Park, G.J., Yoon, J.H., Yahng, S.A., Shin, S.H., Lee, S.E., Eom, K.S., Kim, H.J., Min, C.K., Lee, S., Yim, D.S. **(2015)**. Model-based adaptive phase I trial design of post-transplant decitabine maintenance in myelodysplastic syndrome. *J Hematol Oncol.* **8**, 118.

Harper, J.W., Adams, P.D. **(2001)**. Cyclin-Dependent Kinases. *Chem. Rev.* **101**(8), 2511-26.

Harris, K.S., Brabant, W., Styrchak, S., Gall, A., Daifuku, R. **(2005)**. KP-1212/1461, a nucleoside designed for the treatment of HIV by viral mutagenesis. *Antiviral Res.* **67**(1), 1-9.

Hedeland, R.L., Hvidt, K., Nersting, J., Rosthøj, S., Dalhoff, K., Lausen, B., Schmiegelow, K. **(2010)**. DNA incorporation of 6-thioguanine nucleotides during maintenance therapy of childhood acute lymphoblastic leukaemia and non-Hodgkin lymphoma. *Cancer Chemother Pharmacol.* **66**(3), 485-91.

Heideman, R.L., Gillespie, A., Ford, H., Reaman, G.H., Balis, F.M., Tan, C., Sato, J., Ettinger, L.J., Packer, R.J., Poplack, D.G. **(1989)**. Phase I Trial and Pharmacokinetic Evaluation of Fazarabine in Children. *Cancer Res.* **49**, 5213-6.

Herbst, A., Bayer, C., Wypior, C., Kolligs, F.T. **(2011)**. DRO1 sensitizes colorectal cancer cells to receptor-mediated apoptosis. *Oncology Letters.* **2**(5), 981-4.

Herranz, M., Martín-Caballero, J., Fraga, M.F., Ruiz-Cabello, J., Flores, J.M., Desco, M., Marquez, V., Esteller, M. **(2006)**. The novel DNA methylation inhibitor zebularine is effective against the development of murine T-cell lymphoma. *Blood.* **107**(3), 1174-7.

Hesson, L.B., Patil, V., Sloane, M.A., Nunez, A.C., Liu, J., Pimanda, J.E., Ward, R.L. **(2013)**. Reassembly of nucleosomes at the MLH1 promoter initiates resilencing following decitabine exposure. *PLoS Genet.* **9**(7), e1003636.

Heylen, N., Baurain, R., Remacle, C., Trouet, A. **(1998)**. Effect of MRC-5 fibroblast conditioned medium on breast cancer cell motility and invasion in vitro. *Clin. Exp. Metastasis.* **16**(2), 193-203.

Hitchings, G.H., Elion, G.B. **(1954)**. The chemistry and biochemistry of purine analogs. *Ann N Y Acad Sci*. **60**(2), 195-9.

Hogarth, L.A., Redfern, C.P., Teodoridis, J.M., Hall, A.G., Anderson, H., Case, M.C., Coulthard, S.A. **(2008)**. The effect of thiopurine drugs on DNA methylation in relation to TPMT expression. *Biochem Pharmacol*. **76**(8), 1024-35.

Højfeldt, J.W., Agger, K., Helin, K. **(2013)**. Histone lysine demethylases as targets for anticancer therapy. *Nat Rev Drug Discov.* **12**(12), 917-30.

Holleran, J.L., Beumer, J.H., McCormick, D.L., Johnson, W.D., Newman, E.M., Doroshow, J.H., Kummar, S., Covey, J.M., Davis, M., Eiseman, J.L. **(2015)**. Oral and intravenous pharmacokinetics of 5-fluoro-2'-deoxycytidine and THU in cynomolgus monkeys and humans. *Cancer Chemother Pharmacol.* **76**(4), 803-11.

Holleran, J.L., Parise, R.A., Joseph, E., Eiseman, J.L., Covey, J.M., Glaze, E.R., Lyubimov, A.V., Chen, Y.F., D'Argenio, D.Z., Egorin, M.J. **(2005)**. Plasma pharmacokinetics, oral bioavailability, and interspecies scaling of the DNA methyltransferase inhibitor, zebularine. *Clin Cancer Res.* **11**(10), 3862-8.

Holliday, R., Ho, T. **(2002)**. DNA methylation and epigenetic inheritance. *Methods.* **27**(2), 179-83.

Holoye, P.Y., Dhingra, H.M., Umsawasdi, T., Murphy, W.K., Carr, D.T., Lee, J.S. **(1987)**. Phase II study of 5,6-dihydro-5-azacytidine in extensive, untreated non-small cell lung cancer. *Cancer Treat Rep.* **71**(9), 859-60.

Hong, J.Y., Seo, J.Y., Kim, S.H., Jung, H.A., Park, S., Kim, K., Jung, C.W., Kim, J.S., Park, J.S., Kim, H.J., Jang, J.H. **(2015)**. Mutations in the Spliceosomal Machinery Genes SRSF2,

U2AF1, and ZRSR2 and Response to Decitabine in Myelodysplastic Syndrome. *Anticancer Res.* **35**(5), 3081-9.

Hosokawa, M., Saito, M., Nakano, A., Iwashita, S., Ishizaka, A., Ueda, K., & Iwakawa, S. **(2015)**. Acquired resistance to decitabine and cross-resistance to gemcitabine during the long-term treatment of human HCT116 colorectal cancer cells with decitabine. *Oncol Lett.* **10**(2), 761-7.

Hou, J., Newman, E.M. **(2005)**. The effect of 5-fluoro-2'-deoxycytidine on methylation of the MAGE-1 gene in the 888-mel human melanoma cell line. *Proc Amer Assoc Cancer Res.* **65**, 426.

Huang, E., Cheng, S.H., Dressman, H., Pittman, J., Tsou, M.H., Horng, C.F., Bild, A., Iversen, E.S., Liao, M., Chen, C.M., West, M., Nevins, J.R., Huang, A.T. **(2003)**. Gene expression predictors of breast cancer outcomes. *Lancet.* **361**(9369), 1590-6.

Huang, H.T., Chen, L., Lu, C.X., Xia, C.Q., Xu, Y.M., Zhong, C.J. **(2015)**. Clinical pathological significance of expression of TSPAN-1, KI67 and CD34 in human lung cancer. *Acta Medica Mediterranea.* **31**, 1175.

Hubbard, K.P., Daugherty, K., Ajani, J.A., Pazdur, R., Levin, B., Abbruzzese, J.L. **(1992)**. Phase II trial of fazarabine in advanced colorectal carcinoma. *Invest New Drugs.* **10**(1), 39-42.

Hummel-Eisenbeiss, J., Hascher, A., Hals, P.A., Sandvold, M.L., Müller-Tidow, C., Lyko, F., Rius, M. **(2013)**. The role of human equilibrative nucleoside transporter 1 on the cellular transport of the DNA methyltransferase inhibitors 5-azacytidine and CP-4200 in human leukemia cells. *Mol Pharmacol.* **84**(3), 438-50.

Hurt, E.M., Thomas, S.B., Peng, B., Farrar, W.L. **(2006)**. Reversal of p53 epigenetic silencing in multiple myeloma permits apoptosis by a p53 activator. *Cancer Biol Ther.* **5**(9), 1154-60.

Ikehata, M., Ogawa, M., Yamada, Y., Tanaka, S., Ueda, K., Iwakawa, S. **(2014)**. Different effects of epigenetic modifiers on the cytotoxicity induced by 5-fluorouracil, irinotecan or oxaliplatin in colon cancer cells. *Biol Pharm Bull.* **37**(1), 67-73.

Imanishi, S., Umezu, T., Ohtsuki, K., Kobayashi, C., Ohyashiki, K., Ohyashiki, J.H. **(2014)**. Constitutive activation of the ATM/BRCA1 pathway prevents DNA damage-induced apoptosis in 5-azacytidine-resistant cell lines. *Biochem Pharmacol.* **89**(3), 361-9.

Isella, C., Terrasi, A., Bellomo, S.E., Petti, C., Galatola, G., Muratore, A., Mellano, A., Senetta, R., Cassenti, A., Sonetto, C., Inghirami, G., Trusolino, L., Fekete, Z., De Ridder, M., Cassoni, P., Storme, G., Bertotti, A., Medico, E. **(2015)**. Stromal contribution to the colorectal cancer transcriptome. *Nat Genet.* **47**(4), 312-9.

Issa, J.P., Roboz, G., Rizzieri, D., Jabbour, E., Stock, W., O'Connell, C., Yee, K., Tibes, R., Griffiths, E.A., Walsh, K., Daver, N., Chung, W., Naim, S., Taverna, P., Oganesian, A., Hao, Y., Lowder, J.N., Azab, M., Kantarjian, H. **(2015)**. Safety and tolerability of guadecitabine (SGI-110) in patients with myelodysplastic syndrome and acute myeloid leukaemia: a multicentre, randomised, dose-escalation phase 1 study. *Lancet Oncol.* **16**(9), 1099-110.

Izbicka, E., Davidson, K.K., Lawrence, R.A., MacDonald, J.R., Von Hoff, D.D. **(1999a)**. 5,6-Dihydro-5'-azacytidine (DHAC) affects estrogen sensitivity in estrogen-refractory human breast carcinoma cell lines. *Anticancer Res.* **19**(2A), 1293-8.

Izbicka, E., MacDonald, J.R., Davidson, K., Lawrence, R.A., Gomez, L., Von Hoff, D.D. **(1999b)**. 5,6 Dihydro-5'-azacytidine (DHAC) restores androgen responsiveness in androgen-insensitive prostate cancer cells. *Anticancer Res.* **19**(2A), 1285-91.

Jabbour, E., Kantarjian, H., O'Brien, S., Kadia, T., Malik, A., Welch, M.A., Teng, A., Cortes, J., Ravandi, F., Garcia-Manero, G. **(2013)**. Retrospective analysis of prognostic factors associated with response and overall survival by baseline marrow blast percentage in patients with myelodysplastic syndromes treated with decitabine. *Clin Lymphoma Myeloma Leuk.* **13**(5), 592-6.

Jacinto, F.V., Ballestar, E., Ropero, S., Esteller, M. **(2007)**. Discovery of epigenetically silenced genes by methylated DNA immunoprecipitation in colon cancer cells. *Cancer Res.* **67**(24), 11481-6.

Jain, J.P., Chitkara, D., Kumar, N. **(2008)**. Polyanhydrides as localized drug delivery carrier: an update. *Expert Opin Drug Deliv.* **5**(8), 889-907.

Jain, J.P., Modi, S., Domb, A.J., Kumar, N. **(2005)**. Role of polyanhydrides as localized drug carriers. *J Control Release.* **103**(3), 541-63.

Jeltsch, A., Nellen, W., Lyko, F. **(2006)**. Two substrates are better than one: dual specificities for Dnmt2 methyltransferases. *Trends Biochem Sci.* **31**(6), 306-8.

Jeong, L.S., Zhao, L.X., Choi, W.J., Pal, S., Park, Y.H., Lee, S.K., Chun, M.W., Lee, Y.B., Ahn, C.H., Moon, H.R. **(2007)**. Synthesis and antitumor activity of fluorocyclopentenyl-pyrimidines. *Nucleosides Nucleotides Nucleic Acids.* **26**(6-7), 713-6.

Jeschke, J., Van Neste, L., Glöckner, S.C., Dhir, M., Calmon, M.F., Deregowski, V., Van Criekinge, W., Vlassenbroeck, I., Koch, A., Chan, T.A., Cope, L., Hooker, C.M., Schuebel, K.E., Gabrielson, E., Winterpacht, A., Baylin, S.B., Herman, J.G., Ahuja, N. **(2012)**. Biomarkers for detection and prognosis of breast cancer identified by a functional hypermethylome screen. *Epigenetics.* **7**(7), 701-9.

Jing, Y., Jin, X., Wang, L., Dou, L., Wang, Q., Yao, Y., Lian, S., Zhou, J., Zhu, H., Yao, Z., Gao, L., Wang, L., Li, Y., Bai, X., Fang, M., Yu, L. **(2016)**. Decitabine-based chemotherapy followed by haploidentical lymphocyte infusion improves the effectiveness in elderly patients with acute myeloid leukemia. *Oncotarget.* doi: 10.18632/oncotarget.11183.

Jin, S.H., Akiyama, Y., Fukamachi, H., Yanagihara, K., Akashi, T., Yuasa, Y. **(2008)**. IQGAP2 inactivation through aberrant promoter methylation and promotion of invasion in gastric cancer cells. *Int J Cancer.* **122**(5), 1040-6.

Jones, P.A., Taylor, S.M. **(1980)**. Cellular differentiation, cytidine analogs and DNA methylation. *Cell.* **20**(1) 85-93.

Jones, P.A., Taylor, S.M. **(1981)**. Hemimethylated duplex DNAs prepared from 5-azacytidine-treated cells. *Nucleic Acids Res.* **9**(12), 2933-47.

Jørgensen, H.F., Adie, K., Chaubert, P., Bird, A.P. **(2006)**. Engineering a high-affinity methyl-CpG-binding protein. *Nucleic Acids Res.* **34**(13), e96.

Josling, G.A., Selvarajah, S.A., Petter, M., Duffy, M.F. **(2012)**. The role of bromodomain proteins in regulating gene expression. *Genes (Basel).* **3**(2), 320-43.

Jueliger, S., Lyons, J., Cannito, S., Pata, I., Pata, P., Shkolnaya, M., Lo Re, O., Peyrou, M., Villarroya, F., Pazienza, V., Rappa, F., Cappello, F., Azab, M., Taverna, P., Vinciguerra, M. **(2016)**. Efficacy and epigenetic interactions of novel DNA hypomethylating agent guadecitabine (SGI-110) in preclinical models of hepatocellular carcinoma. *Epigenetics.* **11**, 1-12.

Kanda, T., Sullivan, K.F., Wahl, G.M. **(1998)**. Histone–GFP fusion protein enables sensitive analysis of chromosome dynamics in living mammalian cells. *Curr Biol.* **8**(7), 377-85.

Kantarjian, H.M., Giles, F.J., Greenberg, P.L., Paquette, R.L., Wang, E.S., Gabrilove, J.L., Garcia-Manero, G., Hu, K., Franklin, J.L., Berger, D.P. **(2010)**. Phase 2 study of romiplostim in patients with low- or intermediate-risk myelodysplastic syndrome receiving Azacytidine therapy. *Blood.* **116**(17), 3163-70.

Kantarjian, H., Oki, Y., Garcia-Manero, G., Huang, X., O'Brien, S., Cortes, J., Faderl, S., Bueso-Ramos, C., Ravandi, F., Estrov, Z., Ferrajoli, A., Wierda, W., Shan, J., Davis, J., Giles, F., Saba, H.I., Issa, J.P. **(2007)**. Results of a randomized study of 3 schedules of low-dose decitabine in higher-risk myelodysplastic syndrome and chronic myelomonocytic leukemia. *Blood.* **109**(1), 52-7.

Karantanos, T., Tanimoto, R., Edamura, K., Hirayama, T., Yang, G., Golstov, A.A., Wang, J., Kurosaka, S., Park, S., Thompson, T.C. **(2014)**. Systemic GLIPR1-ΔTM protein as a novel therapeutic approach for prostate cancer. *Int J Cancer.* **134**(8), 2003-13.

Kees, U.R., Avramis, V.I. **(1995)**. Biochemical pharmacology and DNA methylation studies of arabinosyl 5-azacytidine and 5,6-dihydro-5-azacytidine in two human leukemia cell lines PER-145 and PER-163. *Anticancer Drugs.* **6**(2), 303-10.

Kihslinger, J.E., Godley, L.A. **(2007)**. The use of hypomethylating agents in the treatment of hematologic malignancies. *Leuk Lymphoma.* **48**(9), 1676-95.

Kim, C.H., Marquez, V.E., Mao, D.T., Haines, D.R., McCormack, J.J. **(1986)**. Synthesis of pyrimidin-2-one nucleosides as acid-stable inhibitors of cytidine deaminase. *J Med Chem.* **29**(8), 1374-80.

Kim, J.G., Bae, J.H., Kim, J.A., Heo, K., Yang, K., Yi, J.M. **(2014a)**. Combination Effect of Epigenetic Regulation and Ionizing Radiation in Colorectal Cancer Cells. *PLoS ONE*. **9**(8), e105405.

Kim, J.K., Kim, H.J., Chung, J.Y., Lee, J.H., Young, S.B., Kim, Y.H. **(2014b)**. Natural and synthetic biomaterials for controlled drug delivery. *Arch Pharm Res.* **37**(1), 60-8.

Kim, S.J., Tae, C.H., Hong, S.N., Min, B.H., Chang, D.K., Rhee, P.L., Kim, J.J., Kim, H.C., Kim, D.H., Kim, Y.H. **(2015)**. EYA4 Acts as a New Tumor Suppressor Gene in Colorectal Cancer. *Mol Carcinog.* **54**(12), 1748-57.

Kim, Y.H., Kim, W.T., Jeong, P., Ha, Y.S., Kang, H.W., Yun, S.J., Moon, S.K., Choi, Y.H., Kim, I.Y., Kim, W.J. **(2014c)**. Novel Combination Markers for Predicting Survival in Patients with Muscle Invasive Bladder Cancer: USP18 and DGCR2. *J Korean Med Sci.* **29**(3), 351-6.

Kim, Y.H., Lee, H.C., Kim, S.Y., Yeom, Y.I., Ryu, K.J., Min, B.H., Kim, D.H., Son, H.J., Rhee, P.L., Kim, J.J., Rhee, J.C., Kim, H.C., Chun, H.K., Grady, W.M., Kim, Y.S. **(2011)**. Epigenomic analysis of aberrantly methylated genes in colorectal cancer identifies genes commonly affected by epigenetic alterations. *Ann Surg Oncol.* **18**(8), 2338-47.

Kinders, R.J., Wang, L., Kummar, S., Khin, S., Balasubramanian, P., Zhu, W., Parchment, R.E., Newman, E., Tomaszewski, J.E., Doroshow, J.H. **(2011)**. Investigation of 5-fluorodeoxycytidine with tetrahydrouracil as a demethylation regimen in solid tumors. Proceedings of the AACR-NCI-EORTC International Conference; 12-16 November 2011, San Francisco, CA, USA, Abstract A106.

Kipper, M.J., Shen, E., Determan, A., Narasimhan, B. **(2002)**. Design of an injectable system based on bioerodible polyanhydride microspheres for sustained drug delivery. *Biomaterials.* **23**(22), 4405-12.

Kirschbaum, M., Gojo, I., Goldberg, S.L., Bredeson, C., Kujawski, L.A., Yang, A., Marks, P., Frankel, P., Sun, X., Tosolini, A., Eid, J.E., Lubiniecki, G.M., Issa, J.P. **(2014)**. A phase 1

clinical trial of vorinostat in combination with decitabine in patients with acute myeloid leukaemia or myelodysplastic syndrome. *Br J Haematol.* **167**(2), 185-93.

Kobayakawa, S., Miike, K., Nakao, M., Abe, K. **(2007)**. Dynamic changes in the epigenomic state and nuclear organization of differentiating mouse embryonic stem cells. *Genes Cells.* **12**(4), 447-60.

Krug, U., Koschmieder, A., Schwammbach, D., Gerss, J., Tidow, N., Steffen, B., Bug, G., Brandts, C.H., Schaich, M., Röllig, C., Thiede, C., Noppeney, R., Stelljes, M., Büchner, T., Koschmieder, S., Dührsen, U., Serve, H., Ehninger, G., Berdel, W.E., Müller-Tidow, C. **(2012)**. Feasibility of Azacytidine added to standard chemotherapy in older patients with acute myeloid leukemia--a randomised SAL pilot study. *PLoS One.* **7**(12), e52695.

Kuang, Y., El-Khoueiry, A., Taverna, P., Ljungman, M., Neamati, N. **(2015)**. Guadecitabine (SGI-110) priming sensitizes hepatocellular carcinoma cells to oxaliplatin. *Mol Oncol.* **9**(9), 1799-1814.

Kuebler, J.P., Metch, B., Schuller, D.E., Keppen, M., Hynes, H.E. **(1991)**. Phase II study of fazarabine in advanced head and neck cancer. A Southwest Oncology Group study. *Invest New Drugs.* **9**(4), 373-4.

Kumar, S., Horton, J.R., Jones, G.D., Walker, R.T., Roberts, R.J., Cheng, X. **(1997)**. DNA containing 4-thio-2-deoxycytidine inhibits methylation by HhaI methyltransferase. *Nucleic Acids Res.* **25**(14), 2773-83.

Laille, E., Savona, M.R., Scott, B.L., Boyd, T.E., Dong, Q., Skikne, B. **(2014)**. Pharmacokinetics of different formulations of oral Azacytidine (CC-486) and the effect of food and modified gastric pH on pharmacokinetics in subjects with hematologic malignancies. *J Clin Pharmacol.* **54**(6), 630-9.

Lambert, M.P., Herceg, Z. **(2008)**. Epigenetics and cancer, 2nd IARC meeting, Lyon, France, 6 and 7 December 2007. *Mol Oncol.* **2**(1), 33-40.

Langmead, B., Trapnell, C., Pop, M., Salzberg, S.L. **(2009)**. Ultrafast and memory-efficient alignment of short DNA sequences to the human genome. *Genome Biology*. **10,** R25.

Lavelle, D., Saunthararajah, Y., Vaitkus, K., Singh, M., Banzon, V., Phiasivongsva, P., Redkar, S., Kanekal, S., Bearss, D., Shi, C., Inloes, R., DeSimone, J. **(2010)**. S110, a Novel Decitabine Dinucleotide, Increases Fetal Hemoglobin Levels in Baboons (P. anubis). *J Transl Med.* **8**, 92.

Lee, J.H., Jang, J.H., Park, J., Park, S., Joo, Y.D., Kim, Y.K., Kim, H.G., Choi, C.W., Kim, S.H., Park, S.K., Park, E., Min, Y.H. **(2011)**. A prospective multicenter observational study of

decitabine treatment in Korean patients with myelodysplastic syndrome. *Haematologica.* **96**(10), 1441-7.

Lee, K.K., Workman, J.L. **(2007)**. Histone acetyltransferase complexes: one size doesn't fit all. *Nat. Rev. Mol. Cell Biol.* **8**(4), 284-95.

Lee, T.T., Karon, M.R. **(1976)**. Inhibition of protein synthesis in 5-azacytidine-treated HeLa cells. *Biochem Pharmacol.* **25**(15), 1737-42.

Lemaire, M., Momparler, L.F., Bernstein, M.L., Marquez, V.E., Momparler, R.L. **(2005)**. Enhancement of antineoplastic action of 5-aza-2'-deoxycytidine by zebularine on L1210 leukemia. *Anticancer Drugs.* **16**(3), 301-8.

Lemaire, M., Momparler, L.F., Raynal, N.J., Bernstein, M.L., Momparler, R.L. **(2009)**. Inhibition of cytidine deaminase by zebularine enhances the antineoplastic action of 5-aza-2'-deoxycytidine. *Cancer Chemother Pharmacol.* **63**(3), 411-6.

Letsch, A., Keilholz, U., Schadendorf, D., Assfalg, G., Asemissen, A.M., Thiel, E., Scheibenbogen, C. **(2004)**. Functional CCR9 expression is associated with small intestinal metastasis. *J Invest Dermatol.* **122**(3), 685-90.

Liang, J.F., Wang, H.K., Xiao, H., Li, N., Cheng, C.X., Zhao, Y.Z., Ma, Y.B., Gao, J.Z., Bai, R.B., Zheng, H.X. **(2010)**. Relationship and prognostic significance of SPARC and VEGF protein expression in colon cancer. *J Exp Clin Cancer Res.* **29**, 71.

Liao, Y., Smyth, G.K., Shi, W. **(2014)**. featureCounts: an efficient general purpose program for assigning sequence reads to genomic features. *Bioinformatics*. **30,** 923-30.

Li, C., Villacorte, D., Newman, E.M. **(2006)**. 5-Fluoro-2’-deoxycytidine induces re-expression of hypermethylation-silenced genes in the human breast cancer cell line MDA-MB 231. *Proc Amer Assoc Cancer Res.* **66**(8), 381.

Liesveld, J.L., O'Dwyer, K., Walker, A., Becker, M.W., Ifthikharuddin, J.J., Mulford, D., Chen, R., Bechelli, J., Rosell, K., Minhajuddin, M., Jordan, C.T., Phillips, G.L. 2nd. **(2013)**. A phase I study of decitabine and rapamycin in relapsed/refractory AML. *Leuk Res.* **37**(12), 1622-7.

Li, H., Chiappinelli, K.B., Guzzetta, A.A., Easwaran, H., Yen, R.W., Vatapalli, R., Topper, M.J., Luo, J., Connolly, R.M., Azad, N.S., Stearns, V., Pardoll, D.M., Davidson, N., Jones, P.A., Slamon, D.J., Baylin, S.B., Zahnow, C.A., Ahuja, N. **(2014)**. Immune regulation by low doses of the DNA methyltransferase inhibitor 5-azacitidine in common human epithelial cancers. *Oncotarget.* **5**(3), 587-98.

Li, H., Fan, X., Houghton, J. **(2007)**. Tumor microenvironment: The role of the tumor stroma in cancer. *J. Cell. Biochem.* **101**(4), 805-15.

Li, H., Handsaker, B., Wysoker, A., Fennell, T., Ruan, J., Homer, N., Marth, G., Abecasis, G., Durbin, R., 1000 Genome Project Data Processing Subgroup. **(2009)**. The Sequence alignment/map (SAM) format and SAMtools. *Bioinformatics.* **25**(16), 2078-9.

Li, L., Abdel Fattah, E., Cao, G., Ren, C., Yang, G., Goltsov, A.A., Chinault, A.C., Cai, W.W., Timme, T.L., Thompson, T.C. **(2008)**. Glioma pathogenesis-related protein 1 exerts tumor suppressor activities through proapoptotic reactive oxygen species-c-Jun-NH2 kinase signaling. *Cancer Res.* **68**(2), 434-43.

Li, L.C., Dahiya, R. **(2002)**. MethPrimer: designing primers for methylation PCRs. *Bioinformatics.* **18**(11), 1427-31.

Li, L.H., Olin, E.J., Buskirk, H.H., Reineke, L.M. **(1970)**. Cytotoxicity and mode of action of 5-azacytidine on L1210 leukemia. *Cancer Res.* **30**(11), 2760-9.

Li, L., Ren, C., Yang, G., Fattah, E.A., Goltsov, A.A., Kim, S.M., Lee, J.S., Park, S., Demayo, F.J., Ittmann, M.M., Troncoso, P., Thompson, T.C. **(2011)**. GLIPR1 suppresses prostate cancer development through targeted oncoprotein destruction. *Cancer Res.* **71**(24), 7694-704.

Lin, B.R., Chang, C.C., Che, T.F., Chen, S.T., Chen, R.J., Yang, C.Y., Jeng, Y.M., Liang, J.T., Lee, P.H., Chang, K.J., Chau, Y.P., Kuo, M.L. **(2005)**. Connective tissue growth factor inhibits metastasis and acts as an independent prognostic marker in colorectal cancer. *Gastroenterology* **128**(1), 9-23.

Lin, J., Gilbert, J., Rudek, M.A., Zwiebel, J.A., Gore, S., Jiemjit, A., Zhao, M., Baker, S.D., Ambinder, R.F., Herman, J.G., Donehower, R.C., Carducci, M.A. **(2009)**. A phase I dose-finding study of 5-azacytidine in combination with sodium phenylbutyrate in patients with refractory solid tumors. *Clin Cancer Res.* **15**(19), 6241-9.

Linnekamp, J.F., Wang, X., Medema, J.P., Vermeulen, L. **(2015)**. Colorectal Cancer Heterogeneity and Targeted Therapy: A Case for Molecular Disease Subtypes. *Cancer Res.* **75**(2), 245-9.

Liotta, L.A., Kohn, E.C. **(2001)**. The microenvironment of the tumour-host interface. *Nature.* **411**(6835), 375-9.

Liu, Q.Z., Gao, X.H., Chang, W.J., Wang, H.T., Wang, H., Cao, G.W., Fu, C.G. **(2015)**. Secreted protein acidic and rich in cysteine expression in human colorectal cancer predicts postoperative prognosis. *Eur Rev Med Pharmacol Sci.* **19**(10), 1803-11.

Liu, Z., Xie, Z., Aimiuwu, J., Ling, Y., Covey, J., Chan, K. **(2009)**. Cytotoxicity and hypomethylation activity of 5-Fluoro-2'-deoxycytidine and decitabine on human cancer cell lines. AACR Annual Meeting; 18-22 April 2009, Denver, CO, USA, Abstract 3377.

Li, X., Mei, Q., Nie, J., Fu, X., Han, W. **(2015a)**. Decitabine: a promising epi-immunotherapeutic agent in solid tumors. *Expert Rev. Clin. Immunol.* **11**(3), 363-75.

Li, X.Q., Du, X., Li, D.M., Kong, P.Z., Sun, Y., Liu, P.F., Wang, Q.S., Feng, Y.M. **(2015b)**. ITGBL1 Is a Runx2 Transcriptional Target and Promotes Breast Cancer Bone Metastasis by Activating the TGFβ Signaling Pathway. *Cancer Res.* 7**5**(16), 3302-13.

Llinàs, A., Burley, J.C., Box, K.J., Glen, R.C., Goodman, J.M. **(2007)**. Diclofenac solubility: Independent determination of the intrinsic solubility of three crystal forms. *J Med Chem.* **50**(5), 979-83.

Lotti, F., Jarrar, A.M., Pai, R.K., Hitomi, M., Lathia, J., Mace, A., Gantt, G.A. Jr, Sukhdeo, K., DeVecchio, J., Vasanji, A., Leahy, P., Hjelmeland, A.B., Kalady, M.F., Rich, J.N. **(2013)**. Chemotherapy activates cancer-associated fibroblasts to maintain colorectal cancer-initiating cells by IL-17A. *J. Exp. Med.* 210**(13)**, 2851-72.

Love, M.I., Huber, W., Anders, S. **(2014)**. Moderated estimation of fold change and dispersion for RNA-seq data with DESeq2. *Genome biology*. **15,** 550.

Lübbert, M., Suciu, S., Baila, L., Rüter, B.H., Platzbecker, U., Giagounidis, A., Selleslag, D., Labar, B., Germing, U., Salih, H.R., Beeldens, F., Muus, P., Pflüger, K.H., Coens, C., Hagemeijer, A., Eckart Schaefer, H., Ganser, A., Aul, C., de Witte, T., Wijermans, P.W. **(2011)**. Low-dose decitabine versus best supportive care in elderly patients with intermediate- or high-risk myelodysplastic syndrome (MDS) ineligible for intensive chemotherapy: final results of the randomized phase III study of the European Organisation for Research and Treatment of Cancer Leukemia Group and the German MDS Study Group. *J Clin Oncol.* **29**(15), 1987-96.

Lu, C.C., Wang, X.J., Wu, G.L., Wang, J.J., Wang, Y.N., Gao, H., Ma, J.B. **(2014)**. An injectable and biodegradable hydrogel based on poly(alpha,beta-aspartic acid) derivatives for localized drug delivery. *J Biomed Mater Res Part A.* **102**(3), 628-38.

Lu, Z., Luo, T., Nie, M., Pang, T., Zhang, X., Shen, X., Ma, L., Bi, J., Wei, G., Fang, G., Xue, X. **(2015)**. TSPAN1 functions as an oncogene in gastric cancer and is downregulated by miR-573. *FEBS Lett.* **589**(15), 1988-94.

Lyons, J., Bayar, E., Fine, G., McCullar, M., Rolens, R., Rubinfeld, J., Rosenfeld, C. **(2003)**. Decitabine: Development of a DNA methyltransferase inhibitor for hematological malignancies. *Curr Opin Investig Drugs.* **4**(12), 1442-50.

Mack, G.S. **(2010)**. To selectivity and beyond. *Nat Biotechnol.* **28**(12), 1259-66.

MacPhee, D.G. **(1998)**. Epigenetics and epimutagens: some new perspectives on cancer, germ line effects and endocrine disrupters. *Mutat Res.* **400**(1-2), 369-79.

Mahfouz, R.Z., Jankowska, A., Ebrahem, Q., Gu, X., Visconte, V., Tabarroki, A., Terse, P., Covey, J., Chan, K., Ling, Y., Engelke, K.J., Sekeres, M.A., Tiu, R., Maciejewski, J., Radivoyevitch, T., Sauntharajah, Y. **(2013)**. Increased CDA expression/activity in males contributes to decreased cytidine analog half-life and likely contributes to worse outcomes with 5-azacytidine or decitabine therapy. *Clin Cancer Res.* **19**(4), 938-48.

Malik, A., Shoukier, M., Garcia-Manero, G., Wierda, W., Cortes, J., Bickel, S., Keating, M.J., Estrov, Z. **(2013)**. Azacytidine in fludarabine-refractory chronic lymphocytic leukemia: a phase II study. *Clin Lymphoma Myeloma Leuk.* **13**(3), 292-5.

Manetta, A., Blessing, J.A., Look, K.Y. **(1995b)**. A phase II study of fazarabine in patients with advanced ovarian cancer. A Gynecologic Oncology Group study. *Am J Clin Oncol.* **18**(2), 156-7.

Manetta, A., Blessing, J.A., Mann, W.J., Smith, D.M. **(1995a)**. A phase II study of fazarabine (NSC 281272) in patients with advanced squamous cell carcinoma of the cervix. A Gynecologic Oncology Group study. *Am J Clin Oncol.* **18**(5), 439-40.

Manini, I., Sgorbissa, A., Potu, H., Tomasella, A., & Brancolini, C. **(2013)**. The DeISGylase USP18 limits TRAIL-induced apoptosis through the regulation of TRAIL levels: Cellular levels of TRAIL influences responsiveness to TRAIL-induced apoptosis. *Cancer Biol Ther.* **14**(12), 1158-66.

Matei, D., Fang, F., Shen, C., Schilder, J., Arnold, A., Zeng, Y., Berry, W.A., Huang, T., Nephew, K.P. **(2012)**. Epigenetic resensitization to platinum in ovarian cancer. *Cancer Res.* **72**(9), 2197-205.

Matoušová, M., Votruba, I., Otmar, M., Tloušťová, E., Günterová, J., Mertlíková-Kaiserová, H. **(2011)**. 2′-deoxy-5,6-dihydro-5-azacytidine-a less toxic alternative of 2′-deoxy-5-azacytidine: A comparative study of hypomethylating potential. *Epigenetics.* **6**(6), 769-76.

Mayer, J., Arthur, C., Delaunay, J., Mazur, G., Thomas, X.G., Wierzbowska, A., Ravandi, F., Berrak, E., Jones, M., Li, Y., Kantarjian, H.M. **(2014)**. Multivariate and subgroup analyses of a randomized, multinational, phase 3 trial of decitabine vs treatment choice of supportive care or cytarabine in older patients with newly diagnosed acute myeloid leukemia and poor- or intermediate-risk cytogenetics. *BMC Cancer.* **14**, 69.

Mayer, R.J. **(2012)**. Oxaliplatin as part of adjuvant therapy for colon cancer: more complicated than once thought. *J Clin Oncol.* **30**(27), 3325-7.

McMillin, D.W., Negri, J.M., Mitsiades, C.S. **(2013)**. The role of tumour-stromal interactions in modifying drug response: challenges and opportunities. *Nat Rev Drug Discov.* **12**(3), 217-28.

Meador, J.A., Su, Y., Ravanat, J.L., Balajee, A.S. **(2010)**. DNA-dependent protein kinase (DNA-PK)-deficient human glioblastoma cells are preferentially sensitized by Zebularine. *Carcinogenesis.* **31**(2), 184-91.

Melki, J.R., Clark, S.J. **(2002)**. DNA methylation changes in leukaemia. *Semin Cancer Biol.* **12**(5), 347-57.

Merritt, J.A., Meltzer, D.M., Ball, L.A., Borden, E.C. **(1985)**. 2-5A synthetase activity in patients with metastatic carcinoma and its response to interferon treatment. *Prog Clin Biol Res.* **202**, 423-30.

Momparler, R.L., Derse, D. **(1979)**. Kinetics of phosphorylation of 5-aza-2'-deoxyycytidine by deoxycytidine kinase. *Biochem Pharmacol.* **28**(8), 1443-4.

Moran, D.M., Gawlak, G., Jayaprakash, M.S., Mayar, S., Maki, C.G. **(2008)**. Geldanamycin promotes premature mitotic entry and micronucleation in irradiated p53/p21 deficient colon carcinoma cells. *Oncogene.* **27**(42), 5567-77.

Morfouace, M., Nimmervoll, B., Boulos, N., Patel, Y.T., Shelat, A., Freeman, B.B. 3rd, Robinson, G.W., Wright, K., Gajjar, A., Stewart, C.F., Gilbertson, R.J., Roussel, M.F. **(2016)**. Preclinical studies of 5-fluoro-2'-deoxycytidine and tetrahydrouridine in pediatric brain tumors. *J Neurooncol.* **126**(2), 225-34.

Moriwaki, K., Narisada, M., Imai, T., Shinzaki, S., Miyoshi, E. **(2010)**. The effect of epigenetic regulation of fucosylation on TRAIL-induced apoptosis. *Glycoconj J.* **27**(7-9), 649-59.

Morris, M.R., Ricketts, C., Gentle, D., Abdulrahman, M., Clarke, N., Brown, M., Kishida, T., Yao, M., Latif, F., Maher, E.R. **(2010)**. Identification of candidate tumour suppressor genes frequently methylated in renal cell carcinoma. *Oncogene.* **29**(14), 2104-17.

Mullany, S.A., Moslemi-Kebria, M., Rattan, R., Khurana, A., Clayton, A., Ota, T., Mariani, A., Podratz, K.C., Chien, J., Shridhar, V. **(2011)**. Expression and functional significance of HtrA1 loss in endometrial cancer. *Clin Cancer Res.* **17**(3), 427-36.

Mullins, J.I., Heath, L., Hughes, J.P., Kicha, J., Styrchak, S., Wong, K.G., Rao, U., Hansen, A., Harris, K.S., Laurent, J.P., Li, D., Simpson, J.H., Essigmann, J.M., Loeb, L.A., Parkins, J. **(2011)**. Mutation of HIV-1 genomes in a clinical population treated with the mutagenic nucleoside KP1461. *PLoS One.* **6**(1), e15135.

Munshi, P. N., Lubin, M., Bertino, J. R. **(2014)**. 6-thioguanine: a drug with unrealized potential for cancer therapy. *Oncologist.* **19**(7), 760-5.

Nakamura, K., Aizawa, K., Nakabayashi, K., Kato, N., Yamauchi, J., Hata, K., Tanoue, A. **(2013)**. DNA methyltransferase inhibitor zebularine inhibits human hepatic carcinoma cells proliferation and induces apoptosis. *PLoS One.* **8**(1), e54036.

Nakamura, K., Nakabayashi, K., Htet Aung, K., Aizawa, K., Hori, N., Yamauchi, J., Hata, K., Tanoue, A. **(2015)**. DNA methyltransferase inhibitor zebularine induces human cholangiocarcinoma cell death through alteration of DNA methylation status. *PLoS One.* **10**(3), e0120545.

Nand, S., Othus, M., Godwin, J.E., Willman, C.L., Norwood, T.H., Howard, D.S., Coutre, S.E., Erba, H.P., Appelbaum, F.R. **(2013)**. A phase 2 trial of azacytidine and gemtuzumab ozogamicin therapy in older patients with acute myeloid leukemia. *Blood.* **122**(20), 3432-9.

Nelson, J.A., Carpenter, J.W., Rose, L.M., Adamson, D.J. **(1975)**. Mechanisms of action of 6-thioguanine, 6-mercaptopurine, and 8-azaguanine. *Cancer Res.* **35**(10), 2872-8.

Nervi, C., De Marinis, E., Codacci-Pisanelli, G. **(2015)**. Epigenetic treatment of solid tumors: a review of clinical trials. *Clin Epigenetics.* **7**, 127.

Neureiter, D., Zopf, S., Leu, T., Dietze, O., Hauser-Kronberger, C., Hahn, E.G., Herold, C., Ocker, M. **(2007)**. Apoptosis, proliferation and differentiation patterns are influenced by Zebularine and SAHA in pancreatic cancer models. *Scand J Gastroentero.* **42**(1), 103-116.

Newman, E.M., Morgan, R.J., Kummar, S., Beumer, J.H., Blanchard, M.S., Ruel, C., El-Khoueiry, A.B., Carroll, M.I., Hou, J.M., Li, C., Lenz, H.J., Eiseman, J.L., Doroshow, J.H. **(2015)**. A phase I, pharmacokinetic, and pharmacodynamic evaluation of the DNA methyltransferase inhibitor 5-fluoro-2′-deoxycytidine, administered with tetrahydrouridine. *Cancer Chemother Pharmacol.* **75**(3), 537-46.

Newman, E.M., Santi, D.V. **(1982)**. Metabolism and mechanism of action of 5-fluorodeoxycytidine. *Proc Natl Acad Sci U S A.* **79**(21), 6419-23.

Nishihori, T., Perkins, J., Mishra, A., Komrokji, R., Kim, J., Kharfan-Dabaja, M.A., Perez, L., Lancet, J., Fernandez, H., List, A., Anasetti, C., Field, T. **(2014)**. Pretransplantation 5-azacytidine in high-risk myelodysplastic syndrome. *Biol Blood Marrow Transplant.* **20**(6), 776-80.

Noetzel, E., Veeck, J., Niederacher, D., Galm, O., Horn, F., Hartmann, A., Knüchel, R., Dahl, E. **(2008)**. Promoter methylation-associated loss of ID4 expression is a marker of tumour recurrence in human breast cancer. *BMC Cancer.* **8**, 154.

Okano, M., Bell, D.W., Haber, D.A., Li, E. **(1999)**. DNA methyltransferases Dnmt3a and Dnmt3b are essential for de novo methylation and mammalian development. *Cell.* **99**(3), 247-57.

Okano, M., Xie, S., Li, E. **(1998)**. Cloning and characterization of a family of novel mammalian DNA (cytosine-5) methyltransferases. *Nat Genet.* **19**(3), 219-20.

Oki, Y., Jelinek, J., Shen, L., Kantarjian, H.M., Issa, J.P. **(2008)**. Induction of hypomethylation and molecular response after decitabine therapy in patients with chronic myelomonocytic leukemia. *Blood.* **111**(4), 2382-4.

Oki, Y., Kondo, Y., Yamamoto, K., Ogura, M., Kasai, M., Kobayashi, Y., Watanabe, T., Uike, N., Ohyashiki, K., Okamoto, S., Ohnishi, K., Tomita, A., Miyazaki, Y., Tohyama, K., Mukai, H.Y., Hotta, T., Tomonaga, M. **(2012)**. Phase I/II study of decitabine in patients with myelodysplastic syndrome: a multi-center study in Japan. *Cancer Sci.* **103**(10), 1839-47.

Okochi-Takada, E., Ichimura, S., Kaneda, A., Sugimura, T., Ushijima, T. **(2004)**. Establishment of a detection system for demethylating agents using an endogenous promoter CpG island. *Mutat Res.* **568**(2), 187-94.

Oricchio, E., Nanjangud, G., Wolfe, A.L., Schatz, J.H., Mavrakis, K.J., Jiang, M., Liu, X., Bruno, J., Heguy, A., Olshen, A.B., Socci, N.D., Teruya-Feldstein, J., Weis-Garcia, F., Tam, W., Shaknovich, R., Melnick, A., Himanen, J.P., Chaganti, R.S., Wendel, H.G. **(2011)**. The Eph-receptor A7 is a soluble tumor suppressor for follicular lymphoma. *Cell.* **147**(3), 554-64.

Owen, D.J., Ornaghi, P., Yang, J.C., Lowe, N., Evans, P.R., Ballario, P., Neuhaus, D., Filetici, P., Travers, A.A. **(2000)**. The structural basis for the recognition of acetylated histone H4 by the bromodomain of histone acetyltransferase gcn5p. *EMBO J.* **19**(22), 6141-9.

Palii, S.S., Van Emburgh, B.O., Sankpal, U.T., Brown, K.D., Robertson, K.D. **(2008)**. DNA methylation inhibitor 2'-deoxy-5-azacytidine induces reversible genome-wide DNA damage that is distinctly influenced by DNA methyltransferases 1 and 3B. *Mol Cell Biol.* **28**(2), 752-71.

Panayiotou, H., Orsi, N.M., Thygesen, H.H., Wright, A.I., Winder, M., Hutson, R., Cummings, M. **(2015)**. The prognostic significance of tumour-stroma ratio in endometrial carcinoma. *BMC Cancer.* **15**, 955.

Pardini, B., Kumar, R., Naccarati, A., Novotny, J., Prasad, R.B., Forsti, A., Hemminki, K., Vodicka, P., Lorenzo Bermejo, J. **(2011)**. 5-Fluorouracil-based chemotherapy for colorectal cancer and MTHFR/MTRR genotypes. *Br J Clin Pharmacol.* **72**(1), 162-3.

Parent, M., Nouvel, C., Koerber, M., Sapin, A., Maincent, P., Boudier, A. **(2013)**. PLGA in situ implants formed by phase inversion: Critical physicochemical parameters to modulate drug release. *J Control Release.* **172**(1), 292-304.

Passweg, J.R., Pabst, T., Blum, S., Bargetzi, M., Li, Q., Heim, D., Stussi, G., Gregor, M., Leoncini, L., Meyer-Monard, S., Brauchli, P., Chalandon, Y; Swiss Group for Clinical Cancer Research (SAKK). **(2014)**. Swiss Group for Clinical Cancer Research (SAKK). Azacytidine for acute myeloid leukemia in elderly or frail patients: a phase II trial (SAKK 30/07). *Leuk Lymphoma.* **55**(1), 87-91.

Pereira, D.Y., Yip, A.T., Lee, B.S., Kamei, D.T. **(2014)**. Modeling Mass Transfer from Carmustine-Loaded Polymeric Implants for Malignant Gliomas. *J Lab Autom.* **19**(1), 19-34.

Perlíková, P., Rylová, G., Nauš, P., Elbert, T., Tloušťová, E., Bourderioux, A., Slavětínská, L.P., Motyka, K., Doležal, D., Znojek, P., Nová, A., Harvanová, M., Džubák, P., Šiller, M., Hlaváč, J., Hajdúch, M., Hocek, M. **(2016)**. 7-(2-Thienyl)-7-Deazaadenosine (AB61), a New Potent Nucleoside Cytostatic with a Complex Mode of Action. *Mol Cancer Ther.* **15**(5), 922-37.

Peters, G.J., Smid, K., Vecchi, L., Kathmann, I., Sarkisjan, D., Honeywell, R.J., Losekoot, N., Ohne, O., Orbach, A., Blaugrund, E., Jeong, L.S., Lee, Y.B., Ahn, C.H., Kim, D.J. **(2013)**. Metabolism, mechanism of action and sensitivity profile of fluorocyclopentenylcytosine (RX-3117; TV-1360). *Invest New Drugs.* **31**(6), 1444-57.

Piva, R., Belardo, G., Santoro, M.G. **(2006)**. NF-kappaB: a stress-regulated switch for cell survival. *Antioxid Redox Signal.* **8**(3-4), 478-86.

Policianova, O., Brus, J., Hruby, M., Urbanova, M., Zhigunov, A., Kredatusova, J., Kobera, L. **(2014)**. Structural Diversity of Solid Dispersions of Acetylsalicylic Acid As Seen by Solid-State NMR. *Mol Pharmaceutics.* **11**(2), 516-30.

Pollyea, D.A., Kohrt, H.E., Gallegos, L., Figueroa, M.E., Abdel-Wahab, O., Zhang, B., Bhattacharya, S., Zehnder, J., Liedtke, M., Gotlib, J.R., Coutre, S., Berube, C., Melnick, A., Levine, R., Mitchell, B.S., Medeiros, B.C. **(2012)**. Safety, efficacy and biological predictors of response to sequential azacytidine and lenalidomide for elderly patients with acute myeloid leukemia. *Leukemia.* **26**(5), 893-901.

Pollyea, D.A., Zehnder, J., Coutre, S., Gotlib, J.R., Gallegos, L., Abdel-Wahab, O., Greenberg, P., Zhang, B., Liedtke, M., Berube, C., Levine, R., Mitchell, B.S., Medeiros, B.C. **(2013)**. Sequential azacytidine plus lenalidomide combination for elderly patients with untreated acute myeloid leukemia. *Haematologica.* **98**(4), 591-6.

Potu, H., Sgorbissa, A., Brancolini, C. **(2010)**. Identification of USP18 as an important regulator of the susceptibility to IFN-alpha and drug-induced apoptosis. *Cancer Res.* **70**(2), 655-65.

Powell, W.C., Avramis, V.I. **(1988)**. Biochemical pharmacology of 5,6-dihydro-5-azacytidine (DHAC) and DNA hypomethylation in tumor (L1210)-bearing mice. Cancer *Chemother Pharmacol.* **21**(2), 117-21.

Prebet, T., Sun, Z., Ketterling, R.P., Zeidan, A., Greenberg, P., Herman, J., Juckett, M., Smith, M.R., Malick, L., Paietta, E., Czader, M., Figueroa, M., Gabrilove, J., Erba, H.P., Tallman, M.S., Litzow, M., Gore, S.D., Eastern Cooperative Oncology Group and North American Leukemia intergroup. **(2016)**. Azacitidine with or without Entinostat for the treatment of therapy-related myeloid neoplasm: further results of the E1905 North American Leukemia Intergroup study. *Br J Haematol.* **172**(3), 384-91.

Qin, T., Castoro, R., El Ahdab, S., Jelinek, J., Wang, X., Si, J., Shu, J., He, R., Zhang, N., Chung, W., Kantarjian, H.M., Issa, J.P. **(2011)**. Mechanisms of resistance to decitabine in the myelodysplastic syndrome. *PLoS One.* **6**(8), e23372.

Qin, T., Jelinek, J., Si, J., Shu, J., Issa, J.P. **(2009)**. Mechanisms of resistance to 2'-deoxy-5-azacytidine in human cancer cell lines. *Blood.* **113**(3), 659-67.

Qiu, X., Hother, C., Ralfkiær, U.M., Søgaard, A., Lu, Q., Workman, C.T., Liang, G., Jones, P.A., Grønbæk, K. **(2010)**. Equitoxic doses of 5-azacytidine and 5-aza-2'deoxycytidine induce diverse immediate and overlapping heritable changes in the transcriptome. *PLoS One.* **5**(9), e12994.

Qi, Y., Li, Y., Zhang, Y., Zhang, L., Wang, Z., Zhang, X., Gui, L., Huang, J. **(2015)**. IFI6 Inhibits Apoptosis via Mitochondrial-Dependent Pathway in Dengue Virus 2 Infected Vascular Endothelial Cells. *PLoS One.* **10**(8), e0132743.

Rajabi, H., Tagde, A., Alam, M., Bouillez, A., Pitroda, S., Suzuki, Y., Kufe, D. **(2016)**. DNA methylation by DNMT1 and DNMT3b methyltransferases is driven by the MUC1-C oncoprotein in human carcinoma cells. *Oncogene.* **35**(50), 6439-45.

Ravandi, F., Alattar, M.L., Grunwald, M.R., Rudek, M.A., Rajkhowa, T., Richie, M.A., Pierce, S., Daver, N., Garcia-Manero, G., Faderl, S., Nazha, A., Konopleva, M., Borthakur, G., Burger, J., Kadia, T., Dellasala, S., Andreeff, M., Cortes, J., Kantarjian, H., Levis, M. **(2013)**. Phase 2 study of azacytidine plus sorafenib in patients with acute myeloid leukemia and FLT-3 internal tandem duplication mutation. *Blood.* **121**(23), 4655-62.

Rhee, I., Jair, K.W., Yen, R.W., Lengauer, C., Herman, J.G., Kinzler, K.W., Vogelstein, B., Baylin, S.B., Schuebel, K.E. **(2000)**. CpG methylation is maintained in human cancer cells lacking DNMT1. *Nature.* **404**(6781), 1003-7.

Richards, K.L., Zhang, B., Sun, M., Dong, W., Churchill, J., Bachinski, L.L., Wilson, C.D., Baggerly, K.A., Yin, G., Hayes, D.N., Wistuba, I.I., Krahe, R. **(2011)**. Methylation of the candidate biomarker TCF21 is very frequent across a spectrum of early-stage nonsmall cell lung cancers. *Cancer.* **117**(3), 606-17.

Rius, M., Stresemann, C., Keller, D., Brom, M., Schirrmacher, E., Keppler, D., Lyko, F. **(2009)**. Human concentrative nucleoside transporter 1-mediated uptake of 5-azacytidine enhances DNA demethylation. *Mol Cancer Ther.* **8**(1), 225-31.

Robak, T. **(2011)**. New nucleoside analogs for patients with hematological malignancies. *Expert Opin Investig Drugs.* **20**(3), 343-59.

Robertson, K.D. **(2001)**. DNA methylation, methyltransferases, and cancer. *Oncogene.* **20**(24), 3139-155.

Robertson, K.D., Uzvolgyi, E., Liang, G., Talmadge, C., Sumegi, J., Gonzales, F.A., Jones, P.A. **(1999)**. The human DNA methyltransferases (DNMTs) 1, 3a and 3b: coordinate mRNA expression in normal tissues and overexpression in tumors. *Nucleic Acids Res.* **27**(11), 2291-8.

Rogstad, D.K., Herring, J.L., Theruvathu, J.A., Burdzy, A., Perry, C.C., Neidigh, J.W., Sowers, L.C. **(2009)**. Chemical Decomposition of 5-Aza-2 '-deoxycytidine (Decitabine): Kinetic Analyses and Identification of Products by NMR, HPLC, and Mass Spectrometry. *Chem Res Toxicol.* **22**(6), 1194-1204.

Ruiz-Magaña, M.J., Rodríguez-Vargas, J.M., Morales, J.C., Saldivia, M.A., Schulze-Osthoff, K., Ruiz-Ruiz, C. **(2012)**. The DNA methyltransferase inhibitors zebularine and decitabine induce mitochondria-mediated apoptosis and DNA damage in p53 mutant leukemic T cells. *Int J Cancer.* **130**(5), 1195-1207.

Sabatino, M.A., Geroni, C., Ganzinelli, M., Ceruti, R., Broggini, M. **(2013)**. Zebularine partially reverses GST methylation in prostate cancer cells and restores sensitivity to the DNA minor groove binder brostallicin. *Epigenetics.* **8**(6), 656-65.

Saif, M.W., Kaley, K., Penney, R., Hotchkiss, S., Syrigos, K.N., Strimpakos, A.S. **(2011)**. The efficacy of gemcitabine as salvage treatment in patients with refractory advanced colorectal cancer (CRC): a single institution experience. *Anticancer Res.* **31**(9), 2971-4.

Samoszuk, M., Tan, J., Chorn, G. **(2005)**. Clonogenic growth of human breast cancer cells co-cultured in direct contact with serum-activated fibroblasts. *Breast Cancer Res.* **7**(3), R274-83.

Sarkisjan, D., Julsing, J.R., Smid, K., de Klerk, D., van Kuilenburg, A.B., Meinsma, R., Lee, Y.B., Kim, D.J., Peters, G.J. **(2016)**. The Cytidine Analog Fluorocyclopentenylcytosine (RX-3117) Is Activated by Uridine-Cytidine Kinase 2. *PLoS One.* **11**(9), e0162901.

Saunthararajah, Y., Sekeres, M., Advani, A., Mahfouz, R., Durkin, L., Radivoyevitch, T., Englehaupt, R., Juersivich, J., Cooper, K., Husseinzadeh, H., Przychodzen, B., Rump, M., Hobson, S., Earl, M., Sobecks, R., Dean, R., Reu, F., Tiu, R., Hamilton, B., Copelan, E., Lichtin, A., His, E., Kalaycio, M., Maciejewski, J. **(2015)**. Evaluation of noncytotoxic DNMT1-depleting therapy in patients with myelodysplastic syndromes. *J Clin Invest.* **125**(3), 1043-55.

Savickiene, J., Treigyte, G., Borutinskaite, V.V., Navakauskiene, R. **(2012a)**. Antileukemic activity of combined epigenetic agents, DNMT inhibitors zebularine and RG108 with HDAC inhibitors, against promyelocytic leukemia HL-60 cells. *Cell Mol Biol Lett.* **17**(4), 501-25.

Savickiene, J., Treigyte, G., Jonusiene, V., Bruzaite, R., Borutinskaite, V.V., Navakauskiene, R. **(2012b)**. Epigenetic changes by zebularine leading to enhanced differentiation of human promyelocytic leukemia NB4 and KG1 cells. *Mol Cell Biochem.* **359**(1-2), 245-61.

Scandura, J.M., Roboz, G.J., Moh, M., Morawa, E., Brenet, F., Bose, J.R., Villegas, L., Gergis, U.S., Mayer, S.A., Ippoliti, C.M., Curcio, T.J., Ritchie, E.K., Feldman, E.J. **(2011)**. Phase 1 study of epigenetic priming with decitabine prior to standard induction chemotherapy for patients with AML. *Blood.* **118**(6), 1472-80.

Schaefer, M., Hagemann, S., Hanna, K., Lyko, F. **(2009)**. Azacytidine inhibits RNA methylation at DNMT2 target sites in human cancer cell lines. *Cancer Res.* **69**(20), 8127-32.

Schmidt, V.A., Chiariello, C.S., Capilla, E., Miller, F., Bahou, W.F. **(2008)**. Development of hepatocellular carcinoma in Iqgap2-deficient mice is IQGAP1 dependent. *Mol Cell Biol.* **28**(5), 1489-502.

Scott, S.A., Lakshimikuttysamma, A., Sheridan, D.P., Sanche, S.E., Geyer, C.R., DeCoteau, J.F. **(2007)**. Zebularine inhibits human acute myeloid leukemia cell growth in vitro in association with p15INK4B demethylation and reexpression. *Exp Hematol.* **35**(2), 263-73.

Sekeres, M.A., Tiu, R.V., Komrokji, R., Lancet, J., Advani, A.S., Afable, M., Englehaupt, R., Juersivich, J., Cuthbertson, D., Paleveda, J., Tabarroki, A., Visconte, V., Makishima, H., Jerez, A., Paquette, R., List, A.F., Maciejewski, J.P. **(2012)**. Phase 2 study of the lenalidomide and Azacytidine combination in patients with higher-risk myelodysplastic syndromes. *Blood.* **120**(25), 4945-51.

Selby, G.B., Upchurch, C., Townsend, J., Eyre, H.J. **(1994)**. A phase II evaluation of fazarabine in high-grade gliomas: a Southwest Oncology Group study. *Cancer Chemother Pharmacol.* **34**(2), 179-80.

Silverman, L.R., Demakos, E.P., Peterson, B.L., Kornblith, A.B., Holland, J.C., Odchimar-Reissig, R., Stone, R.M., Nelson, D., Powell, B.L., DeCastro, C.M., Ellerton, J., Larson, R.A., Schiffer, C.A., Holland, J.F. **(2002)**. Randomized controlled trial of azacitidine in patients with the myelodysplastic syndrome: a study of the cancer and leukemia group B. *J Clin Oncol.* **20**(10), 2429-40.

Silverman, L.R., Fenaux, P., Mufti, G.J., Santini, V., Hellström-Lindberg, E., Gattermann, N., Sanz, G., List, A.F., Gore, S.D., Seymour, J.F. **(2011)**. Continued azacytidine therapy beyond time of first response improves quality of response in patients with higher-risk myelodysplastic syndromes. *Cancer.* **117**(12), 2697-702.

Simó-Riudalbas, L., Melo, S.A., Esteller, M. **(2011)**. DNMT3B gene amplification predicts resistance to DNA demethylating drugs. *Genes Chromosomes Cancer.* **50**(7), 527-34.

Singal, R., Ramachandran, K., Gordian, E., Quintero, C., Zhao, W., Reis, I.M. **(2015)**. Phase I/II study of azacytidine, docetaxel, and prednisone in patients with metastatic castration-resistant prostate cancer previously treated with docetaxel-based therapy. *Clin Genitourin Cancer.* **13**(1), 22-31.

Singh, S., Singh, U.P., Stiles, J.K., Grizzle, W.E., Lillard, J.W. Jr. **(2004)**. Expression and functional role of CCR9 in prostate cancer cell migration and invasion. *Clin Cancer Res.* **10**(24), 8743-50.

Singh, V., Sharma, P., Capalash, N. **(2013)**. DNA Methyltransferase-1 Inhibitors as Epigenetic Therapy for Cancer. *Curr Cancer Drug Targets.* **13**(4), 379-99.

Skolekova, S., Matuskova, M., Bohac, M., Toro, L., Durinikova, E., Tyciakova, S., Demkova, L., Gursky, J., Kucerova, L. **(2016)**. Cisplatin-induced mesenchymal stromal cells-mediated mechanism contributing to decreased antitumor effect in breast cancer cells. *Cell Commun. Signal. CCS.* **14**, 4.

Smith, L.T., Lin, M., Brena, R.M., Lang, J.C., Schuller, D.E., Otterson, G.A., Morrison, C.D., Smiraglia, D.J., Plass, C. **(2006)**. Epigenetic regulation of the tumor suppressor gene TCF21 on 6q23-q24 in lung and head and neck cancer. *Proc Natl Acad Sci U S A.* **103**(4), 982-7.

Son, C.H., Lee, H.R., Koh, E.K., Shin, D.Y., Bae, J.H., Yang, K., Park, Y.S. **(2016)**. Combination treatment with decitabine and ionizing radiation enhances tumor cells susceptibility of T cells. *Sci. Rep.* **6,** 32470.

Soriano, A.O., Yang, H., Faderl, S., Estrov, Z., Giles, F., Ravandi, F., Cortes, J., Wierda, W.G., Ouzounian, S., Quezada, A., Pierce, S., Estey, E.H., Issa, J.P., Kantarjian, H.M., Garcia-Manero, G. **(2007)**. Safety and clinical activity of the combination of 5-azacytidine, valproic acid, and all-trans retinoic acid in acute myeloid leukemia and myelodysplastic syndrome. *Blood.* **110**(7), 2302-8.

Sorm, F., Píškala, A., Cihák, A., Veselý, J. **(1964)**. 5-Azacytidine, a new, highly effective. *cancerostatic*. *Experientia.* **20**(4), 202-3.

Sorrentino, C., Di Carlo, E. **(2009)**. Expression of IL-32 in human lung cancer is related to the histotype and metastatic phenotype. *Am J Respir Crit Care Med.* **180**(8), 769-79.

Sripayap, P., Nagai, T., Uesawa, M., Kobayashi, H., Tsukahara, T., Ohmine, K., Muroi, K., Ozawa, K. **(2014)**. Mechanisms of resistance to azacitidine in human leukemia cell lines. *Exp Hematol.* **42**(4), 294-306.

Srivastava, P., Paluch, B.E., Matsuzaki, J., James, S.R., Collamat-Lai, G., Karbach, J., Nemeth, M.J., Taverna, P., Karpf, A.R., Griffiths, E.A. **(2014)**. Immunomodulatory action of SGI-110, a hypomethylating agent, in acute myeloid leukemia cells and xenografts. *Leuk Res.* **38**(11), 1332-41.

Srivastava, P., Paluch, B.E., Matsuzaki, J., James, S.R., Collamat-Lai, G., Taverna, P., Karpf, A.R., Griffiths, E.A. **(2015)**. Immunomodulatory action of the DNA methyltransferase inhibitor SGI-110 in epithelial ovarian cancer cells and xenografts. *Epigenetics.* **10**(3), 237-46.

Stelzer, Y., Shivalila, C.S., Soldner, F., Markoulaki, S., Jaenisch, R. **(2015)**. Tracing dynamic changes of DNA methylation at single-cell resolution. *Cell.* **163**(1), 218-29.

Stresemann, C., Lyko, F. **(2008)**. Modes of action of the DNA methyltransferase inhibitors azacytidine and decitabine. *Int J Cancer.* **123**(1), 8-13.

Sun, L., Wang, D., Li, X., Zhang, L., Zhang, H., Zhang, Y. **(2016)**. Extracellular matrix protein ITGBL1 promotes ovarian cancer cell migration and adhesion through Wnt/PCP signaling and FAK/SRC pathway. *Biomed Pharmacother.* **81**, 145-51.

Sun, P., Xia, S., Lal, B., Eberhart, C.G., Quinones-Hinojosa, A., Maciaczyk, J., Matsui, W., Dimeco, F., Piccirillo, S.M., Vescovi, A.L., Laterra, J. **(2009)**. DNER, an epigenetically modulated gene, regulates glioblastoma-derived neurosphere cell differentiation and tumor propagation. *Stem Cells.* **27**(7), 1473-86.

Surbone, A., Ford, H., Kelley, J.A., Ben-Baruch, N., Thomas, R.V., Fine, R., Cowan, K.H. **(1990)**. Phase I and Pharmacokinetic Study of Arabinofuranosyl-5-azacytosine (Fazarabine, NSC 281272). *Cancer Res.* **50**(4), 1220-5.

Suzuki, M., Shinohara, F., Nishimura, K., Echigo, S., Rikiishi, H. **(2007)**. Epigenetic regulation of chemosensitivity to 5-fluorouracil and cisplatin by zebularine in oral squamous cell carcinoma. *Int J Oncol*. **31**(6), 1449-56.

Suzuki, M., Shinohara, F., Rikiishi, H. **(2008)**. Zebularine-induced reduction in VEGF secretion by HIF-1α degradation in oral squamous cell carcinoma. *Mol Med Rep.* **1**(4), 465-71.

Tabata, K., Kurosaka, S., Watanabe, M., Edamura, K., Satoh, T., Yang, G., Abdelfattah, E., Wang, J., Goltsov, A., Floryk, D., Thompson, T.C. **(2011)**. Tumor growth and metastasis suppression by Glipr1 gene-modified macrophages in a metastatic prostate cancer model. *Gene Ther.* **18**(10), 969-78.

Tai, I. T., Dai, M., Owen, D. A., Chen, L. B. **(2005)**. Genome-wide expression analysis of therapy-resistant tumors reveals SPARC as a novel target for cancer therapy. *Journal of Clinical Investigation.* **115**(6), 1492-1502.

Takai, D., Jones, P.A. **(2002)**. Comprehensive analysis of CpG islands in human chromosomes 21 and 22. *Proc Natl Acad Sci USA.* **99**(6), 3740-5.

Tan, W., Zhou, W., Yu, H.G., Luo, H.S., Shen, L. **(2013)**. The DNA methyltransferase inhibitor zebularine induces mitochondria-mediated apoptosis in gastric cancer cells in vitro and in vivo. Biochem Biophys *Res Commun.* **430**(1), 250-5.

Tellez, C.S., Grimes, M.J., Picchi, M.A., Liu, Y., March, T.H., Reed, M.D., Oganesian, A., Taverna, P., Belinsky, S.A. **(2014)**. SGI-110 and entinostat therapy reduces lung tumor burden and reprograms the epigenome. *Int J Cancer.* **135**(9), 2223-31.

Teomim, D., Domb, A.J. **(1999)**. Fatty acid terminated polyanhydrides. *J Polym Sci, Part A: Polym Chem.* **37**(16), 3337-44.

Terzić, J., Grivennikov, S., Karin, E., Karin, M. **(2010)**. Inflammation and colon cancer. *Gastroenterology.* **138**(6), 2101-14.

Thayanithy, V., Park, C., Sarver, A.L., Kartha, R.V., Korpela, D.M., Graef, A.J., Steer, C.J., Modiano, J.F., Subramanian, S. **(2012)**. Combinatorial treatment of DNA and chromatin-modifying drugs cause cell death in human and canine osteosarcoma cell lines. *PLoS One.* **7**(9), e43720.

Thottassery, J.V., Sambandam, V., Allan, P.W., Maddry, J.A., Maxuitenko, Y.Y., Tiwari, K., Hollingshead, M., Parker, W.B. **(2014)**. Novel DNA methyltransferase-1 (DNMT1) depleting anticancer nucleosides, 4'-thio-2'-deoxycytidine and 5-aza-4'-thio-2'-deoxycytidine. *Cancer Chemother Pharmacol.* **74**(2), 291-302.

Tlsty, T.D., Hein, P.W. **(2001)**. Know thy neighbor: stromal cells can contribute oncogenic signals. *Curr. Opin. Genet. Dev.* **11**(1), 54-9.

Traganos, F., Staiano-Coico, L., Darzynkiewicz, Z., Melamed, M.R. **(1981)**. Effects of dihydro-5-azacytidine on cell survival and cell cycle progression of cultured mammalian cells. *Cancer Res.* **41**(3), 780-9.

Trievel, R.C. **(2004)**. Structure and function of histone methyltransferases. *Crit Rev Eukaryot Gene Expr.* **14**(3), 147-69.

Tsai, C.Y., Wang, C.S., Tsai, M.M., Chi, H.C., Cheng, W.L., Tseng, Y.H., Chen, C.Y., Lin, C.D., Wu, J.I., Wang, L.H., Lin, K.H. **(2014)**. Interleukin-32 increases human gastric cancer cell invasion associated with tumor progression and metastasis. *Clin Cancer Res.* **20**(9), 2276-88.

Tsimberidou, A.M., Said, R., Culotta, K., Wistuba, I., Jelinek, J., Fu, S., Falchook, G., Naing, A., Piha-Paul, S., Zinner, R., Siddik, Z.H., He, G., Hess, K., Stewart, D.J., Kurzrock, R., Issa, J.P. **(2015)**. Phase I study of azacitidine and oxaliplatin in patients with advanced cancers that have relapsed or are refractory to any platinum therapy. *Clin. Epigenetics.* **7**, 29.

Tsujino, T., Seshimo, I., Yamamoto, H., Ngan, C.Y., Ezumi, K., Takemasa, I., Ikeda, M., Sekimoto, M., Matsuura, N., Monden, M. **(2007)**. Stromal Myofibroblasts Predict Disease Recurrence for Colorectal Cancer. *Clin. Cancer Res.* **13**(7), 2082-90.

Ueda, J., Maehara, K., Mashiko, D., Ichinose, T., Yao, T., Hori, M., Sato, Y., Kimura, H., Ohkawa, Y., Yamagata, K. **(2014)**. Heterochromatin dynamics during the differentiation process revealed by the DNA methylation reporter mouse, MethylRO. *Stem Cell Reports.* **2**(6), 910-24.

Ulazzi, L., Sabbioni, S., Miotto, E., Veronese, A., Angusti, A., Gafà, R., Manfredini, S., Farinati, F., Sasaki, T., Lanza, G., Negrini, M. **(2007)**. Nidogen 1 and 2 gene promoters are aberrantly methylated in human gastrointestinal cancer. *Mol Cancer.* **6**, 17.

Umetani, N., Takeuchi, H., Fujimoto, A., Shinozaki, M., Bilchik, A.J., Hoon, D.S. **(2004)**. Epigenetic inactivation of ID4 in colorectal carcinomas correlates with poor differentiation and unfavorable prognosis. *Clin Cancer Res.* **10**(22), 7475-83.

Urbanova, M., Brus, J., Sedenkova, I., Policianova, O., Kobera, L. **(2013)**. Characterization of solid polymer dispersions of active pharmaceutical ingredients by F-19 MAS NMR and factor analysis. *Spectrochim Acta A Mol Biomol Spectrosc.* **100**, 59-66.

Valencia, A., Masala, E., Rossi, A., Martino, A., Sanna, A., Buchi, F., Canzian, F., Cilloni, D., Gaidano, V., Voso, M.T., Kosmider, O., Fontenay, M., Gozzini, A., Bosi, A., Santini, V. **(2014)**. Expression of nucleoside-metabolizing enzymes in myelodysplastic syndromes and modulation of response to azacitidine. *Leukemia.* **28**(3), 621-8.

Vanaja, D.K., Ballman, K.V., Morlan, B.W., Cheville, J.C., Neumann, R.M., Lieber, M.M., Tindall, D.J., Young, C.Y. **(2006)** PDLIM4 repression by hypermethylation as a potential biomarker for prostate cancer. *Clin Cancer Res.* **12**(4), 1128-36.

Vanaja, D.K., Grossmann, M.E., Cheville, J.C., Gazi, M.H., Gong, A., Zhang, J.S., Ajtai, K., Burghardt, T.P., Young, C.Y. **(2009)**. PDLIM4, an actin binding protein, suppresses prostate cancer cell growth. *Cancer Invest.* **27**(3), 264-72.

Vermeulen, L., De Sousa, E., Melo, F., van der Heijden, M., Cameron, K., de Jong, J.H., Borovski, T., Tuynman, J.B., Todaro, M., Merz, C., Rodermond, H., Sprick, M.R., Kemper, K., Richel, D.J., Stassi, G., Medema, J.P. **(2010)**. Wnt activity defines colon cancer stem cells and is regulated by the microenvironment. *Nat Cell Biol.* **12**(5), 468-76.

Vertino, P.M., Yen, R.W., Gao, J., Baylin, S.B. **(1996)**. De novo methylation of CpG island sequences in human fibroblasts overexpressing DNA (cytosine-5-)-methyltransferase. *Mol Cell Biol.* **16**(8), 4555-65.

Veselý, J., Píškala, A. **(1984)**. Effects of the alpha-D-anomer of 5-aza-2'-deoxycytidine on L1210 mouse leukemic cells in vitro and in vivo. *Cancer Res.* **44**(11), 5165-8.

Veselý, J., Píškala, A. **(1986)**. Mechanism of action of 1-beta-D-arabinofuranosyl-5-azacytosine and its effects in L1210 mouse leukemia cells. *Neoplasma.* **33**(1), 3-10.

Voytek, P., Beisler, J.A., Abbasi, M.M., Wolpert-DeFilippes, M.K. **(1977)**. Comparative studies of the cytostatic action and metabolism of 5-azacytidine and 5,6-dihydro-5-azacytidine. *Cancer Res.* **37**(7 Pt 1), 1956-61.

Wallace, R.E., Lindh, D., Durr, F.E. **(1989)**. Arabinofuranosyl-5-azacytosine: activity against human tumors in athymic mice. *Cancer Chemother Pharmacol.* **25**(2), 117-23.

Walter, R.B., Medeiros, B.C., Gardner, K.M., Orlowski, K.F., Gallegos, L., Scott, B.L., Hendrie, P.C., Estey, E.H. **(2014)**. Gemtuzumab ozogamicin in combination with vorinostat and azacytidine in older patients with relapsed or refractory acute myeloid leukemia: a phase I/II study. *Haematologica.* **99**(1), 54-9.

Walters, R.S., Theriault, R.L., Holmes, F.A., Hortobagyi, G.N., Esparza, L. **(1992)**. Phase II trial of fazarabine (ARA-AC, arabinosyl-5-azacytosine) in metastatic breast cancer. *Invest New Drugs.* **10**(1), 43-4.

Wang, H., Wang, X.Q., Xu, X.P., Lin, G.W. **(2010)**. ID4 methylation predicts high risk of leukemic transformation in patients with myelodysplastic syndrome. *Leuk Res.* **34**(5), 598-604.

Wang, H., Wang, Y. **(2009)**. 6-Thioguanine perturbs cytosine methylation at the CpG dinucleotide site by DNA methyltransferases in vitro and acts as a DNA demethylating agent in vivo. *Biochemistry.* **48**(10), 2290-9.

Wang, J., Kataoka, H., Suzuki, M., Sato, N., Nakamura, R., Tao, H., Maruyama, K., Isogaki, J., Kanaoka, S., Ihara, M., Tanaka, M., Kanamori, M., Nakamura, T., Shinmura, K., Sugimura, H. **(2005)**. Downregulation of EphA7 by hypermethylation in colorectal cancer. *Oncogene.* **24**(36), 5637-47.

Wang, J., Li, G., Ma, H., Bao, Y., Wang, X., Zhou, H., Sheng, Z., Sugimura, H., Jin, J., Zhou, X. **(2007)**. Differential expression of EphA7 receptor tyrosine kinase in gastric carcinoma. *Hum Pathol.* **38**(11), 1649-56.

Wang, N., Eckert, K.A., Zomorrodi, A.R., Xin, P., Pan, W., Shearer, D.A., Weisz, J., Maranus, C.D., Clawson, G.A. **(2012)**. Down-regulation of HtrA1 activates the epithelial-mesenchymal transition and ATM DNA damage response pathways. *PLoS One.* **7**(6), e39446.

Wang, S., Chen, F., Tang, L. **(2015)**. IL-32 promotes breast cancer cell growth and invasiveness. *Oncol Lett.* **9**(1), 305-7.

Wang, Y., Cardenas, H., Fang, F., Condello, S., Taverna, P., Segar, M., Liu, Y., Nephew, K.P., Matei, D. **(2014)**. Epigenetic targeting of ovarian cancer stem cells. *Cancer Res.* **74**(17), 4922-36.

Welch, J.S., Klco, J.M., Gao, F., Procknow, E., Uy, G.L., Stockerl-Goldstein, K.E., Abboud, C.N., Westervelt, P., DiPersio, J.F., Hassan, A., Cashen, A.F., Vij, R. **(2011)**. Combination decitabine, arsenic trioxide, and ascorbic acid for the treatment of myelodysplastic syndrome and acute myeloid leukemia: a phase I study. *Am J Hematol.* **86**(9), 796-800.

Welch, J.S., Petti, A.A., Miller, C.A., Fronick, C.C., O'Laughlin, M., Fulton, R.S., Wilson, R.K., Baty, J.D., Duncavage, E.J., Tandon, B., Lee, Y.S., Wartman, L.D., Uy, G.L., Ghobadi, A., Tomasson, M.H., Pusic, I., Romee, R., Fehniger, T.A., Stockerl-Goldstein, K.E., Vij, R., Oh, S.T., Abboud, C.N., Cashen, A.F., Schroeder, M.A., Jacoby, M.A., Heath, S.E., Luber, K., Janke, M.R., Hantel, A., Khan, N., Sukhanova, M.J., Knoebel, R.W., Stock, W., Graubert, T.A., Walter, M.J., Westervelt, P., Link, D.C., DiPersio, J.F., Ley, T.J. **(2016)**. TP53 and Decitabine in Acute Myeloid Leukemia and Myelodysplastic Syndromes. *N Engl J Med.* **375**(21), 2023-36.

Wempen, I., Duschinsky, R., Kaplan, L., Fox, J.J. **(1961)**. Thiation of Nucleosides. IV. The Synthesis of 5-Fluoro-2'-deoxycytidine and Related Compounds. *J Am Chem Soc.* **83**(23), 4755-66.

Wilhelm, M., O'Brien, S., Rios, M.B., Estey, E., Keating, M.J., Plunkett, W., Sorenson, M., Kantarjian, H.M. **(1999)**. Phase I study of arabinosyl-5-azacytidine (fazarabine) in adult acute leukemia and chronic myelogenous leukemia in blastic phase. *Leuk Lymphoma.* **34**(5-6), 511-8.

Williamson, S.K., Crowley, J.J., Livingston, R.B., Panella, T.J., Goodwin, J.W. **(1995)**. Phase II trial and cost analysis of fazarabine in advanced non-small cell carcinoma of the lung: A southwest oncology group study. *Invest New Drugs.* **13**(1), 67-71.

Wilson, I.M., Vucic, E.A., Enfield, K.S., Thu, K.L., Zhang, Y.A., Chari, R., Lockwood, W.W., Radulovich, N., Starczynowski, D.T., Banáth, J.P., Zhang, M., Pusic, A., Fuller, M., Lonergan, K.M., Rowbotham, D., Yee, J., English, J.C., Buys, T.P., Selamat, S.A., Laird-Offringa, I.A., Liu, P., Anderson, M., You, M., Tsao, M.S., Brown, C.J., Bennewith, K.L., MacAulay, C.E., Karsan, A., Gazdar, A.F., Lam, S., Lam, W.L. **(2014)**. EYA4 is inactivated biallelically at a high frequency in sporadic lung cancer and is associated with familial lung cancer risk. *Oncogene.* **33**(36), 4464-73.

Winfield, J., Esbitt, A., Seutter, S.F., Desai, B., Abdo, M., Vasconez, M., Laidlaw, W., Green, K., Shamseddin, S.M., Borghaei, R.C. **(2016)**. Effect of Inflammatory Cytokines on DNA Methylation and Demethylation. *FASEB J.* **30**(1), 1053.3.

Woodcock, T.M., Chou, T.C., Tan, C.T., Sternberg, S.S., Philips, F.S., Young, C.W., Burchenal, J.H. **(1980)**. Biochemical, pharmacological, and phase I clinical evaluation of pseudoisocytidine. *Cancer Res.* **40**(11), 4243-9.

Wrangle, J., Wang, W., Koch, A., Easwaran, H., Mohammad, H.P., Vendetti, F., Vancriekinge, W., Demeyer, T., Du, Z., Parsana, P., Rodgers, K., Yen, R.W., Zahnow, C.A., Taube, J.M., Brahmer, J.R., Tykodi, S.S., Easton, K., Carvajal, R.D., Jones, P.A., Laird, P.W., Weisenberger, D.J., Tsai, S., Juergens, R.A., Topalian, S.L., Rudin, C.M., Brock, M.V., Pardoll, D., Baylin, S.B. **(2013)**. Alterations of immune response of Non-Small Cell Lung Cancer with Azacytidine. *Oncotarget.* **4**(11), 2067-79.

Wu, D., Du, X., Jin, J., Xiao, Z., Shen, Z., Shao, Z., Li, X., Huang, X., Liu, T., Yu, L., Li, J., Chen, B., He, G., Cai, Z., Liang, H., Li, J., Ruan, C. **(2015)**. Decitabine for Treatment of Myelodysplastic Syndromes in Chinese Patients: An Open-Label, Phase-3b Study. *Adv Ther.* **32**(11), 1140-59.

Wu, J., Houghton, P.J. **(2010)**. Interval approach to assessing antitumor activity for tumor xenograft studies. *Pharm Stat.* **9**(1), 46-54.

Wu, J. **(2010)**. STATISTICAL INFERENCE FOR TUMOR GROWTH INHIBITION T/C RATIO. *J Biopharm Stat.* **20**(5), 954-64.

Xia, C., Leon-Ferre, R., Laux, D., Deutsch, J., Smith, B.J., Frees, M., Milhem, M. **(2014)**. Treatment of resistant metastatic melanoma using sequential epigenetic therapy (decitabine and panobinostat) combined with chemotherapy (temozolomide). *Cancer Chemother Pharmacol.* **74**(4), 691-7.

Xiao, Y.H., Li, X.H., Tan, T., Liang, T., Yi, H., Li, M.Y., Zeng, G.Q., Wan, X.X., Qu, J.Q., He, Q.Y., Li, J.H., Chen, Y., Xiao, Z.Q. **(2011)**. Identification of GLIPR1 tumor suppressor as methylation-silenced gene in acute myeloid leukemia by microarray analysis. *J Cancer Res Clin Oncol.* **137**(12), 1831-40.

Xie, Y., Yan, J., Cutz, J.C., Rybak, A.P., He, L., Wei, F., Kapoor, A., Schmidt, V.A., Tao, L., Tang, D. **(2012)**. IQGAP2, A candidate tumour suppressor of prostate tumorigenesis. *Biochim Biophys Acta.* **1822**(6), 875-84.

Xu, R.R., Liu, F., Cui, X., Zhang, X.W., Wang, Y. **(2011)**. ID4 promoter methylation in acute myeloid leukemia. *Zhongguo Shi Yan Xue Ye Xue Za Zhi.* **19**(3), 582-4.

Yacqub-Usman, K., Duong, C.V., Clayton, R.N., Farrell, W.E. **(2013)**. Preincubation of pituitary tumor cells with the epidrugs zebularine and trichostatin A are permissive for retinoic acid-augmented expression of the BMP-4 and D2R genes. *Endocrinology.* **154**(5), 1711-21.

Yan, F., Shen, N., Pang, J., Molina, J.R., Yang, P., Liu, S. **(2015)**. The DNA Methyltransferase DNMT1 and Tyrosine-Protein Kinase KIT Cooperatively Promote Resistance to 5-Aza-2'-deoxycytidine (Decitabine) and Midostaurin (PKC412) in Lung Cancer Cells. *J Biol Chem.* **290**(30), 18480-94.

Yang, E., Kang, H.J., Koh, K.H., Rhee, H., Kim, N.K., Kim, H. **(2007)**. Frequent inactivation of SPARC by promoter hypermethylation in colon cancers. *Int J Cancer.* **121**(3), 567-75.

Yang, M.Y., Lee, Y.B., Ahn, C.H.., Kaye, J., Fine, T., Kashi, R., Ohne, O., Smid, K., Peters, G.J., Kim, D.J. **(2014a)**. A novel cytidine analog, RX-3117, shows potent efficacy in xenograft models, even in tumors that are resistant to gemcitabine. *Anticancer Res.* **34**(12), 6951-9.

Yang, P.M., Lin, Y.T., Shun, C.T., Lin, S.H., Wei, T.T., Chuang, S.H., Wu, M.S., Chen, C.C. **(2013)**. Zebularine inhibits tumorigenesis and stemness of colorectal cancer via p53-dependent endoplasmic reticulum stress. *Sci Rep.* **3**, 3219.

Yang, X., Lay, F., Han, H., Jones, P.A. **(2010)**. Targeting DNA methylation for epigenetic therapy. *Trends Pharmacol. Sci.* **31**(11), 536-46.

Yang, Y., Wang, Z., Zhou, Y., Wang, X., Xiang, J., Chen, Z. **(2015)**. Dysregulation of over-expressed IL-32 in colorectal cancer induces metastasis. *World J Surg Oncol.* **13**, 146.

Yang, Z., Li, D.M., Xie, Q., Dai, D.Q. **(2014b)**. Protein Expression and Promoter Methylation of the Candidate Biomarker TCF21 in Gastric Cancer. *J Cancer Res Clin Oncol.* **141**(2), 211-20.

Yegin, Z., Gunes, S., Buyukalpelli, R. **(2013)**. Hypermethylation of TWIST1 and NID2 in tumor tissues and voided urine in urinary bladder cancer patients. *DNA Cell Biol.* **32**(7), 386-92.

Ye, K., Wang, S., Wang, J., Han, H., Ma, B., Yang, Y. **(2016)**. Zebularine enhances apoptosis of human osteosarcoma cells by suppressing methylation of ARHI. *Cancer Sci.* **107**(12), 1851-7.

Yogelzang, N.J., Herndon, J.E. 2nd, Cirrincione, C., Harmon, D.C., Antman, K.H., Corson, J.M., Suzuki, Y., Citron, M.L., Green, M.R. **(1997)**. Dihydro-5-azacytidine in malignant mesothelioma. A phase II trial demonstrating activity accompanied by cardiac toxicity. Cancer and Leukemia Group B. *Cancer.* **79**(11), 2237-42.

Yoo, C.B., Chuang, J.C., Byun, H.M., Egger, G., Yang, A.S., Dubeau, L., Long, T., Laird, P.W., Marquez, V.E., Jones, P.A. **(2008)**. Long-term epigenetic therapy with oral zebularine has minimal side effects and prevents intestinal tumors in mice. *Cancer Prev Res (Phila).* **1**(4), 233-40.

Yoo, C.B., Jeong, S., Egger, G., Liang, G., Phiasivongsa, P., Tang, C., Redkar, S., Jones, P.A. **(2007)**. Delivery of 2'-deoxy-5-azacytidine to cells using oligodeoxynucleotides. *Cancer Res.* **67**(13), 6400-8.

Yoshihara, K., Shahmoradgoli, M., Martínez, E., Vegesna, R., Kim, H., Torres-Garcia, W., Treviño, V., Shen, H., Laird, P.W., Levine, D.A., Carter, S.L., Getz, G., Stemke-Hale, K., Mills, G.B., Verhaak, R.G. **(2013)**. Inferring tumour purity and stromal and immune cell admixture from expression data. *Nat. Commun.* **4**, 2612.

You, B.R., Park, W.H. **(2012)**. Zebularine inhibits the growth of HeLa cervical cancer cells via cell cycle arrest and caspase-dependent apoptosis. *Mol Biol Rep.* **39**(10), 9723-31.

You, B.R., Park, W.H. **(2013)**. Zebularine-induced apoptosis in Calu-6 lung cancer cells is influenced by ROS and GSH level changes. *Tumour Biol.* **34**(2), 1145-53.

You, B.R., Park, W.H. **(2014)**. Zebularine inhibits the growth of A549 lung cancer cells via cell cycle arrest and apoptosis. *Mol Carcinog.* **53**(11), 847-57.

Yousif, N.G., Al-Amran, F.G., Hadi, N., Lee, J., Adrienne, J. **(2013)**. Expression of IL-32 modulates NF-κB and p38 MAP kinase pathways in human esophageal cancer. *Cytokine.* **61**(1), 223-7.

Yuan, B., Zhang, J., Wang, H., Xiong, L., Cai, Q., Wang, T., Jacobsen, S., Pradhan, S., Wang, Y. **(2011)**. 6-Thioguanine reactivates epigenetically silenced genes in acute lymphoblastic leukemia cells by facilitating proteasome-mediated degradation of DNMT1. *Cancer Res.* **71**(5), 1904-11.

Yu, Y., Shao, W., Hu, Y., Zhang, J., Song, H., Zhu, Z. **(2012)**. HtrA1 expression associated with the occurrence and development of esophageal cancer. *World J Surg Oncol.* **10**, 179.

Zhang, J., Bian, Z., Zhou, J., Song, M., Liu, Z., Feng, Y., Zhe, L., Zhang, B., Yuan, Y., Huang, Z. **(2015)**. MicroRNA-638 inhibits cell proliferation by targeting phospholipase D1 in human gastric carcinoma. *Protein Cell.* **6**(9), 680-8.

Zhang, Y., Li, B., Ji, Z.Z., Zheng, P.S. **(2010)**. Notch1 regulates the growth of human colon cancers. *Cancer.* **116**(22), 5207-18.

Zhao, L.X., Yun, M., Kim, H.O., Lee, J.A., Choi, W.J., Lee, K.M., Lee, S.K., Lee, Y.B., Ahn, C.H., Jeong, L.S. **(2005)**. Design, synthesis, and anticancer activity of fluorocyclopentenyl-pyrimidines. *Nucleic Acids Symp Ser (Oxf).* **49**, 107-8.

Zhao, Q., Fan, J., Hong, W., Li, L., Wu, M. **(2012)**. Inhibition of cancer cell proliferation by 5-fluoro-2'-deoxycytidine, a DNA methylation inhibitor, through activation of DNA damage response pathway. *Springerplus.* **1**(1), 65.

Zhou, L., Cheng, X., Connolly, B.A., Dickman, M.J., Hurd, P.J., Hornby, D.P. **(2002)**. Zebularine: a novel DNA methylation inhibitor that forms a covalent complex with DNA methyltransferases. *J Mol Biol.* **321**(4), 591-9.

Ziemba, A., Hayes, E., Freeman, B.B. 3rd, Ye, T., Pizzorno, G. **(2011)**. Development of an oral form of azacytidine: 2'3'5'triacetyl-5-azacytidine. *Chemother Res Pract.* **2011**, 965826.

Zou, H., Osborn, N.K., Harrington, J.J., Klatt, K.K., Molina, J.R., Burgart, L.J., Ahlquist, D.A. **(2005)**. Frequent methylation of eyes absent 4 gene in Barrett's esophagus and esophageal adenocarcinoma. *Cancer Epidemiol Biomarkers Prev.* **14**(4), 830-4.

Zou, Z., Huang, B., Wu, X., Zhang, H., Qi, J., Bradner, J., Nair, S., Chen, L.F. **(2014)**. Brd4 maintains constitutively active NF-κB in cancer cells by binding to acetylated RelA. *Oncogene.* **33**(18), 2395-404.

Zurawa-Janicka, D., Kobiela, J., Galczynska, N., Stefaniak, T., Lipinska, B., Lachinski, A., Skorko-Glonek, J., Narkiewicz, J., Proczko-Markuszewska, M., Sledzinski, Z. **(2012)**.

Changes in expression of human serine protease HtrA1, HtrA2 and HtrA3 genes in benign and malignant thyroid tumors. *Oncol Rep.* **28**(5), 1838-44.

Bibliography

▪ Original research articles and reviews

Hruby, M., **Agrawal, K.,** Policianova, O., Brus, J., Skopal, J., Svec, P., Otmar, M., Dzubak, P., Stepanek, P., Hajduch, M. **(2016)**. Biodegradable system for drug delivery of hydrolytically labile azanucleoside drugs. *Biomed Pap Med Fac Univ Palacky Olomouc Czech Repub*. **160** (2), 222-30.

Agrawal, K., Das, V., Otmar, M., Krečmerová, M., Džubák, P., Hajdúch, M. **(2016)**. Cell-based DNA demethylation detection system for screening of epigenetic drugs in 2D, 3D and xenograft models. *Cytometry A.* **91**(2), 133-43.

Annadurai, N., **Agrawal, K.,** Džubák, P., Hajdúch, M., Das, V. **(2017)**. Microtubule-affinity regulating kinases are potential druggable targets for Alzheimer's disease. *Cell Mol Life Sci.* 10.1007/s00018-017-2574-1.

▪ Articles in preparation/under review

Agrawal, K., Hajdúch, M. **(2017)**. Nucleosidic DNA demethylating epi-drugs – From discovery to clinic.

Agrawal, K., Das, V., Gursky, J., Táborská, N., Miklíková, S., Václavková, J., Džubák, P., Hajdúch, M. **(2017)**. Senescent-stromal cells drive colorectal cancer cell response to DNA demethylating epi-drugs.

Agrawal, K., Vojta, P., Slavkovský, R., Frydrych, I., Das, V., Vrbková, J., Džubák, P., Hajdúch, M. **(2017)**. BET inhibitor in reversal of secondary decitabine resistance in solid tumor.

Agrawal, K., Hajdúch, M. **(2017)**. Non-nucleosidic DNA methyltransferase inhibitors – Getting ready for the clinic.

Hruška, M., Varanasi, L., Voller, J., **Agrawal, K.,** Džubák, P., Hajdúch, M. **(2017)**. A variant peptide identification system for bottom up proteomics.

Patents

Patent: EP 2 924 125 A1, Published: 30.09.2015, Ownership: Palacky University Olomouc, Inventors: **Agrawal Khushboo,** Dzubak Petr, Hajduch Marian, Frydrych Ivo.

▪ Abstracts

Agrawal, K., Džubák, P., Hajdúch, M. **(2011)**. Study of epigenetic 5-azacytidine nucleosides and their derivatives. *Biomed Pap Med Fac Univ Palacky Olomouc Czech Repub.* **155**(4), S1-S10.

Agrawal, K., Frydrych, I., Džubák, P., Hajdúch, M. **(2012)**. Study of epigenetic 5-azacytidine nucleosides and their derivatives. *Onkologie.* **6**, B20-B21.

Agrawal, K., Frydrych, I., Džubák, P., Hajdúch, M. **(2012)**. Study of epigenetic 5-azacytidine nucleosides and their derivatives. *Biomed Pap Med Fac Univ Palacky Olomouc Czech Repub.* **156**(3), S117-S126.

Agrawal, K., Frydrych, I., Džubák, P., Hajdúch, M. **(2013)**. Study of epigenetic therapeutics - 5-azacytidine derivatives. *Proceedings: Conference of Chemical Biology and Genetics.*

Agrawal, K., Frydrych, I., Džubák, P., Hajdúch, M. **(2013)**. Study of epigenetic therapeutics - 5-azacytidine derivatives. *Chem. Listy.* **107**, 403-44.

Agrawal, K., Džubák, P., Frydrych, I., Holub, D., Krečmerová, M., Otmar, M., Hajdúch, M. **(2013)**. Epigenetic study of 5-azacytidine nucleosides and their derivatives. *Abstract Book: IX. Diagnostic, Predictive and Experimental Oncology Days.*

Das, V., **Agrawal, K.,** Džubák, P., Hajdúch, M. **(2013)**. Activity of demethylating agents in a three-dimensional cell culture model. *Abstract Book: IX. Diagnostic, Predictive and Experimental Oncology Days.*

Voller, J., Hruška, M., Džubák, P., **Agrawal, K.,** Holub, D., Vojta, P., Macečková, Z., Hajdúch, M. **(2013)**. A system for identification and quantification of mutations in proteomic data. *Abstract Book: IX. Diagnostic, Predictive and Experimental Oncology Days*.

Agrawal, K., Džubák, P., Frydrych, I., Holub, D., Krečmerová, M., Otmar, M., Hajdúch, M. **(2013)**. Epigenetic study of 5-azacytidine nucleosides and their derivatives. *New Frontiers in the Research of PhD Students: 10th International Medical Postgraduate Conference.*

Agrawal, K., Džubák, P., Frydrych, I., Holub, D., Vojta, P., Krečmerová, M., Otmar, M., Hajdúch, M. **(2014)**. 5-azacytidine nucleosides and their derivatives: Molecular hallmarks of drug resistance. *Proceedings: Young Oncologists Award for the best scientific work in Cancer Research.* ISBN 978 -80 -971621-0-8.

Agrawal, K., Džubák, P., Frydrych, I., Holub, D., Vojta, P., Krečmerová, M., Otmar, M., Hajdúch, M. **(2014)**. 5-azacytidine nucleosides and their derivatives: Molecular hallmarks of drug resistance. *Cancer Res.* **74**, 400.

Agrawal, K., Vojta, P., Holub, D., Frydrych, I., Džubák, P., Otmar, M., Hajdúch, M. **(2014)**. 5-Azacytidine Nucleosides and their Derivatives: Molecular Hallmarks of Drug Resistance & Alternative Therapeutic Regimen. *Abstract Book: X. Diagnostic, Predictive and Experimental Oncology Days.*

Agrawal, K., Vojta, P., Holub, D., Frydrych, I., Džubák, P., Otmar, M., Krečmerová, M., Hajdúch, M. **(2015)**. 5-Azacytidine nucleosides and their derivatives: Molecular hallmarks of drug resistance & alternative therapeutic regimen. *Cancer Res.* **75**, 2944.

Agrawal, K., Das, V., Otmar, M., Krečmerová, M., Džubák, P., Hajdúch, M. **(2015)**. Cell-based DNA demethylation detection system for screening of epigenetic drugs in 2D, 3D and xenograft models. *Mol Cancer Ther.* **14**, B72.

Agrawal, K., Džubák, P., Hajdúch, M., Frydrych, I. **(2016)**. Method of predicting the tumor response to DNA methylation inhibitors and alternative therapeutic regimens for overcoming resistance. *Abstract book: 1st. Annual BioSpot Conference.*

Agrawal, K., Vojta, P., Holub, D., Slavkovský, R., Frydrych, I., Džubák, P., Krečmerová, M., Hajdúch, M. **(2016)**. Molecular hallmarks of drug resistance to DNA methylation inhibitors and alternative therapeutic regimen for overcoming resistance. *Cancer Res.* **76**(14), 4453.

Das, V., Skolekova, S., **Agrawal, K.,** Gursky, J., Kučerová, L., Hajdúch, M. **(2016)**. Stromal cell-induced alterations in the response of colorectal cancer cell to demethylating agents. *Cancer Res.* **76**(14), 4101.

▪ Oral and poster presentations

Khushboo Agrawal, Petr Džubák, Marián Hajdúch. Study of epigenetic 5-azacytidine nucleosides and their derivatives. Doctoral students conference, 25-26 November 2011, Vyškov, Czech Republic.

Khushboo Agrawal, Ivo Frydrych, Petr Džubák, Marián Hajdúch. Study of epigenetic 5-azacytidine nucleosides and their derivatives. VIII. Diagnostic, Predictive and Experimental Oncology Days, 29-30 November 2012, Olomouc, Czech Republic.

Khushboo Agrawal, Ivo Frydrych, Petr Džubák, Marián Hajdúch. Study of epigenetic 5-azacytidine nucleosides and their derivatives. Doctoral students conference, 30 November - 01 December 2012, Vyškov, Czech Republic.

Khushboo Agrawal, Ivo Frydrych, Petr Džubák, Marián Hajdúch. Study of epigenetic therapeutics - 5-azacytidine derivatives. Conference of Chemical Biology and Genetics, 12-14 May 2013, Malá Morávka, Czech Republic.

Khushboo Agrawal, Ivo Frydrych, Petr Džubák, Marián Hajdúch. Study of epigenetic therapeutics - 5-azacytidine derivatives. XIII Interdisciplinary meeting of young biologists, biochemists and chemists, 14-17 May 2013, Žďáru nad Sázavou, Czech Republic.

Khushboo Agrawal, Petr Džubák, Ivo Frydrych, Dušan Holub, Marcela Krečmerová, Miroslav Otmar, Marián Hajdúch. Epigenetic study of 5-azacytidine nucleosides and their derivatives. IX. Diagnostic, Predictive and Experimental Oncology Days, 21-22 November 2013, Olomouc, Czech Republic.

Khushboo Agrawal, Petr Džubák, Ivo Frydrych, Dušan Holub, Marcela Krečmerová, Miroslav Otmar, Marián Hajdúch. Epigenetic study of 5-azacytidine nucleosides and their derivatives. 10th International Medical Postgraduate Conference, 21-22 November 2013, Hradec Králové, Czech Republic.

Khushboo Agrawal, Petr Džubák, Ivo Frydrych, Dušan Holub, Petr Vojta, Marcela Krečmerová, Miroslav Otmar, Marián Hajdúch. 5-azacytidine nucleosides and their derivatives: Molecular hallmarks of drug resistance. Young Oncologists Award for the best scientific work in Cancer Research, 06-07 March 2014, Bratislava, Slovak Republic.

Khushboo Agrawal, Petr Džubák, Ivo Frydrych, Dušan Holub, Petr Vojta, Marcela Krečmerová, Miroslav Otmar, Marián Hajdúch. 5-azacytidine nucleosides and their derivatives: Molecular hallmarks of drug resistance. American Association of Cancer Research Annual Meeting, 05-09 April 2014, San Diego, USA.

Khushboo Agrawal, Petr Vojta, Dušan Holub, Ivo Frydrych, Petr Džubák, Miroslav Otmar, Marián Hajdúch. 5-Azacytidine Nucleosides and their Derivatives: Molecular Hallmarks of Drug Resistance & Alternative Therapeutic Regimen. X. Diagnostic, Predictive and Experimental Oncology Days, 02-03 December 2014, Olomouc, Czech Republic.

Khushboo Agrawal, Petr Vojta, Dušan Holub, Ivo Frydrych, Petr Džubák, Miroslav Otmar, Marcela Krečmerová, Marián Hajdúch. 5-Azacytidine nucleosides and their derivatives: Molecular hallmarks of drug resistance & alternative therapeutic regimen. American Association of Cancer Research 106th Annual Meeting, 18-22 April 2015, Philadelphia, USA.

Khushboo Agrawal, Petr Džubák, Marián Hajdúch, Ivo Frydrych. Method of predicting the tumor response to DNA methylation inhibitors and alternative therapeutic regimens for overcoming resistance. 1st. Annual BioSpot Conference, 24 February 2016, Prague, Czech Republic.

Khushboo Agrawal, Petr Vojta, Dušan Holub, Rastislav Slavkovský, Ivo Frydrych, Petr Džubák, Marcela Krečmerová, Marián Hajdúch. Molecular hallmarks of drug resistance to DNA methylation inhibitors and alternative therapeutic regimen for overcoming resistance. American Association of Cancer Research 107th Annual Meeting, 16-20 April 2016, New Orleans, USA.

▪ Awards and Prizes

2010: Doctoral Scholarship, Palacky University of Olomouc, Olomouc, Czech Republic.

2012: 1st Prize, best presentation at VIII. Diagnostic, Predictive and Experimental Oncology Days, Cancer Foundation and Research, Olomouc, Czech Republic.

2013: Consolation prize, nominated amongst best 5 presentations at XIII. Interdisciplinary Meeting of Young Biologists, Biochemists and Chemists, Sigma Aldrich, Žďáru nad Sázavou, Czech Republic.

2014: Special prize, best scientific work in cancer research at the Conference of Young Oncologists, Slovak Academy of Sciences, Bratislava, Slovak Republic.